

2004

Functional analyses of hTel2 and TRF2 deltaB: Insights Into the Role of a New DNA Damage Pathway and Homologous Recombination in Mammalian Telomere Function

Richard Chih-Chien Wang

Follow this and additional works at: [http://digitalcommons.rockefeller.edu/
student_theses_and_dissertations](http://digitalcommons.rockefeller.edu/student_theses_and_dissertations)

 Part of the [Life Sciences Commons](#)

Recommended Citation

Wang, Richard Chih-Chien, "Functional analyses of hTel2 and TRF2 deltaB: Insights Into the Role of a New DNA Damage Pathway and Homologous Recombination in Mammalian Telomere Function" (2004). *Student Theses and Dissertations*. Paper 48.



**Functional analyses of hTel2 and TRF2^{ΔB}: Insights into the role
of a new DNA damage pathway and homologous
recombination in mammalian telomere function**

A thesis presented to the faculty of the Rockefeller University in partial fulfillment of the
requirements for the degree of Doctor of Philosophy

by

Richard Chih-Chien Wang

Advisor

Titia de Lange

September 2004

The Rockefeller University

New York, New York

© Copyright by Richard Wang, 2004

To my family, who love me no matter who I become;
to my friends, who love me for who I have become;
and to my teachers, who love me for who I can become.

Acknowledgements

I will forever be indebted to Titia de Lange for her mentorship. She has been a great advisor in so many ways...She has been the voice of reason when I have been overly enthusiastic about some hair-brained idea (which is a lot of the time), and she has been a cheerleader when I have been despondent about negative results (which is the rest of the time). She has been a creative muse when I have needed inspiration, and she has *always* been around to answer my questions. However, most importantly, she has shown me by example what it means to be a truly great scientist and teacher. I will always consider her as a role model for my future career in teaching and research. After all, one could not hope to do any better. Titia, thanks for everything. I will not forget.

I would like to thank all of the senior members of the lab, past and present, who have taught me so much, especially when I first started in the lab. I am especially grateful to Jan Karlseder, Jeffrey Ye, Xu-dong Zhu, Diego Loayza, and Giulia Celli who all took time out of their busy schedules to hand-hold me through protocols. In the little time that I have left in the lab, I hope to pay it forward. Although their generosity will be hard to match, I will try my very best.

I would like to thank all of the scientists who contributed reagents towards my studies. Kiyoshi Miyagawa was especially generous not only with his XRCC3 null cells but also with his time. John Petrini, especially Travis Stracker in his lab, provided me with many mouse cell lines and related reagents. Lincoln Bickford, a fellow MD-PhD student took time to help me purify copious amounts of hTel2, a process that was essential for generating a good antibody. I also got reagents from Jean Pierre de Villartay, Tadahiro Shiomi, Paul Hasty, Lexicon Genetics, Fred Alt, Margeret Zdzienicka, Thomas Kunkel, Alan Clark, Winfried Edelman, Hein te Reile, Michael Liskay, and Hao Gu. These investigators and their assistants patiently responded to my requests for reagents even when I was not quite as patient. These studies would not have been complete with their generosity.

So many people in the lab have made it a great place to work. I have to thank Xu-dong, my benchmate of many years, for putting up with my constant nagging questions. Through them, we have had many arguments sometimes enlightening, always entertaining. Thanks to all of my fellow graduate students for their camaraderie. With Agata Smogorzewska, Josh Silverman, Jill Donigian, Kristina Hoke, Dirk Hockemeyer, Megan van Overbeek, and Nadya Dimitrova, I have enjoyed innumerable, lunches, movie nights, barbecues, and beers together. I cannot imagine how lab would have been without all of them. I would also like to thank Hiro Takai for all of his sage advice on protocols and experiments. I've truly enjoyed working with him on the Tel2 project. We haven't had our big break on the stubborn molecule yet, but I have every confidence that Hiro will succeed where I have not.

A special thanks also goes to a so many people who make out lab a great place to do science. Rita Rodney, Heidi Moss, Amy Himelblau, Heather Parsons, Vanessa Marrero, Devon White, Sara Hooper, Stephanie Blackwood, and Kaori Takai are all amazingly good at their jobs. But I think even more importantly, they are all great people and have made and continue to make the lab a fun place to work.

When Stewart Barnes first started managing computers in the lab, I think they were still monochrome Apple II's. Now, he takes care of our 800 G lab server. Regardless, he has always done the job with efficiency and skill. I thank him for all his help.

The MD/PhD office at Weill Medical College and Dean's office at The Rockefeller University have always been extremely helpful and patient. Special thanks goes to Ruth Gotian, Elaine Velez, Renee Horton, Sue Ann Chong, Kristen Cullen, and Marta Delgado because they have had to deal with me the most and have always done so with patience and good humor.

When selecting faculty members to be on my thesis committee, I chose Fred Cross, Hiro Funabiki, and Maria Jasin because their area of research interests had the potential of being very helpful for my projects. They have been everything that I had hoped and more. My committee has been attentive and interested about my work; even more, they have given me insightful suggestions, necessary criticisms, and caring encouragement. I greatly appreciate their time and efforts. Dr. Joachim Lingner also deserves recognition for agreeing to be the outside examiner of my thesis. I thank him for taking time away from his work and family to do so.

To my friends, thank you for putting up with me for four years. Some people deserve special recognition. There is, of course, the Stanford in New York crew: Doug, Caroline, and Tim. I already had so many great memories from our time at Stanford. I feel especially lucky that our friendship has been able to grow here in NYC.

Howie, with whom I have lifted weights just about every weekend for our entire PhD's, also deserves special thanks for putting up with me. I'm glad we're both finishing together. I'm not sure how long I would last as a PhD student without our weekend lifts. Mac and I have been roommates for most of graduate school, and I'd like to think we're both better people for it (at least I know I am). Mac, thanks for the late night Ramen philosophy sessions; thanks for commiserating with me about Houston sports; thanks for the many delicious meals. I'm looking forward to spending more time with you both as we eventually go on to finish med school.

A very special thank you goes to Pauline. More than anyone else, she has experienced and patiently endured the highs and lows of graduate school. I really cannot imagine what the past few years would have been like without you. Thanks for being there through the good times and the bad.

Finally, to my parents and Emily, thanks for always being there for me. Regardless of how things are going, I know you will be there to support me; this has and always will buoy me in everything that I do.

Table of Contents

<i>Acknowledgements</i>	<i>iii</i>
<i>Table of Contents</i>	<i>v</i>
<i>List of Figures</i>	<i>vi</i>
<i>List of Tables</i>	<i>viii</i>
<i>List of Abbreviations</i>	<i>ix</i>
ABSTRACT	1
CHAPTER: INTRODUCTION	3
Replicative Senescence	4
Telomerase	8
Telomere binding proteins	14
DNA Damage Proteins and Telomeres	32
CHAPTER 2: ANALYSIS OF TEL2 IN HUMAN CELLS	41
INTRODUCTION	42
RESULTS	46
CONCLUSION	86
CHAPTER 3: GENETIC AND MOLECULAR ANALYSIS OF TRF2ΔB INDUCED HOMOLOGOUS RECOMBINATION AT MAMMALIAN TELOMERES	92
INTRODUCTION	93
RESULTS	105
DISCUSSION	149
CHAPTER 4: DISCUSSION	162
Introduction	163
Possible roles of Tel2 in mammalian cells	164
TRF2 protects chromosome ends from HR	168
CHAPTER 5: MATERIALS AND METHODS	177
REFERENCES	196

List of Figures

Figure 1-1. Cellular senescence in human somatic cells.	6
Figure 1-2. Telomerase in <i>S. cerevisiae</i> and humans.	9
Figure 1-3. Schematic of human TTAGGG repeat binding factors, TRF1 and TRF2. ...	20
Figure 1-4. Telomere structure and proteins in mammals.	27
Figure 2-1. Schematic and alignment of hTel2.	49
Figure 2-2. Expression of hTel2 assessed by Western and IF.	52
Figure 2-3. Endogenous hTel2 does not associate with telomeres.	55
Figure 2-4. Tel2 does not interact with telomeric proteins by IP.	57
Figure 2-5. hTel2 foci do not colocalize with PCNA foci, centromeres, or IRIFs.	59
Figure 2-6. hTel2 foci co-localizes with PML nuclear bodies.	61
Figure 2-7. hTel2 localization in meiotic spermatocytes.	63
Figure 2-8. hTel2 localizes to centrosomes in mouse and human cells.	65
Figure 2-9. Effect of Myc_Tel2 alleles on TRF length in HTC75 and IMR90 cells.	68
Figure 2-10. Effect of FLAG_Tel2 on TRF length in BJ/hTERT and HeLa1.2.11.	69
Figure 2-11. Effect of Tel2 on TRF length in HTC75 and SK-HEP-1 cells.	72
Figure 2-12. Effect of Tel2 on TRF length in HTC75 and SK-HEP-1 cells.	73
Figure 2-13. Depletion of Tel2 by siRNA results in cell death.	76
Figure 2-14. Depletion of Tel2 by siRNA results in the accumulation of abnormal early metaphases.	78
Figure 2-15. Depletion of Tel2 by siRNA results in the accumulation of abnormal early metaphases.	80
Figure 2-16. Tel2 depletion causes defects in chromosome condensation.	82
Figure 2-17. hTel2 expression rescues Tel2 depletion mediated defects in chromosome condensation.	83
Figure 2-18. Overexpression of Tel2 impairs the accumulation of cells in G2 after IR. ...	85
Figure 3-1. A Model for Telomere Rapid Deletion (TRD) in <i>S. cerevisiae</i>	99
Figure 3-2. ChIP of telomeric proteins in cells expressing TRF2 Δ B.	106
Figure 3-3. Growth arrest, senescence, and TIF induction by TRF2 Δ B.	108
Figure 3-4. TRF2 Δ B results in the loss of duplex telomeric DNA in human and mouse cells.	110
Figure 3-5. Quantitation of telomere blots after TRF2 Δ B expression.	112
Figure 3-6. TRF2 Δ B induces increased single-stranded DNA at telomeres.	114
Figure 3-7. TRF2 Δ B induces stochastic telomere loss telomere associations.	117

Figure 3-8. TRF2 Δ B preferentially induces the loss of leading strand telomeres.	120
Figure 3-9. TRF2 Δ B preferentially induces the loss of leading strand telomeres.	122
Figure 3-10. XRCC3 is required for TRF2 Δ B-induced telomere loss.	124
Figure 3-11. Nbs1 is required for TRF2 Δ B-induced telomere loss.	126
Figure 3-12. Telomeres from Nbs ^{ΔB/ΔB} still undergo TRF2 Δ B-mediated shortening.	127
Figure 3-13. TRF2 Δ B induces an arc consistent with relaxed telomeric circles detectable by 2D gels.	133
Figure 3-14. TRF2 Δ B-induced arc comigrates with circular marker.	134
Figure 3-15. TRF2 Δ B-induced relaxed telomeric circles are detected in mouse cells. .	135
Figure 3-16. TRF2 Δ B-induced circular telomeric DNAs do not contain subtelomeric DNA.	136
Figure 3-17. Comparison of telomeric circles in primary IMR90 and Nbs1 fibroblasts.	138
Figure 3-18. TRF2 Δ B induces ss DNA that does not comigrate with telomeric circles in native 2D in-gel hybridizations.	141
Figure 3-19. Telomeric circles can be visualized after UV crosslinking in the presence of psoralen.	142
Figure 3-20. Depletion of Ku86 does not induce telomeric circles.	144
Figure 3-21. DNA damaging agents induce t-loop HR.	146
Figure 3-22. ALT cell lines have increased amounts of circular telomeric DNA.	148
Figure 3-23. Telomere protein expression in ALT cells.	149
Figure 3-24. Model for t-loop HR.	152
Figure 4-1. Possible functions in S-phase for hTel2.	165
Figure 4-2. Possible contributions of telomeric circles in ALT telomere lengthening. .	174

List of Tables

Table 1-1. Summary of general features of telomeres and telomere binding proteins in <i>S. pombe</i> , <i>S. cerevisiae</i> , and humans.	15
Table 1-2. DNA damage proteins in telomere maintenance.....	32
Table 3-1. Quantification of TRF2 Δ B-induced telomeric signal loss.....	118
Table 3-2. Human mutant cells that do not abrogate TRF2 Δ B-induced telomere signal loss	128
Table 3-3. Mouse mutant cells that do not abrogate TRF2 Δ B induced telomere signal loss	130
Table 5-1. Antibodies used in Chapter 2.	180
Table 5-2. Antibodies used in Chapter 3.	181

List of Abbreviations

ALT	alternative lengthening of telomeres
APB	ALT-associated PML bodies
A-T	ataxia-telangiectasia
ATLD	ataxia-telangiectasia like disorder
ATM	ataxia-telangiectasia mutated
ATR	ATM- and rad3- related
BrdU	bromo-deoxyuridine
bp	base pair
CO-FISH	chromosome-orientation FISH
ChIP	chromatin immunoprecipitation
CX3	RAD51C/XRCC3 heterodimer
DAPI	4,6-diamidino-2-phenylindole
DNA-PK	DNA-dependent protein kinase
DNA-PKcs	catalytic subunit of DNA-dependent prot
DKC	dyskeratosis congenita
DSB	double-strand break
EMSA	electromobility shift assay
est	ever shorter telomeres
FISH	fluorescence in-situ hybridization
FITC	fluorescein isothiocyanate
HR	homologous recombination
hTERT	human telomerase reverse transcriptase
hTR	human telomerase reverse RNA
HU	hydroxyurea
IF	immunofluorescence
IP	immunoprecipitation
IR	ionizing radiation
IVT	in vitro transcription / translation
IRIF	ionizing radiation induced foci
kb	kilobase pairs
MEF	mouse embryonic fibroblast
NBS	Nijmegen breakage syndrome
NHEJ	non-homologous end joining

NLS	nuclear localization sequence
O/N	overnight
PARP	poly(ADP-ribose) polymerase
PCNA	proliferating cell nuclear antigen
PCD	premature centromere dissociation
PD	population doubling
PIKK	PI3-related kinases
PML	promyelocytic leukemia
PML-NB	PML nuclear body
PNA	peptide nucleic acid
RAP1	repressor and activator protein 1
RDS	radioresistant DNA synthesis
SA β -gal	senescence associated β -galactosidase
SCE	sister chromatid exchange
SCID	severe combined immunodeficiency
SD	standard deviation
SIR	Silent information regulator
TIF	telomere dysfunction-induced focus
TPE	telomere position effect
hTR	human telomerase RNA
TRF	terminal restriction fragment
TRF1	TTAGGG repeat binding factor 1
TRF2	TTAGGG repeat binding factor 2
TRFH	TRF homology domain
TRD	telomere rapid deletion
UV	ultraviolet

ABSTRACT

Tel2 influences telomere length in *S. cerevisiae* and DNA-damage signaling in *C. elegans*. We found that endogenous human Tel2 (hTel2) localized in a diffuse, granular pattern to the nuclei of human cells where it was enriched in PML nuclear bodies, but not telomeres. Surprisingly, hTel2 also localized to centrosomes. Although hTel2 did not detectably interact with telomeric proteins or telomeric chromatin, the overexpression of untagged hTel2 resulted in the slow elongation of telomeres in HTC75 and SK-HEP-1 cells. Furthermore, hTel2 overexpression suppressed the accumulation of cells in G2 after ionizing radiation. The depletion of hTel2 in HeLa cells by RNA interference resulted in apoptotic cell death. Furthermore, hTel2 depletion resulted in the accumulation of aberrant mitotic cells that possessed disorganized metaphase chromosomes. The metaphase chromosomes of hTel2 depleted cells were curly suggesting that hTel2 played a role in chromosome compaction. A role for hTel2 in establishing chromatin structure during S-phase could explain its multiple localizations and phenotypes.

TRF2 protects telomeres from non-homologous end joining (NHEJ), possibly through the formation of a t-loop structure. A mutant allele of TRF2, TRF2 Δ B, retained the ability to suppress NHEJ but induced dramatic deletions of telomeric DNA. This catastrophic telomere shortening was accompanied by a DNA damage response and senescence. Using FISH and CO-FISH, TRF2 Δ B was found to induce rapid, stochastic deletions that preferentially affected leading strand telomeres (parental C-strand) after DNA replication. Genetic analyses demonstrated that TRF2 Δ B-induced deletions required Nbs1, a component of the Mre11 complex, and XRCC3, a component of the RAD51C/XRCC3 Holliday junction (HJ) resolvase, suggesting the involvement of homologous recombination (HR) in the deletions. Consistent with a role for HR, TRF2 Δ B induced the formation of t-loop-sized telomeric circles. These telomeric circles were also

detected in unperturbed cells suggesting that t-loop deletion by HR could explain the stochastic nature of telomere shortening and senescence in somatic cells. Furthermore, telomerase-negative ALT cells had abundant telomeric circles, suggesting that recombination-mediated elongation of ALT telomeres could involve telomeric circles. These findings show that TRF2 regulates both NHEJ and HR at mammalian telomeres and that HR at telomeres influences the integrity and dynamics of mammalian telomeres.

**CHAPTER 1:
INTRODUCTION**

Replicative Senescence

Hayflick's observation on cellular mortality

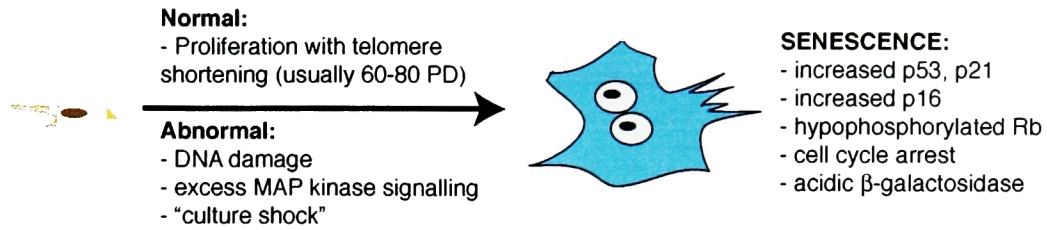
Since the turn of the century, cells isolated from different vertebrate tissues, including human, have been cultured *in vitro*. Alexis Carrel claimed that cells derived from the chicken heart, if given the right growth conditions, could divide indefinitely in a culture dish. Flaws in Carrel's experiments went unrecognized, and the notion that cells were immortal *in vitro* became widely accepted scientific fact. For most of the twentieth century, it was thought that the cessation of cellular division in tissue culture was due to inadequate growth conditions [1]. However, in 1961, Hayflick and Moorhead reported that normal diploid fibroblasts stopped dividing despite the fact that they had been cultured under optimal growth conditions. Although senescent fibroblasts remained metabolically active, they were unable to proliferate despite the presence of the appropriate growth signals. This state has been described as "replicative senescence," or more recently as the "Hayflick limit" [2, 3]. Although the original observations were met with some skepticism, repeated independent observations of replicative senescence in a large variety of cell types—including fibroblasts, keratinocytes, epithelial, endothelial, glial, and smooth muscle cells—have demonstrated the robustness of replicative senescence as a feature of human somatic cells [4, 5].

Many recent studies have yielded some insight into the molecular foundations of replicative senescence. FACS analyses of cells in replicative senescence indicate that very few cells are in S-phase with higher than normal numbers with $2n$ and $4n$ DNA content. This profile is distinct from that of quiescent cells, which show most cells to be arrested with a G1 DNA content. Genetic studies have demonstrated that senescence is maintained by two partially redundant tumor suppressor pathways—Rb and p53. In senescent cells, the activation of p53 pathway is accompanied by the upregulation of the cyclin dependent kinase inhibitor, p21. Cells undergoing replicative senescence also

activate p16 resulting in hypophosphorylated Rb [6] (Fig. 1-1A). Both of these modifications serve to inhibit the activity of several cyclin dependent kinases to halt cell cycle progression. The involvement of the two major tumor suppressor pathways in establishing senescence is no coincidence. It is likely that cellular senescence has evolved as a mechanism to prevent inappropriate cell proliferation especially in the context of neoplastic transformation.

As early as the 1972, it was speculated that the inability of lagging strand synthesis to replicate the ends of linear chromosomes, called telomeres, could be the cause of replicative senescence [7, 8]. Consistent with a role for the end-replication problem in replicative senescence, it has been found that telomeres of many eukaryotes shorten in the absence of telomerase at a rate of ~3-5 bp/end/cell division. Curiously, the telomeres of cultured human and mouse cells that lack telomerase activity have been found to shorten faster, ~50-150 bp/end/cell division [9-11]. Thus, it is likely that the active degradation of telomeric DNA exacerbates the end replication problem in mammalian cells. The mechanism and possible nucleases that cause the accelerated rate of progressive telomere attrition in mammalian cells are not known.

A



B

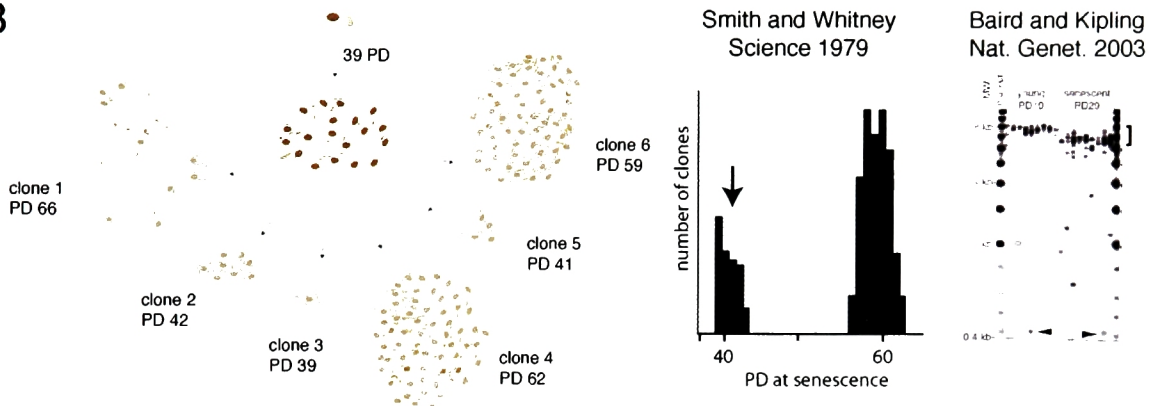


Figure 1-1. Cellular senescence in human somatic cells.

(A) Normal fibroblasts have a limited proliferative capacity *in vitro*. Although telomere shortening is thought to be the primary cause of senescence *in vitro*, inadequate growth conditions, abnormal mitogenic signaling, or DNA damage can drive a cell into "premature" senescence. (B) Cellular senescence does not happen progressively for primary diploid fibroblasts. Individual cells derived from a clonal population are capable of strikingly different numbers of divisions *in vitro*. The clonal sizes formed by individual cells have a bimodal distribution [12]. These rapidly senescent cells (arrow) are thought to be caused by stochastic telomere shortening events that can be detected by STELA (right) [13]. Progressive shortening happens at ~ 50 -150 bp/PD (bracket) while stochastic shortening events can delete the entire telomeric tract (arrowheads). Figures were adapted from Titia de Lange.

Although progressive telomere shortening likely contributes to replicative senescence in human cells, it does not explain some prominent features of cellular senescence. Although mass populations of cells derived from the same tissue undergo roughly the same number of population doublings (PDs) before entering senescence, individual cells derived from that population can have dramatically different replicative capacities. For example, while most cells separated from an intra-clonal population of fibroblasts are capable of as many PDs as the mass population, many other isolated cells divide only a few times (or not at all) before senescing (Fig. 1-1B) [12]. Thus, the

colonies formed by fibroblasts isolated from an intra-clonal population were bimodal in their size. Although factors other than telomere shortening, like spontaneous DNA damage, inadequate growth conditions, and inappropriate mitogenic signals, have been shown to induce cells to undergo a “premature” cellular senescence, recent studies have shown that the prematurely senescent cells have shorter telomeres than the bulk population [14]. In addition, the analysis of single telomere lengths using STELA has demonstrated that the Xp/Yp telomeres from individual cells undergo stochastic deletions while the majority of cells have telomeres that shorten at previously predicted rates [13]. Thus, large-scale, stochastic shortening events play a critical role in determining the number of divisions that a cell can undergo. Oxidative damage, telomeric recombination, and replication slippage have all been postulated to contribute to the stochastic element of telomere shortening [15-17]. However, mechanistic details of this important contributor to telomere shortening had not been clear.

Although the mechanisms of telomere shortening are still not completely understood, there is little doubt that telomere shortening ultimately drives replicative senescence. The early evidence for the relationship between replicative senescence and telomere shortening had been correlative in nature. In addition to the progressive telomere shortening that had been noted for most somatic cells, it was also noted that a significant correlation existed between the telomere length of a cell population and its proliferative capacity [18]. However, definitive proof for a causal role of telomere shortening in replicative senescence was possible only after the cloning of telomerase, the enzyme that adds telomeric repeats to chromosome end. The ectopic expression of telomerase in somatic cells prevented the onset of replicative senescence [19]. Telomerase is normally expressed in germline tissues and stem cells and explains why telomeres of those cell types are longer than those of somatic cells [20, 21].

Telomerase

The telomerase core enzyme—the RNA and protein subunits

Telomerase is a ribonucleoprotein enzyme that adds telomeric repeats to the ends of linear chromosomes [22]. It consists of two parts—a template RNA, the telomerase RNA component (TERC, TR, or TER) and a catalytic subunit, the telomerase reverse transcriptase (TERT) [23-27]. Although telomerase RNA components from different species have a high degree of sequence variability, they appear to have a well-defined secondary structure (Fig. 1-2A) [28, 29]. One well conserved feature of ciliate, yeast, and vertebrates telomerase RNAs is the pseudoknot domain. This pseudoknot domain is thought to contain a conserved pseudoknot structure, a potential TERT-binding site, and the template sequence that is used by TERT to synthesize telomeric repeats. In addition, several features of the TERC secondary structure are important for the maturation, stability, and association of the RNA with telomerase [28]. Some of other important structural features of the telomerase RNA along with the proteins that bind them will be discussed later in the introduction. TERT, the protein subunit of telomerase, is a reverse transcriptase that is most closely related to group II intron-encoded reverse transcriptase [30]. Together with the RNA, telomerase aligns itself on the chromosome terminus and uses the short template sequence to add DNA to the 3' end of DNA substrates. *In vitro*, the enzyme is capable of repeated steps of alignment and elongation making it highly processive [31, 32]. In addition, in both humans and *S. cerevisiae*, active telomerase is found as a dimer [33, 34]; the functional significance of telomerase dimerization is still unclear.

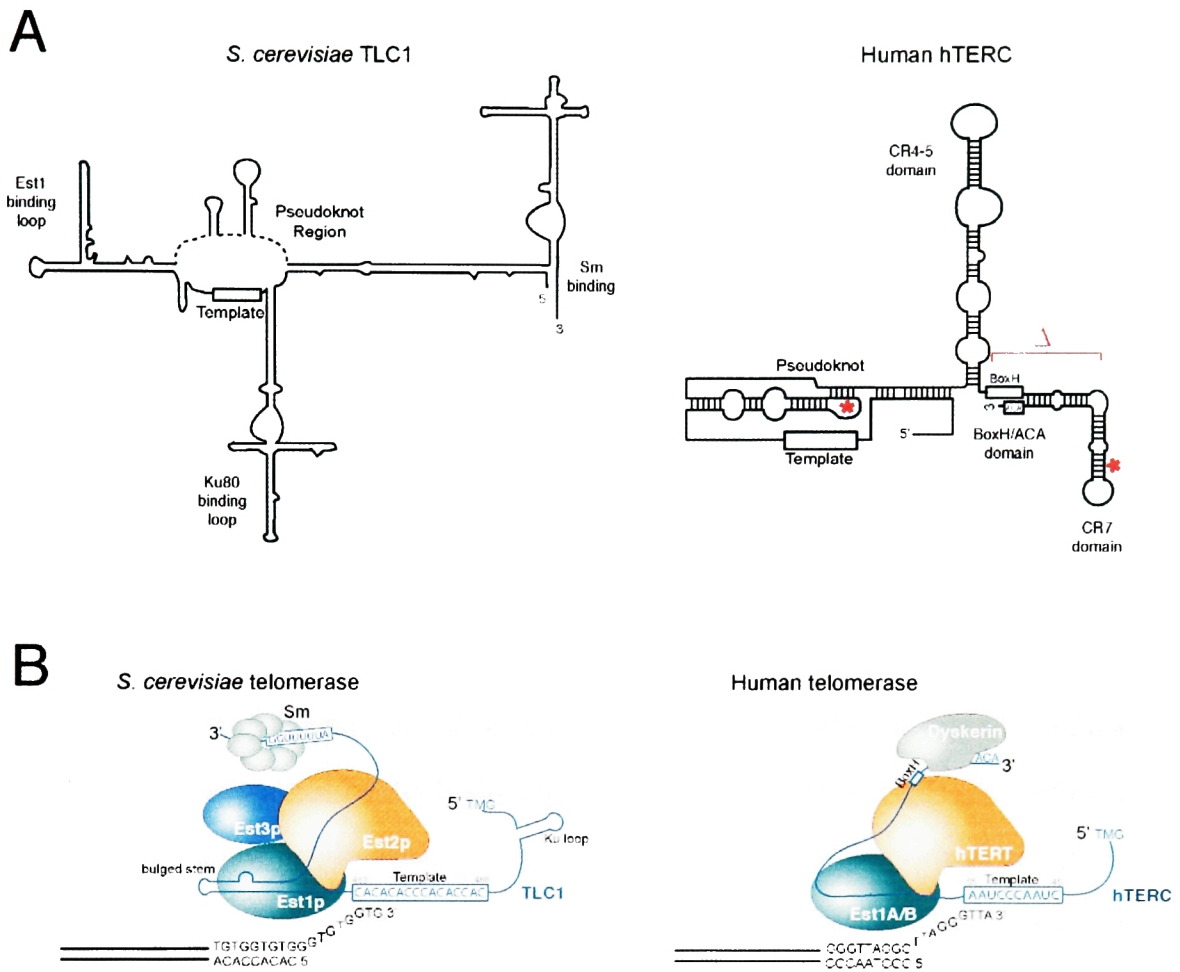


Figure 1-2. Telomerase in *S. cerevisiae* and humans.

(A) The predicted secondary structure of yeast TLC1 and human hTERC. Shaded boxes represent structural motifs demonstrated to be important for telomerase function. Deletions noted in autosomal dominant DKC patients are marked in red. (B) Telomerase RNA associated with known protein binding partners. (Figures adapted from [29, 35])

Telomeres reside in either an extendible or a non-extendible state; shorter telomeres are more likely to be extendible [36]. Telomere length regulates the access of telomerase, likely through the recruitment of protein factors that act in *cis*; these factors will be discussed in detail later in this chapter. Upon recruitment to extendible chromosome ends, telomerase adds a variable number of specific repeat sequences to the 3' overhang of telomeres. Telomere length does not appear to influence the processivity of telomerase [36]. Although it is thought that telomerase mediated extension of the G

strand is coordinated with lagging strand synthesis of the C-strand, precisely how these events are coordinated are not understood.

In contrast to unicellular organisms and mice, the expression of telomerase in human cells is highly regulated. In most somatic cells, the expression of hTERT and telomerase activity, though detectable, is limiting for long term growth [37]. Somatic cells repress hTERT expression in through multiple overlapping tumor suppressor pathways including Mad/c-Myc, TGFb, and Mad/c-Myc [38]. A functional deficiency of telomerase in somatic cells would be consistent with their progressive telomere shortening and limited proliferative capacity *in vitro*. This relationship between telomere shortening and replicative senescence was demonstrated definitively by the immortalization of three otherwise mortal cell types through the ectopic expression of hTERT [19]. The fundamental importance of regulating TERT levels in mammalian cells is further supported by the finding that mice heterozygous for a deletion of mTERT (mTERT+/-) show haploinsufficiency and telomere shortening when compared to mTERT+/+ mice [39]. Despite its repression in somatic tissues, hTERT is normally expressed in the germline, stem cells, and highly proliferative tissues [21, 40].

TERT expression may be repressed in human cells because telomerase activity is required for unlimited cell proliferation, a characteristic of many tumor cells. Approximately 85% of all human tumors have reactivated telomerase [41, 42]. Of the remaining tumors, some may have undetectable amounts of telomerase activity that are still sufficient to promote growth of the tumor; others may have reached a pathological size without reactivating telomerase [43]; still others could have activated an alternative means of telomere elongation (ALT) (discussed in Chapter 3). For most tumors, replicative senescence caused by telomere attrition seems to limit the outgrowth of cells undergoing repeated cycles of inappropriate division. Consistent with this model, tumorigenesis is impaired in cancer prone mice in the absence of mTR [44]. Although it is possible to generate transformed, oncogenic cells without reactivating telomerase [45],

the majority of human cancers have reactivated telomerase or another telomere maintenance mechanism and no longer show progressive telomere loss with proliferation [46, 47].

Telomerase accessory factors

Although hTERT and hTR are the only essential factors in telomerase *in vitro*, a number of factors have been identified in genetic and biochemical assays that appear to promote telomere elongation *in vivo*. In *S. cerevisiae*, genetic screens for yielded Est1 and Est3, in addition to the RNA template (TLC) and catalytic protein subunit (Est2) of telomerase. Est1 localizes to chromosome ends via an interaction with a G-strand binding protein (Cdc13) and also interacts with a conserved bulged stem in TLC (yeast telomerase RNA component) [48]. Consistent with its interacting partner, Est1 has been implicated in loading telomerase onto telomeres [49]. Est3 is also a component of the telomerase holoenzyme in yeast; however, its precise function in promoting telomerase recruitment is not understood [50]. Recent investigations have also demonstrated that Ku80 specifically binds to a specific stem loop in TLC1 promoting its recruitment to telomeres. Although yeast that express a yKu80 that is defective for TLC1 binding have shorter telomeres, these yeast do not senesce like est mutants. Thus, Ku promotes, but is not essential for, telomere elongation by telomerase. The details of Ku's recruitment of telomerase will be discussed in more detail later in this introductory chapter.

Based on weak homology to *S. cerevisiae* Est1, three homologs in humans (Est1A, B, and C) and one homolog in *S. pombe* have been identified [51-53]. In both fission yeast and human cells, Est1 is closely associated with telomerase activity suggesting that Est1's role as an essential component of telomerase is widely conserved. The overexpression of Est1A in human cells results in defects in telomere capping; in addition, the concomitant loss of both Est1 and Taz1 in fission yeast resulted in a lethal germination phenotype suggesting that Est1 may have a role in telomere capping in

addition to a role as an telomerase accessory factor. In contrast to Est1, no homologs of Est3 have been found in other organisms.

In addition to factors that interact with the core enzyme, a number of proteins have been shown to be important for the maturation and folding of the RNA subunit. In *S. cerevisiae*, the TLC1 RNA associates with Sm proteins using a binding motif near its 3' end (Fig. 1-1A). In concert with its 5' trimethylguanosine cap, TLC1 is very likely a small nuclear ribonucleoprotein particle [54].

Like TLC1, hTERC associates with accessory factors and undergoes secondary processing that is required for its maturation. Human telomerase RNA localizes to Cajal bodies, an intranuclear structure for RNP processing and assembly [55-57]. Like other small Cajal body RNAs (scaRNAs), the localization to Cajal bodies is dependent on a specific sequence motif in the CR7 domain. An additional protein factor that is important for the maturation of telomerase is dyskerin (Fig. 1-2). Dyskerin binds to a conserved 3' box H/ACA motif in hTERC. Dyskerin is a component of small nucleolar ribonucleoproteins (snoRNAs) and scaRNAs that convert specific uridine residues to pseudouridine residues, a process which is especially important for the maturation of rRNA.

Dyskerin is mutated in patients who suffer from dyskeratosis congenital (DKC), a disease that is characterized by muco-cutaneous abnormalities and severe bone marrow failure [58]. In the absence of dyskerin, hTERC is unstable and becomes limiting for telomerase activity. DKC patients have extremely short telomeres, and an inability to maintain telomere capping in stem cell populations can explain all of the disease symptoms in DKC, many of which are reminiscent of premature ageing syndromes. Because the dyskerin gene is located on the X chromosome, the more common form of the disease is usually inherited in an X-linked recessive pattern. A subset of DKC patients, who have an autosomal dominant version of the disorder (AD-DC), possess mutations in hTERC RNA itself (Fig. 1-2A), excluding the possibility that the

phenotypes of DKC are secondary to defects in ribosome biogenesis [59, 60]. Studies on eight families affected with AD-DC indicate that the disease shows genetic anticipation in that successive generations become symptomatic at earlier ages. The disease anticipation is associated with progressively shorter telomeres [61]. hTERC's interactions with dyskerin and Cajal bodies and TLC's interactions with Sm accessory proteins are likely to be related to the observation that telomerase shuttles to and from nucleoli in both human and yeast cells [62, 63].

Telomerase is not enough

The activity of telomerase alone cannot explain many features of telomere maintenance. For example, germ cells or immortalized cells that possess very high telomerase activity do not progressively lengthen their telomeres, but rather keep their telomeres within a (usually) narrow length distribution [19, 64]. Furthermore, the ends of linear plasmids introduced into budding yeast will be lengthened by telomerase until they match the size of the endogenous telomeres [65]. These results suggest that there are factors that act in *cis* at individual telomeres to regulate the access of telomerase. In addition to regulating telomerase activity, these *cis* acting factors have additional unique functions in maintaining the ends of chromosomes.

Although the overexpression of hTERT is sufficient to immortalize many human cell lines, the addition of any sequence is not sufficient to circumvent the problem of chromosome ends. In fact, the expression of mutant versions of telomerase, which synthesize altered telomeric repeats in ciliates, yeast, or human cells, results in the rapid loss of viability [66-68]. Furthermore, in human cells, an alteration in telomere state rather than the complete loss of telomeric sequence induces senescence [11]. Collectively, these observations are consistent with a model in which telomerase synthesizes repetitive sequences that are the binding sites for sequence-specific binding proteins and additional associated proteins. Together with the DNA, these proteins complexes protect natural chromosome ends from being recognized and processed as

DNA damage. This definition of telomeres is consistent with the original cytological description of telomeres as essential chromosomal elements that prevent fusions [69, 70].

Although the telomere specific binding factors that mediate this protection are evolutionarily divergent, I will compare the telomere proteins of several organisms—primarily ciliates, *S. cerevisiae*, *S. pombe* and humans—to highlight some of the conserved features of general telomere biology and to examine what remains unresolved about telomere structure and function. A summary of some of the proteins and features of telomeres in these diverse organisms are included in Table 1-1.

Telomere binding proteins

The telomere end binding proteins of macronuclei – a simple solution for ciliates

Many unicellular ciliated protozoans including *Oxytricha*, *Euplotes*, and *Tetrahymena* possess two distinct nuclei—a diploid, transcriptionally silent germline nucleus (micronucleus) and a polyploid, transcriptionally active, vegetative nucleus (macronucleus). The *Oxytricha* macronucleus, possesses ~24 million short, linear, gene-sized chromosomes of no more than a few kilobases. The abundance of telomeres in these nuclei allowed for the isolation and sequencing of telomeric DNA, the purification of telomerase, and the identification of the first telomere binding proteins [30, 71, 72]. The telomere end binding proteins (TEBP) of *Oxytricha nova* has been characterized most thoroughly. It has two subunits, TEBP α and β . TEBP α binds specifically to the single stranded G-rich 16 nucleotide overhangs using three oligonucleotide binding (OB) domains; TEBP β interacts with the α subunit via an additional OB-like fold to form a very stable ternary complex with DNA [73]. In addition, telomeric DNA complexed with TEBP α and β are completely inaccessible to telomerase [74]. Based on the crystal structure and *in vitro* function of the TEBP α / β of *Oxytricha*, it was speculated that the tightly bound complex might both regulate telomerase activity and protect telomeres from

fusion, nucleases, and recombination. However, evidence for the functions of single stranded telomere binding proteins required the analysis in other model systems.

Table 1-1. Summary of general features of telomeres and telomere binding proteins in *S. pombe*, *S. cerevisiae*, and humans.

	Vertebrates	<i>S. cerevisiae</i>	<i>S. pombe</i>
Telomere sequence	TTAGGG	TG ₁₋₃	TTACAGG
Telomere structure	t-loop	Folded back	Unknown
Telomerase			
- RNA	hTERC (hTR, hTER)	TLC1	
- Protein	hTERT	Est2p	spTrt1p
- Accessory	Dyskerin, Est1A	Est1, Est3	Est1A
ds telomeric DNA binding protein	TRF1 TRF2 Ku?	Tbf1p? Rap1p Ku	Taz1 Ku?
ss telomeric DNA binding protein	POT1	Cdc13p	scPot1p
Telomere recruited proteins	<i>TRF1 interacting:</i> Tin2, Tankyrase1/2, PinX1, Ku? <i>TRF2 interacting:</i> Tin2, hRap1, Mre11 complex, ERCC1/XPF, BLM, WRN, Ku? <i>POT1 interacting:</i> PIP1	<i>Rap1p interacting:</i> Rif1/2, Sir3/4 <i>Cdc13 interacting:</i> Est2, Stn1, Ten1 <i>Ku interacting:</i> Est2 (via TLC)	<i>Taz1p interacting:</i> spRap1p, spRif1p
Telomerase independent survival	ALT pathway - HR dependent?	<i>Type I:</i> Y' repeat amp. - Rad52, Rad51, Rad54, Rad55, Rad57 <i>Type II:</i> - telomere repeat amp. - Rad 52, MRX, Rad59, Sgs1	Chromosome circularization Telomere repeat amp. - recombination dependent?

Cdc13 and the roles of single stranded DNA binding proteins in budding yeast

A role for the OB fold in binding ssDNA at telomeres appears to be conserved in most eukaryotes. Cdc13, the single stranded telomere binding protein of *S. cerevisiae*,

also binds to the G-overhang with an OB fold [75]. Cdc13 functions to regulate both telomerase recruitment and end protection. The protective functions of Cdc13 were highlighted by the original identification of *cdc13-1* as a mutant that arrested in G2 with long, single-stranded DNA at telomere at restrictive temperatures in a Rad9 dependent fashion [76]. Cdc13 recruits both Stn1 and Ten1 to prevent the recognition of the telomere as DNA damage and its subsequent resection by 5'-3' exonucleases. Overexpression of Stn1 or Ten1 or the tethering of Stn1 to telomeres with the Cdc13 DNA binding domain can rescue the defects of the *cdc13-1* mutant [77]. Stn1 and Ten1 also play a role in telomere length homeostasis, as mutations in either of the proteins results in telomere elongation. Cdc13 is likely to coordinate the actions of telomerase and lagging strand DNA synthesis because mutations in Stn1 and Ten1 result in defects in C strand synthesis and further Cdc13 interacts directly with DNA polymerase α [78]. In addition to its role in end protection, Cdc13 also has a role in telomere length maintenance via the recruitment of Est1. This function of Cdc13 was uncovered in a senescence screen through the isolation of the *cdc13-2^{est}* mutation. The *cdc13-2* mutant is defective in its ability to interact with Est1 but can be rescued by the fusion of Est2 to telomeres with the Cdc13 DBD or by a compensatory charge swap mutation in Est1 (*est1-60*) [49]. Although the details of how Cdc13 coordinates the actions of so many different protein complexes is not yet clear, it is apparent that this single stranded binding protein in *S. cerevisiae* plays a crucial role in both end protection and length regulation.

Pot1 – a conserved single stranded telomere binding protein

Using the OB fold of TEBPa, an ortholog of this protein, Pot1, was found in *S. pombe*. Pot1 binds single-stranded telomeric DNA *in vitro* with very high specificity. Deletion of Pot1 in fission yeast results in the rapid loss of both telomeric and subtelomeric sequences. *Pot1-* survivors possess telomere fusions and are only viable when the three chromosomes become circularized [79]. Like TEBPa, Pot1 possesses an OB fold that is sufficient for its specific interaction with ss telomeric DNA [80]. It is

possible that the other OB folds of scPot1 mediate interactions with other proteins. In addition, any role for scPot1 in telomerase recruitment and telomere length regulation remains an interesting question.

Found based on homology in the amino terminal OB fold of spPot1, the human homolog of Pot1 binds to single-stranded G-rich DNA and regulates telomere length. Human Pot1 (hPot1) binds with extremely high specificity to the single-stranded nonamer 5'-TAGGGTTAG-3' [81]. Human Pot1 localizes to telomeres [82]. Surprisingly, a mutant allele of hPot1 that lacks its N-terminal OB fold (Pot1 Δ OB) and no longer binds DNA still localizes to telomeres. The DNA binding-independent recruitment of Pot1 to telomeres is mediated by an interaction between hPot1 and the Pot1 Interacting Protein 1 (PIP1) [83, 84]. Although PIP1 does not directly bind to telomeric DNA, it is indirectly recruited to telomeres by duplex telomeric repeat binding proteins. Once targeted to the telomere, hPot1 negatively regulates telomere length. This has been demonstrated by two complementary approaches. First, in fibrosarcoma cells, the expression of hPot1 Δ OB results in a loss of endogenous hPot1. The hPot1 Δ OB allele results in rapid telomere elongation presumably because it can no longer inhibit telomerase mediated elongation due to the loss of its ability to bind single-stranded DNA [85]. Second, reducing levels of hPot1 through stable RNA interference also results in telomere elongation [84]. In some settings, it seems that hPot1 may promote modest telomere elongation although these findings need to be further substantiated [86, 87]. Thus, it is possible that hPot1 may also have a role in telomerase recruitment and activation, so, like Cdc13, hPot1 would have both negative and positive regulatory functions on the action of telomerase. However, there is currently no evidence that hPot1 is associated with telomerase activity (Loayza and de Lange, unpublished). Furthermore, the addition of purified hPot1 inhibits the extension of primers by telomerase *in vitro* (Lingner, unpublished data). More studies will be necessary to dissect the relationship

between hPot1 and its regulation of telomerase. More studies are also needed to address whether hPot1 has a role in telomere capping like Cdc13 or spPot1.

With the exception of ciliated protozoans, single-stranded telomeric DNA constitutes only a very small fraction of the DNA present at telomeres. For example, *S. cerevisiae* only has long G-overhangs in S-phase but possesses double stranded telomeric repeats of ~350 bp throughout the cell cycle [88, 89]. The G overhangs of human telomeres are longer (~150 nt); however, they still constitute only a small fraction of the total telomeric DNA which ranges from ~2-30 kb in most cells. Not surprisingly, these ds telomeric repeats recruit many different binding proteins with essential telomere functions.

Rap1 – the double-stranded telomeric binding protein of *S. cerevisiae*

The ds telomeric binding protein of *S. cerevisiae*, Rap1p, affects both telomere length and telomere position effect (TPE). Two Myb DNA binding domains in the ~120 kDa protein mediate Rap1p's localization to telomeres through a degenerate recognition sequence present in yeast telomeres. Rap1p also binds to numerous chromosome internal sites where it can mediate either transcription at various upstream activating sites or silencing at the *HML* and *HMR* mating loci. Because of these dual roles, it was originally deemed a Repressor/activator protein [90].

In addition to its roles at chromosome internal loci, Rap1 also plays an essential role in the establishment of silenced chromatin at telomeres. Genes placed near telomere in *S. cerevisiae* are transcriptionally silenced, a process known as telomere position effect (TPE). Rap1 establishes silencing at telomeres (and silent mating loci) by interacting with the silent information regulators, Sir3 and Sir4, with its carboxy terminus [91-94]. Deletion of Sir3/4 results in the complete loss of telomere position effect (TPE) [95].

The overexpression of Rap1 results in telomere elongation while temperature-sensitive Rap1 mutants result in telomere shortening when grown at semipermissive temperatures [96]. Rap1 regulates telomere length by recruiting Rif1 and 2 to telomeres.

Rif1 and 2 are negative regulators of telomere length as their deletion results in dramatic telomere elongation [97, 98]. The mechanism through which Rif1/2 inhibit telomere elongation is not completely clear but the proteins may limit the accessibility of telomeric chromatin to telomerase [36].

As Rap1 was the first ds telomere repeat binding proteins known in any organism, telomere length regulation by Rap1 has been established as a paradigm for the negative regulation of telomerase in *cis* by binding proteins. This model is often described as the “protein-counting” model of telomere length homeostasis. Simply put, longer telomeres recruit more negative regulators of telomerase, like Rap1 and its associated factors Rif1/2. As telomeres shorten, binding sites for the negative regulators are lost, and telomerase can once again lengthen the telomere [99].

TTAGGG Repeat Binding Factors

The long ds repeat arrays of vertebrate telomeres recruit two distinct binding factors called TTAGGG Repeat binding Factors, TRF1 and TRF2. The proteins share extensive homology in their C-terminal Myb DNA binding domain and throughout the protein’s central helices, the TRF homology (TRFH) domain [100]. Based on specific interactions in the TRFH domain, TRF1 and 2 form homodimers, but not heterodimers, to telomeric DNA through a Myb-type DNA binding domain at their C-termini. TRF homodimers bind two 5’-YTAGGGTTR-3’ half-sites with spatial and orientational flexibility [101]. The spatial flexibility of DNA binding by the TRF molecules has been shown to promote the bending and pairing of telomeric substrates *in vitro* [102]. Although TRF1 and 2 do share extensive sequence and structural similarities through the TRFH and Myb DNA binding domains, the proteins differ extensively in their amino termini and recruit different proteins to the telomeres (Fig. 1-2) [100].

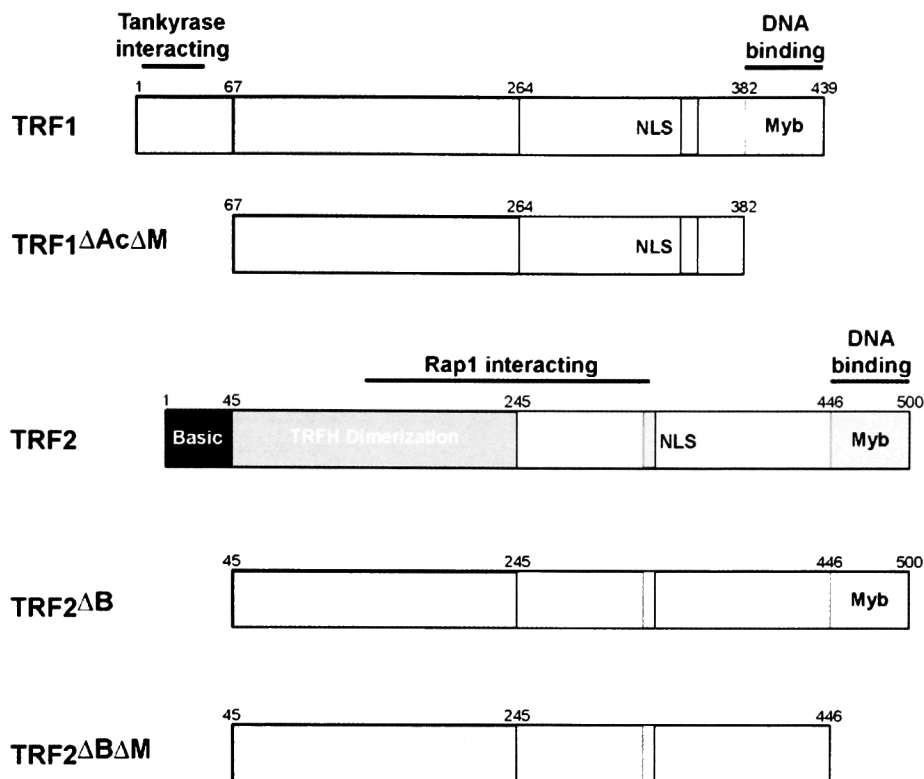


Figure 1-3. Schematic of human TTAGGG repeat binding factors, TRF1 and TRF2.

TRF1 and TRF2 share similarity through most of the molecule except for the amino-terminus that is acidic in TRF1 and basic in TRF2. TRF1 Δ Ac Δ M, TRF2 Δ B, and TRF2 Δ B Δ M are mutant alleles of each of the proteins that have been used to study the roles of TRF1 and TRF2 in capping and length regulation.

TRF1 is a negative regulator of telomere length

Studies of TRF1 have firmly established its role as a negative regulator of telomere length. The overexpression of TRF1 using an inducible gene expression system results in telomere shortening without affecting telomerase expression or activity [103]. In addition, in telomerase positive cells, the expression of a lacI-TRF1 fusion protein results in a shortening of telomeres tagged with LacO arrays confirming that the negative length regulation happened in *cis* [104]. If TRF1 homeostatically regulates telomere length in an analogous fashion to scRap1's 'protein counting model', then disruption of TRF1 activity should result in telomere elongation. An allele of TRF1 that lacks the Myb DNA binding domain and the acidic N terminus functions as a dominant negative allele of the protein by impairing its ability to bind DNA. The partial inhibition of TRF1

through the expression of the dominant negative allele results in telomere elongation. Furthermore, the stable depletion of TRF1 by RNA interference (shRNA) results in telomere elongation (van Overbeek and de Lange, unpublished). In primary cells that do not express appreciable amounts of telomerase, TRF1 does not affect the shortening rate of the telomeres and thus indicates that TRF1's effects on telomere length are telomerase-dependent. How TRF1 inhibits telomerase is not clear, but the recruitment of hPot1 to single stranded telomeric DNA is likely to play a role in the process. In addition to hPot1, TRF1 recruits a number of other binding partners that modulate its length regulatory functions.

Tankyrase, Tin2, and PinX1 – TRF1 binding partners

In the acidic amino-terminus of hTRF1, a conserved motif (RXXPDG) mediates TRF1's interaction with tankyrase 1 and 2 [105]. Curiously, the interaction between tankyrase and TRF1 does not appear to be conserved in murine TRF1, which lacks this conserved tankyrase binding motif. The tankyrases are poly(ADP-ribose) polymerases (PARPs) that oligomerize and can ADP ribosylate both TRF1 and itself [106-108]. ADP-ribosylation of TRF1 interferes with TRF1's ability to bind telomeric DNA *in vitro* [106, 109]. The overexpression of a nuclear targeted tankyrase 1 or 2 results in a partial removal of TRF1 from telomeres *in vivo* [85]. Consistent with other mechanisms of TRF1 inhibition, the partial removal of TRF1 by tankyrase 1 results in telomere elongation. Importantly, the tankyrase mediated telomere elongation is dependent on an active PARP domain [110].

The ADP-ribosylation of TRF1 by tankyrases is inhibited by Tin2, a small protein that interacts with TRF1. The expression of an allele of Tin2 that lacks its N terminus (Tin2-13) but still interacts with TRF1 results in rapid telomere elongation [111]. *In vitro*, Tin2 forms a stable trimeric complex with both TRF1 and tankyrase and further protects TRF1 from ADP ribosylation. Consistent with its telomere elongation phenotype, Tin2-13 does not protect TRF1 from ADP-ribosylation *in vitro*. Furthermore,

the inhibition of Tin2 through RNA interference results in a reduction of TRF1 at telomeres detectable by IF; this loss of TRF1 from telomeres can itself be rescued by the inhibition of tankyrase with 3AB, a PARP inhibitor, or a dominant negative allele of tankyrase. Finally, the inhibition of Tin2 also results in telomere elongation as would be expected for a factor that promotes the stabilization of TRF1 on telomeres [112]. Collectively, these results demonstrate that Tin2 is a negative regulator of telomere length and that Tin2 exerts at least part of its regulatory effects through the stabilization of TRF1 on telomeres.

Another member of the TRF1 complex that may play a role in length regulation is PinX1. Like tankyrase and Tin2, PinX1 was found to interact with TRF1 in a yeast two-hybrid screen. The overexpression of PinX1 or a truncated allele of PinX1 shortens telomeres and can inhibit telomerase activity *in vitro*. However, the effects of PinX1 on telomerase are complicated by its additional role in the processing of rRNAs and snoRNAs [113]. Curiously, the function of PinX1 in inhibiting rRNA maturation and potentially telomerase RNA maturation may be conserved in *S. cerevisiae* [114]. More studies will be necessary to determine how PinX1 inhibits telomerase and whether how this activity might be integrated with other members of the TRF1 complex.

Tankyrase, and possibly other members of the TRF1 complex, have important functions outside of telomere length maintenance. The transient inhibition of tankyrase by RNA interference results in a mitotic arrest with an apparent defect in the separation of telomeres in metaphase [115]. Although tankyrase's role in sister telomere cohesion is dependent on its PARP activity, there is no evidence to suggest that it is necessarily related to the TRF1 complex. Furthermore, although it can be localized to telomeres if expressed with TRF1, most of the tankyrase in the cell localizes to the Golgi complex of interphase cells and mitotic spindle in dividing cells. Direct interactions with IRAP, a component of GLUT4 vesicles, and NUMA, a component of the spindle, suggest that tankyrase may have a role in regulating these two other organelles [105].

Roles of TRF2 in telomere length maintenance

TRF2, the other duplex repeat binding protein, has also been shown to have a role in the regulation of telomere length. Similar to TRF1, the overexpression of TRF2 through an inducible expression system results in telomere shortening in telomerase positive cells [116]. In contrast to TRF1, however, the expression of TRF2 also increases the rate of telomere shortening in primary cells suggesting that it promotes the active degradation of telomeres [11]. This finding was confirmed by the targeting of a lacI-TRF2 fusion protein to LacO-marked telomeres. Targeted telomeres shortened in the presence of telomerase activity but shortened even faster when telomerase was inhibited suggesting that targeted telomeres were being actively degraded [117]. Although it is likely that TRF2 is involved in regulating the rate of telomere attrition, the possible nucleases and details of the process are unknown.

TRF2 binding proteins regulate telomere length

One multi-subunit nuclease with which TRF2 is known to interact is the Mre11 complex [118]. In human cells, the Mre11 complex, which includes Mre11, Rad50, and Nbs1, has essential functions in DNA damage signaling and maintaining genomic stability [119]. The Mre11 complex may also be involved in telomere length maintenance. Fibroblasts derived from patients that have hypomorphic alleles of Nbs1 have short telomeres [120]. Nbs1 associates with TRF2 in S phase suggesting a possible role in telomere replication. A better understanding of the precise contributions of the Mre11 complex to telomere length has been complicated by the essential, non-telomeric functions of the complex.

In addition to the Mre11 complex, TRF2 also recruits hRap1 to telomeres [121]. hRap1 is a small protein with homology to Rap1 of *S. cerevisiae* in the N-terminal BRCT domain, a Myb domain, and the C-terminal acidic (RCT) domain. Rap1 of *S. cerevisiae* possesses a transcription activation domain and a second Myb domain that is lacking in vertebrates. Despite the presence of a Myb domain, hRap1 does not bind directly to

telomeric DNA. Instead, it localizes to telomeres by interacting with TRF2 through its RCT domain. Inducible overexpression of hRap1 results in telomere elongation [121]. In addition, the overexpression of many deletion mutants of hRap1 lacking various combinations of the BRCT, Myb, and RCT domains all resulted in telomere elongation. In addition to elongating telomeres, the overexpression of hRap1 Δ BRCT promotes a more homogeneous length distribution when compared to alleles that possess the BRCT domain [122]. hRap1 also possessed a coiled region situated between its Myb domain and RCT domain. A deletion of a small linker region between the Myb and Coil domains does not appear to elongate telomeres [123]. The overexpression of hRap1 alleles, even ones that still possess the TRF2 interaction domain, result in a large amounts of hRap1 that is not localized to telomeres and accumulates in the nucleoplasm where it might titrate other proteins away from telomeres. One way to explain the results obtained with Rap1 mutants is that hRap1 recruits a negative regulator of telomere elongation to telomeres. More work will be necessary to identify this putative length regulator and to understand its function in regulating telomere length and heterogeneity.

TRF2 protects telomeres from uncapping and fusion

The expression of a dominant negative allele of TRF2 lacking both its C-terminal Myb DNA binding domain and its basic N-terminus (TRF2 Δ B Δ M) effectively removes endogenous TRF2 from telomeres [85, 124]. When TRF2 is depleted from telomeres, they become recognized and processed as sites of DNA double stranded breaks. Thus, TRF2 maintains telomeres in a “capped” structure. The depletion of TRF2 by RNA interference and its conditional deletion in mouse fibroblasts have all confirmed the essential role of TRF2 in protecting telomeres [125] (Celli, unpublished results). After the depletions of TRF2, many telomeres behave as sites of DNA damage and recruit DNA damage response proteins including 53BP1 and g-H2AX. The uncapped telomeres can be visualized cytologically as structures called Telomere Dysfunction Induced Foci (TIFs) [125-127]. One very important transducer of the DNA damage signal from

uncapped telomeres is the ATM kinase. In its absence, the formation of TIFs is less efficient. In addition, ATM is known to be a major kinase responsible for the activation of p53. After the activation of a DNA damage response by uncapped telomeres, the induction of apoptosis in primary lymphocytes and mouse fibroblasts is dependent on both ATM and p53 [128]. In other cell types, including primary fibroblasts, the expression of TRF2 Δ B Δ M induces a cell cycle arrest that has all of the hallmarks of replicative senescence [129]. Telomeres uncapped by TRF2 Δ B Δ M signal through both Rb and p53 signaling pathways to induce senescence. In addition, ATM-deficient (A-T) primary fibroblasts still senesce in response to the inhibition of TRF2 suggesting that other PIKK kinases like ATR or DNA-PK can also transmit the telomere damage signal to induce senescence [125].

In addition to the activation of DNA damage checkpoints, uncapped telomeres are recognized as double-strand breaks and processed by NHEJ. This processing of telomeres creates chromosome end-to-end fusions with the preservation of telomeric DNA [124]. Prior to their ligation by LigaseIV, the overhangs must be processed by the ERCC1/XPF nuclease [130, 131]. The frequency and class of telomere end-to-end fusions can be monitored by Fluorescent In Situ Hybridization (FISH) on spreads of metaphase chromosomes. The expression of the dominant negative TRF2 Δ B Δ M results in at least a 10-fold increase in the number of telomere fusions compared to control cells. In mouse cells conditionally deficient for TRF2, virtually all chromosome ends undergo end-to-end fusions in the absence of TRF2 (Celli and de Lange, unpublished). Fusions that occur in the G1 phase of the cell cycle result in chromosome type fusions in which both arms of different chromosomes are fused [130]. Interestingly, when fusions occur in G2, telomere fusions between sister chromatids generated by leading strand replication seem to predominate [132]. The preferential fusion of leading strand sister telomeres is consistent with the observation that often only one of a pair of telomere signals, presumably representing replicated sister telomeres, is associated with DNA damage

response factors [125]. TRF2 inhibition may be a good model for the telomere induced replicative senescence, as it has been reported that TRF2 is often undetectable from shortened, uncapped telomeres [133].

Telomere protection by TRF2: t-loop formation and ATM suppression

TRF2 may prevent the recognition and processing of telomeres as DNA breaks by NHEJ through the formation of a unique DNA architecture at chromosome ends. By EM, it has been observed that the 3' overhang of telomeres invade the proximal ds telomeric sequence and displace the corresponding G-strand yielding a short stretch of single stranded G-strand DNA at the base of the loop (Fig. 1-4A) [134]. The resultant structure, called a t-loop, has been visualized by EM in a variety of organisms and appears to be an evolutionarily conserved feature of most eukaryotic telomeres; it can be found in mammals [134], plants [135], trypanosomes [136], ciliates [137], and chickens [138]. The size of the t-loop varies greatly in different eukaryotes but can be as small as a few hundred base pairs or may also encompass an entire mouse telomere (>40 kb). In mammalian cells, TRF2 may have an important role in t-loop formation, as it can catalyze the formation of t-loops on model substrates *in vitro* as demonstrated by EM [139]. By hiding the 3' overhang and the DNA end within the adjacent ds DNA, the t-loop appears to provide a structural solution to the capping problem posed by telomeres. Although purified TRF2 has the ability to form t-loops *in vitro*, several TRF2 binding partners like the Mre11 complex and RecQ helicases have also been proposed to facilitate the formation of t-loops [140, 141].

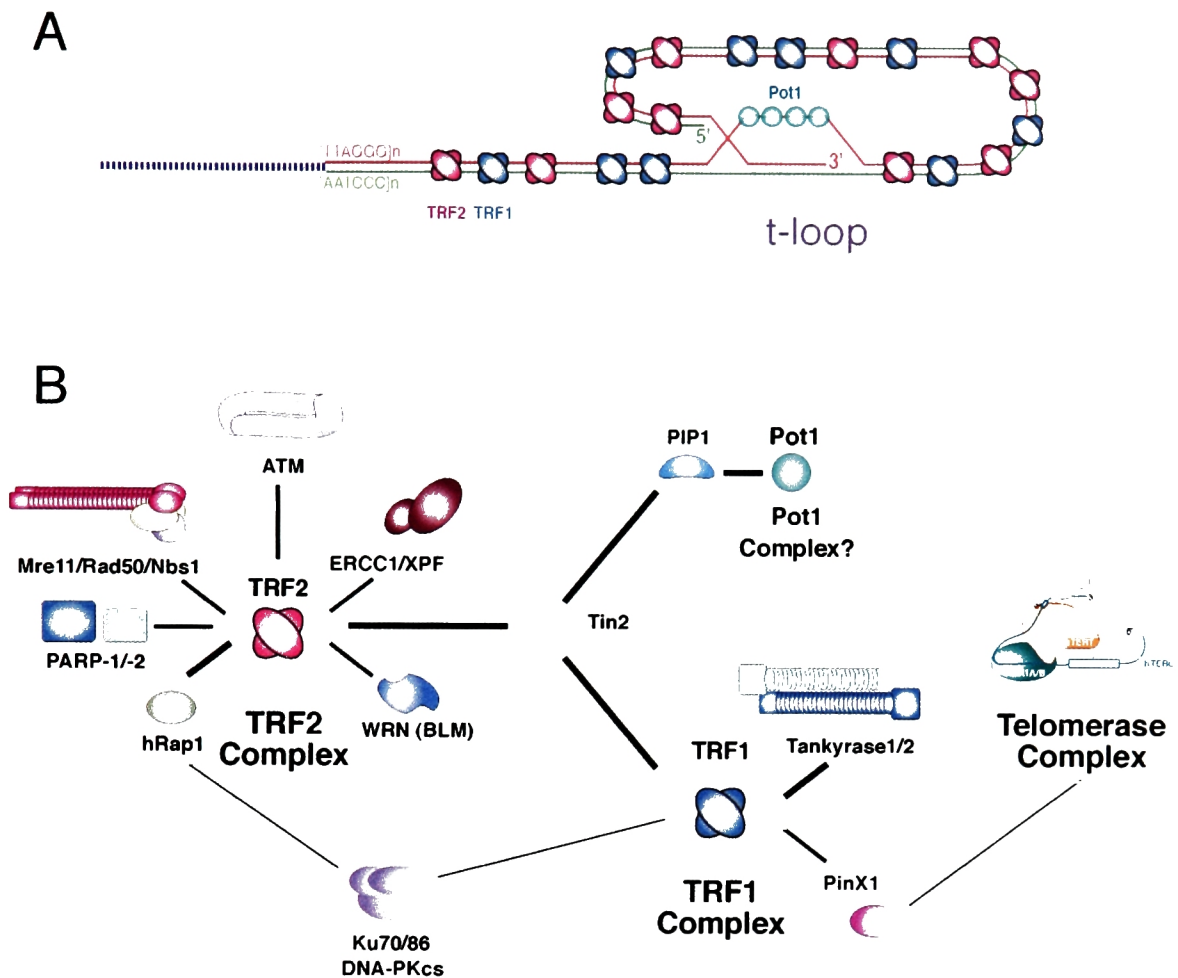


Figure 1-4. Telomere structure and proteins in mammals.

(A) Proposed structure of the t-loop based on EM [134]. Shown bound to the t-loop are proteins with specific binding activity for telomeric DNA *in vitro*. The precise length of the displaced single stranded DNA proposed to be bound by hPot1 is not known, but it is estimated to be between 50-100 nt. The loop of ds telomeric DNA can encompass the entire telomere. (B) Human telomeric proteins. Lines between proteins represent reported direct interactions. Thick lines connect proteins which have been identified as a part of a large telomeric protein complex [142].

In addition to sequestering chromosome ends in t-loops, an additional function of TRF2 that may help to protect telomeres from being recognized as DNA damage is the direct suppression of the ATM kinase. Long telomeres, like those found in primary cells, are likely to bear more than 1000 TRF2 molecules each [143]. The overexpression of TRF2 results in a global suppression of ATM activation as monitored by several factors,

including the phosphorylation and accumulation of p53. In addition, TRF2 can bind directly to ATM and inhibit its kinase activity [144].

Because the inhibition of TRF2 may also result in a concomitant loss of its binding partners, like hRap1 and the Mre11 complex, from telomeres, it cannot be excluded that TRF2 binding partners have important roles in capping telomeres. It has been difficult to address the possible contributions of either hRap1 or the Mre11 complex to telomere capping as both are essential for cellular viability. Because the Mre11 complex has nuclease activity and has been reported to modulate recombination, it is possible that the complex participates in the formation of t-loops.

In addition to the Mre11 complex nuclease, the ERCC1/XPF endonuclease complex is normally recruited to telomeres by TRF2. ERCC1/XPF is a structure specific endonuclease that participates in nucleotide excision repair and in the processing of HR intermediates; it cleaves on the 5' side of bubble structures containing damaged DNA and can cleave off the 3' overhang of flapped structures [145, 146]. As described previously, when telomeres are uncapped by TRF2 Δ BAM, ERCC1/XPF has a role in cleaving the 3' overhang in preparation for telomere fusions [131]. However, ERCC1/XPF also functions in normal telomere metabolism to suppress the formation of telomeric double-minutes (TDM), which may arise from inappropriate recombination events between telomeres and interstitial telomeric sites [131].

Another TRF2 binding partner that may contribute to telomere protection is the nuclear poly(ADP-ribose) polymerases, PARP-1 and -2. TRF2 interacts with and is modified by PARP-2 and may interact with PARP-1 [123, 147, 148]. PARP-1 and -2 promote base excision repair (BER) by binding and modifying many proteins in the BER pathway including XRCC1, DNA polymerase, and DNA ligase III [149, 150]. Poly ADP-ribosylation of TRF2 interferes with its ability to bind DNA, but it is unclear how this affects TRF2's roles in telomere protection. Mice that are deficient in PARP-2 possess marked genomic instability and also have some evidence of telomere dysfunction

[147, 151] although the latter defect is a matter of some debate [152, 153]. Because of the important roles of PARP-1 and -2 in other types of DNA repair, it is difficult to dissect how much of the telomere dysfunction and genomic instability is caused by TRF2 *per se*. Ultimately, for hRap1, the Mre11 complex, PARP-1 and -2, and other potential TRF2 binding partners, finding mutants that are telomere-loss-of-function mutants will be necessary to assess their specific roles in telomere protection.

TRF orthologs in yeast

S. cerevisiae and other budding yeasts may have a distant ortholog of the vertebrate TRFs in Tbf1p. Although this protein will bind to human telomeric repeats introduced into yeast by a mutant telomerase [154], it does not bind the degenerate TG_{1,3} repeat of normal *S. cerevisiae* telomeres (Table 1-1). This rather dramatic shift in telomere binding protein architecture may have occurred secondary to a mutation in the telomerase in the budding yeast [121]. Consistent with this hypothesis, the telomeric sequences of budding yeast are heterogenous, divergent, and drastically different in sequence compared with most other eukaryotes. It is proposed that, despite the proposed alteration of telomeric sequences in budding yeast, scRap1 and Cdc13 were still able to bind to telomeric repeats and mediate chromosome end protection on the now altered telomeres.

In contrast to the budding yeasts, *S. pombe* possesses a TRF ortholog, Taz1 [155]. Like the TRFs, Taz1 dimerizes and binds DNA using a Myb domain [156]. Both the telomere capping and length maintenance functions of the vertebrate TRF molecules appear to be conserved in Taz1. In the absence of Taz1, telomeres show dramatic elongation consistent with a role for the protein in the negative length regulation [155]. In addition, G1-arrested *taz1* deficient cells undergo Ku and ligase IV dependent end fusions implicating the protein in end protection [157]. Similar to TRF2, Taz1 recruits the *S. pombe* ortholog of Rap1 to telomeres; spRap1 deleted cells show telomere elongation and loss of telomere position effect [158, 159]. Furthermore, Taz1 also

recruits the ortholog of Rif1 to telomeres in *S. pombe*. Although milder than the deficits exhibited by scRap1, spRif1 also has a role in negatively regulating telomere length [158]. In addition to the expected defects in telomere length regulation and capping, Taz1, spRap1, and spRif1 mutants all have severe defects in meiotic segregation implicating telomeres in the process of meiotic clustering [159-161].

Interactions between telomere binding proteins

Currently, it appears that vertebrate cells possess more telomere specific binding proteins than either *S. cerevisiae* or *S. pombe*. TRF1, TRF2, and hPot1 all have the ability to bind to DNA *in vitro*. However, interactions between each of these telomere binding proteins and their binding proteins appears to play an important role in the recruitment of the complexes to telomeres *in vivo*, especially with regards to the TRF2 and Pot1 complexes. Although Tin2 was first identified as a binding partner of TRF1, Tin2 also binds directly to TRF2 with its N terminus [142, 162]. Importantly, *in vitro*, Tin2 can interact simultaneously with both TRF1 and TRF2 [142]. The Tin2-13 allele, which still binds TRF1 but no longer protects TRF1 from ADP-ribosylation, is also defective in its interaction with TRF2. Thus, in addition to stabilizing TRF1 on telomeres, Tin2 may also regulate telomere length via the recruitment of the TRF2 complex. The localization of TRF1 and Tin2 to telomeres is especially important for the recruitment of TRF2 and its associated proteins. After the depletion of either TRF1 or Tin2 by siRNA, TRF2 and hRap1 are lost from telomeres by IF. This explains the observation that mouse embryonic stem (ES) cells deficient for TRF1 show a defect in the telomeric localization of both Tin2 and TRF2 by both IF and ChIP. Consistent with the loss of TRF2, ES cells deficient for TRF1 also showed telomere fusions indicative of defects in telomere protection [163]. Furthermore, lentiviral expression of Tin2 mutants that have lost their ability to bind either TRF1 or TRF2 results in a displacement of TRF2 from telomeres and the induction of TIFs [162]. Though TRF1 and TRF2 have similar DNA binding properties, the depletion of TRF2 by siRNA or the expression of the

dominant negative TRF2 does not result in an obvious displacement of TRF1 from telomeres. In general, the localization of TRF2 to telomeres may be more tenuous than TRF1 because of TRF2's direct interaction with many abundant non-telomeric DNA binding proteins including the Mre11 complex, ERCC1/XPF, and ATM. These interactions could titrate TRF2 to chromatin at non-telomeric sites.

The recruitment of hPot1 to telomeres is also reinforced by its interactions with other telomere binding proteins. By binding simultaneously to hPot1 and Tin2, PIP1 recruits and stabilizes hPot1 on telomeres [83, 84]. Tin2 can bind simultaneously to PIP1 and TRF1 *in vitro*. By gel filtration, complexes containing TRF2, hRap1, Tin2, and hPot1 but not TRF1 have been identified suggesting that Tin2 can also interact simultaneously with PIP1 and TRF2 [142]. However, it is not known whether Tin2 can interact simultaneously with all three of its binding partners—TRF1, TRF2, and PIP1. Both TRF1 and TRF2 appear to contribute to the recruitment of hPot1 as interfering with the telomeric localization of TRF1 or TRF2 results in a decreased amount of hPot1 on telomeres by ChIP [85]. The extensive interactions between TRF1, TRF2, and hPot1 complicate the analysis of individual proteins in their specific telomere functions as perturbing one protein will likely affect the status of the entire telomere complex. It will be an interesting problem for the future to dissect how these proteins are coordinated in mediating telomere length regulation and protection.

Table 1-2. DNA damage proteins in telomere maintenance.

Each row represents a conserved DNA damage response protein that has been implicated in telomere metabolism in at least one species. Putative homologs are in parentheses. Proteins that have been implicated in telomere length regulation or capping are in bold.

Mammals	<i>S. cerevisiae</i>	<i>S. pombe</i>	<i>C. elegans</i>
ATR	Mec1	Rad3	(Atl1)
ATM	Tel1	Tel1	(Atl1)
DNA-PK	--	--	--
Mre11/Rad50/Nbs1	Mre11/Rad50/Xrs2	Rad32/Rad50/Nbs1	Mre11/--/--
ERCC1/XPF	Rad10/Rad1	Swi10(Rad23)/Rad16	--/xpf
Ku70/86	Ku70/80	Ku70/80	--
RAD9	Ddc1	Rad9	Rad9
RAD1	Rad17	Rad1	Mrt-2
HUS1	Mec3	Hus1	Hus1
RPA70/RPA32	Rfa1/Rfa2	Rad11	--
Tel2 (CLK-2)	Tel2	spTel2	Rad-5 / Clk-2
PARP-1/2	--	--	PME-1/2/5
BLM/WRN	Sgs1	Rqh1	Him-6
Rad54	Rad54	Rhp54	--
Rad51D	(Rad55, Rad57)	(Rhp55, Rhp57)	--
Rif1	Rif1/2	Rif1	--

DNA Damage Proteins and Telomeres

PIKK kinases in telomere maintenance—ATM, ATR, and DNA-PKcs

Although telomeres resemble double strand breaks (DSBs), telomere binding proteins protect them from being recognized as such. In addition to specialized telomere binding proteins, the general DNA damage response pathways of all eukaryotes may have also adapted to function at telomeres in ways that differ from their function in the response to global DNA damage. Central to the DNA damage response of most eukaryotes is the PIKK (phosphatidyl inositol 3-kinase-like kinase) family. As previously described, in human cells, the activation of ATM and possibly ATR and/or DNA-PKcs at uncapped telomeres results in the generation of a DNA damage signal,

which if unrepaired, would likely result in senescence or apoptosis. The recognition of “damaged” telomeres may be related to the positive roles of ATM and ATR in telomere maintenance. The loss of ATM (Tel1p) or ATR (Mec1/Rad3) in *S. cerevisiae* or *S. pombe* results in telomere shortening [164-166]. Even more strikingly, the concomitant loss of both Tel1 (ATM) and Mec1 (ATR) in *S. cerevisiae* results in progressive telomere shortening ultimately causing senescence and the outgrowth of telomerase independent survivors [166]. Similarly, the combined deletion of *S. pombe* Tel1 and Rad3 results in the loss of telomeric sequences and the survival of yeast with circularized chromosomes without telomeric sequences [167]. Recently, it has been shown that Tel1p and Mec1p associate with telomeres in *S. cerevisiae*, Mec1p during S phase, and Tel1p during other phases of the cell cycle [168]. Human fibroblasts deficient for ATM have been reported to have defects in telomere length and maintenance [169, 170].

In addition to telomere shortening, the loss or overexpression of Mec1, but not Tel1, in *S. cerevisiae* results in defects in telomere silencing [171]. In *Drosophila*, the homolog of ATM, rather than ATR, is involved in the establishment of a protective chromatin structure at telomeres. In the absence of ATM, HP1 is no longer localized to telomeres and massive end-to-end fusions result [172-174]. The fusions happen despite the presence of retrotransposon type telomere repeat elements being present at the ends.

The PIKK kinases exert their effects on telomere maintenance through a variety of pathways. In *S. cerevisiae*, Tel1p affects telomere elongation in the same pathway as Rif1 and Rif2, the scRap1-recruited, negative regulators of telomere elongation. Thus, in the *tell*-deleted cells, the deletion of *rif1/2* does not result in elongation [175]. Like *S. cerevisiae*, the human homolog of Rif1 is in the ATM (Tel1) signaling pathway. Curiously, however, hRif1 does not localize to telomeres, but rather is involved in the response to DNA damage. hRif1 localizes to DNA damage foci in an ATM, 53BP1 dependent manner and is also required for the intra-S phase DNA damage checkpoint (Silverman and de Lange, in press).

Tel1 or Mec1 may also mediate its effects on telomere elongation through an effect on replication protein A (RPA), which includes Rfa1p/Rfa2p in yeast and RPA70/RPA32 in humans. A number of *rfa* mutants including *rfa1-D228Y*, *rfa2-210*, *rfa2-55*, *rfa2Δ40* have shortened telomeres [176, 177]. In *rfaΔ40* mutants, the binding of Est1p to telomeric DNA is impaired while the binding of Cdc13, Est2, and Ku80 is unimpaired. Although RPA has been shown to interact with Mec1 (ATR) to activate DNA damage checkpoints, with regards to the telomere, *rfa2-55* and *rfa2-55* appear to be in the same pathway as Tel1. Whether RPA plays in telomere elongation in human cells is not known.

A recent study in *S. pombe* has demonstrated that Rad3 (ATR) may exert some of its telomere length regulatory effects via components of the Rad9, Rad1, and Hus1 complex. Fission yeast mutant for the 9-1-1 complex have short telomeres that are epistatic with Rad3, but not Tel1. In addition, the components of the 9-1-1 complex were found to be associated with telomeric DNA by ChIP [178]. Together with Rad9 and Hus1, Rad1 forms a trimeric, PCNA-like complex, called the 9-1-1 complex, which is thought to be loaded by Rad17 onto damaged DNA substrates to act as a sensor in a DNA damage signalling pathway. A role for the 9-1-1 complex in telomere maintenance was first identified noted in a *C. elegans* screen. Ahmed and colleagues found that worms mutated for *ceRad1*, called MRT-2, experienced progressive telomere shortening in their germline which ultimately resulted in infertility and senescence of the population after several generations (i.e., the worms possessed a mortal germline) [179]. A role for the 9-1-1 complex in *C. elegans* telomere maintenance was confirmed by a Hus1 mutant of *C. elegans*, which also shows progressive telomere shortening and mortality of the germline [180]. It is not clear that mutations in the *S. cerevisiae* homologs of the Rad9, Rad1, Hus1 complex (Ddc1, Rad17, Mec3) have defects in telomere maintenance [181-184]. The roles of the human 9-1-1 complex in telomere maintenance have not been explored.

Though diverse in their mechanisms of action, clearly the homologs of ATM and ATR in all organisms have essential roles in telomere maintenance.

Mammalian cells possess a third PIKK kinase, DNA-PKcs, which has also been shown to have a role in telomere maintenance. Different mutations in DNA-PKcs appear to have discordant effects on telomere length. Mice with a severe combined immunodeficiency (scid) mutation in DNA-PKcs have slightly longer telomeres than isogenic controls [185]. In contrast, DNA-PKcs null mice have been reported to have telomeres that are slightly shorter or similar in length to wild-type mice [186-188]. The absence of DNA-PKcs may exacerbate telomere shortening in telomerase deficient mice [189]. DNA-PKcs deficient mouse cells or cells treated with chemical inhibitors of DNA-PKcs both show increased telomere fusions [188, 190-192]. Finally, consistent with its potential function in telomere maintenance, DNA-PKcs associated with telomeric DNA can be detected by immunoprecipitation [193]. In diverse organisms, the PIKK kinases—ATM, ATR, and DNA-PK—have evolved different, but important roles in telomere function; it will be an interesting challenge for the future to understand how telomerase, telomere binding proteins, and PIKK kinases interact to affect telomere maintenance.

NHEJ—the Ku heterodimer in telomere biology

The Ku heterodimer, which consists of two subunits of ~70 and 80 kDa, has a high affinity for DNA ends and has an essential role in DNA repair. In mammals, the Ku heterodimer associates with catalytic subunit to form the DNA dependent protein kinase. Ku has an evolutionarily conserved role in mediating non-homologous end joining together with DNA ligase IV and XRCC4. Because end-to-end fusions are a major threat to telomere integrity, it is somewhat surprising that the Ku heterodimer should play a role in telomere maintenance. However, in most organisms, the Ku heterodimer has special telomeric functions that are distinct from its role in general DNA repair.

Early indications of a role for Ku in telomere biology came from studies in *S. cerevisiae*. The deletion of Ku results in several defects in telomere function including shortened telomeres, an increased amount of single-stranded DNA, and the loss of TPE [194-197]. Ku promotes telomere elongation by a specific interaction with a stem-loop in TLC1 (Fig. 1-2A) [198, 199]. This stem loop is not conserved in other organisms, so this feature seems to have evolved specifically in *S. cerevisiae*. The disruption of either the Ku binding stem loop of TLC1 or the expression of a mutant Ku allele that is specifically defective for TLC1 binding (yKu80-135i) results in short, but stable telomeres [199]. Ku80's specific interaction with TLC explains how the catalytic subunit of telomerase (Est2) is recruited to telomeres in G1 despite the absence of both Cdc13 and Est1 from the telomeric chromatin (Zakian, unpublished). This localization is independent of Cdc13's localization to the single-stranded overhangs at telomeres in S phase [200].

Ku also has essential functions in telomere maintenance that are independent from telomerase recruitment. The deletion of Ku70 or 80 combined with an Est2 deletion is synthetically lethal [196, 201]. Defects in lagging-strand telomere synthesis and/or increased access of telomeres to nucleases, including Exo1, could explain the excess single-stranded DNA in Ku deletion strains and the synthetic lethality caused by the loss of telomerase [201, 202]. Finally, in *S. cerevisiae*, Ku interacts with SIR4 and may stabilize it on telomeric DNA to promote TPE [203]. The Ku heterodimer appears to have similar functions in telomere function in *S. pombe*. Telomeres are shorter but stable after the loss of Ku. Although the combined deletion of *trt* and a Ku subunit is not lethal, it does result in the immediate loss of all telomeric repeats in *S. pombe*. In addition, subtelomeric repeats showed striking rearrangements [204]. Thus, the *S. pombe* Ku protein is important for the protection of telomeres from nucleolytic degradation and recombination.

In mammalian cells, Ku70 and Ku86 associate with telomeric DNA by ChIP [193, 205]. This association with telomeres could be mediated by a direct binding to telomeric

DNA, as Ku has been reported to do *in vitro*, or it could be recruited to telomeres by one of its proposed direct interactions with TRF1, TRF2, or hRap1 [123, 206-208]. Potential functions of the Ku heterodimer in mammalian telomere maintenance have been revealed by genetic studies. Ku is an essential gene in HCT116 colon carcinoma cells [209]. However, in addition to the expected increase in genomic instability, the inactivation of one allele of Ku86 resulted in HCT116 cells with shorter telomeres and increased single stranded G strand overhangs [210]. These findings are corroborated by the reported shortened telomeres in mouse fibroblasts or ES cells that lack either partner of the Ku heterodimer [193]. Although many studies confirm that cells deficient for Ku70 or Ku86 have increased amounts of chromosomal fusions, it is not clear whether the fusions are telomeric or simply a result of increased genomic instability [190, 193, 210, 211]. However, in all studies, the reported frequency of fusion in Ku deficient cells pales in comparison to fusions caused by the inhibition of TRF2. Thus, the Ku heterodimer probably has an accessory role in end protection in comparison to the role of the bona fide telomere binding proteins like TRF2.

The analysis of Ku in other eukaryotes highlights how Ku at telomeres possesses different functions. This could either be due to the interactions with telomere specific binding factor, an evolution of Ku to have particular functions at telomeres, or a combination of both processes. Another example of unique functions for Ku at telomeres come from *Arabidopsis*. *Arabidopsis* telomeres are usually maintained within a very narrow distribution such that each telomere is visible as an individual band. However, the loss of Ku results in a loss of telomere homogeneity and telomere elongation [212]. Despite the unexpected telomere elongation in the absence of Ku70, plants deficient for both *ku70* and *tert* shorten their telomeres much faster than single *tert* deficient plants; this observation is consistent with observations of yeast deficient for both Ku and telomerase [212]. Also consistent with finding from *S. cerevisiae*, plants deficient for Ku have excess single stranded G-rich overhangs regardless of presence of telomerase,

indicating defects in telomeric C-strand synthesis and/or the protection of the C strand from exonucleases [212]. In contrast to other eukaryotes, Ku does not appear to have an important role in telomere maintenance in chicken DT40 cells. The telomere length and G-overhangs of Ku70 deleted DT40 cells were comparable to control cells [213]. Overall, in most eukaryotes, in addition to its general role in NHEJ, the Ku heterodimer functions appears to regulate telomere elongation and to maintain telomere capping by protecting them from nucleolytic activity and recombination.

Roles of Mre11 complex at the telomere

The Mre11 complex appears to have a conserved role in promoting telomere elongation in a number of organisms. The loss of components of the *S. cerevisiae* Mre11, Rad50, Xrs2 complex (MRX) results in shorter but stable telomeres without defects in TPE [214]. This shortening is epistatic with telomere shortening caused by deletion of Tel1 suggesting that the Mre11 complex may function in concert with Tel1p to promote telomerase mediated elongation of telomere ends [196]. Moreover, the deletion of *rad50*, *mre11*, or *xrs2* in a *mec1-21* mutant mimics a *tell1*, *mec1-21* double mutant; both sets result in a senescence phenotype [215]. In fission yeast, the Mre11 complex and Tel1 (ATM) also appear to function in the same pathway of telomere length maintenance that collaborates with Rad3 (ATR) to maintain telomeres [178, 216-219].

Precisely how the MRX complex promotes telomere elongation is unclear. In concert with other nucleases, the MRX complex is required for the generation of the short 12-14 nt overhangs present on *S. cerevisiae* outside of S phase which may then be resected in S phase prior to telomere elongation [89]. The presence of ss G rich DNA is thought to be necessary for Cdc13 binding, which would in turn promote the recruitment of telomerase. Consistent with this hypothesis, *de novo* telomere formation outside of S-phase requires the Mre11 complex [220]. However, even in the absence of the Mre11 complex, the formation of long ss GG-rich overhangs appears to be normal [89]. Alternatively, the MRX complex may be involved in the recruitment of telomerase

activity [221]. As previously mentioned, the mammalian Mre11 complex—Mre11, Rad50, and Nbs1—is recruited to mammalian telomeres by TRF2 [118]. Although the complex has been implicated in telomere length regulation, much remains to be understood about the function of this complex at mammalian telomeres [120]. Finally, in *Drosophila*, Mre11 and Rad50 appear to work in the same pathway as ATM to prevent chromosome fusions [172, 222]. In their absence, HP1 and HOAP are no longer efficiently localized to telomeres and massive end-to-end fusions result [222].

Homologous recombination at the telomere

Compared with NHEJ, homologous recombination (HR) is the more accurate mechanism of DNA repair in eukaryotes. In addition to studies that have implicated the Mre11 complex in telomere functions, other systems have illustrated important relationships between HR and telomeres. The earliest studies on the relationships between HR and telomeres have come in the setting of telomere dysfunction. For example, Telomere Rapid Deletions (TRD) resizes over-elongated budding yeast telomeres to wild-type length in a process that depends on HR. In another setting, it was found that *S. cerevisiae* escape senescence through the activation of survivor pathways that depend on HR for telomere elongation and survival. Similarly, human cells that are immortal, but telomerase-negative may also maintain their telomeres through HR in a mechanism called Alternative Lengthening of Telomeres (ALT). More recently, studies have implicated both Rad54 and Rad51D in telomere length regulation and capping in mammals. Finally, the structure of the t-loop structure is reminiscent of an intramolecular Holliday junction. The relationships between telomeres and HR will be discussed in detail in the introduction of Chapter 3.

Emerging connections between telomeres and the DNA damage pathways

As our understanding of the mechanisms of both DNA damage signalling and telomere maintenance improve, new ways in which the two processes intersect will become apparent. For example, a poorly understood upstream DNA damage repair

protein of *C. elegans*, called Rad-5/Clk-2, may have a role in telomere length regulation. The *S. cerevisiae* homolog of Rad-5/Clk-2 called Tel2p has a definitive role in telomere maintenance. The details of these mutants will be described in detail in the introduction of Chapter 2. Despite the significant differences between the telomere biology of diverse eukaryotes, there are enough parallels to make comparisons very informative for both human telomere function and DNA damage pathways. A more comprehensive understanding of telomere biology in all of these organisms should uncover the possible roles that telomeres play in human aging and disease.

CHAPTER 2:
ANALYSIS OF TEL2 IN HUMAN CELLS

INTRODUCTION

Lessons from altered telomere length in *S. cerevisiae*

Perhaps the best-known mutations that affect yeast telomere length are the Ever shorter telomere, or est mutations [223, 224]. Mutations of this class progressively shorten yeast telomeres until they are too short to be compatible with telomere capping resulting in cell senescence. However, the majority of mutations that affect telomere length in *S. cerevisiae* cause them to lengthen or shorten until a new length equilibrium is established. A survey of the ~4800 viable haploid deletion mutants of *S. cerevisiae* mutants reported ~150 strains with altered telomere length. Deletion strains were designated as having slight (<50 bp), moderate (50-150 bp), or severe (>150 bp) alterations in telomere length. Most of the mutants with "severely" (>150 bp) shorter telomeres were deletions of genes previously known to affect telomere metabolism including Tel1 (ATM), the Mre11 complex, and the Ku heterodimer. However, deletions of many novel genes involved in diverse processes, including DNA metabolism, chromatin modification, and PolIII transcription and ribosome biogenesis, also showed moderate defects in length maintenance. It will be interesting to establish how these new genes, and the pathways in which they function, influence telomere metabolism.

Tel2 was one of the first mutants of *S. cerevisiae* known to affect telomere length [164]. Despite its identification in 1986, still very little is known about the protein and its role in telomere maintenance. The *tel2* mutation causes a significant telomere shortening of ~150 bp, to about about half wild-type length, when yeast are shifted to a non-permissive temperature. When crossed with a wild-type strain, telomeres return to WT lengths indicating that *tel2* is a recessive mutation. *Tel2* was isolated from a collection of

temperature sensitive mutants and has a growth defect at 37°C. Based on this phenotype, the gene encoding wild-type TEL2 was cloned by complementation and characterized [225]. The *tel2* mutation is a missense mutation causing a serine to asparagine mutation at AA 129. In *S. cerevisiae*, TEL2 is essential, and its deletion causes cells to die with multiple surface projections or “blebs.” In addition to shorter telomeres, *tel2* mutant strains are unable to silence telomeric loci as effectively as wild-type yeast. This defect in silencing is limited to telomeres, as mating type loci are still effectively silenced. Importantly, this defect in TPE was not due to shortened telomeres of *per se* mutants, as yeast with telomeres that are even shorter than *tel2* mutants have no noticeable defect in telomere silencing [225]. Dual defects in TPE and length maintenance in *tel2* yeast suggest that the gene plays an important role in the maintenance of chromosome ends. In addition to telomere defects, diploid strains heterozygous for *tel2*Δ had modestly higher (10-20 folds) rates of chromosome loss. The *tel2* S129N mutation did not have elevated rates of chromosome loss when grown at permissive temperatures.

In vitro, Tel2p from *S. cerevisiae* (scTel2p) binds telomeric DNA [225]. Tel2p bound yeast telomeric DNA in a sequence specific manner. Tel2p also has a high affinity for single stranded telomeric DNA and induces the formation of secondary structures, likely to be held together by G-G interactions, in G-rich single stranded telomeric DNA of *S. cerevisiae* [226]. Because the expression of full length scTel2p is toxic to bacteria, the DNA binding studies of Tel2p could only be done with a fusion of the C-terminal two-thirds of the protein with MBP. Despite the biochemical analyses of Tel2p, still very little is known about the essential function of the protein. The sequence of scTel2 did not

possess any domains of known function. However, the gene does appear to be conserved in all eukaryotes, including *Caenorhabditis elegans*.

***Clk-2* and *rad-5*: *C. elegans* mutations in Tel2p**

The *rad-5* worm was found in a screen for UV irradiation hypersensitivity [227]. The *rad-5* mutant is hypersensitive to a variety of DNA damage agents (UV, EMS, and X-rays). Unlike the other *rad* mutants, *rad-5* is lethal at 25°C and is also a general spontaneous mutator. Specifically, in tests for either *unc-58* reversion (31/34 vs. 0/35 plates) or spontaneous levamisole-resistance (4/15 vs. 0/15 plates), *rad-5* animals showed very high rates of spontaneous mutation [227]. Consistent with the spontaneous accumulation of DNA damage, it was found that *rad-5* mutants were synthetically lethal with other DNA damage checkpoint mutants including *hus1* and *mrt-2* (*rad1*) [228]. Furthermore, compared to normal worms, *rad-5* worms possessed a greater number of Hus1:GFP nuclear foci both before and after X-irradiation suggesting an impairment in the ability to repair spontaneous and induced DNA damage [180]. In addition to a potential role in repairing damage, *rad-5* mutants prevented the DNA damaged-induced apoptosis and cell proliferation arrest in the germline [229] suggesting that it may also have a checkpoint function. Unlike *mrt-2/rad1* or *hus1* mutants, *rad-5/clk-2* worms have impaired S-phase DNA damage checkpoints in response to hydroxyurea (HU) [228]. The unique phenotypes of *rad-5* compared to the other *rad* mutants generated great interest in its gene product. Curiously, when the gene for *rad-5* was positionally cloned, it was found to be allelic with a different mutant, *clk-2*, found in a completely different screen [228].

Clk-2 was one of several mutant worms found in a screen for altered biological rhythms [230]. In addition to a ~25% increase in mean lifespan, *clk-2* worms possess slower rhythmic behavior like feeding and egg-laying [231]. The extended lifespan of the *clk-2* worms may be related to their generally slowed development and metabolic activity. Like *rad-5*, *clk-2* is essential; adults that are shifted to non-permissive temperatures cannot produce viable offspring. The *clk-2* mutant possesses similar DNA damage checkpoint defects as *rad-5* and is unique among *clk* mutants for these defects. Curiously, despite its other known function in DNA damage repair, CLK-2::GFP was reported to localize to the cytoplasm of various cell types in *C. elegans*. When the sequence of the gene encoding for *rad-5/clk-2* was analyzed, it was found to be homologous to *TEL2* in yeast [228, 231, 232]. Given its role in regulating DNA damage signaling and lifespan in *C. elegans*, there was considerable interest in determining whether it also affected telomere length. It was exciting to speculate about the possibility that *tel2/rad-5/clk-2* was a conserved regulator of telomere length, DNA damage, and organismal life-span.

Three different groups studied the effects of the mutations on telomere length and reached three different conclusions [228, 231, 232]. The first study concluded that *clk-2* mutants possessed shortened telomeres compared to a wild-type N2 strain [232]. More recent studies suggested that *clk-2* results in telomere elongation [231]. This elongation was rescued by expression of functional CLK-2. However, the most extensive analyses of both *rad-5* and *clk-2* mutant on telomere length concluded that neither mutation has a strong influence on telomere length [228]. In *C. elegans*, there is considerable strain variability in telomere length [233]. In addition, the telomere length of wild-type worms

fluctuates over time (Ahmed S., personal communication). Neither *rad-5* nor *clk-2* mutants show significant telomere length changes compared to normal worms. Additionally, combining either *rad-5* or *clk-2* with *mrt-2/rad1* does not affect the telomere shortening caused by *mrt-2*. It is likely that the strain variability and generational fluctuations in telomere length of *C. elegans* contributed to the disparate observations reported by the initial two studies. There are Tel2 orthologs in all eukaryotes, including humans. To understand the function of Tel2 and its possible role in telomere metabolism, we have studied the human ortholog of Tel2.

RESULTS

Identification of human Tel2 (hTel2)

When it was originally cloned, Tel2 had no homologs or known domains [234]. I tested whether Tel2 had homology to any more recent submissions. Because the sequence from *C. elegans* Tel2 (ceTel2) was not yet known, we used scTel2 as a starting point. Some proteins in *S. pombe* are less diverged from mammals than those of budding yeast, so any potential homologs identified in *S. pombe* could then be used to search for potential mammalian homologs of Tel2. A BLAST search yielded significant homology to a predicted ORF/protein in *S. pombe*. I used this region of high similarity between the *S. cerevisiae* (aa 281-668) and *S. pombe* (aa 305-750) in an iterative BLAST (BLAST2) search. This search revealed potential Tel2 homologs in humans (XP_008121), *Mus musculus* (BAB23388), *Arabidopsis thaliana* (CAB88328), *Drosophila melanogaster* (AAF55990), and *Caenorhabditis elegans* (T22976). Although the amino-termini of the various proteins are not well conserved, the latter two-thirds of the various homologs demonstrated regions of significant similarity (Fig. 2-1B). The *C. elegans* ortholog was

not included in the alignment because this protein was least conserved amongst the different orthologs. There is ~20% identity in pairwise comparisons between each of the divergent species in the aligned regions (ClustalW). Conserved domains have not been described for any of the putative Tel2 homologs. The conservation of Tel2 in *D. melanogaster* strongly suggests that Tel2's functions are not limited to telomere maintenance, as *Drosophila* (and other dipterans) possess a unique mechanism of telomere maintenance and lack most of the otherwise conserved genes involved in telomere biology, including telomerase and telomere repeat binding factors [235]. The mutations responsible for the *tel2*, *rad-5*, and *clk-2* phenotypes were localized to regions of the protein that were not well conserved in humans. Thus, it was not possible for me to generate the analogous mutants in the human protein.

Based on structural prediction programs, hTel2 has no well-conserved functional domains; however, it does appear to have a conserved secondary structure (PSI-PRED, <http://insulin.brunel.ac.uk/psipred>) (Fig. 2-1A). Because the amino-terminal 200aa of the protein is not conserved, it was not possible to make predictions about its secondary structure. The next segment of 120 AA is rich in helices and possesses one highly conserved loop. The next 100 AA are coiled or globular and probably consist of a less conserved linker region. This linker is followed by another conserved helical region and a less conserved carboxy-terminus composed of leucine-rich, hydrophobic helices. The predicted secondary structure of hTel2 is also conserved among the different homologs of Tel2.

Using a Reverse Position Specific BLAST (RPS-BLAST) program, I found that scTel2 had some homology to the MutS/MSH family of mismatch repair proteins. The

homology begins from AA 329 of scTel2 and extends for approximately 200 AA. Despite the relative conservation of this region amongst the different homologs, only the scTel2 protein RPS-BLAST revealed the extensive homology with MutS. Using the crystal structure of the MutS homodimer [236], I found the region of homology corresponded to the clamp, levers, and core of the homodimer and included α -helices 11-21 and β -sheets 14-17. These regions of the MutS homodimer are involved in encircling DNA. The significance of this homology to MutS is unclear. As scTel2p has been reported to bind a variety of DNA structures, it is possible that this homology is relevant to this activity. However, it is also possible that the homology is not representative of Tel2 function and is simply a remnant of an ancestral protein from which the eukaryotic Tel2 evolved.

Cloning and Expression of hTel2

To clone hTel2, I ordered clones that possessed the predicted full length cDNA from BLAST searches of GenBank. The ORF from the cDNA is predicted to have a molecular mass of ~92 kDa and a pI of 5.54. Restriction digests of various cDNA clones had suggested that a few clones, including one from a sequencing consortium (RZPD ID: DKFZp434A073), were full length. The presumed full length cDNAs and a negative control (N-terminal truncation of Tel2) were included in an *in vitro* transcription and translation reaction. Only the RZPD clone yielded a detectable product running at the predicted size of just less than 100 kDa (Fig. 2-2A).

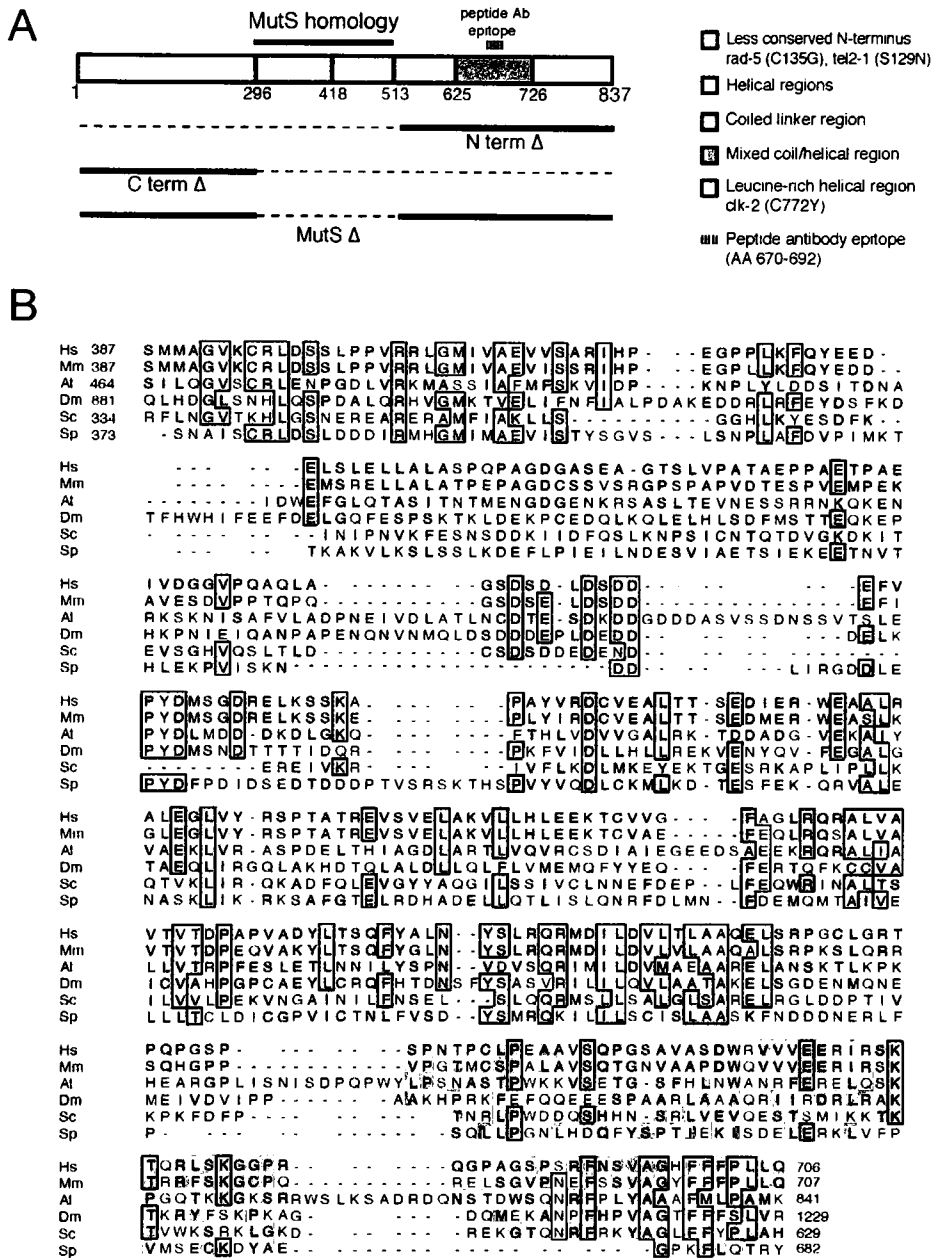


Figure 2-1. Schematic and alignment of hTel2.

(A) Predicted structural domains of hTel2. The region of hTel2 showing some homology to the MutS/MSH protein is marked above the schematic (AA 296-513). Deletion alleles generated for expression studies are marked below the schematic; dashed lines represent the deleted regions. The peptide used to generate antibodies Tel2A and Tel2B is marked above the schematic with a dashed line. (B) Multiple sequence alignment of Tel2 orthologs in the conserved terminal two-thirds. (*Hs*, human [XP_008121], *Mm* mouse [BAB23388], *At Arabidopsis* [CAB88328], *Dm Drosophila* [AF55990], *Sc S. cerevisiae* [P53038], *Sp S. pombe* [CAB93845]). Sequences were aligned using ClustalX with the Gonnet

series matrix. The alignment is displayed with SeqVu. If residues are identical or similar to the human sequence, they are boxed or shaded, respectively.

Tel2 was expressed both with and without epitope tags (Myc and FLAG) after the full-length cDNA was cloned by PCR into retroviral expression vectors that included a puromycin resistance marker. In order to generate purified hTel2 protein, the gene was also cloned into a baculovirus expression vector for expression in insect cells. In addition to the full-length constructs, based on the putative homology to the MutS protein, I generated several truncated alleles of Tel2. These included the following: a deletion of the N-terminus yielding AA 513-837 (Nterm Δ), a deletion of the C-terminus yielding AA 1-296, and an in-frame deletion of the MutS domain yielding AA 1-296 + 513-837 (MutS Δ). These deletion alleles were also cloned into retroviral vectors and were used for subsequent expression studies.

In order to detect hTel2, I generated 3 antibodies against the protein. I ordered a peptide of hTel2 (AA 670-692) that was predicted to be hydrophilic and immunogenic (Fig. 2-1A). The two polyclonal rabbit serum generated against this peptide were affinity purified over a peptide column to generate the two antibodies, Tel2A and Tel2B. In addition, polyclonal rabbit serum was produced against full-length Tel2 produced in insect cells; this serum was also affinity purified to generate an antibody, Tel2C. Finally, a polyclonal mouse serum was also produced against a GST_Tel2 (AA 296-837) fusion protein for a mouse α -Tel2 serum (Parsons, Marrero, and de Lange, unpublished). These antibodies were used for subsequent analysis of both endogenous hTel2 and overexpressed Tel2 proteins.

The transient transfection of either tagged Tel2 expression vector, but not a control vector, resulted in the expression of a protein that migrated at the expected MW of ~100 kDa (Fig. 2-2A). Although the transfection of full-length hTel2 in 293T cells

and Phoenix cells (293T-derived retroviral packaging cells) resulted in large amounts of cell death within 48 hours of transfections, the cell death did not interfere with the production of viral particles for the stable transduction of hTel2 into a number of different cell lines. Full length and truncated alleles of Tel2 were expressed in a number of cell lines including HTC75, HeLa1.2.11, BJ/hTERT, IMR90, SK-HEP1, and U2-OS. Most full length and truncated alleles of hTel2 were clearly overexpressed above the endogenous hTel2 in each of the cell lines tested (Fig. 2-2B, 2-9 to 2-11). Only the Cterm Δ allele appeared to be produced less efficiently than the other alleles and was detected very weakly in HTC75 and IMR90 cells (Fig. 2-2B, 2-9 to 2-11). Although it was reported that the overexpression of hTel2 resulted in an increased growth rate in SK-HEP-1 cells, we did not detect an altered growth rate in any cell lines that we tested (Fig. 2-9 to 2-11) [237]. It is not clear what caused the discrepancy in growth rates.

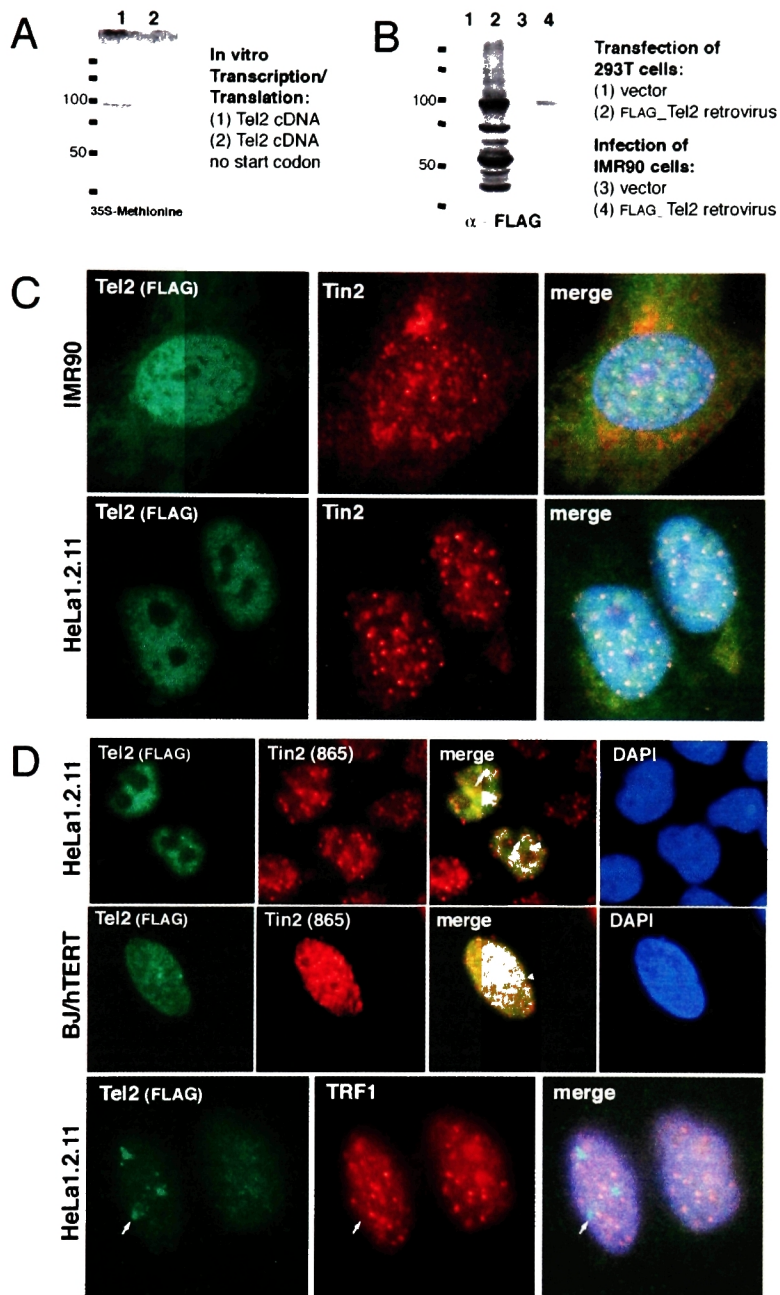


Figure 2-2. Expression of hTel2 assessed by Western and IF.

(A) *In vitro* transcription and translation from a full length cDNA (RZPD DKFZp434A073) (lane 1) and a truncated cDNA lacking the predicted start codon. Detected with ³⁵S-methionine on PhosphorImager. (B) Western blots from Phoenix packaging (293T) cells transiently transfected with vector control (lane 1) or Myc_Tel2 (lane 2), or IMR90 fibroblasts infected with pLPC vector control (lane 3) or Myc_Tel2 (lane 4). (C) IF of cells overexpressing FLAG_Tel2. Cells (type indicated on left) were stained with FLAG (9E10, green) and Tin2 (865; red). FLAG_Tel2 shows weak cytoplasmic and strong, diffuse nuclear staining in methanol fixed IMR90 and HeLa1.2.11 cells. (D) Some foci of overexpressed FLAG_Tel2 colocalize with Tin2. Cells were extracted with Triton X-100 prior to formaldehyde fixation and staining with FLAG and Tin or TRF1 (371; red). Arrowheads indicate sites of putative colocalization with telomeric markers. Arrows indicate FLAG_Tel2 foci that do not colocalize with telomeric markers.

Endogenous hTel2 does not localize to telomeres

We also investigated the subcellular localization of hTel2 in the Tel2 overexpressing cell populations. With methanol or formaldehyde fixation, overexpressed hTel2 has a strong, diffuse nuclear staining (Fig. 2-2C). Because the overexpressed Tel2 was enriched strongly and diffusely in the nucleus, it was difficult to localize Tel2 with known telomeric markers in a definitive fashion. Pre-extraction of cells with a TritonX-100 buffer prior to fixation removes nucleoplasmic proteins and can reveal foci of highly expressed nuclear proteins [118]. Upon Triton extraction, both HeLa1.2.11 and BJ/hTERT cells overexpressing FLAG_Tel2 possessed nuclear foci. Unlike the known telomeric proteins, overexpressed FLAG_Tel2 showed very few nuclear foci (usually <5). Using either Myc (9E10) or FLAG (M2) antibodies, I found that some of the nuclear foci colocalized with the telomeric marker Tin2 (Fig. 2-2C). However, these foci were reduced in number and larger in size than typical telomeric foci. Furthermore, these foci of overexpressed Tel2 did not consistently co-localize with all telomeric markers like TRF1 (Fig. 2-2D). Thus, I conclude that these foci of co-localization are unlikely to represent telomeres. It is unclear what these foci represent. Although it is possible that overexpressed Tel2 localizes with telomeric marker at extra telomeric sites, it is possible that these sites are an artifact of either the epitope tagging or Triton extraction of the cells.

To address the localization of endogenous Tel2 more accurately, I used an affinity-purified serum generated against full length Tel2 (Tel2C). Using this antibody, I examined the localization of endogenous Tel2 in a variety of cell types (BJ, IMR90, HeLa1.2.11). Consistent with the overexpressed FLAG_Tel2, most Tel2 localized in the nucleus (Fig. 2-3A). However, endogenous hTel2 had a more punctate staining pattern

than overexpressed Tel2. The foci of Tel2 enrichment did not colocalize with telomeres (Fig. 2-3A). An antibody against mouse Tel2 (mTel2) also showed a granular nuclear staining pattern in NIH/3T3 mouse fibroblasts (Fig. 2-3B) (Takai and de Lange, unpublished). Like hTel2, mTel2 foci also do not significantly colocalize with telomeres.

ChIP is an alternative and quantitative method of assessing the presence of proteins at telomeres. To better address a possible localization of hTel2 to telomeres, I performed ChIP on HeLa1.2.11 and HTC75 cells. Crosslinked lysates from HeLa cells that stably expressed FLAG_Tel2 were subjected to ChIP. Known telomeric proteins efficiently precipitated telomeric DNA. However, polyclonal sera raised against peptides of hTel2 did not precipitate telomeric DNA more efficiently than pre-immune sera. Furthermore, monoclonal antibodies against the FLAG peptide did not efficiently bring down telomeric DNA (Fig. 2-3C left). In two separate clones of HTC75 cells, the affinity-purified antibody raised against full length hTel2 (Tel2C) also did not precipitate telomeric DNA while sera against TRF1 or TRF2 did so very efficiently. Antibodies Tel2A, Tel2B, and Tel2C recognize Tel2 by both Western blot and IP (Fig. 2-3D, 2-4C). Based on the ChIP experiments from HeLa1.2.11:pLPC cells and the HTC75 clones, it seems that that neither overexpressed nor endogenous Tel2 are abundant telomeric protein.

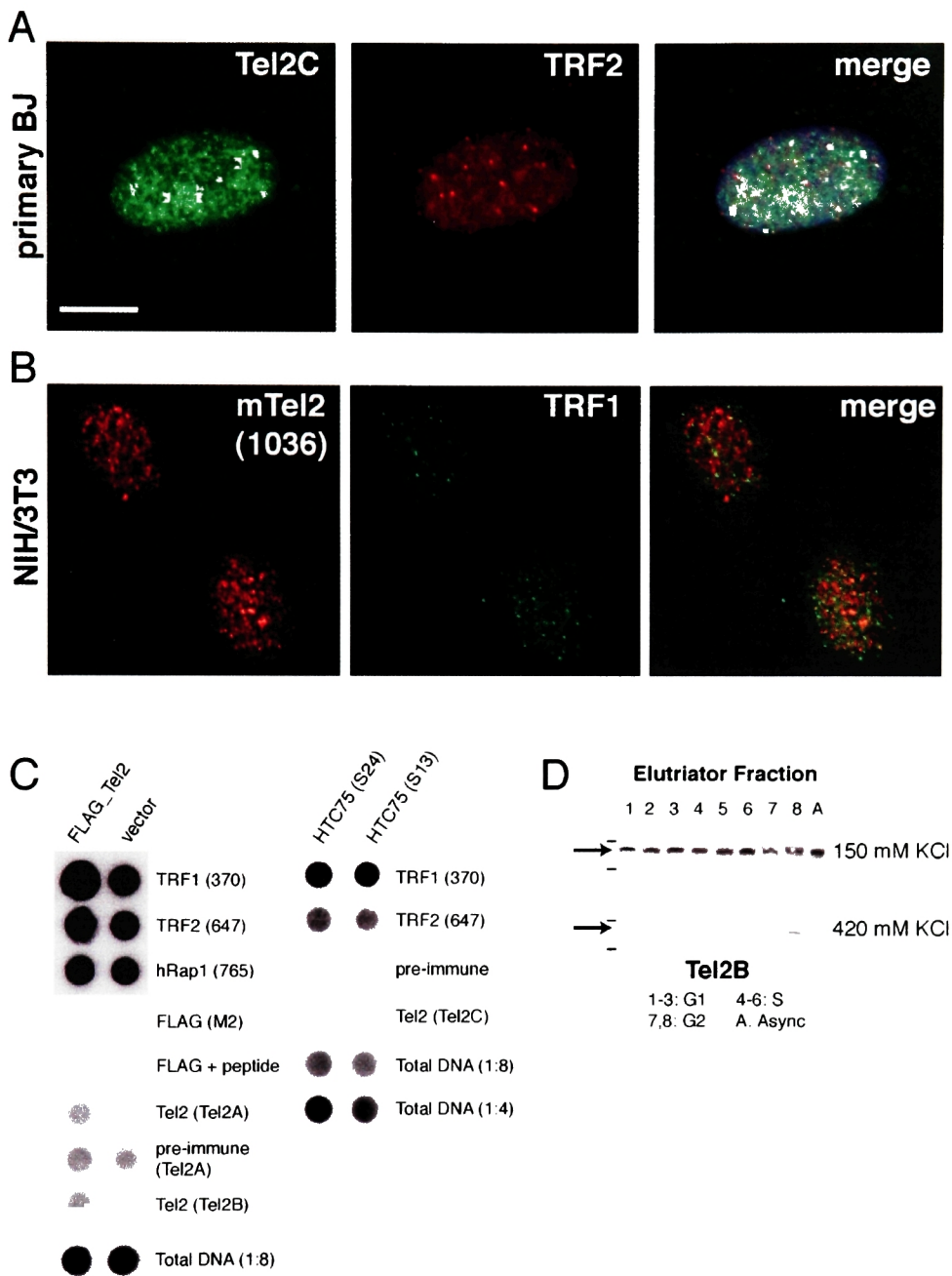


Figure 2-3. Endogenous hTel2 does not associate with telomeres.

(A) Localization of endogenous Tel2 by IF. Primary BJ fibroblasts were fixed with formaldehyde and co-stained for Tel2 (Tel2C; green) and TRF2 (Upstate anti-TRF2; red). Image is merged with DAPI (blue) on right. (B) NIH/3T3 mouse fibroblasts were stained for mTel2 and mTRF1. This experiment was performed by Hiro Takai. (C) hTel2C does not associate with telomeric DNA by ChIP. Telomeric ChIP on HeLa1.2.11 cells (left) infected with pLPC or pLPC-FLAG_Tel2 or two clones of HTC75 cells that do not express exogenous Tel2 (right) using the indicated antibodies or pre-immune serum (PI). Dot blots were hybridized with a TTAGGG repeat probe. All Tel2 sera interacted with <1% of the input telomeric DNA. (D) Western blot of centrifugally elutriated HeLa cells demonstrates that the Tel2B serum recognizes a band of the expected size. Levels of hTel2 do not vary through the cell cycle. Elutriated lysates were provided by J. Ye. Scale bar ~ 10 μ m.

The ability of hTel2 to bind telomeric DNA was assessed with *in vitro* assays. Full-length hTel2 purified from insect cells did not bind to telomeric DNA *in vitro* (Parsons and de Lange, unpublished). In previous studies of scTel2, only the C-terminal two-thirds of scTel2p fused to maltose binding protein were used in the telomeric DNA binding assays. Because it was possible that the N-terminal third of Tel2 might interfere with efficient binding, the C-terminal two-thirds of the protein was fused to GST and tested for DNA binding; it also did not bind to telomeric DNA (Parsons and de Lange, unpublished).

The dearth of telomeric colocalization of endogenous hTel2, lack of telomeric DNA in ChIP assays, and inability of purified hTel2 to bind telomeric DNA suggest that hTel2 is not an abundant telomeric protein. However, some proteins, like the BLM and WRN RecQ helicases, are thought to have important roles in telomere maintenance, but also do not obviously colocalize with telomeres by IF [141, 238]. BLM and WRN may be targeted to telomeres via an interaction with TRF2. To test whether hTel2 might be brought to telomeres via interactions with known telomere binding proteins, I co-transfected 293T cells with hTel2 and various known telomere binding proteins to test for direct interactions. I found that Tel2 did not interact directly with the known telomeric proteins TRF1, Tin2, TRF2, or tankyrase; however, it did interact with itself indicating some level of protein oligomerization (Fig. 2-4A). To test for indirect protein interactions, lysates from IMR90 cells expressing Myc_Tel2 were immunoprecipitated with Myc (9E10). Myc_Tel2 did not pull down abundant amounts of hRap1, TRF1, TRF2, Nbs1, or Rad50.

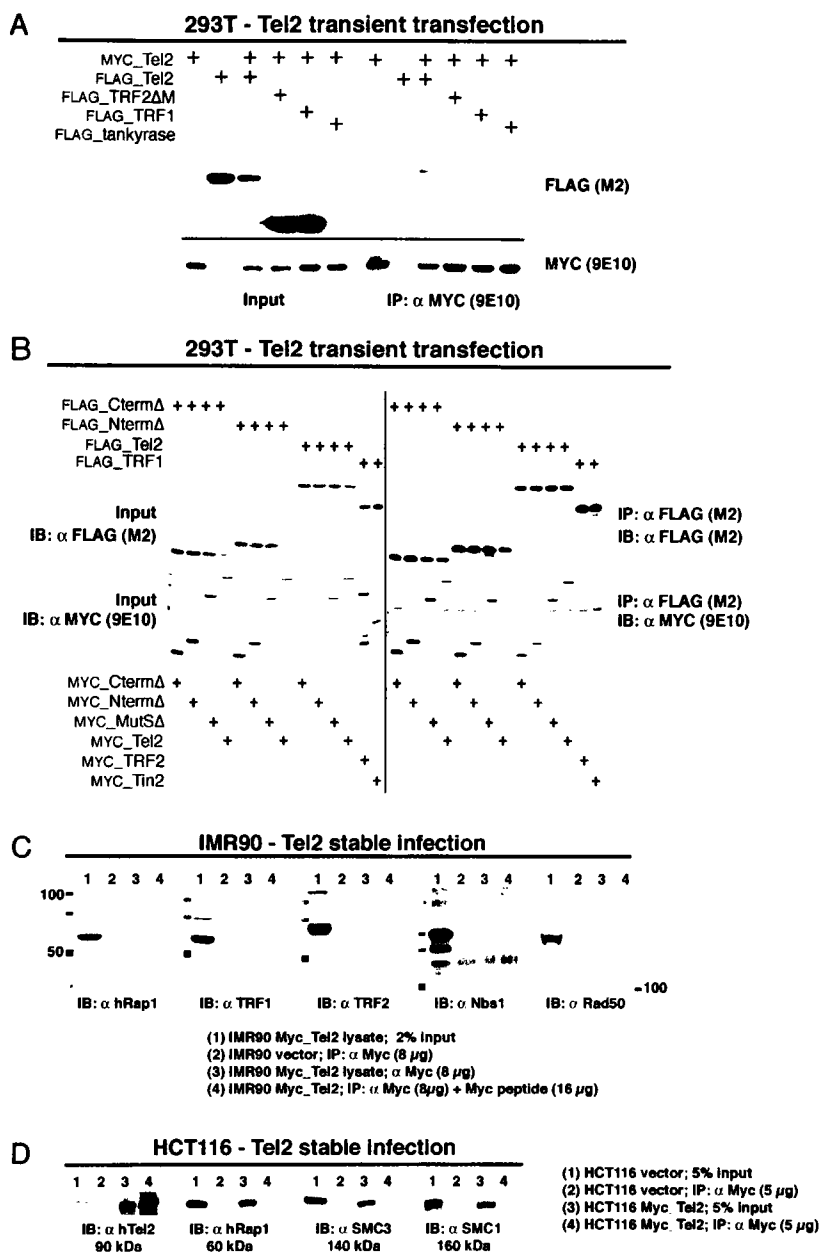


Figure 2-4. Tel2 does not interact with telomeric proteins by IP.

(A) Co-immunoprecipitation of hTel2 with itself but no other telomeric proteins. FLAG and Myc tagged constructs were transfected into 293T cells in various combinations and subjected to co-IP using antibodies against a monoclonal Myc antibody (9E10). Input lysates indicate that proteins are expressed. (FLAG_tankyrase is expressed more weakly than other proteins.) Immunoblots were done with the Myc antibody; bands in the FLAG blot (upper right) indicate a positive interaction. (B) Interaction of hTel2 with itself can not be localized to a domain of hTel2 by 293T Co-IP. FLAG_TRF1 + Myc_TRF2 and FLAG_TRF1 + Myc_Tin2 serve as negative and positive controls for the Co-IP. (C) Myc_Tel2 does not interact with telomeric proteins when stably expressed in IMR90 fibroblasts. IPs were performed from Buffer C extracts with the indicated amounts of Myc (9E10) antibody and analyzed by immunoblotting with antibodies to the indicated proteins. IPs were performed in the presence of 100 μg/ml of ethidium bromide to inhibit non-specific interactions mediated by DNA tethering. (D) Myc_Tel2 does not interact with telomeric proteins when stably expressed in HCT116 cells. IPs were performed as in (C).

Collectively, the IF, IP, ChIP, and in vitro DNA binding assays strongly suggest that hTel2 does not interact with telomeres. However, because of hTel2's diffuse localization in the nucleus, I cannot exclude the possibility that transient interactions between hTel2 and telomeric chromatin exist.

Tel2 co-localizes with PML nuclear bodies

I next determined whether the foci of hTel2 enrichment colocalize with known nuclear structures. Fixation and permeabilization of nuclei with methanol or the pre-extraction of nuclei with Triton buffer or a cytoskeletal extraction buffer (CSK) enhanced, but were not required, for the visibility of the enriched foci. The foci did not significantly colocalize with foci of DNA replication marked by PCNA, centromeres (CREST or CENP), or ionizing radiation induced foci (IRIFs) (Fig. 2-5A and B). However, they did show significant colocalization with PML nuclear bodies (PML-NBs, also called PODs or ND10). This colocalization was assessed using two distinct antibodies for Tel2, Tel2C and α Tel2, and two separate markers for PML-NBs, PML and Mre11 (Fig. 2-6A). The colocalization with PML-NBs was visible under three different extraction conditions (methanol, CSK buffer, Triton X-100 buffer) making it unlikely that the colocalization was an artifact of the fixation conditions (Fig. 2-6A, B). Most, if not all, PML-NBs colocalized with hTel2 foci; however, there were frequent hTel2 foci that were not associated with PML-NBs (Fig. 2-6, merged images). The function of PML-NBs is not well understood, though they have been implicated in many functions including apoptosis, transcriptional regulation, RNA processing, and DNA repair/replication [239, 240].

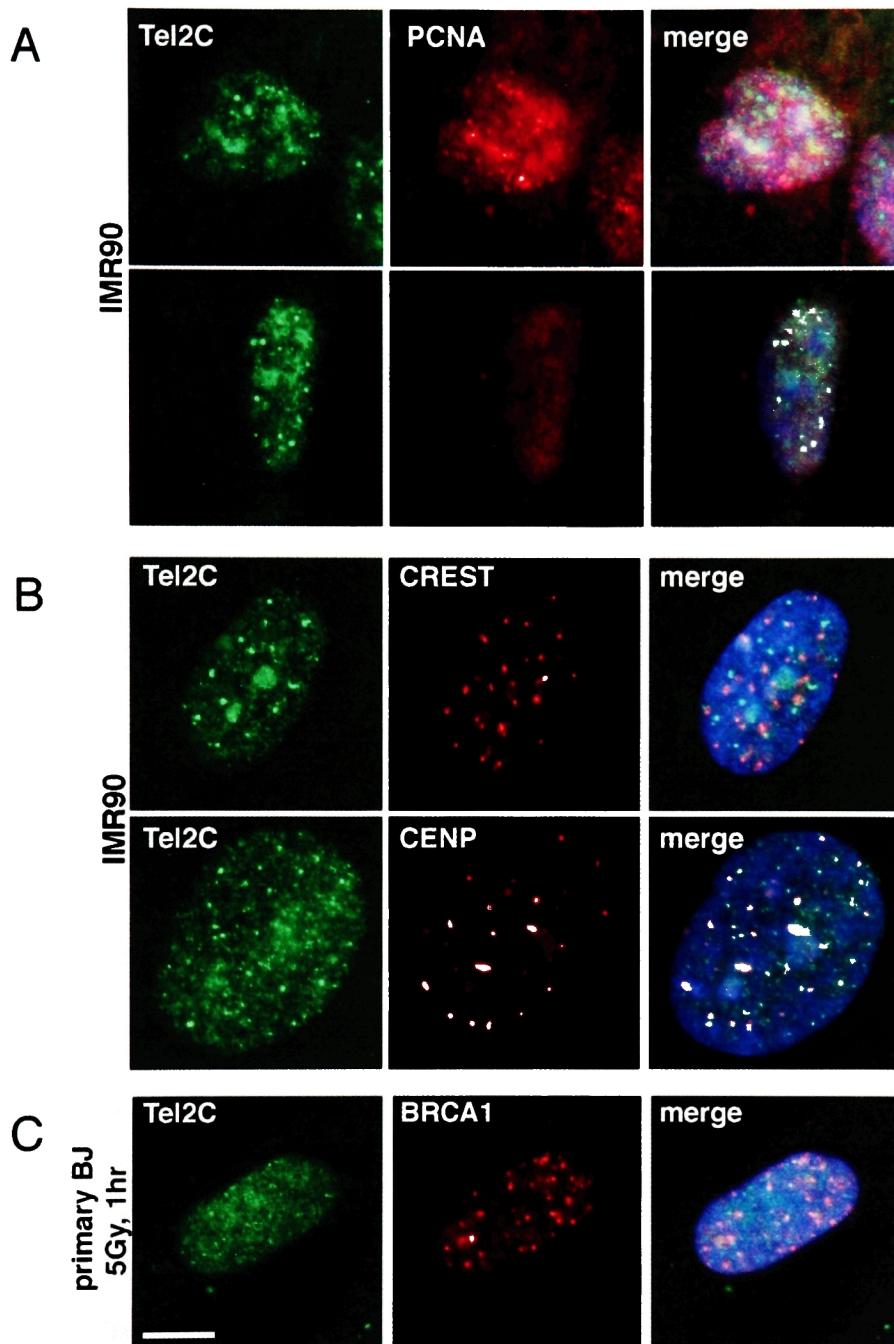


Figure 2-5. hTel2 foci do not colocalize with PCNA foci, centromeres, or IRIFs.

(A) hTel2 does not localize to replication centers. hTel2 (Tel2C; green) and PCNA (Calbiochem NA03; red) IF of IMR90 cells extracted with CSK extraction buffer prior to fixation with formaldehyde. The majority of PCNA foci do not colocalize with hTel2. As only cells in S phase possess PCNA, the lack of colocalization is especially apparent in G1 cells (*bottom*). (B) hTel2 does not localize to centromeres. hTel2 (Tel2C; green) and centromere (CREST serum, gift from T. Kapoor; red) (CENP-F [BN-S188B8] , gift from E. Tan; red) IF of IMR90 cells fixed with methanol. (C) hTel2 does not localize to IRIFs, presumably sites of DNA damage and repair. hTel2 (Tel2C) and BRCA1 (Oncogene Ab-1; red) IF of BJ cells fixed with formaldehyde 1hr after 5 Gy of IR. Images are merged with DAPI (blue) in the right panels. Scale bar ~ 10 μ m.

A partial list of proteins that associate with PML-NBs include the following: the Mre11 complex, Sp100, ISG20, p53, Daxx, BLM, RPA, and Rad51. It is not clear which, if any, of the diverse functions associated with PML-NBs are related to hTel2 function.

Immortal telomerase negative ALT cells possess a unique kind of PML body called ALT associated PML bodies (APBs or AA-PBs). These nuclear structures not only contain all of the previously described components of PML-NBs but also possess telomere binding proteins, telomeric DNA, and many DNA repair complexes (reviewed in the Chapter 3). We found that hTel2 colocalized to APBs in both VA13 cells and GM847 cells (Fig. 2-5C). The telomeric foci that were not associated with APBs, notable for their smaller size and diminished intensity, did not localize with hTel2. This pattern of localization was consistent with other PML-NB proteins that do not normally colocalize with telomeres, including PML itself.

PML-NBs have been implicated in DNA repair, and some of the components that localize to these bodies (Mre11 complex, RPA, and BLM) relocate to sites of DNA damage after cells are treated with IR or clastogens. Although primary BJ cells irradiated with 5 Gy had distinct IRIFs as assessed by BRCA1 staining, but Tel2 did not localize to the IRIFs and its pattern of localization did not appear dramatically altered (Fig. 2-5C).

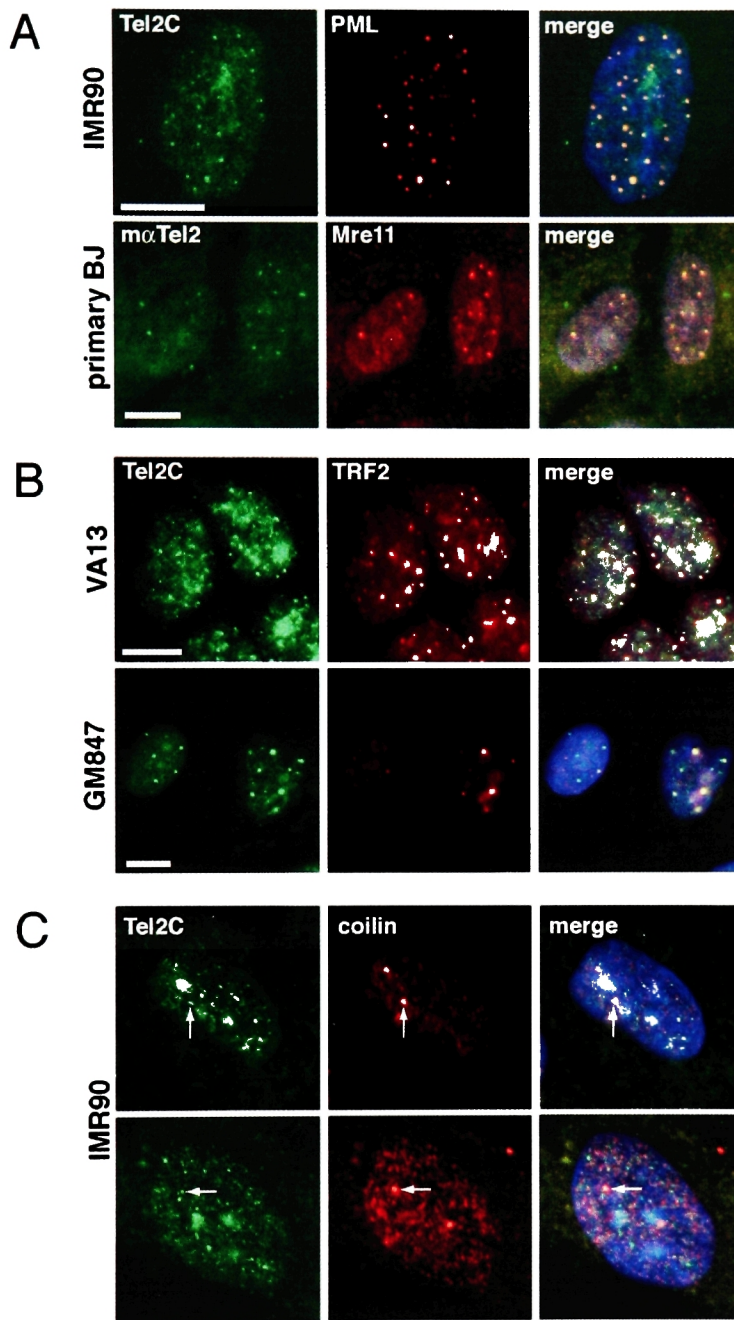


Figure 2-6. hTel2 foci co-localizes with PML nuclear bodies.

(A) hTel2 localizes to PML-NBs in telomerase-positive cells. hTel2 (Tel2C; green) and PML (Santa Cruz PG-M3; red) IF of IMR90 cells (*top*) fixed with methanol. hTel2 (Tel2C) and Mre11 (864; red) IF of primary BJ cells (*bottom*) fixed with methanol. (B) hTel2 localizes to PML-NBs in telomerase-negative ALT cells. hTel2 (Tel2C) and TRF2 (647; red) IF of VA-13 cells (*top*) extracted with Triton X-100 and fixed with formaldehyde. hTel2 (Tel2C) and TRF2 (647) IF of GM847 cells (*bottom*) extracted with Triton X-100 buffer and fixed with formaldehyde. Tel2 co-localizes with the larger TRF2 foci, corresponding to APBs, but not to smaller ones, corresponding to telomeres. (C) hTel2 co-localizes with some Cajal bodies. hTel2 (Tel2C) and coilin (BD C28020; red) IF of BJ cells fixed with methanol. Arrows indicate sites of colocalization with hTel2; not all Cajal bodies contain Tel2. Images are merged with DAPI (blue) in right panels. Scale bars ~ 10 μ m.

In most cells, it has been noted that at least one PML body is associated with Cajal bodies, an intranuclear structure for small ribonucleoprotein processing and assembly [241, 242]. Consistent with these findings, hTel2 occasionally colocalized with one or more Cajal bodies stained with p80 coilin (Fig. 2-6C). As there were Cajal bodies that did not localize with hTel2, it is unlikely that the co-localization is due to bleed-through from coilin staining; however, these experiments should be repeated using separate markers for both hTel2 and Cajal bodies to confirm the finding. Some components of PML-NBs and Cajal bodies have been noted to have cell cycle variations in their localization. Thus, I assessed the cell cycle variation in levels of hTel2 using cell lysates prepared from centrifugally elutriated HeLa cells and found that it did not vary with the cell cycle (Fig. 2-3D). More careful IF and biochemical studies are necessary to address whether there are more subtle variations in the localization of hTel2 through the cell cycle.

Localization of hTel2 in meiotic cells

Microarray analyses of *S. cerevisiae* genes have also suggested that scTel2 is one of a limited number of genes that are highly induced after yeast are induced to undergo meiosis on sporulation medium. Using affinity purified Tel2C serum, our collaborators examined the localization of hTel2 in meiotic nuclei prepared from testis suspensions. Overall, both somatic and meiotic cells shared a diffuse nuclear staining pattern.

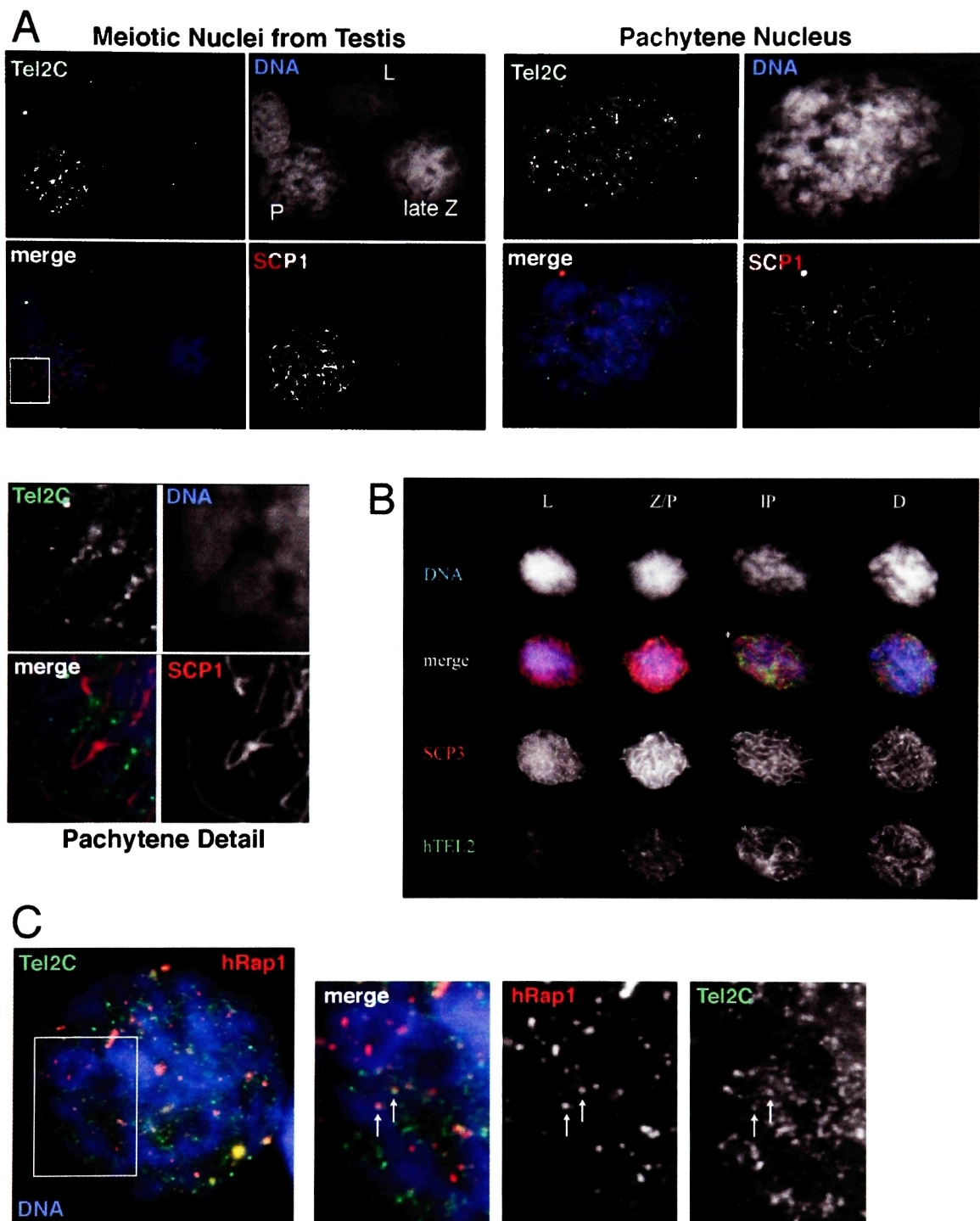


Figure 2-7. hTel2 localization in meiotic spermatocytes.

(A) Localization of hTel2 in meiotic spermatocytes. hTel2 (Tel2C) and SCP1 IF of spermatocytes in leptotene (L), zygotene (Z), pachytene (P), or diplotene (D) as labeled. (*Inset*) Detail of hTel2 localization from white box. (B) Variation in staining pattern of hTel2 through meiosis. Meiotic chromosomes are localized with SCP3. (C) Small amounts of hTel2 co-localizes with hRap1 in meiotic nuclei. Arrows denote sites of putative co-localization. Some images are merged with DAPI staining in right panels. These experiments were performed by H. Scherthan.

However, some subtleties were noted in meiotic cells. In particular, the diffuse granular staining pattern was most apparent in late pachytene and diplotene meiotic nuclei. Interestingly, it appeared that the strongest granular staining was excluded from the dense chromatin of late pachytene and diplotene nuclei. The meiotic chromosomes were visualized by DAPI staining for components of the synaptonemal complex (SCP1, SCP3). The progressive condensation of meiotic chromosomes and exclusion of hTel2 from this condensed chromatin could explain the apparent increase in the intensity of hTel2 during the late stages of meiosis. The exclusion of hTel2 from regions of dense chromatin may be consistent with the finding that PML-NB and Cajal bodies are also excluded from dense chromatin in interphase cells [243]. Curiously, in late pachytene and diplotene nuclei, some foci of hTel2 colocalized with foci of hRap1. It is not clear whether the infrequent foci of co-localization represented telomeres. In addition, not all telomeres colocalized with hTel2. Because it is possible that the occasional colocalization between hTel2 and hRap1 was a trivial result of the abundant and diffuse staining of hTel2, the possible co-localization of hTel2 with telomeres in meiotic cells will need to be addressed with additional markers.

Localization of mammalian Tel2 to centrosomes

During their analyses of hTel2 localization in meiotic cells, our collaborators noted that a strong extra-nuclear focus of hTel2 staining was often visible (Scherthan, unpublished). The size and localization of this focus next to the nucleus was consistent with that of the centrosome.

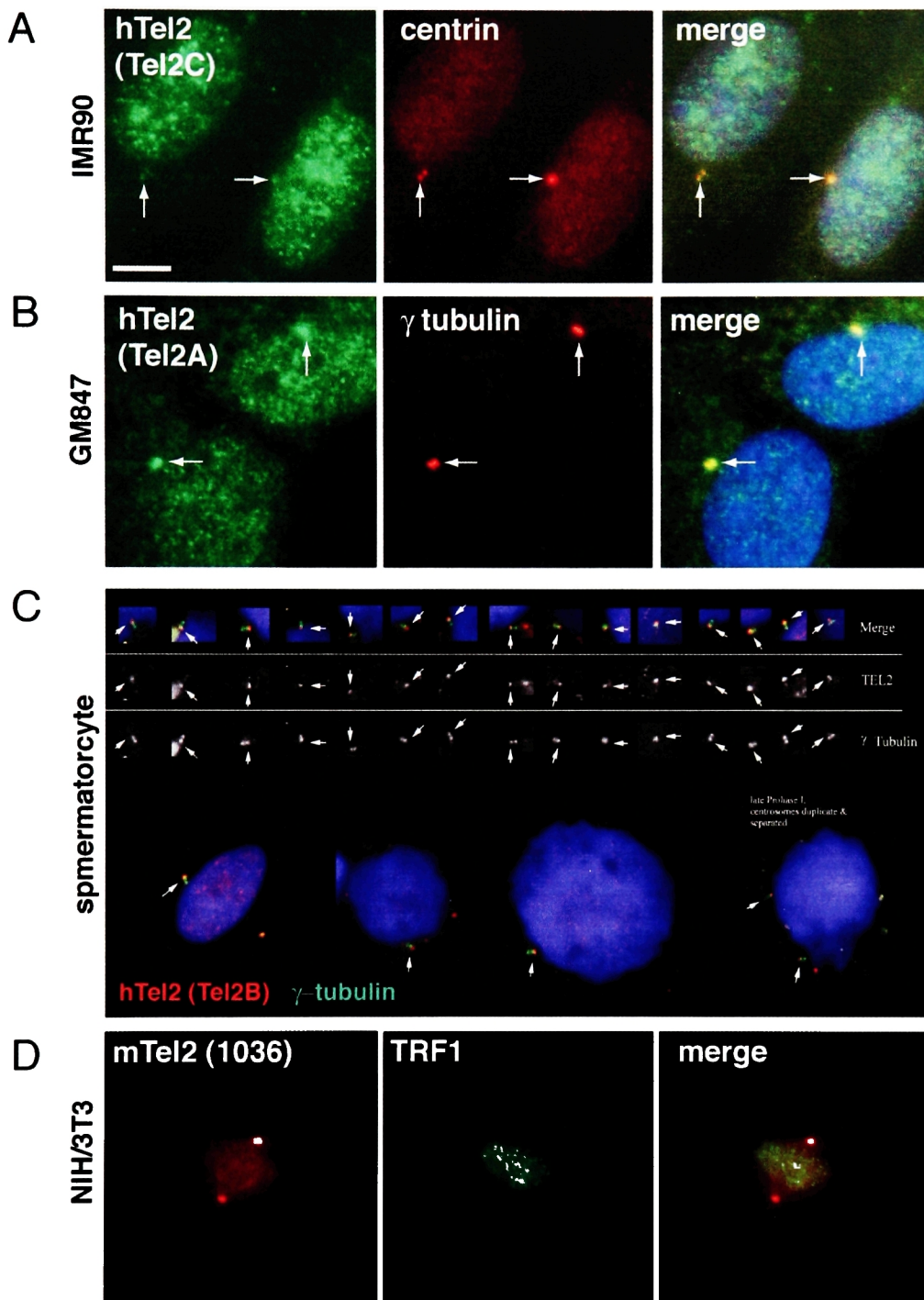


Figure 2-8. hTel2 localizes to centrosomes in mouse and human cells.

(A) hTel2 (Tel2C) and centrin (gift from J. Salisbury; red) IF of IMR90 cells fixed with formaldehyde. (B) hTel2 (Tel2A) and γ -tubulin (Sigma GTU88; red) IF of GM847 cells fixed with methanol. (C) hTel2 (Tel2B; red) and γ -tubulin (green) IF of spermatocytes. Note the asymmetric staining of centrosomes by hTel2 in spermatocytes. Experiment performed by H. Scherthan. (D) mTel2 (1036) and mTRF1 IF of a mitotic NIH/3T3 cell. Experiment performed by H. Takai. Some images are merged with DAPI staining in right panels. Scale bars $\sim 10 \mu\text{m}$.

I have found that hTel2 localized to centrosomes in somatic cells using three different affinity purified antibodies against hTel2 (Tel2A, Tel2B, and Tel2C) and several different markers for centrosomes (centrin, γ -tubulin) (Fig. 2-8A, B). Independently from the studies of our collaborator, using two distinct peptide antibodies against mTel2, a post-doctoral fellow in our lab has found that mTel2 also colocalized with centrosomes (Fig. 2-8E and data not shown) (Takai and de Lange, unpublished). The centrosomal staining of mTel2 was especially intense in mitotic cells where mTel2 very clearly stained the centrosomes at the core of the mitotic spindles.

Curiously, the staining of hTel2 in spermatocytes with Tel2B resulted in an asymmetric staining pattern on most centrosomes (Fig. 2-8C). However, this asymmetric localization of Tel2 was not noted in mitotic human and mouse cells (Fig. 2-8A, B, D). Although some components of the centrosome (e.g. ϵ -tubulin) have been previously noted to be asymmetrically distributed between the mother and daughter centrioles, it is not known whether Tel2's distribution is related to the asymmetric distribution of these centrosomal markers. Furthermore, the asymmetric centrosomal staining by hTel2 appears to be specific to meiotic cells. Importantly, in at least the spermatocytes, the incomplete overlap between the IF signals for hTel2 and centrosomes suggests that the localization of hTel2 is not an artifact of the staining process (e.g. bleed through). One concern of these IF studies is that the intensity of the centrosomal staining varies considerable between different antibodies. To address this concern, it may be helpful to determine the localization of a GFP_Tel2 fusion protein. Alternatively, it will be important to determine whether mouse Tel2 still localizes to telomeres in mouse cells that

have been targeted for Tel2. These additional studies should establish the importance of the apparent localization of mammalian Tel2 localization to centrosomes.

hTel2 overexpression induces telomere elongation

In *S. cerevisiae*, *Tel2* mutants have short telomeres. The hypomorphic alleles of *ceTel2* (*clk-2/rad-5*) may subtly elongate telomeres, though this effect is disrupted. I expressed different Myc tagged alleles of *Tel2*—Nterm Δ , Cterm Δ , MutS Δ , and full length—in the telomerase-positive HTC75 cell line and the primary, telomerase-negative cell line IMR90. Most truncation alleles of *Tel2* were expressed efficiently; however, the C-terminal deletion of *Tel2* (Cterm Δ) was unstable and expressed only weakly. In HTC75 cells, after ~60PD, the overexpression of Myc_Tel2 or truncation mutants did not have obvious effects on telomere length or growth rate (Fig. 2-9B). In IMR90 cells, the expression of *Tel2* did not affect the rate of telomere shortening or growth rate (Fig. 2-9C). To extend my analysis on the possible effects of hTel2 on telomere length, I expressed FLAG_Tel2 in the telomerase-positive BJ/hTERT and HeLa1.2.11 cells. In BJ/hTERT cells, even the vector control expressing cells demonstrated significant telomere elongation. However, the expression of FLAG_Tel2 did not obviously alter the baseline TRF (terminal restriction fragment) elongation.

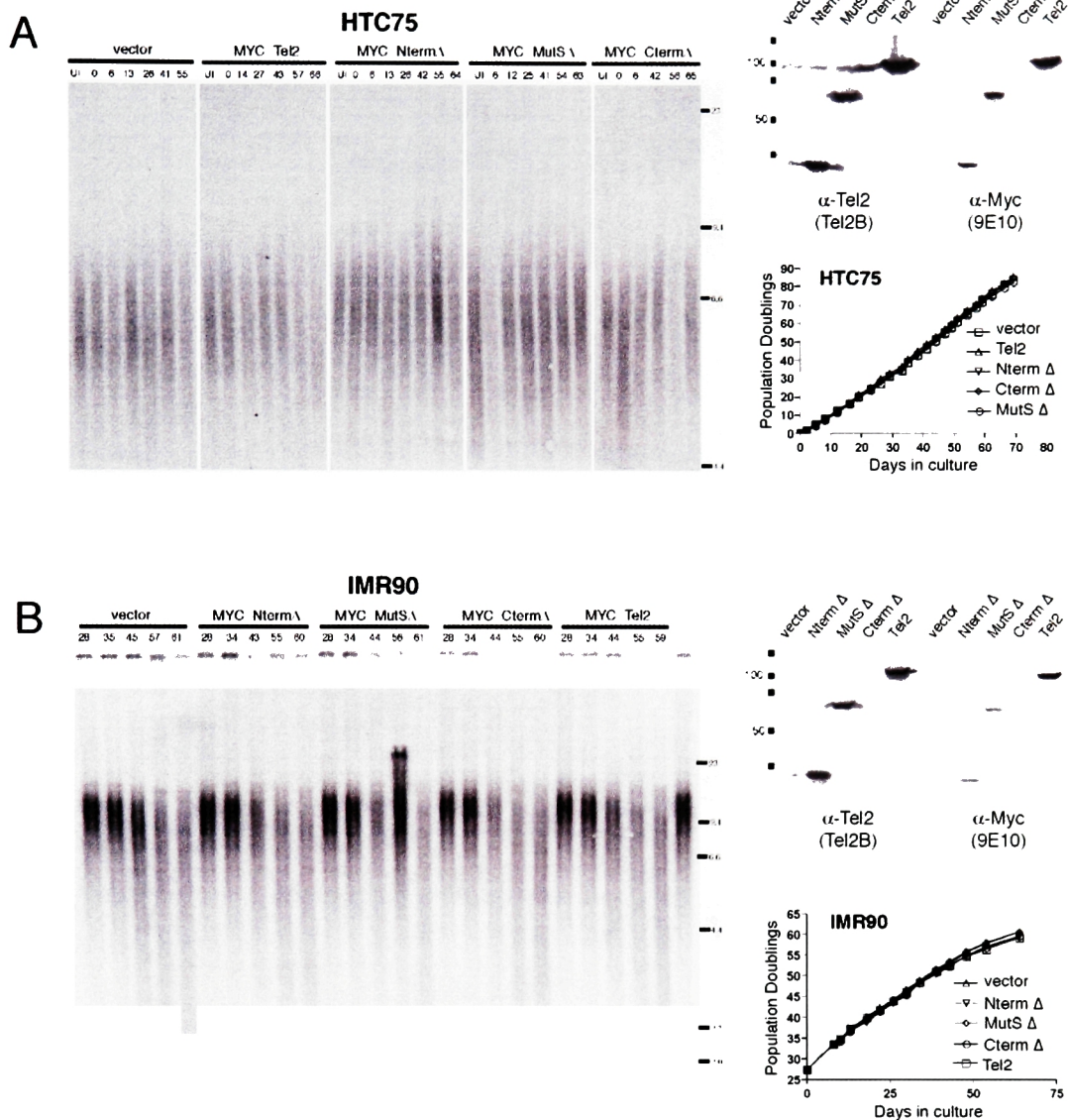


Figure 2-9. Effect of Myc_Tel2 alleles on TRF length in HTC75 and IMR90 cells.

(A) Analysis of telomeric restriction fragments (TRFs) and growth curves of HTC75 cells expressing Myc_Tel2 alleles. HTC75 cells were infected with Myc_Tel2, Myc_NtermΔ, Myc_MutSΔ, Myc_CtermΔ, or vector control retroviruses. Cells were passaged every 2-3 days by seeding 4.0×10^5 cells into a 10 cm dish. DNA was harvested at the indicated PDs, digested with *Mbo*I and *Alu*I, and analyzed by genomic blotting using a TTAGGG repeat probe. Growth curve of HTC75 cells (right, bottom) calculated from cell numbers taken at each cell splitting. "UI" indicates DNA harvested from cells prior to infection. Western blot of Myc_Tel2 allele expression (right, top). About 5 PD after selection from infection, lysate from $\sim 1.5 \times 10^5$ cells infected with the indicated virus were blotted with Tel2B (left) or Myc (right). Deletion alleles all run at the predicted MW; endogenous hTel2 is detected with Tel2B at ~ 100 kDa. Myc_Tel2ΔCterm is expressed very weakly (right) and is not detected by Tel2B, which recognizes a C-terminal epitope. (C) Analysis of TRFs, growth curves, expression in IMR90 cells expressing Myc_Tel2 alleles. IMR90 fibroblasts (ATCC) were infected at PD27 and passaged every 4 days by seeding 1.5×10^6 cells into a 15-cm dish. PD56 of Myc_MutSΔ was not fully digested.

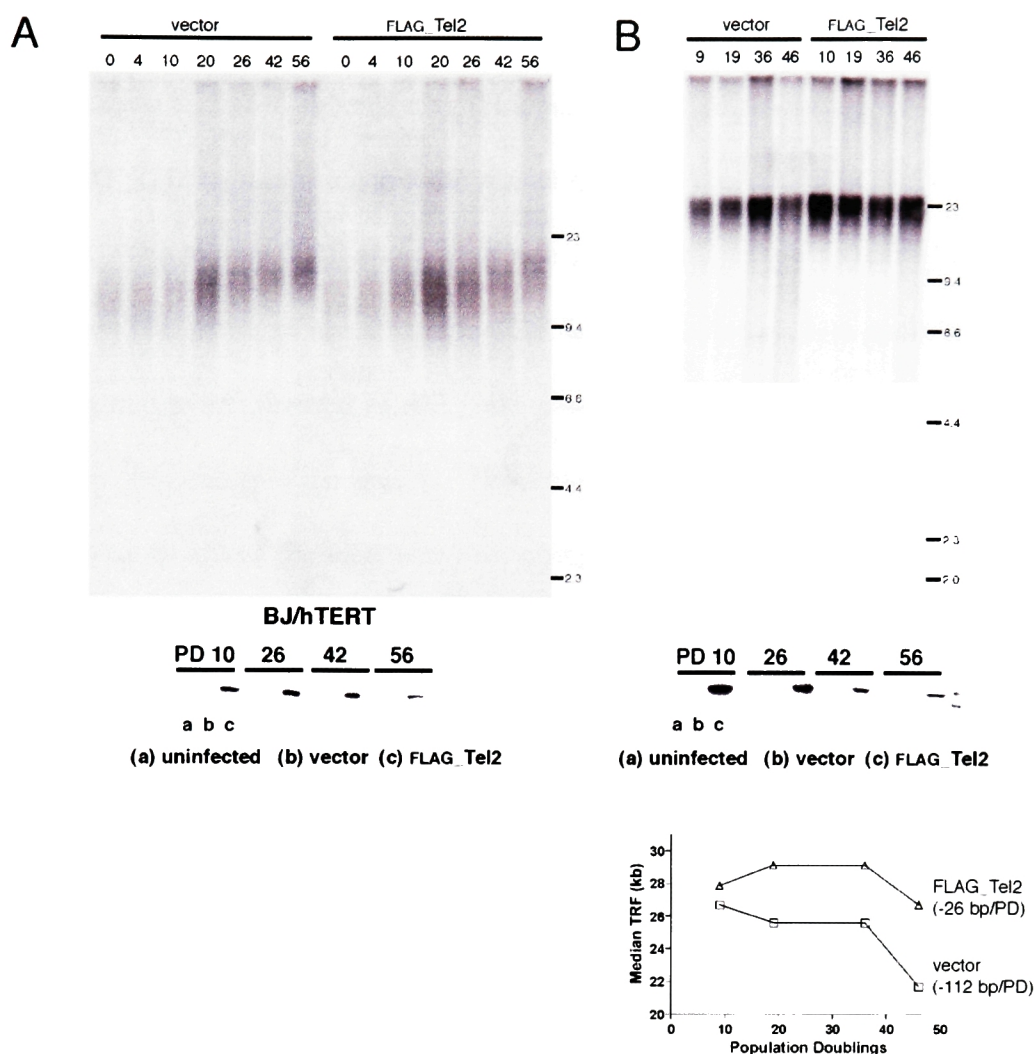


Figure 2-10. Effect of FLAG_Tel2 on TRF length in BJ/hTERT and HeLa1.2.11.

(A) TRF analysis of BJ/hTERT expressing vector control or FLAG_Tel2. Genomic blot was performed as described in Fig. 2-9A. BJ/hTERT cells were passaged every 3 days by seeding 7.0×10^5 cells into a 10 cm dish. Expression of FLAG_Tel2 was confirmed throughout the course of the experiment by the α -FLAG western (*left bottom*) (B) TRF analysis of HeLa1.2.11 cells. HeLa1.2.11 cells were passaged every 2-3 days by seeding 4.0×10^5 cells into a 10 cm dish. Expression of FLAG_Tel2 was confirmed throughout the course of the experiment by the α -FLAG western (*right middle*). Samples were prepared as described in Fig. 2-9A. The change in median TRF length was determined in ImageQuant and plotted (*right bottom*). Telomere shortening rate was calculated by linear regression.

The HeLa1.2.11 subclonal line has extremely long telomeres (>23 kb) that shorten upon extended subculturing (Hooper and de Lange unpublished). The expression of FLAG_Tel2 appeared to slow the rate of telomere shortening in HeLa1.2.11 cells (Fig. 2-10B). The slower TRF shortening rate persisted through at least 100 PD (data not shown). The cause of the unstable TRF length in HeLa1.2.11 cells is unclear. It is possible that overexpressed FLAG_Tel2 could either promote TRF elongation or prevent telomere shortening in these cells. However, as the overexpression of Tel2 alleles does not appear to affect the telomere shortening in primary IMR90 cells, it may be more likely that FLAG_Tel2 promotes telomere elongation. To exclude the possibility that the altered telomere shortening rates were caused by population variability in HeLa1.2.11 populations, it will be necessary to repeat this infection; it may further be helpful to determine whether the deletion mutant of Tel2 may also slow the TRF shortening rate in HeLa1.2.11 cells or other cells with long, but unstable telomeres.

Recently, it was reported that the overexpression of hTel2 (CLK-2) was reported lengthen telomeres in the hepatocellular adenocarcinoma cell line, SK-HEP-1 [237]. This report conflicted with my finding that Myc_Tel2 overexpression did not promote telomere elongation in HTC75 cells. However, there were some differences in the way the two studies were performed. At least three factors--differences in the cell line used (SK-HEP-1 vs. HTC75), the presence of an N-terminal epitope tag in my expression vector, and the longer term culturing of infected cells by the Hekimi group-- could all contribute to the reported differences. To address these discrepancies, I repeated the experiment using the same conditions as Hekimi and colleagues. Consistent with findings from the Hekimi group, I found that the expression of untagged Tel2 gradually increased

the median TRF length in both HTC75 and SK-HEP-1 (Fig. 2-10B, C). The rates of telomere elongation were calculated by linear regression to be roughly 11 bp/PD and 22 bp/PD in HTC75 and SK-HEP-1 cells, respectively. In HTC75 cells, this rate of telomere elongation is ~3 fold lower than the rate of elongation caused by hRap1 overexpression and ~20 fold lower than the telomere elongation caused by expressing Pot1 Δ OB [85, 122].

In both SK-HEP-1 and HTC75 cells, untagged Tel2 overexpression appeared to yield qualitatively better TRF elongation than FLAG_Tel2 overexpression. However, quantitative analyses of changes in median telomere length (ImageQuant) indicated that FLAG_Tel2 overexpression in SK-HEP-1, but not HTC75, cells also induced telomere elongation. Thus, it is unclear whether an N-terminal epitope tag on Tel2 impedes the protein's ability to promote telomere elongation after overexpression. More experiments may be necessary to determine whether untagged deletions mutants of Tel2 affect telomere length in HTC75 and HeLa1.2.11 cells.

I previously noted that hTel2 colocalizes with telomeric markers in the APBs of ALT cells. To determine whether hTel2 contributes to telomere elongation in ALT cells, I expressed hTel2 in the ALT osteosarcoma cell line, U2-OS cells, and found that its expression did not strongly affect telomere length dynamics (Fig. 2-12A). However, the very long and heterogeneous telomeres of ALT cells are difficult to resolve through standard electrophoresis, which can only resolve fragments <25 kb in length. Thus, a more thorough TRF analysis of these U2-OS cells should be performed using a CHEF gel. This will help to exclude the possibility that hTel2 exerts subtle effects on telomere maintenance in ALT cells.

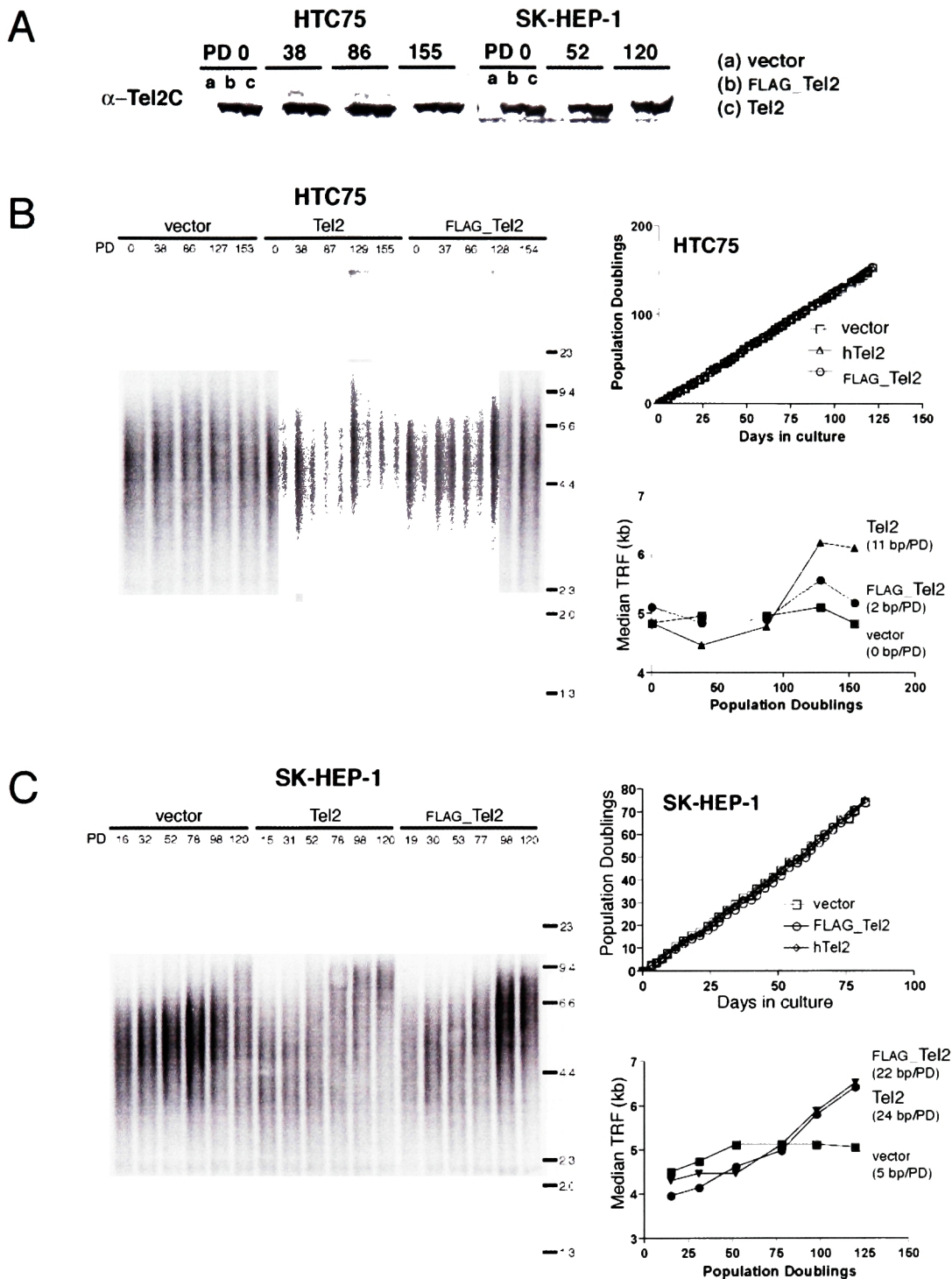


Figure 2-11. Effect of Tel2 on TRF length in HTC75 and SK-HEP-1 cells.

(A) Levels of endogenous, FLAG_Tel2, and untagged Tel2 in HTC75 (left) and SK-HEP-1 (right) cells detected by Tel2C. Samples were prepared as described in Fig. 2-9A. (B) TRF analysis of HTC75 cells expressing indicated virus. Genomic blot and growth rates (upper right) were performed as described in Fig. 2-9A. The change in median TRF length was determined in ImageQuant and plotted (right bottom). Telomere growth rate was calculated by linear regression. (C) TRF analysis of SK-HEP-1 cells. SK-HEP-1 cells (from ATCC) cells were passaged every 3 days by seeding 7.0×10^5 cells into a 10 cm dish.

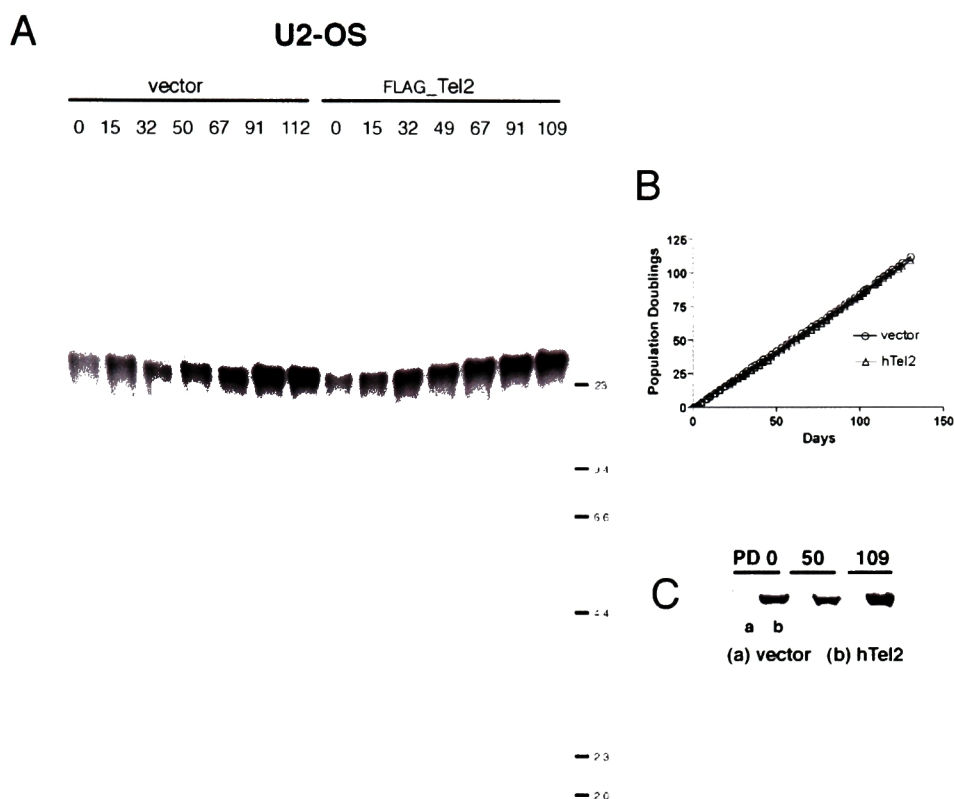


Figure 2-12. Effect of Tel2 on TRF length in HTC75 and SK-HEP-1 cells.

(A) TRF analysis of U2-OS expressing vector control or FLAG_Tel2. Genomic blot was performed as described in Fig. 2-9A. U2-OS cells were passaged every 3 days by seeding 7.0×10^5 cells into a 10 cm dish. The apparent increase in MW of TRFs in the outer lanes is caused by an artifact of the gel running conditions. (B) Growth rate of U2-OS cells expressing vector control or hTel2 were determined as described in Fig. 2-9B. (C) Expression of FLAG_Tel2 was confirmed throughout the course of the experiment by the α -Tel2C western.

The overexpression of Tel2 can promote modest telomere elongation in many settings. The effect appears to be dependent on telomerase as IMR90 cells and U2-OS cells overexpressing Tel2 alleles did not have altered telomere length dynamics compared to control cells. However, because an N-terminal epitope tag may affect the function of Tel2 alleles, it may be helpful to reassess whether untagged alleles of Tel2 can affect rates of telomere shortening in telomerase negative cell lines. Perturbing the function in almost any of the abundant telomere binding proteins (TRF1, TRF2, hRap1, Tin2, PTP, or Pot1) results in rapid (visible in < 50 PD) and substantial (>30 bp/PD) changes in telomere length. Consistent with the findings that endogenous hTel2 is not an abundant

telomeric protein, Tel2's effects on telomere length are very modest. To better address the role of Tel2 in telomere maintenance, it will be necessary to study the effect of hTel2 depletion on telomere maintenance. However, the depletion of hTel2 by RNA interference suggests that it is essential for cell viability; thus, it will be necessary to reduce levels of endogenous hTel2 to levels that are still compatible with cellular viability to assess any possible functions on telomere length homeostasis.

Tel2 is essential in human cells

To assess the possible roles of Tel2, I depleted Tel2 by transfections of short interfering RNA (siRNA) [244]. Two independent siRNA duplexes, Tel2.2 and Tel2.3, resulted in a reduction of hTel2 levels to ~30% and ~10% of normal levels, respectively (Fig. 2-13A, B). For some experiments, HeLa2 cells that overexpressed FLAG_Tel2 of untagged hTel2 (HeLa2:FLAG_Tel2, HeLa2:hTel2) were used as a control in some experiments. Although the exogenously introduced Tel2 constructs have the same coding sequence as endogenous Tel2, the transfection of siRNA duplexes did not reduce overexpressed Tel2 below normal levels in HeLa2:FLAG_Tel2 or HeLa2:Tel2 cells as assessed by Western (Fig. 2-13B). For most analyses, HeLa2 cells were analyzed 48 hours after 2 siRNA transfections spaced by 24 hrs.

Most of the HeLa2 cells transfected with the Tel2.2 duplex (Tel2.2i) were rounded and refractile or had lifted off of the plate by 72 hours after the 2nd transfection. Consistent with their refractile appearance, HeLa2 cells were positive for TUNEL labeling (for DNA fragmentation) between 12-60 hours after the 2nd transfection with Tel2.2i (Fig. 2-13C, D). Apoptotic cells also have <2n DNA content. Indeed, HeLa cells transfected with the Tel2.3 siRNA (Tel2.3) had ~21% sub-G1 DNA content as assessed

by FACS compared to ~8% for a GFP siRNA (GFPi) transfected control (Fig. 2-13C, D). Importantly, this effect was almost fully rescued by the overexpression of either FLAG_Tel2 or untagged Tel2. Finally, it is possible to score apoptotic cells microscopically by the highly condensed nature of their chromatin (Fig. 2-14A). The apoptotic nuclei can be easily distinguished from mitotic nuclei by co-staining with phospho-Histone H3 antibody that stains mitotic chromatin. In three independent transfections of Tel2.3i, there was an average of ~3 fold more apoptotic nuclei compared to GFPi control (18.6% compared to 6.4%). Furthermore, Tel2.3i transfected cells incorporated a 1 hr pulse of BrdU less efficiently than GFPi control (33% compared to 48%).

The induction of apoptosis by two different duplexes targeting Tel2 and the rescue of the apoptosis by Tel2 overexpression excluded the possibility that the cell death was due to non-specific effects of the siRNA. Thus, I conclude that, like scTel2 and ceTel2, hTel2 is essential for cellular viability. In agreement with my findings from somatic human cells, mouse cells with targeted deletions of mTel2 are not viable (Takai and de Lange, unpublished).

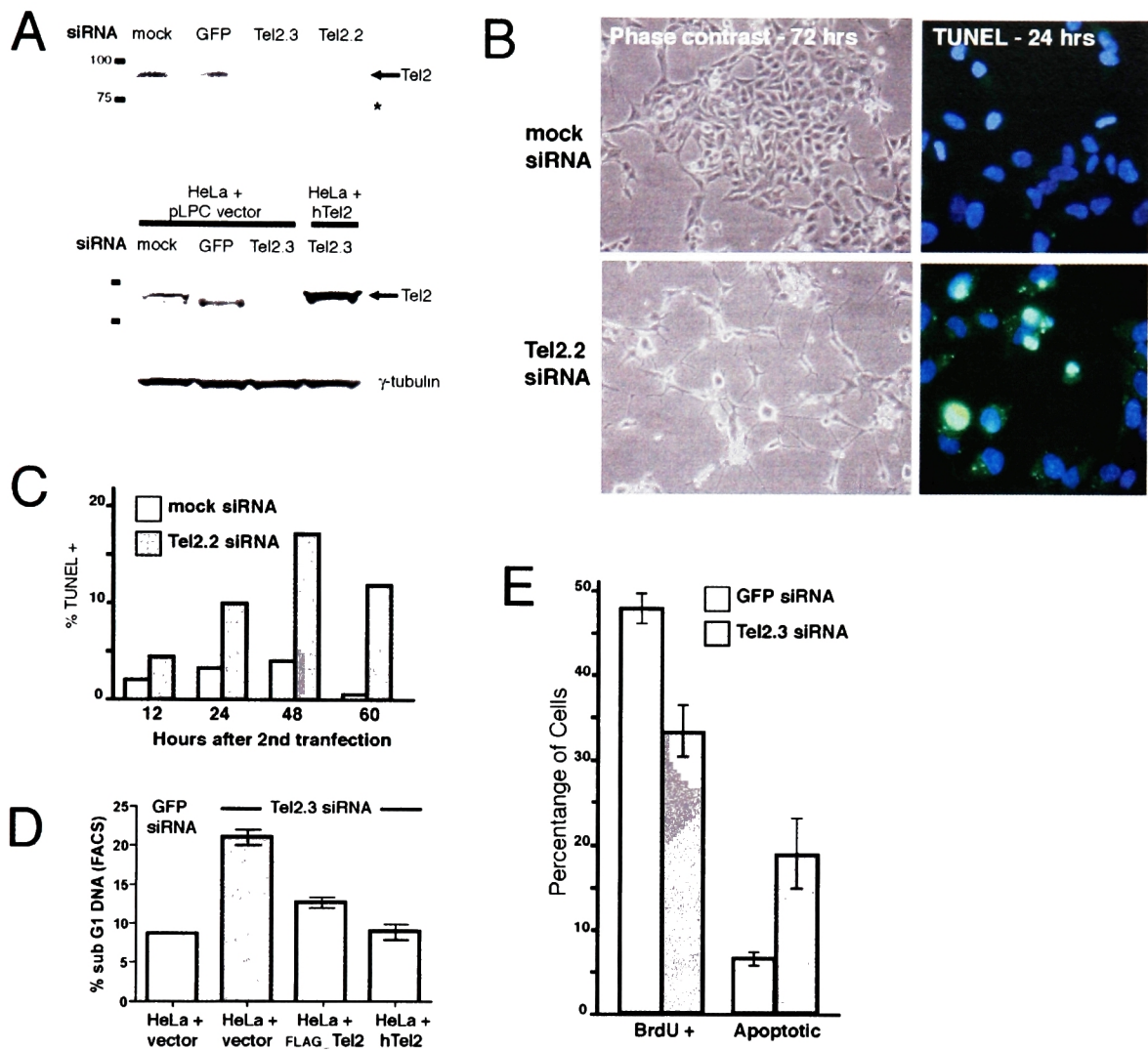


Figure 2-13. Depletion of Tel2 by siRNA results in cell death.

(A) Western blot showing that HeLa2 cells have reduced amounts of hTel2 after transfection with Tel2.2 or Tel2.3 siRNA duplexes. Western analysis performed with Tel2C. The star indicates a non-Tel2 band, which can be used as loading reference. (B) The overexpression of hTel2 rescues the depletion of endogenous Tel2 by siRNA. HeLa2 cells stably expressing pLPC hTel2, but not pLPC vector, continue to express hTel2 after depletion by Tel2.3i. (top) Tel2C (bottom) γ -tubulin loading control. The apparent doublet in the endogenous Tel2 lanes is an artifact of gel separation. (C) Phase contrast and fluorescent micrographs of TUNEL staining in HeLa2 cells 72 and 60 hrs after a 2nd transfection. TUNEL assay was performed using. (D) Percentage of sub-G1 cells increases after transfection with Tel2.3i in HeLa2 cells (with pLPC vector) but not HeLa2 cells expressing FLAG_Tel2 or hTel2. Bars represent the mean and SD of three independent FACS analyses performed on 3 transfections performed in parallel. Samples were processed 48 hrs after the 2nd transfection. (E) HeLa2 cells possess more apoptotic nuclei and fewer BrdU-labeled nuclei after Tel2.3 transfection. Cells were scored for BrdU labeling 1 hr after a 10 μ M BrdU pulse. Cells were scored as apoptotic nuclei if they possessed condensed DAPI staining and did not stain positively for phospho-Histone H3 (Cell Signaling). >400 nuclei were scored for each assay.

Additional phenotypes of hTel2 depleted cells

The depletion of Tel2 by both Tel2.2i and Tel2.3i duplexes also resulted in a modest enrichment of mitotic cells. The condensed chromatin of mitotic nuclei was markedly distinct from that of apoptotic nuclei. Furthermore, mitotic cells, but not apoptotic nuclei, stained strongly for Cyclin B and phospho-Histone H3 (Fig. 2-15A). 48 hrs after transfection with GFPi siRNA, there were 2-3 fold more mitotic cells in Tel2.3i transfected cells compared to GFPi (3.1% compare to 1.1%, respectively) (Fig. 2-15B). The mitotic arrest induced by hTel2 depletion was significantly less striking than the arrest induced by the depletion of proteins directly required for the formation of the mitotic spindle (e.g. TPX2, Aurora A kinase, and Plk1) [245-247]. The depletion of these spindle components by siRNA results in a 10-fold increase in the number of mitotic cells. Thus, it is unlikely that hTel2 is directly involved in mitotic spindle assembly.

Many of the accumulated mitotic cells had appeared to be arrested in early metaphase; the metaphase chromosomes of these mitotic figures appeared less organized than the mitotic figures of GFPi or mock controls (Fig. 2-15A, 2-16). The accumulation of the abnormal metaphase cells was noted with both Tel2.2i and Tel2.3i (Fig. 2-15B, C). Many of the cells that had accumulated in mitosis were abnormal and appeared to be arrested in prometaphase with misaligned chromosomes. Mitotic cells were scored as abnormal if they had chromatin that was dispersed away from the bulk chromatin (e.g. lagging chromosomes or misaligned chromosomes) (Fig. 2-16B). Based on these criteria, after Tel2 depletion with either Tel2.2i or Tel2.3i, I found that ~20% of the mitotic cells were abnormal.

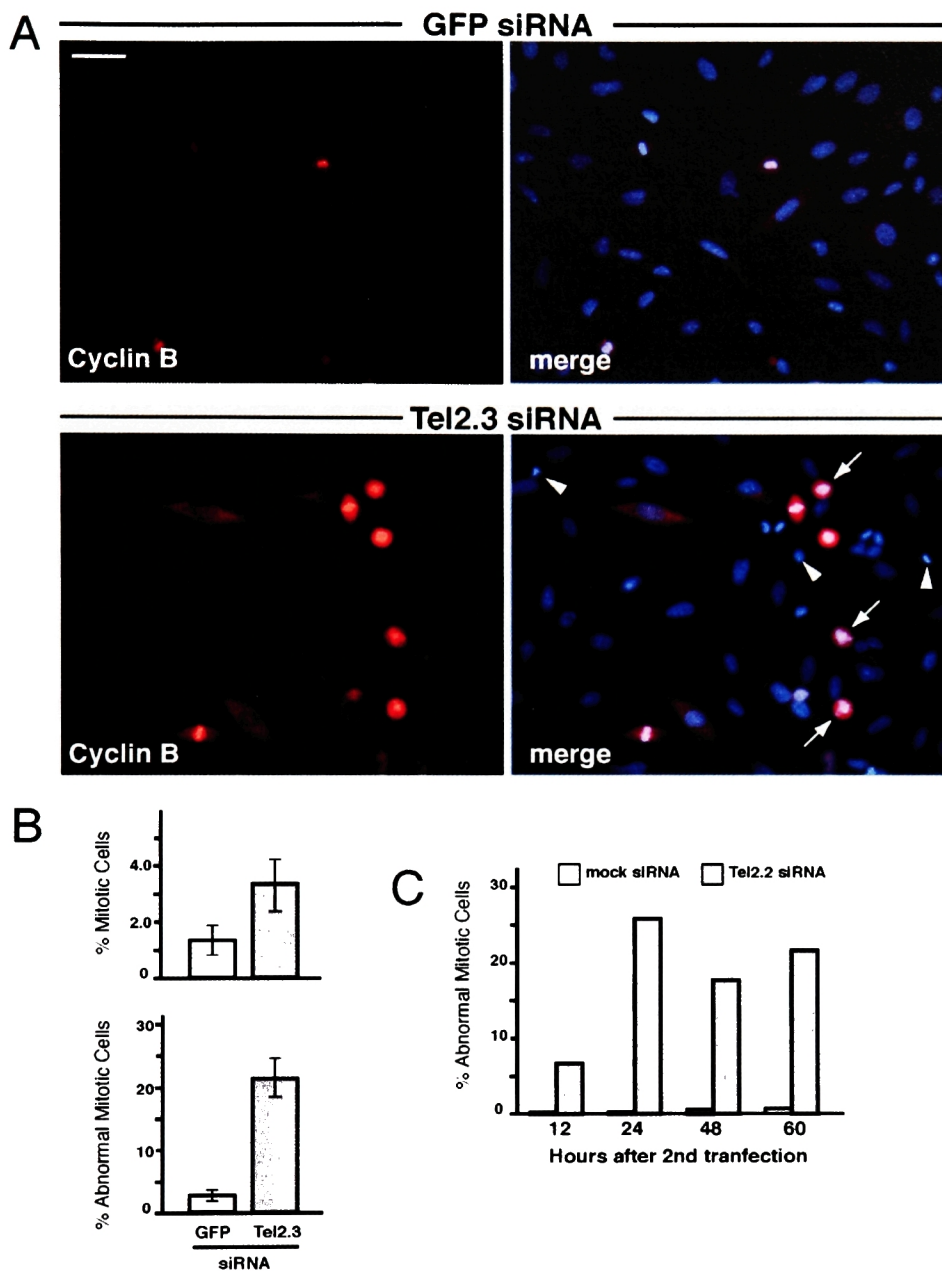


Figure 2-14. Depletion of Tel2 by siRNA results in the accumulation of abnormal early mitotic cells.

(A) Depletion of Tel2 results in an accumulation of abnormal early mitotic figures. Scale bar $\sim 50 \mu\text{m}$. HeLa2 cells were fixed and stained for Cyclin B (Santa Cruz; red) and DNA (DAPI, blue) after Tel2.3i transfection. Arrows indicate cells with defects in metaphase chromosome condensation that have arrested in early metaphase. Arrow heads indicate apoptotic nuclei which are compact DAPI staining nuclei that lack strong Cyclin B staining. (B) Quantitation of the metaphase accumulation induced by Tel2.3i. (Top) Percentage of mitotic cells as scored by Histone H3 (Cell Signaling) staining; >400 cells were scored for each experiment. (Bottom) Percentage of abnormal metaphases in all mitotic cells; cells were scored as abnormal when the chromatin was not organized on the metaphase plate or when masses of chromatin were separated from the bulk of the chromatin; >100 metaphases were scored for each experiment. Bars represent mean and SD from three experiments. (C) Time course of abnormal mitotic accumulation induced by Tel2.2i. >200 mitotic cells were scored for each time point.

In addition, staining for γ or α -tubulin revealed that most of the aberrant mitotic cells also had multiple (>3) centrosomes or defects in the assembly of the spindle around the chromatin. The accumulation of abnormal metaphase cells in Tel2.2i and Tel2.3i transfected cells is unlikely to be generated by off-target effects of the siRNA (e.g. depletion of spindle components) as the phenotype was notable with non-overlapping duplexes. However, recently it has been found that Dicer, a core component of the RNAi machinery involved in the cleavage of ds RNA, is required for the formation of normal heterochromatin. When Dicer is deleted in DT40 cells, the cells arrest in metaphase, show premature sister chromatid dissociation (PCD), and undergo apoptosis [248]. In my experiments, although the transfection of GFPi did not result in the gross accumulation of abnormal mitotic cells and apoptosis, the GFP siRNA duplex may not be the best control because it has no cognate mRNA and, thus, may be less detrimental to the RNAi machinery than those that do have *in vivo* targets.

In future experiments, to address the possible contribution of inhibiting the RNAi machinery to the potential Tel2 depletion phenotypes, it will be necessary to rescue the mitotic abnormalities through the overexpression of exogenous hTel2. Alternatively, mouse cells with a targeted deletion of mTel2 will help to discern the specific defects associated with the loss of Tel2 function.

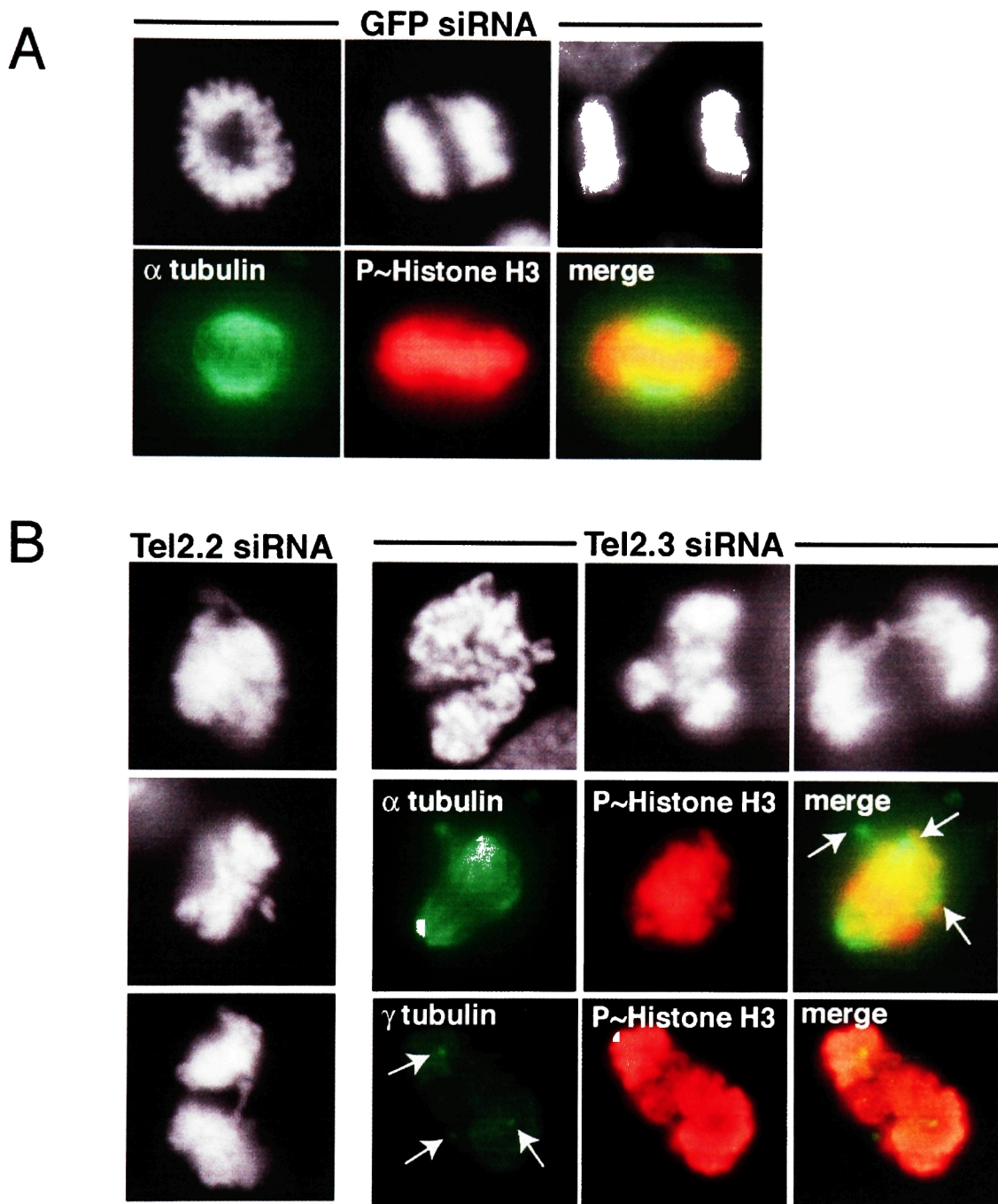


Figure 2-15. Depletion of Tel2 by siRNA results in the accumulation of abnormal early metaphases.

(A) HeLa cells after GFPi control transfection. (Top) Typical mitotic nuclei stained with DAPI after GFPi transfection. (Bottom) Cells were transfected and fixed in formaldehyde followed by staining for α -tubulin (Sigma; green) and phospho-Histone H3 (red). (B) Abnormal mitoses from Tel2.2i and Tel2.3i depleted cells. 48 hrs after 2 transfections of the indicated duplex, HeLa cells were fixed and stained for DAPI (white), α -tubulin (green), γ -tubulin (green), or phospho-Histone H3 (red) as labeled. Arrows indicate defects in the mitotic spindle or cells with defects in the mitotic spindle (middle) or extra centrosomes (bottom).

Metaphase chromosome abnormalities

After Tel2 depletion, there was an accumulation of abnormal metaphase cells with abnormal chromatin. To assess the appearance of the metaphase chromosomes more precisely, I performed metaphase spreads on cells that had been depleted for hTel2. 48 hours after transfection with Tel2 siRNA duplexes, metaphase spreads were harvested from colcemid arrested HeLa2 cells. After Tel2 depletion, an induction of chromosome end fusions was not detected; telomeres in Tel2 depleted cells also appeared to be intact when analyzed by telomere FISH (Fig. 2-16B). However, many spreads from hTel2-depleted cells had metaphase chromosomes with aberrantly condensed chromosomes. In contrast to GFPi or mock transfected HeLa2 cells, these chromosomes appeared very curly, though the chromatid arms were still relatively compact. After hTel2 depletion, ~15% of the metaphases spreads possessed abnormally condensed chromosomes (Fig. 2-17B). Metaphases were scored as abnormal if more than 10 chromosomes on the spread possessed > 3 turns/chromatid (Fig. 2-17B).

Sister chromatids were roughly symmetrical in their curling pattern (Fig. 2-17A). This mirror symmetric uncoiling is consistent with previous descriptions of the higher-order structuring of mitotic chromosomes. Extended incubations (>1 hr) in hypotonic saline or the depletion of the linker Histone H1 have revealed that mitotic chromosomes possess an underlying coiled structure [249, 250]. In these experiments, the chromosome defects are not an artifact of sample preparation as GFPi control cells that were processed in parallel did not show the same defects.

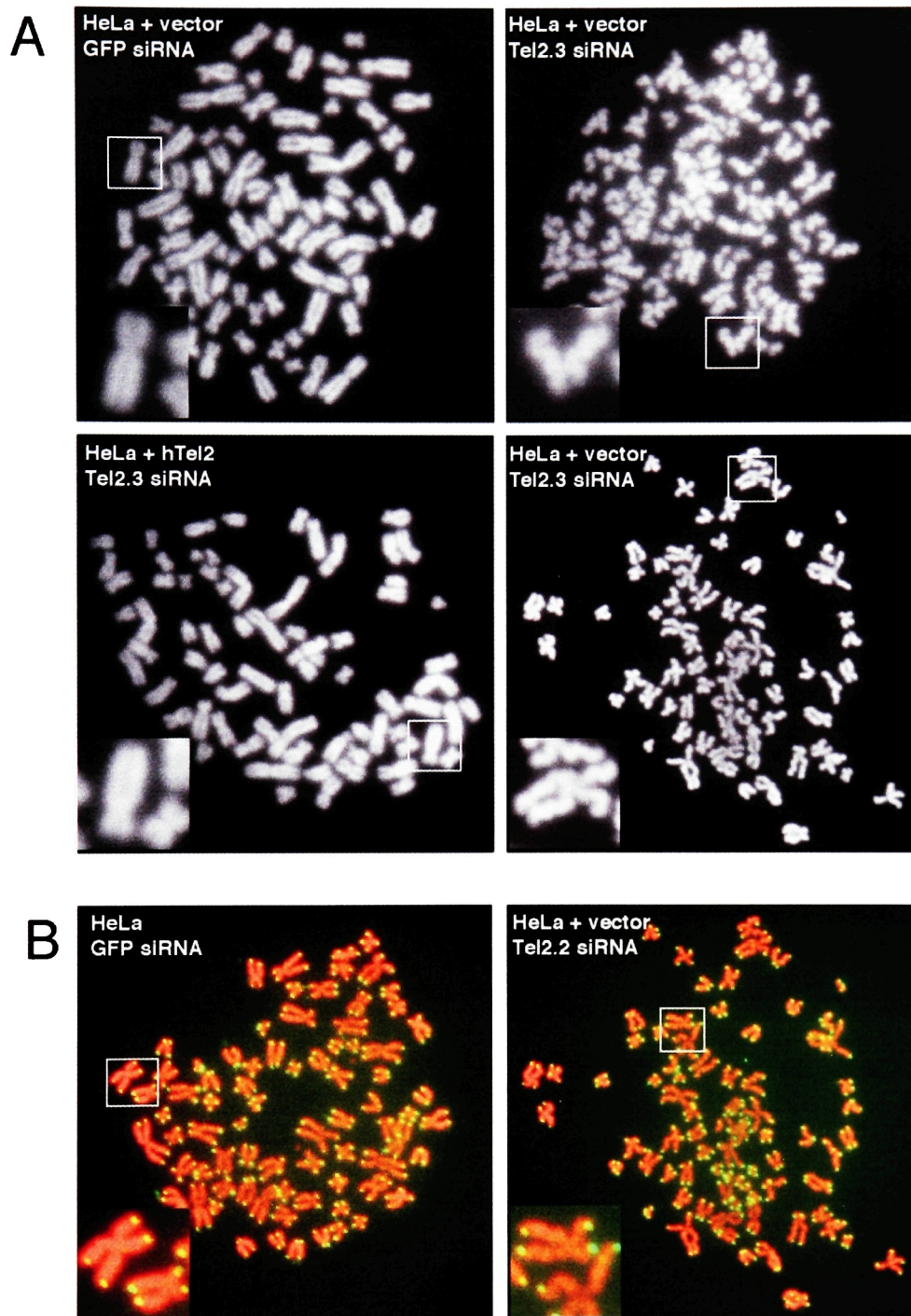


Figure 2-16. Tel2 depletion causes defects in chromosome condensation.

(A) Metaphase spreads of Tel2 depleted cells reveal defects in chromosome condensation. HeLa2 cells were transfected with Tel2.2i or Tel2.3i, enriched for metaphases with colcemid, and fixed in methanol:acetic acid (3:1) for metaphase spreads 48 hrs after transfection. Tel2 depletion results in the accumulation of metaphase chromosomes with defects in condensation. (*Bottom left*) Stable expression of hTel2 rescues the metaphase abnormalities. (Insets) Magnification of individual chromosomes from each spread. (B) Telomere PNA-FISH on Tel2.2 depleted spreads. There were no obvious telomere aberrations in 10 metaphases each of Tel2.2i and Tel2.3i transfected cells.

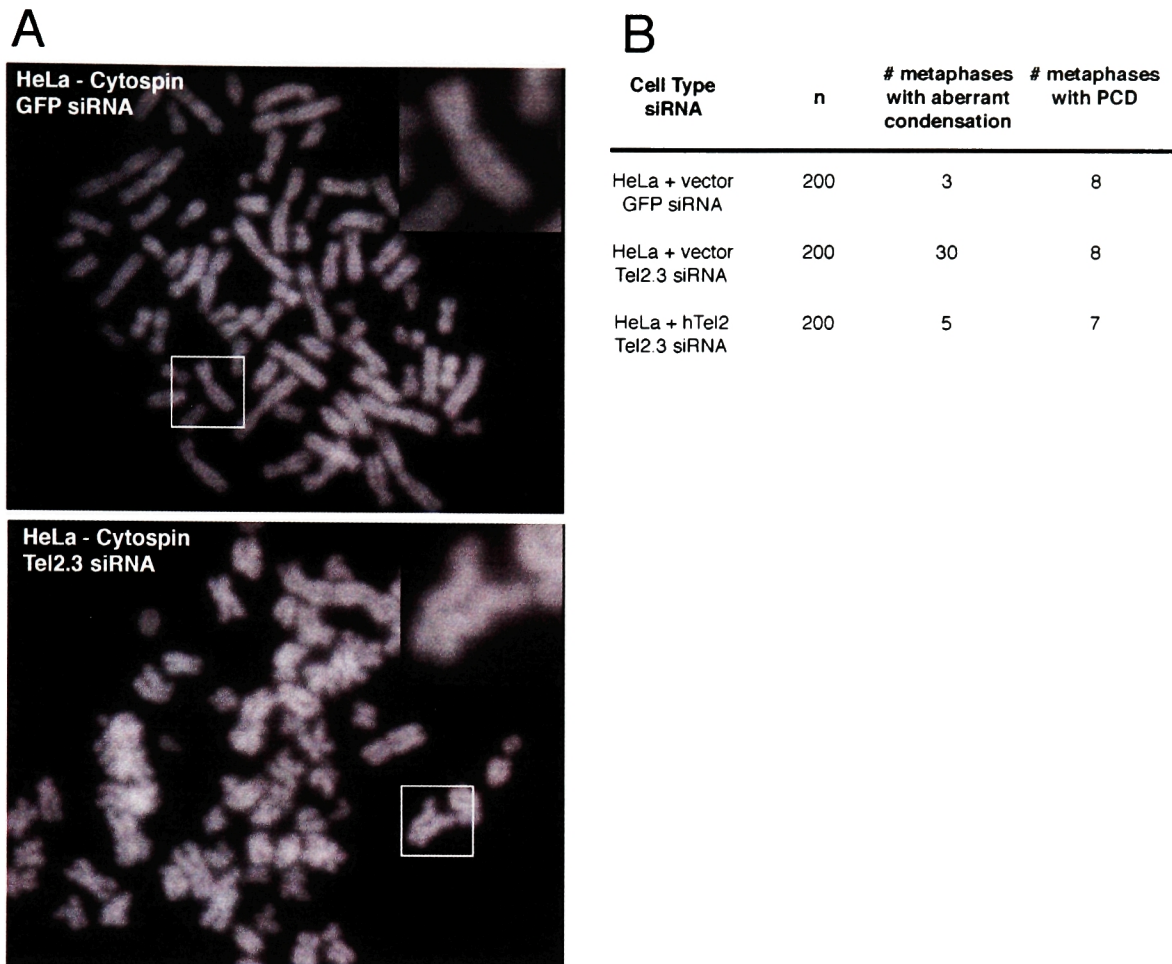


Figure 2-17. hTel2 expression rescues Tel2 depletion mediated defects in chromosome condensation.

(A) Metaphase chromosomes prepared by Cytospin also had defects in condensation after Tel2 depletion. (*Inset*) Magnification of individual chromosomes. (B) Scoring of chromosome abnormalities caused by Tel2.3 transfection. 200 metaphases were scored for each condition. Metaphases were scored as abnormal if >10 chromosomes in each spread had 3 or more curls per chromatid. Metaphases were scored as PCD+ only if <10 chromosomes in each spread had completely separated sister chromatids.

In addition, I found that defects in chromosome compaction were also apparent under non-spreading conditions when mitotic cells were fixed on coverslips (Fig. 2-15B). As an additional control, after the preparation of metaphase chromosomes by Cytospin, Tel2 depleted, but not GFPi transfect cells, still showed similar defects in chromosome coiling (Fig. 2-17A). Finally, the overexpression of hTel2 in HeLa2 cells rescued the metaphase chromosome abnormalities caused by Tel2.3i transfection back to levels of the

GFPi transfection control (Fig. 2-17B). Because Tel2.3i transfection did not induce premature centromere dissociation (PCD) in the same set of experiments, it is unlikely that the metaphase abnormalities are secondary to defects in the formation of heterochromatin caused by an inhibition of Dicer. However, it is possible that the depletion of Tel2 causes a synthetic phenotype with additional unrecognized defects in HeLa cells. Thus, it will be important to confirm the possible role of Tel2 in chromosome condensation in a separate cell line or in knockout mouse fibroblasts.

Overexpression of hTel2 overrides DNA damage checkpoints

In *C. elegans*, both *rad-5* and *clk-2* mutants are defective in DNA damage dependent cell cycle arrest and apoptosis. Because hTel2 is essential for viability, we assessed the DNA damage checkpoint responses of IMR90 cells overexpressing hTel2. We irradiated vector control or hTel2 overexpressing IMR90 with increasing doses of ionizing radiation (1, 2, 6 Gy) and allowed them to recover for 16 hrs in the presence of colcemid. As expected, increasing doses of irradiation inhibited the accumulation of mitotic figures for both control and hTel2 overexpressing cells (Fig. 2-18A). However, we found that cells overexpressing hTel2, but not truncated version of N-terminally tagged Tel2, consistently possessed more mitotic figures than control cells (Fig. 2-18A). After exposure to IR, mammalian cells experience two distinct G2 "checkpoints": a transient (<2 hrs), ATM-dependent, dose-independent mitotic arrest and a more prolonged (12-72 hrs), ATM independent, dose dependent G2 accumulation [251].

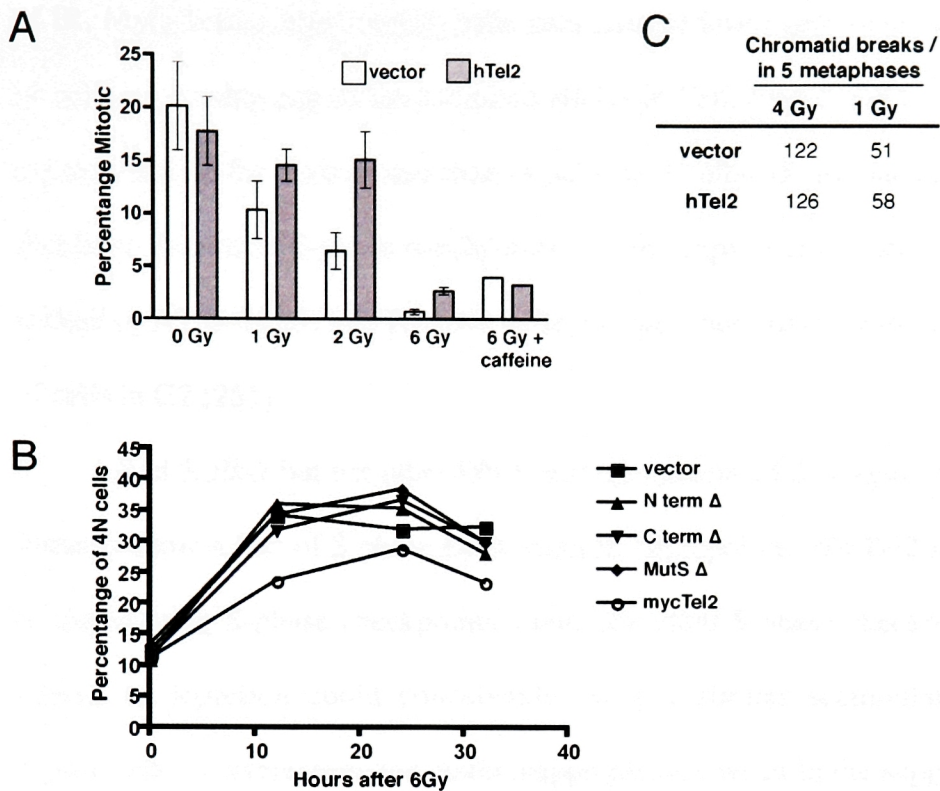


Figure 2-18. Overexpression of Tel2 impairs IR-induced arrest prior to mitosis.

(A) Tel2 overexpression results in the accumulation of. IMR90 cells were irradiated as indicated and transferred to colcemid for 16 hr. Cells were then fixed and stained for phospho Histone H3 to identify mitotic cells. Bars represent the mean and SD from 3 experiments with >400 cells. As a control, caffeine was added at 15 mM, 1 hr prior to IR to abrogate the "G2/M checkpoint" (B) IMR90 cells expressing various alleles of Tel2 were irradiated with 6 Gy and harvested for FACS at 12, 24, and 32 hrs. Data are plotted as the percentage of cells with 4N DNA vs. total cells. (C) Cells were incubated in 15 mM caffeine for 1 hr, irradiated at indicated dose, and harvested for metaphases after 4 hrs. Breaks were scored in 5 metaphases.

Thus, it was possible that the accumulation of mitotic cells 16 hr after IR could reflect an abrogation of either of the two checkpoints. However, hTel2 overexpression appeared to suppress the accumulation of mitotic cells in a IR-dose dependent fashion; the disparity between control and Tel2 expressing cells was most evident at 2 and 6 Gy of IR (Fig. 2-18A).

To confirm that hTel2 overexpressing cells were defective in G2 accumulation rather than mitotic arrest after IR, I analyzed IMR90 cells expressing different alleles of hTel2 by FACS after IR. At three sequential time points (12, 24, and 32 hr) after 6 Gy

of IR, Myc_Tel2 overexpressing cells accumulated fewer cells in G2 than vector control or cells expressing any of the truncated alleles of Tel2 (Fig. 2-18C). The pathways that are responsible for the accumulation of cells in G2 after IR are unclear. However, cells that have defects in S-phase checkpoints (i.e, undergo radio-resistant DNA synthesis)--including ATM, Nbs1, and BRCA1 deficient cell lines--have a prolonged accumulation of cells in G2 [251].

Rad-5/clk-2 but not other DNA damage mutants of *C. elegans* (*hus1*, *mrt-2/rad1*) mutants show a loss of S-phase DNA damage checkpoints. If hTel2 were also involved in maintaining S-phase checkpoints, then, like other S-phase checkpoint deficient-cell types, its depletion could conceivably cause a similar accumulation of G2 cells. Conversely, its overexpression could inappropriately result in the suppression of this G2 checkpoint. Because the accumulation of cells in G2 is so poorly defined, the possible relationships with the S-phase DNA damage checkpoint are highly speculative. In future experiments, it will be helpful to determine the effects of hTel2 overexpression on better defined DNA damage checkpoints (G1, S phase, and G2/M mitotic). Furthermore, it may be informative to determine whether hTel2 overexpression affects viability after IR or S-phase stressors (HU, aphidicolin). Preliminary experiments suggest that hTel2 expression does not increase the repair of cells after IR as cells overexpressing hTel2 possess similar levels of breaks as vector control cells at two different doses of IR.

CONCLUSION

hTel2 is not an abundant component of mammalian telomeres

In somatic human cells, we find that endogenous hTel2 is not enriched at telomeres by IF, does not precipitate telomeric DNA in ChIP assays, does not interact

with telomere binding proteins, and does not affect telomere length maintenance when overexpressed. Furthermore, hTel2 does not bind telomeric DNA (Parsons and de Lange, unpublished). We conclude that hTel2 is not an abundant component of telomeres. Like hTel2, Ku70/80, DNA-PK, and the WRN helicase do not localize to telomeres in telomerase positive cells by IF. However, these proteins, which are not abundant or exclusive components of mammalian telomeres, have been shown to affect telomere function. As described in detail in the introduction, the absence or mutation of the NHEJ joining factors results in both telomere length and capping defects. In *Terc*^{-/-} mice, the Werner helicase is required for optimal telomere maintenance [252]. The subtle effects of Ku on telomere capping could be explained by the vigorous ability of the Ku heterodimer to bind DNA ends, including telomeric DNA ends, *in vitro*, thus targeting it to telomeres [206]. In contrast to Ku, hTel2 has no affinity for telomeric DNA *in vitro*. In addition, the effects of WRN or Ku on telomeres could be mediated by their interactions with telomere binding proteins, thereby targeting the proteins to telomeric DNA. However, in contrast to WRN and Ku, hTel2 does not detectably interact with known telomere binding proteins.

hTel2 overexpression induces telomere elongation

Although hTel2 does not appear to associate with telomeres, I found that the overexpression of untagged hTel2 resulted in slow telomere elongation in HTC75 and SK-HEP-1 cells. In addition, its overexpression may slow telomere shortening in HeLa1.2.11 cells, which possess very long, but unstable telomeres. Curiously, the expression of an N-terminal epitope tag may impair hTel2's ability to mediate telomere elongation. However, these results are preliminary, and need to be confirmed. It is

plausible that Tel2 mediate telomere lengthening exerts its effects through promoting telomerase rather than inhibiting telomere shortening. This is based on the observation that the expression of Myc tagged Tel2 alleles do not affect shortening rates in primary IMR90 cells. However, because N-terminal epitope tagging protein might have interfered with its function, these experiments should be repeated. Consistent with a requirement for telomerase in hTel2-mediated elongation, the overexpression of hTel2 in U2-OS cells did not grossly affect telomere length. In future studies, it may be informative to assess whether the depletion of hTel2 by shRNA results in telomere shortening. Because hTel2 is probably essential, a partial knock-down of Tel2 may be informative about its role in telomere length. HTC75 fibrosarcoma may be useful for these studies, as RNA interference appears to happen less efficiently in this cell type.

It is not clear how hTel2 might promote telomere elongation. ScTel2 affects the telomeric chromatin as assessed by the loss of TPE. It is possible that hTel2 affects the telomeric chromatin of human cells to promote elongation. Alternatively, overexpression of Tel2 could promote the stability and activity of telomerase. Intriguingly, hTel2 co-localizes with PML-NBs and also a fraction of Cajal bodies. Cajal bodies are known to be involved in hTERC stability and processing. To test the possible effects relationship between hTel2 and Cajal bodies, it may be useful to visualize PML-NBs and Cajal bodies after hTel2 depletion. If the structure of Cajal bodies is perturbed after hTel depletion, it may be interesting to investigate possible relationships between Tel2 and hTERC.

A role for Tel2 in mitotic progression?

The depletion of Tel2 in HeLa2 cells results in cell death, and the targeted deletion of mTel2 in mouse cells results in the induction of senescence (Takai and de

Lange, unpublished). The telomeres of HeLa2 cells after Tel2 depletion are intact (Fig. 2-17A), so it becomes clear that Tel2 has an essential function(s) away from the telomere. What are those essential functions? Clues about hTel2's function may come from the phenotypes of hTel2 depleted HeLa2 cells. In addition to apoptotic cells, the depletion of hTel2 by siRNA in HeLa2 cells resulted in a mild mitotic arrest. The mitotic arrest induced by hTel2 depletion is much less pronounced than the mitotic arrest induced by the depletion of either mitotic kinases or spindle components (e.g. Plk1 or TPX2). However, perhaps consistent with a role in mitosis, Tel2 localizes to centrosomes in both human and mouse cells. Many proteins involved in mitotic progression and spindle assembly are localized to centrosomes. The localization of other mitotic kinases—Plk family, CyclinB-Cdk1, and Aurora family—exhibits dynamic changes between centrosomes, kinetochores, and the spindle (reviewed in [253]) as cells progress from G2 through mitosis. I did not note a dynamic pattern of Tel2 localization through cell cycle progression. Furthermore, the majority of Tel2 was localized to the nucleus suggesting significant extra-centrosomal roles.

Thus, the significance of Tel2's localization to centrosomes should be confirmed and dissected more carefully either by monitoring the localization of a GFP-Tel2 fusion protein in real time or observing the localization of the protein in synchronized cells. In addition, the availability of Tel2^{-/-} fibroblasts should be able to confirm the specificity of Tel2's localization to centrosomes. Although it is unlikely that hTel2 is directly involved in mitotic progression, the accumulation of aberrant mitotic cells and centrosomal localization of Tel2 may hint at an indirect function in regulating the G2 to M transition.

A role for Tel2 in chromosome condensation?

We find that metaphase spreads from hTel2 depleted cells have a coiled and contorted appearance. The process of chromosome condensation from G2 to M is a complex and involves several protein complexes and is likely to be coordinated by mitotic kinases. Condensin and topoisomerase II play are known to be essential for the higher-order structuring of chromosomes from G2 to M [254, 255]. Their deletion or inhibition results in severe defects in chromosome structure. Under hypotonic spreading conditions, the compact structure of mitotic chromosome is completely dispersed by the depletion of either topoisomerase II or condensin I [254, 255]. Curiously, the depletion of a second, vertebrate-specific condensin complex (condensin II) resulted in coiled chromosome aberrations that appear very similar to the defects resulting from Tel2 depletion [256]. However, despite phenotypic similarities between Tel2 and Condensin II depletion, the localization of Tel2 and the condensins are distinct. Importantly, condensins localize to mitotic chromosomes while Tel2 does not. It would be worthwhile testing whether there a direct interaction between hTel2 and any component of the condensin proteins. IP of Myc_Tel2 did not detect an interaction between Myc_Tel2 and the cohesin subunits SMC1 or SMC3 (Fig. 2-4C).

Because the depletion of Tel2 results in a weaker defect in chromosome organization than has been previously noted for proteins directly involved in the process, it is unlikely that Tel2 is an essential component of these protein complexes. Recently, it has become clear that chromosome condensation and mitotic progression are intimately linked processes. The disruption of one process results in defects in the other; for example, the depletion of condensin causes the aberrant localization of the INCENP complex and vice versa [255, 257]. Thus, it is possible that the defects in chromosome

condensation and the aberrant mitotic spindles are related phenomenon. Unfortunately, this gives us no insight on the primary defect caused by Tel2 depletion.

A role for hTel2 in DNA damage checkpoints?

Rad-5/clk-2 has a role in recognizing and/or repairing DNA damage. The mutants are unique in their requirement for the recognition of damage induced by HU. The chromosome instability evident in *tel2Δ/Tel2* diploid yeast cells would also be consistent with a role for Tel2p in DNA damage signaling. Our finding that overexpressing hTel2 inhibits the accumulation of cells in G2 after DNA damage suggests that hTel2 may have a checkpoint regulatory functions in mammalian cells. The G2 accumulation checkpoint is not well defined, so it is speculative to draw conclusions about more specific roles of hTel2 in other DNA damage checkpoints. It would be best to assess the function of Tel2 in loss-of-function experiments. However, because Tel2 is essential, these questions may be difficult to assess. Further analysis of the effects of hTel2 overexpression on G1, S and G2-M DNA damage checkpoints may yield some insights into the role of the mammalian Tel2 in DNA damage recognition and repair.

CHAPTER 3:

GENETIC AND MOLECULAR ANALYSIS OF TRF2 Δ B

INDUCED HOMOLOGOUS RECOMBINATION AT

MAMMALIAN TELOMERES

INTRODUCTION

Homologous Recombination (HR) and the repair of double strand breaks

Compared to single strand DNA lesions, double strand breaks (DSBs) are particularly troubling for a genome because there is a greater potential for the loss of genetic information. DSBs can arise as a result of a variety of stresses including irradiation, genotoxic agents, or replication fork collapse. Eukaryotes have two distinct pathways for the repair of these lesions. Of non-homologous end joining (NHEJ) and HR, the latter is the preferred repair pathway because it relies on a homologous template to ensure the accuracy of repair.

Groundbreaking principles in the process of HR were first proposed by Robin Holliday in 1964 to explain the features of allelic segregation in meiotic recombination [258]. He speculated that single stranded DNA from one chromosome could anneal to a homologous chromosome by displacing the corresponding strand and form a four-stranded heteroduplex structure, now called a Holliday Junction (HJ). Holliday's original proposal has provided a framework for numerous models to explain the mechanisms of DSB repair [259]. Although mechanistic details of different DSB repair models differ, several processes are necessary for all of the models. These include the formation and stabilization of a single stranded DNA molecule, the invasion of the single stranded DNA into homologous DNA to form heteroduplex DNA, and the ultimate resolution of the heteroduplex structure, often a HJ. Importantly, many of the proteins essential for HR are known to have biochemical functions that correspond to these fundamental processes. I will introduce some of the important factors in HR and their potential roles in telomere maintenance.

Conserved Members of the Rad52 Epistasis Group—Rad51, Rad52, and Rad54

In *S. cerevisiae*, genetic studies have identified a large group of genes that are required for efficient DSB repair by HR. One member, RAD51, is a small (~38 kDa)

protein that can form long nucleoprotein filament together with single-stranded DNA [260, 261]. Homologs of RAD51 can be found in all organisms including prokaryotes (RecA) and archaea (RadA) and have been shown to promote the invasion and strand exchange of single stranded DNA into homologous duplex DNA [262, 263]. ATP binding by conserved Walker boxes is required for the heteroduplex promoting activity.

In *S. cerevisiae*, *rad52* mutants are hypersensitive to IR and have severe defects in DSB mediated HR (reviewed in [264]). Consistent with an important role in HR, RAD52 was shown to interact with RAD51 to promote strand invasion [265, 266]. However, these functions are either not conserved or redundant with other HR proteins in most vertebrates as chicken and mouse cells that lack Rad52 show very modest (<2 fold) defects in HR and no sensitivity to IR [267, 268].

Another molecule that promotes the formation and stability of heteroduplex DNA is Rad54. In addition to interacting with RAD51, RAD54 and its homolog Rdh54 (Rad54B in humans) are DNA dependent ATPases with helicase motifs [269, 270]. In both *S. cerevisiae* and mouse cells, deletion of Rad54 confers sensitivity to IR. Furthermore, Rad54^{-/-} mouse cells deficient for Rad54 have defects in DSB repair [271, 272].

Some components of the Rad52 epistasis group appear to have roles in telomere maintenance. In chicken DT40 cells deficient in Rad51, telomeric overhangs appear to be >1.5 fold longer [213]. Also, Rad54^{-/-} mouse cells appear to have slightly shorter telomeres and moderate defects in telomere capping [187]. Chicken cells deficient for Rad54 may show slight telomere elongation [213]. Thus, although the mechanisms are unclear, it appears that Rad54 may have a role in telomere maintenance in vertebrates.

Additional mediators of HR—BRCA1, BRCA2, and the Rad51 paralogs

Not all factors important for HR in vertebrates are conserved in *S. cerevisiae*. Mutations in BRCA2 impair HR, predispose cells to genomic instability, and promote the development breast and/or ovarian cancers [273-275]. BRCA2 is a large (~384 kDa)

protein that interacts with Rad51 through central and C-terminal BRC motifs and single stranded DNA through C-terminal OB folds [276, 277]. BRCA1, a ~208 kDa protein encoded by a distinct breast cancer susceptibility gene, is also required for efficient HR in mammalian cells [278, 279]. BRCA1 may itself bind DNA and also interacts with a number of proteins that are known to bind and modify DNA including BARD1, the Mre11 complex, and BRCA2. The exact mechanism through which BRCA2 and BRCA1 promote HR is not known. Neither BRCA1 nor BRCA2 have been implicated in telomere maintenance in mammalian cells.

Two paralogs of Rad51 were cloned by complementation of radiosensitive rodent cell lines, XRCC2 and XRCC3 [280]. An additional three paralogs of Rad51—RAD51B, RAD51C, and RAD51D—were cloned by virtue of their homology to Rad51/RecA [280-284]. Although *S. cerevisiae* does possess two additional Rad51-homologs, Rad55 and Rad57, it is unclear whether they are functional homologs of any of the vertebrates Rad51-like genes [285]. Biochemical studies indicate that the Rad51 paralogs form at least two subcomplexes—one containing RAD51B, C, D, and XRCC2 (BCDX2) and one containing Rad51C and XRCC3 (CX3) [286, 287]. Both BCDX2 and CX3 subcomplexes bind ssDNA *in vitro* and may promote homologous pairing [287-289].

Hamster cell lines deficient for RAD51C (CL-V4B, *irs3*), XRCC2 (*irs1*), or XRCC3 (*irs1SF*) are hypersensitive to IR [280, 281]. Cell lines deficient for RAD51C or XRCC3 showed additional defects in HR as assessed by transposon integration, reduced SCE, and abnormal repair products [290-293]. Human cells deficient for XRCC3 are sensitive to cisplatin, impaired in the formation of Rad51 foci, and show decreased levels of HR as assessed by SCE and gene targeting [294]. DT40 cells deleted for any of the Rad51 orthologs and *Xrcc2*^{-/-} deficient hamster cells all showed hypersensitivity to DNA damage, impaired HR, and impaired Rad51 foci formation [295, 296].

Moreover, recent results have demonstrated not only that Rad51C promoted the cleavage of model HJ *in vitro* but also that extracts from cells deficient for RAD51C or

XRCC3 were severely impaired for HJ resolution [297]. Collectively, these data suggest that the Rad51C and, in particular, the CX3 subcomplex are closely associated with HJ resolution activity in mammalian cells. Importantly, Rad51D^{-/-} mouse fibroblasts had shorter telomeres and showed a modest increase in the number of telomere fusions (~2 fold). Rad51D may be unique amongst Rad51-like genes in its role in telomere maintenance, as it was the only ortholog found to associate with telomeric chromatin by IF and ChIP [298].

The RecQ helicases—complex roles in HR

The RecQ helicases are evolutionarily conserved helicases that are critical for the maintenance of genome stability. Humans have 5 RecQ helicase homologs; strikingly, three of these helicases—WRN, BLM, or RECQ4—are mutated in human diseases, Werner's syndrome, Bloom's syndrome, and Rothmund-Thomson syndrome, respectively. These diseases have similar symptoms that include cancer predisposition and premature ageing. The RecQ helicases may be involved in the suppression or resolution of certain types of HR. Strong evidence for this role comes from the observation that the lethal phenotype of an *sgs1, srs2* (a non RecQ helicase) double mutant can be rescued by the concomitant deletion of *rad51* [299]. This function appears to be conserved for the WRN helicase in mammalian cells [300]. Furthermore, these findings are also consistent with the ability of RecQ helicases to promote branch migration and unwinding of HJs *in vitro* [301, 302]. Recent studies have demonstrated that the RecQ helicases suppresses crossovers during DSB repair by HR [303, 304].

Many of the RecQ helicases appear to play roles in telomere maintenance. The G-rich repeat strand of telomeres in most organisms have the ability to form intramolecular G-G base-paired quadruplex DNA, or G-quartets. RecQ helicases are unique amongst nucleases in their ability to unwind G quartets; thus, the recruitment of the helicases could be important to the unwinding of these structures, especially during S-phase to promote efficient replication [305]. Consistent with a role for these helicases in

telomere maintenance, TRF2 was found to bind both the WRN and BLM helicases and stimulate their helicase activity [306]. Furthermore, mice deficient for both the WRN helicase and hTERC showed more dramatic telomere dysfunction and accelerated ageing phenotypes when compared with either single mutant [252]. Finally, the RecQ helicases appear to play an important role in telomere maintenance in the absence of telomerase for both human ALT cells and *S. cerevisiae* survivors, a subject which will be discussed in more detail in the upcoming sections.

The modulation of HR by other DNA repair pathways

In addition to the RecQ helicase family, DNA repair proteins that are not directly involved in catalyzing HR affect the process. For example, the endonuclease ERCC1/XPF (Rad10/Rad1 in *S. cerevisiae*) is unique among the nucleotide excision repair (NER) factors in its ability to regulate homologous recombination [307]. Studies indicate that the endonuclease may promote the removal of non-homologous sequences or inter-strand crosslinks (ICLs) to promote HR [308, 309]. In addition, recent studies have expanded the role of the ERCC1/XPF in HR and suggested that it may promote HR of identical sequences in the absence of ICLs or non-homologous tails and inhibit the recombination of imperfectly matched heteroduplexes [310, 311]. As described previously, the ERCC1/XPF endonuclease complex is recruited to telomeres by TRF2 and may prevent the inappropriate recombination of telomeric sequences and formation of telomeric double minutes [131].

Mismatch repair (MMR) proteins also inhibit the HR of slightly divergent sequences (homeologous recombination) [310]. MutS family members (Msh2, Msh3, and Msh6) and MutL family members (Mlh1, Pms1) may inhibit homeologous recombination by recognizing mismatches in heteroduplex DNA and promoting its rejection through unwinding by the Sgs1 helicase [310, 312, 313]. The mismatch repair proteins have not been shown to have a role in normal telomere maintenance.

A final DNA repair pathway known to modulate HR is the other major DSB repair pathway, NHEJ. In mammalian cells, NHEJ competes with HR to repair DSBs [314, 315]. This could occur if the binding of Ku or DNA-PKcs to DSBs prevented the nucleolytic resection of the DSB into ss DNA, a step which is thought to be required for repair by HR. The role of NHEJ factors in telomere maintenance is discussed in detail in Chapter 1.

HR in telomere shortening—Telomere Rapid Deletion (TRD)

Although there had been considerable circumstantial evidence for the involvement of HR in telomere function, some of the earliest direct evidence of a role for recombination in normal telomere maintenance came from the work of Art Lustig and colleagues in budding yeast. *S. cerevisiae* normally maintain their telomeres at ~350 bp in length. However, the expression of *rap1'* alleles, in which there is a deletion of ~150 residues at the C-terminus, results in telomeres elongating by as much as 4 kb. This elongation is due to the inability of the *rap1'* alleles to recruit the negative length regulators Rif1 and Rif2 to the telomere. The elongated telomeres generated in *rap1'* expressing cells are unstable and frequently delete themselves to shorter lengths in a process later called telomere rapid deletion (TRD) [316, 317]. The analysis of the deletion products by Southern blot indicated that TRD stochastically deleted the telomeres to near wild-type lengths without the apparent accumulation of products of intermediate lengths. Genes located adjacent to long telomeres may be transcriptionally silenced; the longer the telomere, the more likely it is that a gene will be silenced. Based on the phenomenon of TPE, Li and Lustig developed a colony color assay to monitor the repression of the *ADE2* gene and, indirectly, the rate of TRD [317]. They found that the rate of TRD was ~1 event/100 cell divisions in haploid yeast.

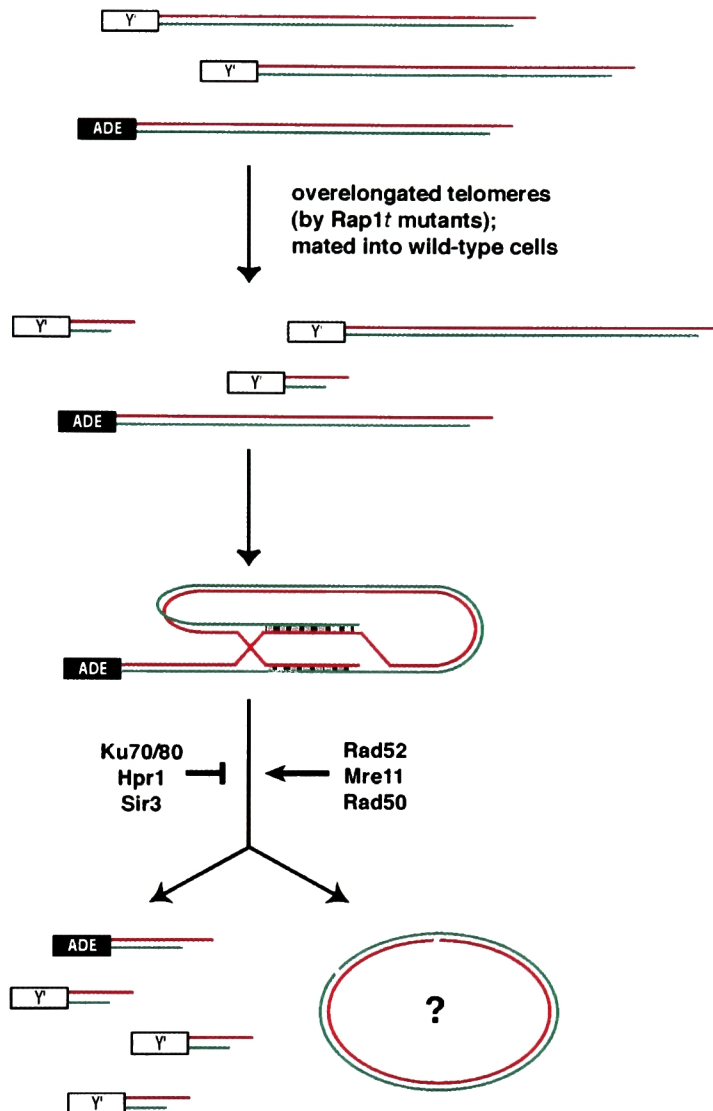


Figure 3-1. A Model for Telomere Rapid Deletion (TRD) in *S. cerevisiae*.

The expression of *rap1t* alleles in *S. cerevisiae* results in telomere elongation. These overelongated telomeres can be mated into wild-type yeast. The longer telomeres are stochastically resized to normal telomere length in a process called telomere rapid deletion (TRD). The rate of TRD can be monitored through experiments using an *ADE2* marked telomere [317]. Using this marked telomeres, Lustig and colleagues found that TRD was promoted by Mre11, Rad50, and Rad52. Ku70/80, Hpr1, and Sir3 inhibited TRD. It has been proposed that TRD occurs through an intrachromatid recombination event. However, it is not known whether a circle of telomeric DNA is generated as a result of this process.

Using the silencing assay, it was found that the deletion of *rad52* resulted in a three-fold decrease in the efficiency of TRD [317]. The loss of *hpr1* promotes the intrachromatid recombination of long or G+C rich repeat sequences in a manner that is dependent on transcription through the region [318, 319]. Consistent with a role for HR

in promoting TRD, *hpr1* mutants had a ten-fold increase in the rate of TRD. The promotion of TRD by *hpr1* is upstream to *rad52*-dependent HR, as an *hpr1rad52* double mutant cell still showed a two-fold suppression of TRD. Another conclusion of this study was that the *sir3* protein, involved in telomeric silencing, also increased the rate of TRD and decreased the precision of its deletion products causing the accumulation of telomeres of intermediate deletion lengths. Sir3p is recruited to telomeres by the Ku heterodimer. Consistent with their interaction, it was found that the deletion of Ku also increased the rate of TRD while decreasing the precision of its deleted products [197]. More recently, Mre11 and Rad50, but not Xrs2, seem to be required for efficient TRD [320].

As overelongated telomeres were being shortened by TRD, it was not possible to detect reciprocally elongated telomeres by Southern [316, 317]. Furthermore, TRD is strongly stimulated by the *hpr1* mutant, which is implicated in promoting intrachromatid deletions. These two pieces of evidence suggested that the TRD occurred through an intrachromatid rather than interchromatid mechanism. To address the mechanism of TRD more directly, Lustig and colleagues marked an elongated telomere with *HaeIII* restriction sites and found that the sites were not transferred to other telomeres making intertelomeric exchanges unlikely [320]. Based on these genetic and molecular assays, Lustig and colleagues conclude that TRD in yeast occur through end-initiated intrachromatid homologous recombination events.

HR in telomere elongation: survivor pathways in *S. cerevisiae*

In addition to contributing to rapid deletion events, homologous recombination has been implicated in telomere elongation in *S. cerevisiae*. Most yeast that are mutated in the *est* pathway (*tlc1Δ*, *est1Δ*, *est2Δ*, *est3Δ*, *cdc13-2*) shorten telomeres until they senescence after 40-60 generations [224, 321]. However, in the absence of sufficient telomerase activity, some percentage of yeast cells can maintain their telomeres through one of two survivor pathways [322]. Both survivor pathways absolutely require Rad52

and result in the amplification of repeats to protect the chromosome ends. However the two pathways have are significantly different. The Type I pathways also requires Rad51, Rad54, Rad55, and Rad57 and result in the amplification of subtelomeric Y' repeats. Furthermore, the Type I pathway is unstable and often converts to the TypeII survivor pathway upon extended culturing. Type II survivors require the MRX complex, Rad59, and the RecQ helicase Sgs1. Type II survivors amplify just telomeric repeats in order to maintain their chromosome ends. The genetic or epigenetic changes that determine the frequency and type of survivor pathway are not understood.

Additional insight into possible mechanisms of recombination mediated telomere elongation comes from *Kluyveromyces lactis*. These budding yeast can also elongate their telomeres without telomerase in a Rad52 dependent manner [323]. A minority of the *K. lactis* survivors possessed telomeres that had restriction patterns consistent with replication from small circles of telomeric DNA. Transforming *K. lactis* with small circles of telomeric DNA increases the efficiency of this type of alternate telomere maintenance [324]. Rolling circle telomere replication appears to be another possible result of homologous recombination at telomeres. Mismatch repair appears to inhibit the ability of survivors to arise from senescent cells lacking telomerase. The loss or mutation of Msh2 in either both *S. cerevisiae* and *K. lactis* enhances the growth of telomerase null strains [325]. As mismatch repair was not previously known to have a role in telomere maintenance, the mechanism through which MMR inhibits the survivor pathways is unclear.

A possible role for HR in telomere maintenance without telomerase

Although most human tumors have reactivated telomerase, some portion of them may maintain telomeres by alternative means, collectively referred to as alternative lengthening of telomeres (ALT). By definition, ALT cells are capable of maintaining the lengths of their telomeres without detectable telomerase activity. However, because a clear mechanism for ALT has yet to be defined, it is likely that there is more than one

non-telomerase mechanism for telomere maintenance. ALT cells are characterized by very heterogeneous telomeres; while the mean TRF length is ~20 kb, the length can range from 3 kb to over 50 kb [326]. The heterogeneity of telomere lengths occurs individual cells, as FISH on ALT cells reveal that some chromosome ends have no detectable signal while other cells ends have very long telomeres [327].

In addition to telomere heterogeneity, ALT cells are also characterized by the presence of a unique nuclear body, the ALT associated PML bodies (APBs). PML nuclear bodies (PNBs) are subnuclear structures that have been implicated in a number of cellular processes including the regulation of transcription, apoptosis, and senescence [239, 240]. A minority of exponentially cycling ALT cells (up to 20%) display the APBs, which appear to be enriched in G2 [328-330]. APBs are a unique subpopulation of PML bodies in ALT cells that contain many proteins that normal PNBs do not. In addition to the expected PNB proteins, APBs also contain telomeric DNA, telomere binding proteins (TRF1, TRF2, hRap1, hPot1, the Mre11 complex), recombination proteins (RAD51, RAD52), RecQ helicases (BLM and WRN), and DNA damage response proteins (RPA, 9-1-1 complex, and γ -H2AX) [118, 141, 328, 330-333]. The repression of ALT through somatic cell hybrids results in a loss of the APBs [334]. These observations have led to the hypothesis that APBs are the sites of telomeric DNA synthesis in immortal, telomerase negative cells.

Another notable feature of some ALT lines is the presence of extra-chromosomal telomeric repeats (ECTR). ECTR have been detected in a number of ALT lines. These ECTR repeats are thought to be relatively small (<3 kb) and linear [335, 336]. ATM deficient fibroblasts and EBV-transformed B lymphoblasts, which are not ALT cells, also seem to possess to possess ECTR [169, 337, 338]. Repetitive sequences, including telomeric sequences, have been found as extra-chromosomal circles in some cell lines [338, 339]. Interestingly, the treatment of these cells with carcinogens induced the accumulation of these extra-chromosomal circular DNAs [338]. Thus, it is unclear

whether ECTR have a functional role in the ALT mechanism or whether they are a more general marker of genomic instability in ALT cells.

The pathways that are altered to allow cells to undergo ALT cells have not been identified. Some studies suggest that ALT is caused by a recessive mutation, as somatic cell hybrids between ALT cells and some normal cells results in a repression of ALT [334]. However, in a different study, hybrids between a distinct set of ALT and non-ALT cell types did not disrupt ALT activity [340]. The diverse responses of different ALT cells to somatic cell hybrids suggests that there might be multiple pathways through which ALT can be activated. Interestingly, there is evidence that the inactivation of the p53 pathway is an important event for ALT progression. ALT is found frequently in tumors or fibroblasts from Li-Fraumeni patients who are heterozygous for p53. In addition, the reexpression of various p53 alleles arrests the growth of ALT cells, but not telomerase positive cell lines [341]. Finally, ALT activation seems to happen more readily in tissues of mesenchymal origin (e.g. fibroblasts); the reason for this preference is unknown [326].

Cytogenetic studies on the composition of telomeres in one ALT cell line, GM847, have implicated recombination as a possible mechanism of telomere elongation in ALT cells. The study by Reddel and colleagues found that a tagged telomeric sequence was transferred to other chromosomes in GM847 (ALT immortalized) but not HT1080 (telomerase immortalized) cells [342]. In another study, it was found using a sister chromatid specific FISH protocol (CO-FISH) that ALT cells possessed much higher levels of post-replicative telomere exchange events when compared with other telomerase positive cells [343]. There are a number of specific mechanisms that could allow for telomeric sequence transfer to occur. These include inter-telomeric replication, rolling circle replication from an extrachromosomal telomeric template, or intertelomeric recombination. In addition, the studies have not fully excluded the possibility that NHEJ

of linear tracts of telomeric DNA could contribute to telomere elongation in ALT telomere maintenance.

T-loops: a structural solution to the end of the chromosome

Another intriguing connection between telomeres and HR is the proposed structure of the t-loop (description in Chapter 1). Although the t-loop structure may prevent the recognition and NHEJ processing of telomeres as DNA breaks, the t-loop is no panacea to potential problems posed by telomeres. The t-loop structure resembles a Holliday Junction, a repair intermediate used by HR. Single-strand binding protein from *E. coli* can be loaded near the base of t-loop *in vitro* [134] suggesting that primarily one strand (likely the G-rich strand) has been displaced in a small D-loop. However, it is possible that a small degree of branch migration can occur near the base of the t-loop allowing for the formation of a short, but genuine HJ. The protection of the t-loop structure from cleavage and resolution by HJ resolvases is likely to be an important feature of telomere metabolism.

Exploring possible roles of TRF2 in HR at telomeres

Although several processes have indicated that HR can function at the telomere, there is no explanation for how this process might be regulated. TRF2 has been shown to be essential for the protection of telomeres from NHEJ, possibly through the formation of t-loops. To extend our understanding of the roles of TRF2 in regulating telomere metabolism, we have studied an allele of TRF2 that lacks its basic amino-terminus, called TRF2 Δ B. Unlike the acidic N terminus of TRF1, the first 45 AA of TRF2 are enriched in arginines. The domain is not predicted to form an obvious secondary structure and lacks significant homology to any known protein domains. While all vertebrates appear to have a homolog of TRF2, the basic N-terminus appears to be conserved only amongst mammals. For example, chicken TRF2 has only a short (~23 AA) extension at its N-terminus, which is not enriched in basic residues [344]. The TRF2 homologs of zebrafish

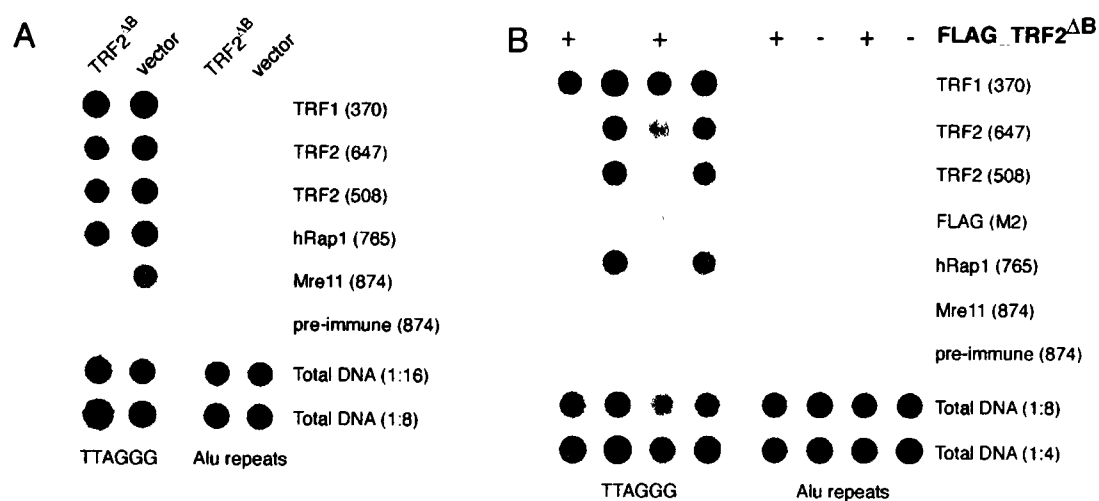
and *Xenopus* appear to lack an N-terminal extension [345] (Ishikawa F., personal communication).

TRF2 and TRF2 Δ B proteins behave similarly, *in vitro*. For example, TRF2 Δ B still binds telomeric DNA *in vitro* [100]. TRF2 Δ B has a modestly higher (~2-fold) affinity for telomeric DNA than full length TRF2 (van Breugel and de Lange, unpublished). Furthermore, although both TRF2 and TRF2 Δ B form oligomers, a greater proportion of TRF2 Δ B appears to reside in higher order oligomers (probably octamers) than TRF2 (Steensel and Griffith, unpublished; van Breugel and de Lange, unpublished). Thus, the slightly higher affinity for telomeric DNA may be related to the altered oligomeric state of TRF2 Δ B. In addition, as indicated by the EM visualization of model telomeric substrates, TRF2 Δ B was still capable of generating t-loops *in vitro*, albeit at a slightly lower efficiency (~2-3 fold) than full length TRF2 (Steensel, de Lange, and Griffith, unpublished data). In addition, the size of the t-loops formed by TRF2 Δ B were similar to those formed by TRF2. TRF2 Δ B can still interact with hRap1, XPF/ERCC1, and the Mre11 complex by IP [118, 121, 131]. Consistent with the ability of the protein to bind telomeric DNA and recruit its known interacting proteins *in vitro*, TRF2 Δ B still localizes to telomeres and does not induce telomere end-to-end fusions [124]. Curiously, despite its ability to prevent NHEJ at telomeres, TRF2 Δ B expression results in the rapid induction of senescence in HT1080 cells [124]. In this study, using the TRF2 Δ B allele, we find that TRF2 has an essential function in preventing HR at mammalian telomeres and use it to explore the roles of HR in mammalian telomere metabolism.

RESULTS

TRF2 Δ B associates with telomeric chromatin

To confirm that the expression of TRF2 Δ B did not diminish the presence of known proteins on telomeric chromatin, telomeric chromatin immunoprecipitation (ChIP) was performed on HeLa1.2.11 and HTC75 with or without expression of TRF2 Δ B.



C Telomeric ChIP quantitation (% TTAGGG repeat signal in ChIP)

Cell line	TRF2 Δ B ^a	TRF1	TRF2 ^b	TRF2 ^c	FLAG	hRap1	Mre11	PI
HeLa1.2.11		43	14	16	ND	17	4	<1
HeLa1.2.11	+	43	12	12	ND	12	3	<1
HTC75 (S24)		40	13	13	<1	9.4	1.4	<1
HTC75 (S24)	+	16	4.4	1.9	1.9	3.0	1.0	<1
HTC75 (S13)		47	15	10	<1	10	1.0	<1
HTC75 (S13)	+	33	13	1.1	7.9	3.9	1.1	<1

ChIP was performed as described by Loayza and de Lange (2003). Numbers indicate the percentage of total TTAGGG repeat signal recovered in ChIPs with antibodies for the indicated proteins. PI = preimmune serum. ND = not done.

^a TRF2 Δ B was introduced to HeLa1.2.11 cells by retrovirus. The HTC75 lines, S24 and S13, were induced to express FLAG-TRF2 Δ B in by doxycycline withdrawal (van Steensel et al., 1998)

^b TRF2 ChIP with Ab 647 derived against full-length TRF2 (TRF2 Δ B and endogenous)

^c TRF2 ChIP with Ab 508 derived against the basic domain of TRF2 (endogenous only)

Figure 3-2. ChIP of telomeric proteins in cells expressing TRF2 Δ B.

(A) ChIP on HeLa1.2.11 cells infected with pLPC or pLPC-TRF2 Δ B using the indicated antibodies. Duplicate blots were hybridized with a TTAGGG repeats or an Alu repeat probe. (B) HTC75 clones S24 and S13 were induced (+) to express FLAG-TRF2 Δ B for 5 days and were processed alongside uninduced cells (-). Duplicate blots were hybridized with a TTAGGG repeats or an Alu repeat probe. (C) Quantification of the data in A and B representing per cent TTAGGG repeat DNA recovered in each ChIP. Averaged duplicate signals obtained with total DNA samples from the lysate were used as baseline value for the quantification. TRF2 antibody 508 was derived against the basic domain and only recognizes endogenous TRF2.

HeLa1.2.11 cells expressing TRF2 Δ B still retained TRF1, TRF2, hRap1, and Mre11 on telomeres after TRF2 Δ B expression (Fig. 3-2A). Quantitation of the ChIP revealed that comparable amounts of telomeric DNA were precipitated in vector control and TRF2 Δ B expressing HeLa1.2.11 cells (Fig. 3-2C). Two doxycycline-inducible HTC75 lines (S24

and S13), which express TRF2 Δ B in a doxycycline inducible manner, were induced to express TRF2 Δ B for 5 days. After the induction of FLAG_TRF2 Δ B, HTC75 also retained TRF1, TRF2, hRap1, and Mre11 on telomeres (Fig. 3-2B, C). In contrast to TRF2 Δ B, the expression of TRF2 Δ B Δ M results in a two-fold reduction of TRF2 and a six-fold reduction in hRap1 [85]. Furthermore, unlike the dominant-negative TRF2 Δ B Δ M allele, the expression of TRF2 Δ B did not result in the rapid induction of telomere end-to-end fusions mediated by NHEJ.

TRF2 Δ B and TRF2 Δ B Δ M induce senescence and telomere dysfunction

Because TRF2 Δ B seemed capable of binding telomeric and preventing fusions, it was unexpected that its expression resulted in the induction of senescence in HTC75 cell [124]. We expressed TRF2 Δ B in primary IMR90 fibroblasts and found that it inhibited the proliferation of these cells (Fig. 3-3A). The extended culturing (> 14 days) of cells infected with TRF2 Δ B or TRF2 Δ B Δ M will result in the outgrowth of cells that do not express the exogenous allele. Despite the presence of some non-expressors in the population, after WI-38 fibroblasts were selected for the expression of TRF2 Δ B for 10 days, many of the cells were large and flat. There was a ~3 fold increase in the proportion of cells that stained positively for senescence-associated (SA) β -galactosidase (24% in TRF2 Δ B vs. 7% for control) (Fig. 3-3B). Consistent with the induction of senescence, TRF2 Δ B expressing IMR90 cells had elevated levels of p53, p21, and p16 as well as hypophosphorylated Rb and decreased cyclin A [346], all markers consistent with senescent cell. The expression of TRF2 Δ B inhibited the growth of a number of additional cell lines including BJ/hTERT, HeLa2, and HeLa1.2.11 cells (Fig. 3-3A). In all cell types, the growth arrest was more complete in TRF2 Δ B Δ M expressing cells compared to TRF2 Δ B expressing cells. This may be consistent with the observation that TRF2 Δ B but not TRF2 Δ B Δ M is still proficient for preventing telomere end-to-end fusions [124, 128].

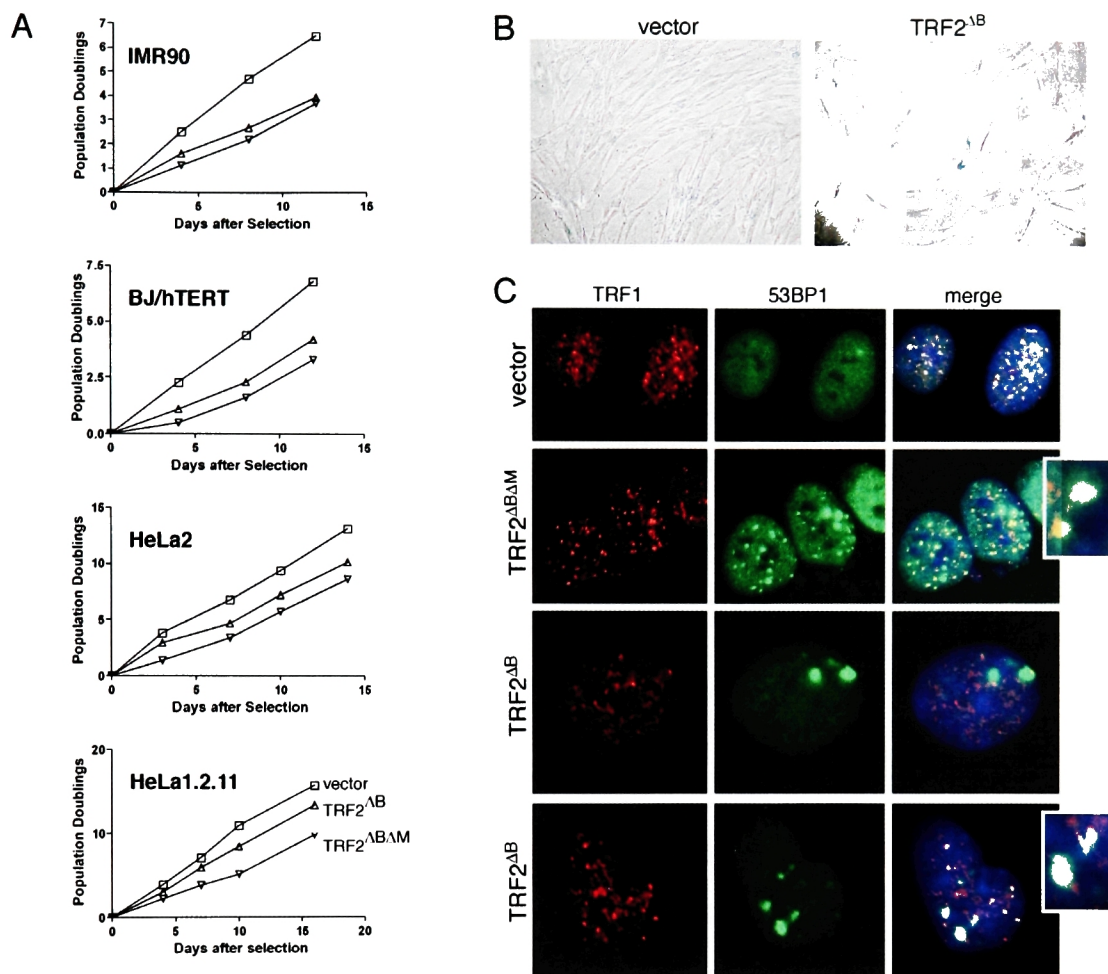


Figure 3-3. Growth arrest, senescence, and TIF induction by TRF2 Δ B.

(A) Growth curve cells expressing TRF2 Δ B Δ M, TRF2 Δ B, or vector control cells. (B) TRF2 Δ B induced senescent morphology and SA- β -gal expression. 3×10^4 WI38 cells infected with the indicated retrovirus were plated in chamber slides on day 8 of selection. After 2 days, cells were fixed and stained for β -gal activity. (C) TRF2 Δ B induces large 53BP1 foci that co-localize with TRF1. BJ/hTERT expressing the indicated virus were fixed 1 day after infection (no selection) and stained for DNA (DAPI; blue), 53BP1 (gift from T. Halazonetis; green) and TRF1 (370; red). The enlarged images show 53BP1 foci at telomeres from these nuclei (TIFs). (D) Quantitation of DNA damage foci induced by the expression of TRF2 Δ B.

BJ/hTERT cells were infected for 24 hours with the indicated viruses and harvested after 2 days without selection. A 53BP1 focus was scored as a TIF if the focus colocalized with TRF1 (370) when merged. The number of foci and number of TIFs were only scored for cells that were 53BP1-positive.

The cytologic colocalization of telomeres labeled by TRF1 with sites of DNA damage is described as a telomere dysfunction induced focus (TIF) and has been established as a marker for uncapped telomeres [125]. IF for 53BP1 in BJ/hTERT cells harvested after expressing TRF2 Δ B revealed the presence of DNA damage foci in 72% of the cells (~5 foci/cell) compared to 32% of vector control cells (~2 foci/cell) (Fig. 3-3D). Of the cells that possessed DNA damage foci, most (>60%) had foci that colocalized with telomeres marked with TRF1. Of cells that possessed 53BP1 foci, TRF2 Δ B expressing cells possessed an average of 1.8 TIFs/cell while vector control cells possessed ~0.16 TIFs/cell. The presence of TIFs in TRF2 Δ B-expressing cells suggested that the TRF2 Δ B allele induced growth arrest could be due to telomere dysfunction.

The expression of TRF2 Δ B Δ M or the conditional deletion of TRF2 in mouse fibroblasts results in a marked induction of DNA damage foci that colocalize with telomeres [125](Celli and de Lange, unpublished). TRF2 Δ B Δ M-induced foci are abundant (>10 TIFs/cell) and relatively small (usually <1 μ m). In contrast, TRF2 Δ B-induced foci were notably larger (usually >1 μ m) and less frequent than those caused by TRF2 Δ B Δ M expression (Fig. 3-3C, D). The morphology of TRF2 Δ B-induced foci are more reminiscent of the “senescent foci” described in cells undergoing passage induced senescence than the TIFs described in TRF2 Δ B Δ M expressing cells [347, 348]. The differences in the appearance and frequency of TIFs would be consistent with distinct mechanisms of action for the TRF2 Δ B and TR2 Δ B Δ M alleles. Because of its proficiency in inhibiting telomere end-to-end fusions and distinct TIF morphology, I surmised that the telomere dysfunction and senescence induction induced by TRF2 Δ B was a fundamentally distinct process.

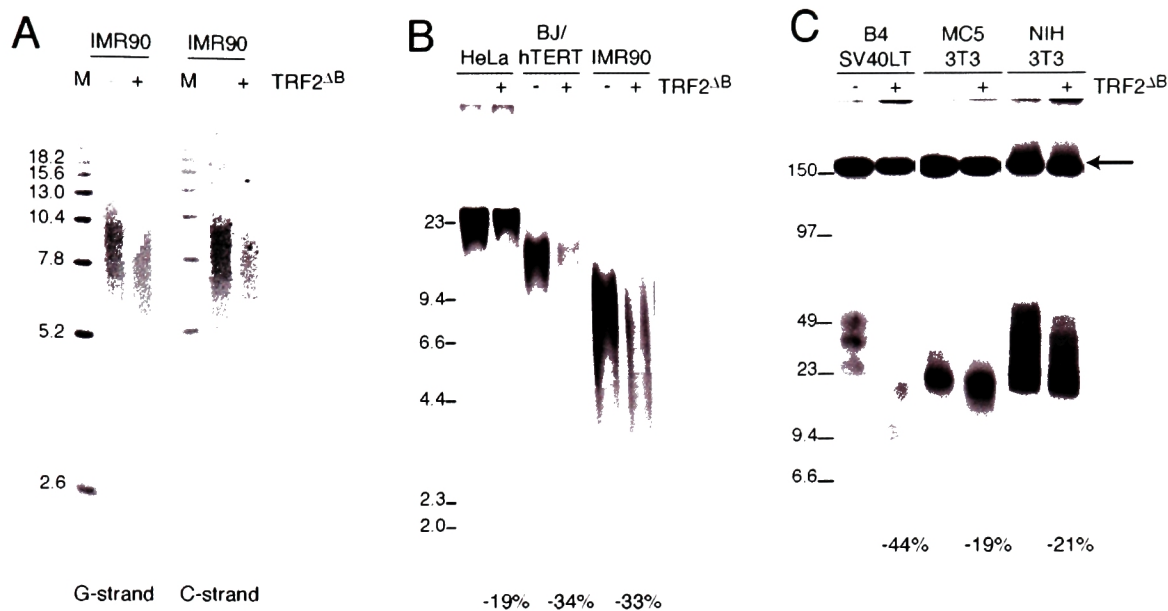


Figure 3-4. TRF2 Δ B results in the loss of duplex telomeric DNA in human and mouse cells.

(A) Denaturing gel electrophoresis comparison of C and G strand length after expression of TRF2 Δ B. IMR90 fibroblast were harvested on day 5 of selection. Genomic DNA was digested with *Mbo*I and *Alu*I and quantitated prior to loading. Equal loading was not confirmed due to the alkaline condition of the electrophoresis. Two alkaline gels were run in parallel, neutralized, blotted onto a Nylon membrane and hybridized with end-labeled (CCCTAA)₄ and (TTAGGG)₄ repeat oligos. The molecular weight marker were prepared by digesting a TTAGGG repeat bearing 2.6 kb pTH5 plasmid with *Hind*III and self ligation of the cut plasmid. (B) Telomere blots of human cells after TRF2 Δ B expression. HeLa, BJ/hTERT, and IMR90 cells were harvested on day 4 after selection. Genomic DNA was digested with *Mbo*I and *Alu*I and quantitated prior to loading. Equal loading was confirmed by EtBr staining. Blots were hybridized with a TTAGGG repeat probe (Sty11) and exposed on phosphor screens. The telomere smear, excluding the wells, was quantified using Imagequant software. The number below each lane indicates the telomere signal relative to a vector control infection that was done in parallel. The loss of telomere signal from each of these cell lines was similar in multiple independent infections. (C) CHEF gel telomere blots from mouse cells after TRF2 Δ B expression. The indicated wild-type mouse cells were harvested 5 days after infection. Genomic DNA from 1.5 x 10⁶ cells was prepared in plugs, digested with *Hind*III, and separated by CHEF gel. Blots were controlled for loading and quantitated as described in Fig. 3-5. (Arrow) Many short arm telomere fragments migrate >150kb because they possess long subtelomeric arrays that are not digested by *Hind*III. Genomic DNAs digested with *Mbo*I show similar losses of telomeric repeats despite the absence of the strong short arm telomere band.

TRF2 Δ B induces rapid telomere shortening – quantitative genomic telomere blots

To address the mechanism of senescence induction by TRF2 Δ B, I examined the telomeres of TRF2 Δ B expressing cells by telomere Southern blots. TRF2 Δ B induced a rapid loss of telomeric DNA when compared to vector control. The loss of telomeric DNA could be observed both as a shortening of telomere restriction fragment (TRF)

length and also an obvious decrease in hybridization intensity. Telomere shortening was noted in a variety of primary and transformed human cells types including IMR90, WI38, BJ, BJ/hTERT, HTC75, HCT116, and HeLa1.2.11 (Fig. 3-4B, Table 3-4).

The examination of the C-rich and G-rich telomeric strands separately using denaturing gel electrophoresis indicated that both strands became shortened upon exposure to TRF2 Δ B (Fig. 3-4A). Median TRF decreased by at least ~16% (from 8.4 to 7.1 kb) after the expression of TRF2 Δ B in IMR90 fibroblasts (Fig. 3-11F). However, this is likely to be an underestimate of the actual amount of telomere sequence loss as TRFs possess variable amounts (at least 0.5 kb) of non-telomeric repetitive sequence which are not separated from the telomeric repeats after restriction digest [13, 349].

As an alternative means of measuring telomeric sequence loss, I performed quantitative Southern blots on telomeric sequences with or without expression of the TRF2 Δ B allele. For all experiments, samples were first normalized by Hoechst fluorometry prior to loading. Additionally, for most experiments, the amount of genomic DNA was further normalized by first probing blots for a chromosome internal sequence (Fig. 3-5A, B). Using quantitative Southern blots, I found that human cells expressing TRF2 Δ B consistently lost at least 15% and up to 30% of their telomeric repeat sequences regardless of their starting telomere length. Although the telomere sequence loss was very rapid and could be easily detected as early as 2 days after selection (4 days after introduction of virus), most experiments were performed after 4-6 days of selection. I also expressed TRF2 Δ B in mouse cells and found that telomeric sequences were lost at comparable rates (~30% in 4 days) despite the much longer telomeres of mouse cells (Fig. 3-4C). The rate of telomeric sequence loss caused by TRF2 Δ B (~1000-2000 bp/PD) rate of loss is too high to be explained by the progressive erosion predicted by the end replication problem that is estimated to erode telomeres at between 50-150 bp/PD.

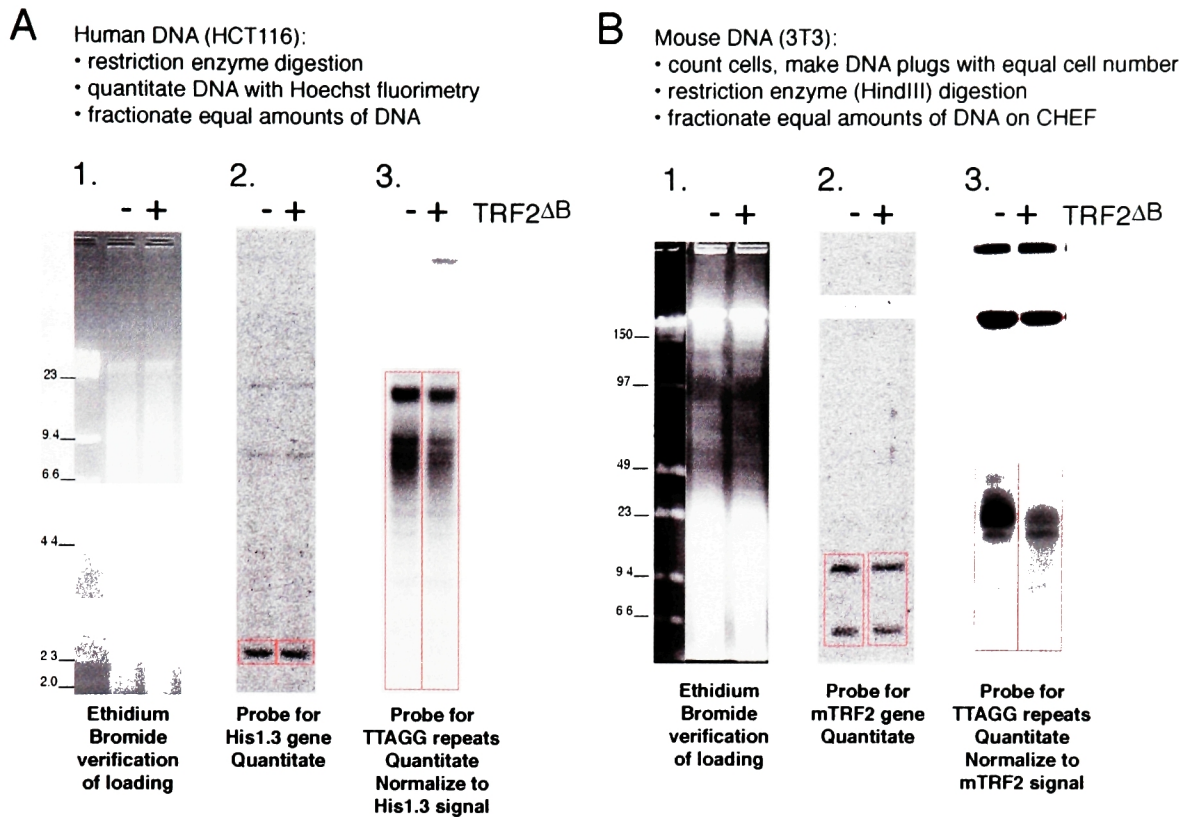


Figure 3-5. Quantitation of telomere blots after TRF2 Δ B expression.

Human (A) or mouse (B) genomic DNA treated in parallel with vector or TRF2 Δ B retroviruses was digested with the indicated restriction enzymes and quantitated by Hoechst fluorimetry prior to loading. Blots were probed for the indicated loading control, exposed on Phosphor screens, and quantitated in Imagequant. The blots were then stripped, hybridized with a TTAGGG repeat probe (Sty11), and the telomere smear was quantified in Imagequant. The loading control normalized signal was compared to between parallel vector and TRF2 Δ B samples.

TRF2 Δ B alters telomere end structure – non-denaturing in-gel hybridization

The expression of TRF2 Δ B Δ M or deletion of the TRF2 gene greatly reduces the amount of single stranded G-strand overhang at telomeres ([124]; G. Celli and T. de Lange, in preparation). To assess the effects of TRF2 Δ B on single-stranded DNA (ssDNA) at telomeres, I performed non-denaturing in-gel hybridizations with oligonucleotide probes specific for the G-rich or C-rich strands of telomeres. Under non-denaturing conditions, a telomeric smear is detected only for the TelC probe consistent with the presence of short (50-150 bp) G-rich overhangs thought to be present on all telomeres

[350]. Subsequent to quantitation, the same gels are denatured *in situ* and rehybridized to the probes. Thus, quantity of overhang is always normalized to amount of telomeric DNA loaded in a particular sample lane. In IMR90 and BJ/hTERT fibroblasts, expression of TRF2 Δ B increased the amount of single stranded G-strand DNA at telomeres (Fig. 3-6A). Three days after selection, TRF2 Δ B-expressing BJ/hTERT cells had 45% more ss G-rich telomeric DNA than vector control cells. IMR90 cells had ~25% and 70% more ss G strand telomere DNA without selection or 3 days after selection, respectively. Cells selected for TRF2 Δ B expression for >7 days appeared to lose the excess single stranded DNA [346]. Thus, the aberrant ss DNA induced by TRF2 Δ B may be a transient intermediate. Consistent with previous observation, the expression of TRF2 Δ B Δ M resulted in a modest but consistent decrease in the amount of ss overhang signal in my experiments. Most of the additional ss DNA at telomeres induced by TRF2 Δ B did not migrate in a pattern consistent with TRFs, but rather smeared upwards and downwards from the expected signal. The signal from shorter TRFs is likely to represent the ss G-overhangs of telomeres shortened by TRF2 Δ B. However, the upwards smearing signal is unlikely to represent longer telomeres as standard electrophoresis conditions can only resolve linear fragments of DNA <25 kb. Thus, the upwards-smearing signal may represent aberrant structures (e.g. G quartets, strand invaded intermediates) formed by the additional ss DNA. These structures are non-covalent because they are not detectable when gels are run under denaturing conditions (Fig. 3-4A).

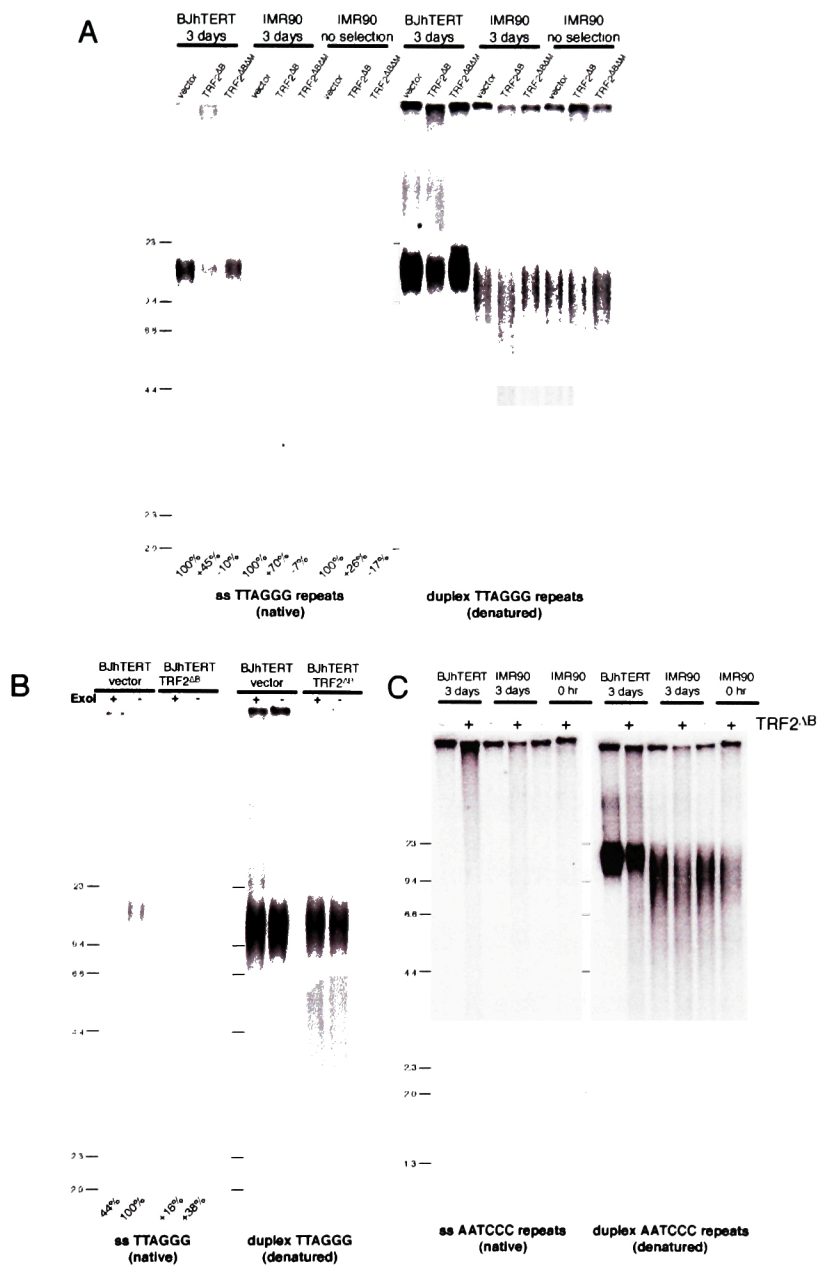


Figure 3-6. TRF2 Δ B induces increased single-stranded DNA at telomeres.

(A) In-gel hybridization of TRFs from cells expressing TRF2 Δ B. BJ/hTERT and IMR90 fibroblasts were harvested at the indicated time points after selection. Genomic DNA was digested with *Mbo*I and *Alu*I and fractionated on a 0.8% agarose gel. Equal loading was confirmed by EtBr staining. The same gel was probed under native (left) and denaturing (right) conditions with an end-labeled (CCCTAA)₄ probe. The overhang signal was normalized for loading and then compared to the vector control sample (set to 100%). (B) The excess single stranded DNA induced by TRF2 Δ B is resistant to Exo1. TRFs were treated with Exo1 at 5 units/ μ g genomic DNA for 1hr prior to digestion and fractionation. Overhang signal was normalized for loading against the denatured gel (right) and then compared to the vector control sample without Exo1 treatment, set to 100%. (C) Expression of TRF2 Δ B induces ss C-rich DNA at telomeres. Native gels performed as described in (A) except that gels were hybridized with an end-labeled (TTAGGG)₄ probe.

Normally, the ss G-overhangs of telomeres are sensitive to ExoI, a 3'→5' exonuclease. In vector control cells, treatment of TRFs with ExoI resulted in a 44% decrease in the overhang signal. After the expression of TRF2ΔB, a fraction of the ss DNA was digested by ExoI, which suggested that some telomeres maintained a normal end structure. However, the majority of the excess ss G-strand signal induced by TRF2ΔB was resistant to ExoI as the signal intensity only dropped from 138% to 116% of vector control levels (Fig. 3-6B). ExoI requires a free 3' terminus to degrade ssDNA; thus, resistance to ExoI suggests that the DNA could be extremely long, lack a free 3' terminus, or form otherwise aberrant structures (e.g. G quartets).

Consistent with the possibility of altered telomere structure caused by TRF2ΔB, I found that a TelG probe specific for C rich DNA hybridized with TRFs from TRF2ΔB-expressing cells (Fig. 3-6C). Telomeres are not thought to possess ss C-rich telomeric repeats. Thus, vector control TRFs did not hybridize with telomeric DNA in non-denaturing conditions. However, after the expression of TRF2ΔB, ss C-rich DNA became obvious (Fig. 3-6C). This TRF2ΔB induced ss C-rich DNA may share many of the same features as the ss G-rich DNA as it also migrates at very high apparent MW suggesting the presence of secondary structures. Thus, in addition to causing the loss of duplex telomeric repeats, these non-denaturing in-gel analyses suggest that the normal telomeric structure is also altered by the expression of TRF2ΔB.

TRF2ΔB induced deletions are stochastic telomere loss by FISH

To clarify the mechanism of TRF2ΔB-mediated telomere loss, I visualized the telomeres by Fluorescent In Situ Hybridization (FISH) with a telomere peptide nucleic acid (PNA) probe. Consistent with telomere blots, TRF2ΔB expression caused an overall decrease in the strength of telomeric FISH signals (Fig. 3-7A, B). I was surprised to find that telomere attrition did not affect all chromatids equally. While some telomeres appeared relatively unaffected, others were very weak or lost completely. Under optimal conditions, PNA-FISH can detect as little as 500-1000 bp of telomeric DNA on

metaphase spreads ([351] and P. Lansdorp, personal communication). The strikingly asymmetric pattern of loss in many of the metaphase chromosomes indicated that TRF2 Δ B-mediated telomere loss was likely to occur during or after S-phase. Though less frequent, I also visualized deletions in which both sister telomeres appeared to be affected suggesting either a loss prior to DNA replication or duplicate deletion events after metaphase. Thus, we do not exclude that possibility that a minority of telomere deletions occur prior to S-phase.

Scoring metaphases from several independent infections of mouse fibroblasts, I found that TRF2 Δ B expression resulted in a ~10 fold increase in the number of chromatids lacking detectable telomere signals (Table 3-1). I found that TRF2 Δ B induced telomere loss at similar rates in BJ and BJ/hTERT cells (Fig. 3-7B, Table 3-1). Curiously, even in the control spreads, there was a low proportion of chromatids that lacked telomeric signal. Although it is possible that these signal free ends could be an artifact of sample preparation, these baseline loss events were noted in several independent experiments and have also been previously reported to occur in both mouse and human cells.

In NIH/3T3 cells, after two days of TRF2 Δ B expression, 8.5% of telomeres had been lost completely while most other telomeres had also decreased in length notable as an overall decrease hybridization intensity. While a more precise quantification of telomere loss on metaphase spreads requires the use of the Quantitative-FISH (Q-FISH) [352], I estimate that the rate of loss visualized by FISH is roughly consistent with the 21% decrease in telomere hybridization intensity that I observed through quantitative genomic blots after four days of selection.

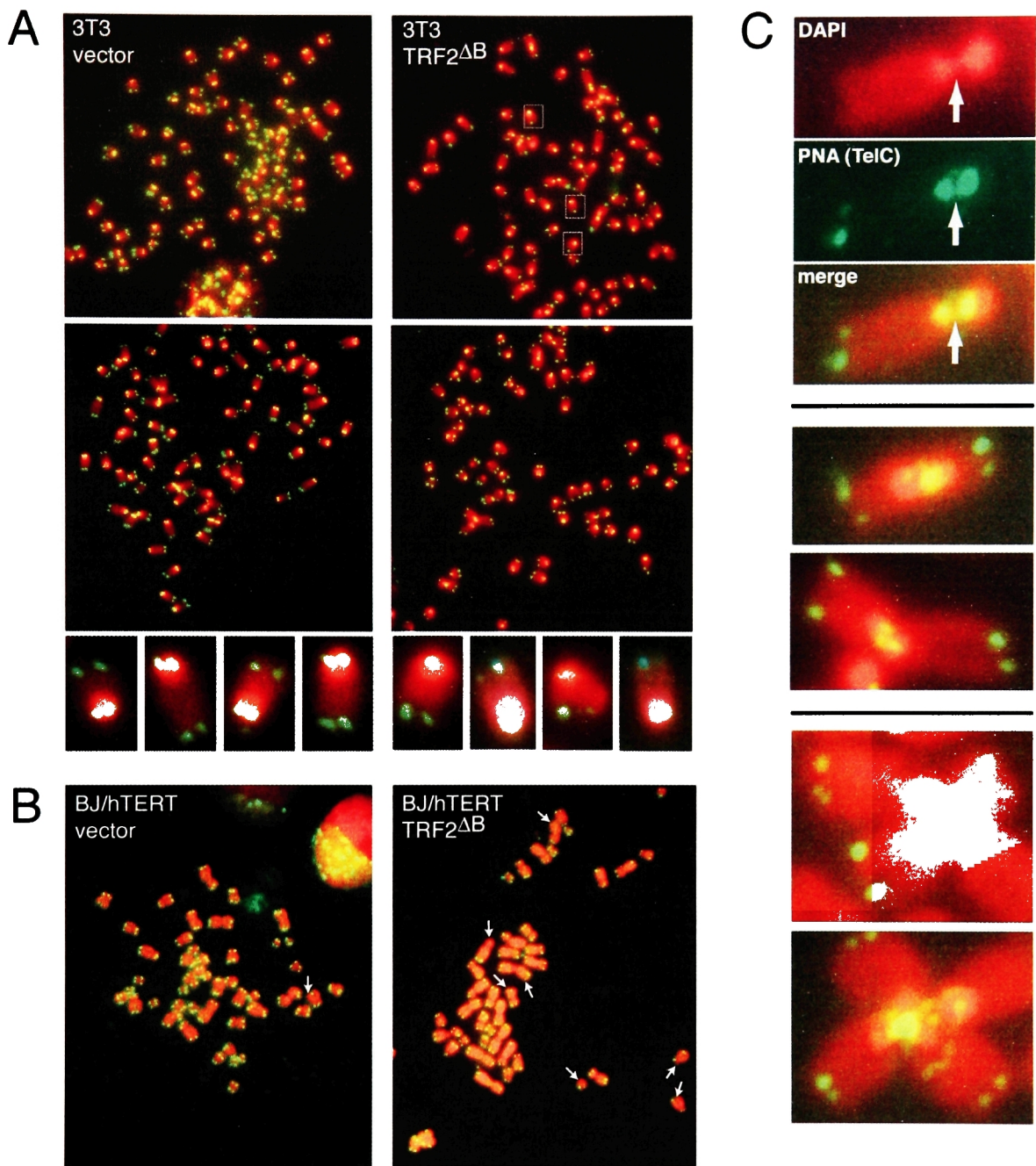


Figure 3-7. TRF2 Δ B induces stochastic telomere loss telomere associations.

(A) Telomere FISH on metaphase spreads from NIH/3T3 cells expressing TRF2 Δ B or vector control retrovirus. NIH/3T3 cells were harvested for metaphase spreads one day after infection (no selection). Metaphases were stained with DAPI (red) and a telomere specific FISH probe, FITC-(CCCTAA)₃ (green). The enlarged images below the metaphases show individual chromosomes from control and TRF2 Δ B expressing slides. (B) Telomere FISH on spreads from BJ/hTERT cells. BJ/hTERT cells were harvested for metaphases five days after selection. Arrows point to signal free ends; the occasional signal free end can be noted in vector control cells (*left*). (C) Telomere associations (TAs) induced by TRF2 Δ B. (*Top*) TAs are distinct from fusions. Neither the DAPI nor PNA-FISH staining are continuous between the telomeres linked by TAs, something which would be expected from fusions. Additional examples of TAs between two chromosomes (*middle*) or multiple chromosomes (*bottom*) are shown.

Table 3-1. Quantification of TRF2ΔB-induced telomeric signal loss.

Cell line	Retrovirus	Chromosomes/ Ends scored	Signal free ends	Telomere associations (10 metaphases)
NIH/3T3	vector	784/3136	28 (0.9%)	12
NIH/3T3	TRF2ΔB	706/2824	240 (8.5%)	28
B4-SV40LT	vector	722/2888	18 (0.6%)	6
B4-SV40LT	TRF2ΔB	833/3332	133 (4.0%)	38
MC5	vector	1004/4016	22 (0.5%)	12
MC5	TRF2ΔB	898/3592	197 (5.5%)	46
BJ/hTERT	vector	444/1776	10 (0.6%)	ND
BJ/hTERT	TRF2ΔB	448/1792	83 (4.6%)	ND
BJ	vector	392/1568	22 (1.4%)	ND
BJ	TRF2ΔB	416/1664	96 (5.8%)	ND

The indicated cells lines were infected with vector or TRF2ΔB retrovirus and harvested after one day for mouse cells and two days for human cells. Metaphase spreads were hybridized with a telomere PNA probe and examined for telomeric signal loss as shown in Fig. 3-7A and B. Metaphase spreads from mouse cells were also scored for telomere associations (TAs). A TA event was scored when two or more PNA-FISH signals from separate chromosomes were continuous or almost continuous while the DAPI staining of the separate chromatid arms remained distinct; thus, TAs were only scored between separate chromosomes.

TRF2ΔB induces telomere associations (TAs)

In addition to telomeric signal loss, the expression of TRF2ΔB also increased the number of telomeric associations (TAs). Like telomere end-to-end fusions, TAs appeared as continuous or nearly continuous PNA-FISH staining between two or more different chromosomes. However, unlike fusion, TAs do not show continuous DAPI staining. By definition, continuous telomere FISH staining between more than two telomeres must represent at least one TA because it cannot be due to an end-to-end fusion between two ends. Furthermore, because the spatial proximity between FISH signals on adjacent sister chromatids (especially on the short p arms that are situated next to the centromeric heterochromatin) made it difficult to discern the continuity of DAPI staining, only TAs between separates chromosomes were scored in our analyses. Thus, the number of TAs presented in Table 3-1 are likely to be a conservative estimate of the

frequency of occurrence. Even so, after the expression of TRF2 Δ B, there was a ~three-fold increase (30 total in vector compared to 112 in TRF2 Δ B) in the total number of TAs in metaphases from three separate infections. In contrast to telomere fusions, TAs do not possess continuous DAPI staining and condensed chromatin between the adjacent PNA-FISH signals (Fig. 3-7C). TAs often involved more than two telomeres (Fig. 3-7C) making it even more unlikely that associations were covalent end fusions. Finally, as previously described, the expression of TRF2 Δ B did not result in the accumulation of larger MW TRFs on denaturing gels, representing fused telomeres, a process which occurs after the expression of TRF2 Δ B Δ M [130]. I conclude that in addition to causing stochastic telomere deletions, TRF2 Δ B also induces non-covalent associations between different telomeres.

TRF2 Δ B preferentially deletes the parental C-strand telomeres

Metaphase spreads harvested within 2 days after the expression of TRF2 Δ B suggested that telomere loss preferentially affected one of the two sister telomeres (Fig. 3-8A). TRF2 Δ B mediated deletions were frequent and often resulted in the loss of two signals from the same chromosome. When 1 sister telomere was lost from a single chromosome, the telomere situated diagonally on the opposite side of the centromere was also lost or very weak (Fig. 3-9A). This configuration of anti-parallel signal loss happened very infrequently in control metaphases. Because all telomeres terminate with G-rich 3' overhangs, barring any sister chromatid exchange events, anti-parallel sister telomeres possess the same parental sequence after DNA replication. Thus, it is likely that the anti-parallel configuration of telomere loss caused by TRF2 Δ B would be consistent with a preferential loss of the products of either the leading or lagging strand telomeres [353].

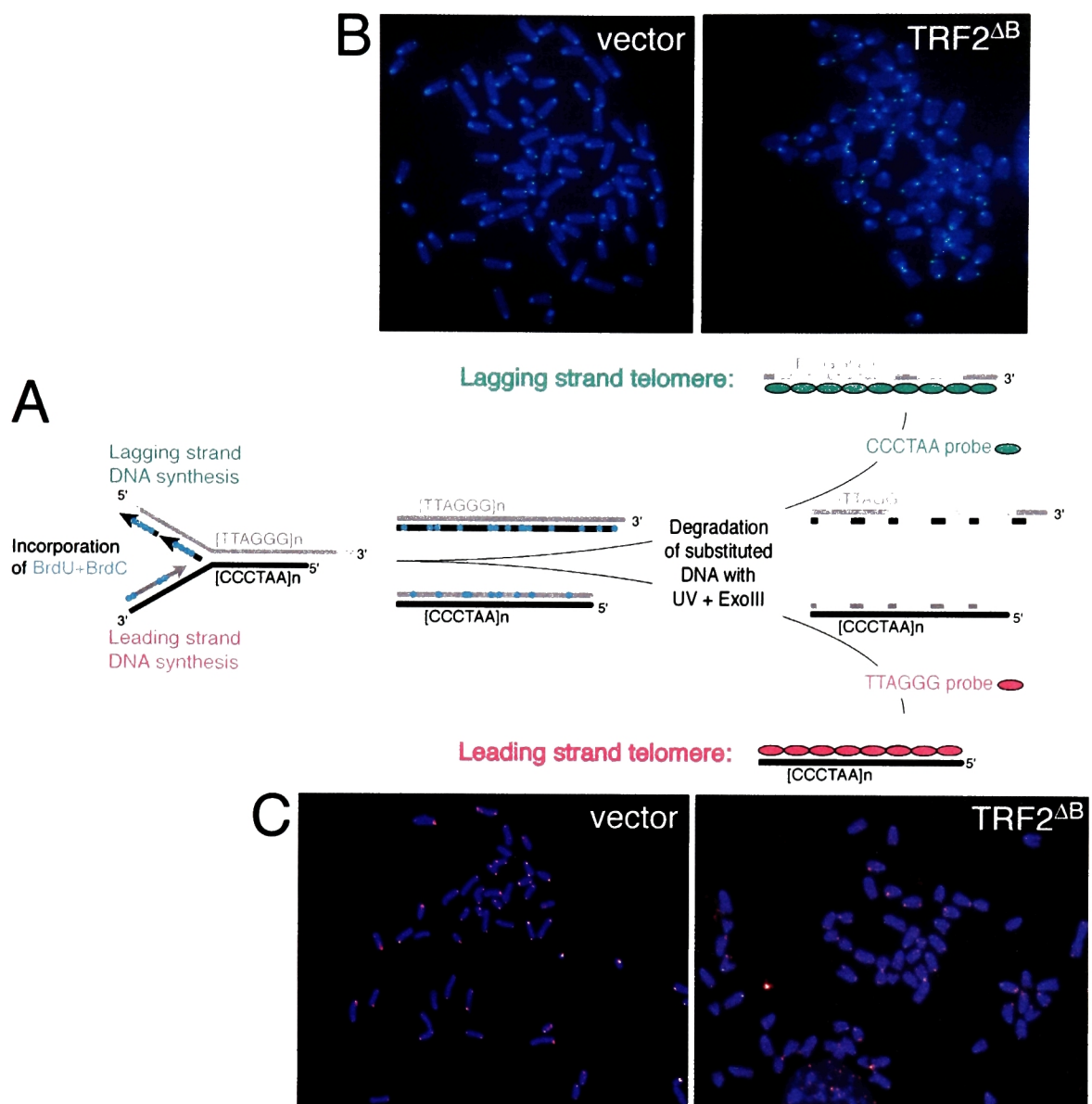


Figure 3-8. TRF2^{ΔB} preferentially induces the loss of leading strand telomeres.

(A) CO-FISH schematic. Cells are grown in the presence of BrdU and BrdC for one S-phase. These nucleotide analogs are incorporated only into the newly replicated strand. After preparation of metaphase spreads, DNA is treated with UV light which nicks DNA preferentially at sites of halogenated pyrimidine incorporation. After treatment of the slides with ExoIII, the newly synthesized DNA strand is lost and only parental telomeric sequences remain. (B) Lagging strand telomeres are relatively preserved in TRF2^{ΔB} expressing metaphases. Metaphase spreads were prepared from NIH/3T3 cells 48 hours after introduction of TRF2^{ΔB} and ~20 hours after BrdU/C labeling. The spreads were subjected to CO-FISH and stained with DAPI (red) and a G-rich specific FISH probe FITC-(CCCTAA)₃ (green). (C) Leading strand telomeres are preferentially deleted after TRF2^{ΔB} expression. After metaphases were treated with the CO-FISH protocol, they were stained with DAPI (blue) and a lagging strand specific FISH probe TAMRA-(TTAGGG)₃ (red).

The specificity of this anti-parallel configuration for identifying telomeres with the same parental strand could be misleading if TRF2 Δ B also induce a higher frequency of sister chromatid exchange. However, I found that levels of SCE were comparable between vector control and TRF2 Δ B expressing cells (12.3 vs. 13.3 SCEs/metaphase, respectively). It is possible to determine the parental sequence of a particular sister telomere by degrading the newly synthesized strand using a protocol developed by Goodwin and colleagues called Chromosome Orientation FISH, CO-FISH (Fig. 3-8A) [354]. To minimize the number of cell divisions that occurred after the expression of TRF2 Δ B, I performed CO-FISH on metaphases from NIH/3T3 cells 48 hours after the introduction of TRF2 Δ B in order to determine whether deletions happened preferentially on leading or lagging strand telomeres.

Using a probe specific for the parental G strand, I found that lagging strand telomeres were not lost in TRF2 Δ B expressing cells (Fig. 3-9B). The number of G-strand signals remained relatively constant (2.1 in the vector control and 1.93 after TRF2 Δ B expression (n=700 chromosomes)). Although there was a slight increase in the number of G-strand signals per chromosome, this increase was slight (<0.2 additional signals/chromosome) and may be a consequence of the overall diminution of telomere signal strength after TRF2 Δ B expression (i.e. lowered ratio of signal to noise). In contrast, a probe specific for the parental C strand showed a striking loss after expression of TRF2 Δ B (Fig. 3-9B). In contrast to vector control, CO-FISH treated metaphases from TRF2 Δ B infected cells possessed fewer than half the expected number of the leading strand telomere signals per chromosome, from \sim 0.74 after compared to 2.2 in the vector control (n=650 chromosomes) (Table 3-2). This high rate of loss argues that most of the asymmetric signal free ends visible after TRF2 Δ B expression were due to loss of the leading strand replication product.

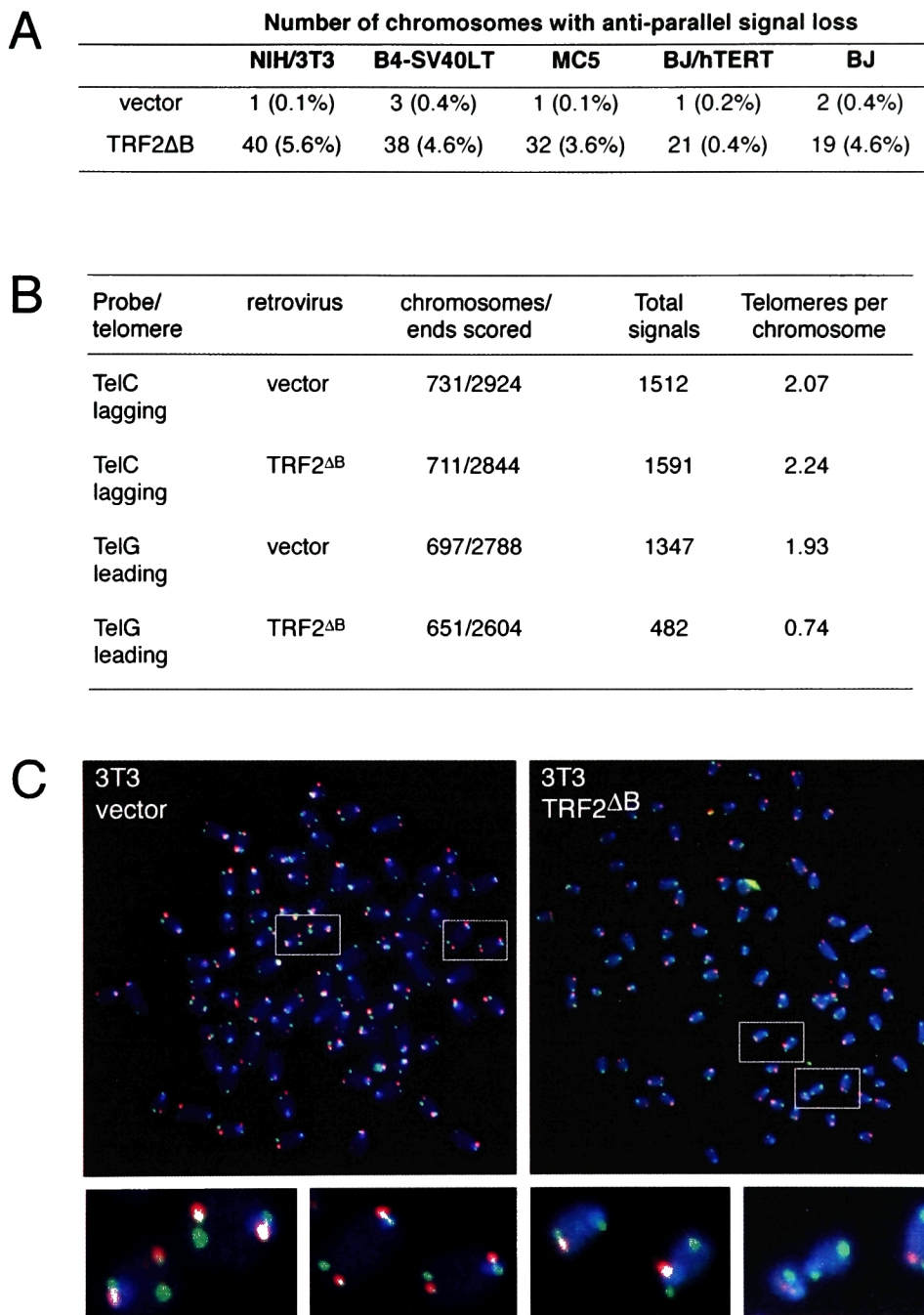


Figure 3-9. TRF2 Δ B preferentially induces the loss of leading strand telomeres.

(A) Quantitation of frequency of chromosomes with loss of anti-parallel signals. Metaphase spreads from Table 3-1 were scored for chromosomes that possessed absent or weaker signals on anti-parallel arms. (B) Quantitation of CO-FISH staining demonstrated that leading strand telomeres are lost more frequently than lagging strand telomeres. (C) Dual CO-FISH confirms that leading strand telomeres are preferentially deleted by TRD after dB expression. After metaphases were treated with UV and ExoIII only the parental DNA remains intact. They were then stained simultaneously with a TAMRA-(TTAGGG)₃ leading strand telomere probe (red), and a FITC-(CCCTAA)₃ lagging strand FISH probe (green), and DAPI (blue).

It was possible that the two telomere probes (TelC-FITC, TelG-TAMRA) hybridized with different efficiencies on particular metaphase spreads. Thus, if the TelG probe specific for leading strand telomeres were less efficient overall, it might result in an apparent loss of leading strand telomeres. To address this possibility, in a separate set of infections, I visualized both leading and lagging strand telomeres on the same metaphase spread. Control metaphases possessed strong leading and lagging (red and green, respectively) strand signals on adjacent sister telomeres (Fig. 3-9C). However, TRF2 Δ B metaphases fewer leading strand telomeres than expected. This dual CO-FISH served as additional evidence for the leading strand specificity of the telomere deletion mediated by TRF2 Δ B.

XRCC3 is required for TRF2 Δ B-induced deletions

TRF2 Δ B mediated deletions were rapid, stochastic, and post-replicative. These characteristics could be consistent with deletion events mediated by HR at telomeres. To test this, I introduced TRF2 Δ B into cell lines impaired in HR and determined whether the deletion of telomeric sequences still occurred as through quantitative genomic blots. I chose to perform the genetic epistasis analysis of TRF2 Δ B-mediated telomere sequence loss by quantitative Southern blots because it has several advantages over FISH analysis. First, sample sizes are much larger (e.g. 1.5×10^6 cells per lane for mouse blots) in quantitative blots than in FISH. In addition, many cell types (e.g. HCT116 and HTC75) have very short telomeres that are refractory to analysis by FISH due to their short length.

I tested HCT116 (colon carcinoma) cells in which both alleles of XRCC3 have been eliminated by targeted deletion for their ability to undergo TRF2 Δ B-mediated telomere deletions [294]. Genomic DNAs digested with *EcoRI/XbaI* were first probed with a chromosome internal locus (Histone1.3) to normalize for loading and then reprobed with a telomeric probe (Fig. 3-5A).

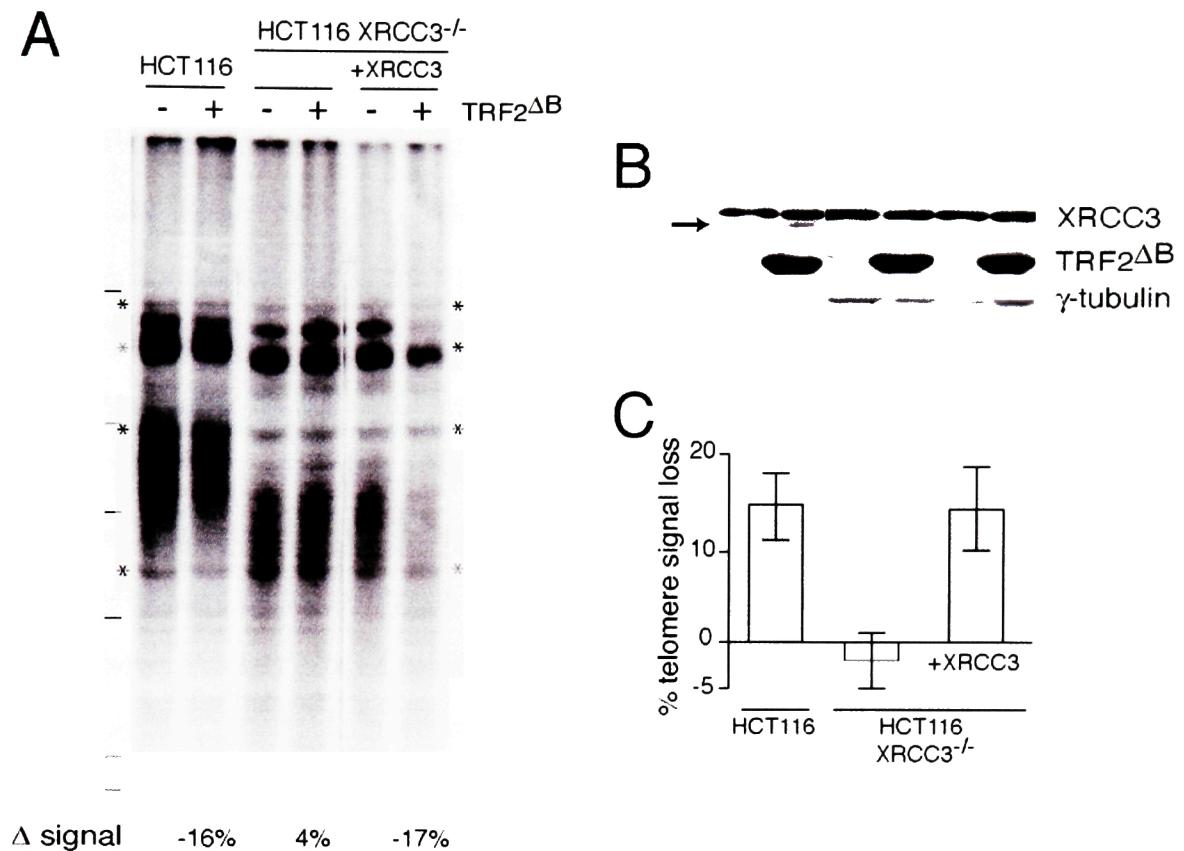


Figure 3-10. XRCC3 is required for TRF2 Δ B-induced telomere loss.

(A) XRCC3 is required for TRF2 Δ B mediated TRD. HCT116 cells, HCT116 (cells) with targeted deletions of both XRCC3 alleles (XRCC3^{-/-}), and XRCC3 deficient cells stably transfected with exogenous cDNA (XRCC3^{-/-} + X3 cDNA) were infected with TRF2 Δ B or a vector control and were harvested on day 5 after selection for DNA and protein from the same population. Genomic DNA was digested with *Eco*RI and *Xba*I, and probed for a chromosome internal locus (Histone 1.3), stripped, and re-probed for telomeric repeats (Sty11). All subsequent calculations were made using the loading control normalized telomere signal. The number below each lane indicates the telomere signal relative to a vector control infection that was done in parallel. Asterisks represent intersitial telomeric bands that are not affected by TRF2 Δ B expression. Gray bars represent the bulk telomeric repeats. (B) Western blots for XRCC3, TRF2, and γ -tubulin. XRCC3 (arrow) migrates just below a non-specific band. TRF2 Δ B is expressed at similar levels in all three cell types. (C) Graph summarizing requirement of XRCC3 for TRD. The graph plots the mean loss of telomeric sequence (\pm SD) induced by TRF2 Δ B from 5 independent genomic preps (3 separate infections).

Five genomic preps from 3 independent infections experiments were used for the quantification of the effect of XRCC3 status of TRF2 Δ B-induced deletions. Although the XRCC3^{-/-} cells expressed the same level of TRF2 Δ B as the control cells (Fig. 3-10B), they did not show telomere deletions after TRF2 Δ B expression (Fig. 3-10A, C). HCT116 cells are deficient in Mlh1 and may contain other mutations. Telomere

deletions were restored to wild-type levels by the expression of XRCC3 from a stably introduced cDNA (Fig. 3-10A, C) excluding the possibility that the rescue of TRF2 Δ B mediated deletions was due to another defect in the HCT116-derived cell line. These results are consistent with a requirement for the CX3-associated Holliday junction resolvase in cleaving and resolving t-loops. However, we cannot exclude that possibility that XRCC3 is also involved in early steps of HJ formation.

Nbs1 is required for TRF2 Δ B induced deletions

The Mre11 complex, which includes Mre11, Rad50, and Nbs1, has diverse functions in the DNA repair, some of these activities may promote HR [355]. I assessed the requirement of Nbs1 for the action of TRF2 Δ B in primary human Nbs deficient fibroblasts. Primary Nbs1 fibroblasts from patients with Nijmegen breakage syndrome do not express detectable levels of the Nbs1 protein (Fig. 3-11G) and also have a defect in the nuclear localization of Mre11 and Rad50 [356]. The expression of TRF2 Δ B in these cells did not result in the appreciable loss of telomeric repeats as assessed by both telomere hybridization intensity (Fig. 3-11D) and change in median TRF length (Fig. 3-11F).

The specificity of Nbs1 in the abrogation of TRF2 Δ B-mediated deletion was confirmed in SV40 transformed Nbs1 fibroblasts (NBS1-LB1) derived from a separate patient [357]. Like primary Nbs cells, NBS1-LB1 cells were impaired for TRF2 Δ B-mediated telomere shortening (Fig. 3-11A, C). As a control, HTC75 cells, which express functional Nbs1 and have telomeres comparable length, deleted ~25% of their telomeric repeats after TRF2 Δ B expression. Retroviral expression of either wildtype Nbs1 or signaling deficient mutant of Nbs1 (S343A; [358]) restored the ability of TRF2 Δ B to degrade telomeres to levels approximating those of HTC75 cells (Fig. 3-11A, C).

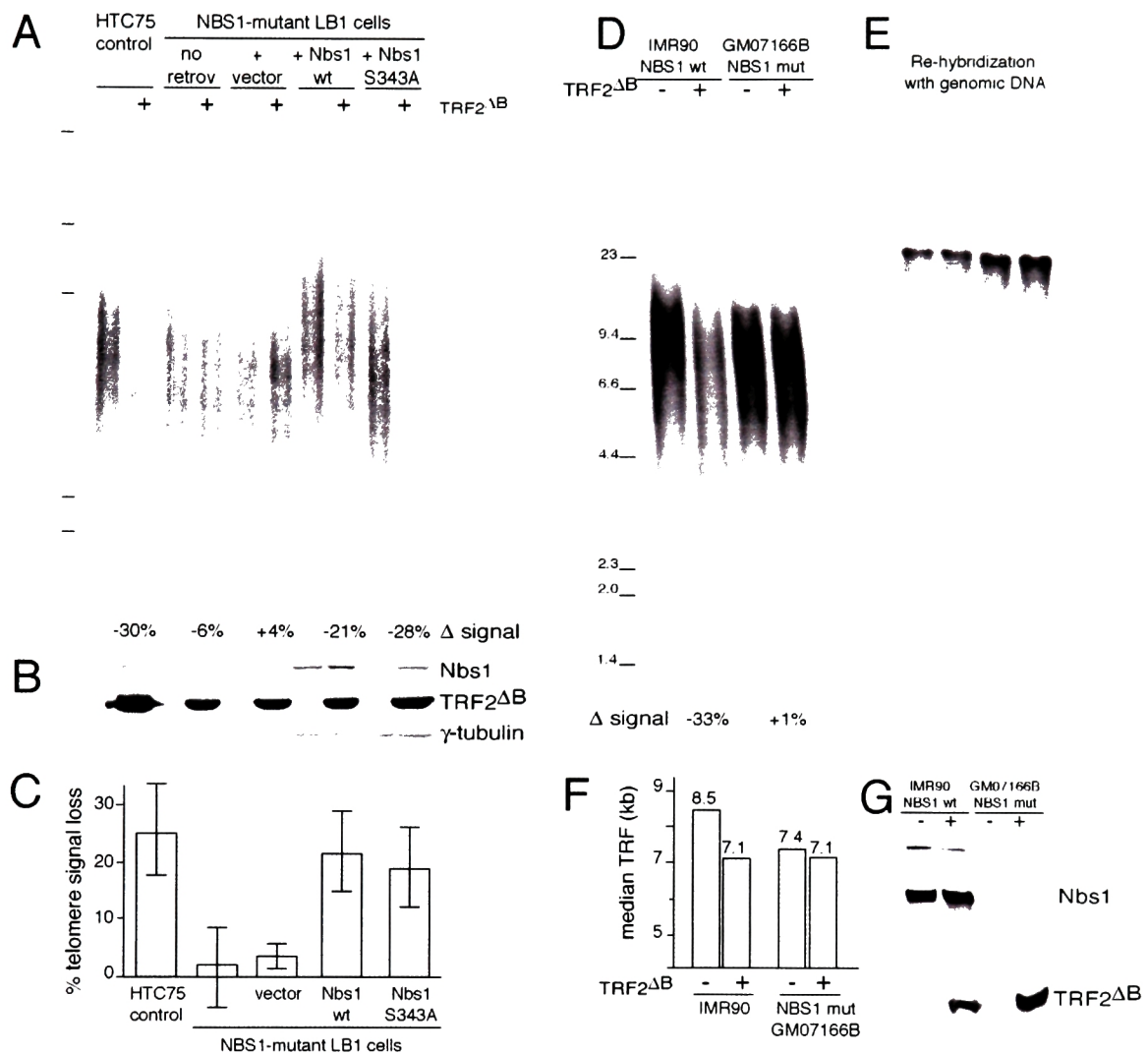


Figure 3-11. Nbs1 is required for TRF2^{ΔB}-induced telomere loss.

(A) Nbs1-LB1 cells were rescued for Nbs1 expression with a wild-type Nbs1 (Nbs1_wt) retrovirus or a phosphorylation deficient Nbs1 (Nbs_S343A) retrovirus. HTC75 fibrosarcoma, Nbs1-LB1 cells, and its derivatives were infected with TRF2^{ΔB} or a vector control and were harvested on day 5 as described in Fig. 3-10. Genomic DNA was digested with *Mbo*I and *Alu*I and probed for telomeric repeats (Sty11). In Nbs1-LB1 cell derivatives (+vector, +Nbs1_wt, +Nbs1_S343A), TRF2^{ΔB} was introduced with using a separate selectable marker (hygromycin). (B) Western blots for Nbs1, TRF2, and g-tubulin. TRF2^{ΔB} is expressed at similar levels in all five cell types. (C) Graph summarizing requirement of Nbs1 for TRD. The graph plots the mean loss of telomeric sequence (\pm SD) induced by TRF2^{ΔB} telomeric repeats from ≥ 4 independent genomic preps (≥ 4 independent infections). (D) Nbs1 fibroblasts (Coriell; GM07166B) were infected with TRF2^{ΔB} or a vector control and harvested on day 6 after selection to prepare DNA and protein. Genomic DNA was digested with *Mbo*I and *Alu*I and 3 μ g was fractionated and blotted for telomeric signals (D). The same blot was stripped and probed to confirm equal loading using a non-specific genomic probe (E). The blots were quantitated and normalized as described previously (Fig. 3-5). The numbers below the lane represent the change in signal intensity after normalization relative to the vector control. (F) The median TRF for both samples were calculated from ImageQuant. (G) Absence of Nbs1 protein in Nbs1 fibroblasts and expression of TRF2^{ΔB} was confirmed by immunoblot. Note that a band corresponding a C-terminal truncation product (p80) is absent from human Nbs1 fibroblasts.

Mouse cells that express a hypomorphic allele of Nbs1 (p80, Nbs1^{ΔB/ΔB}) still delete their telomeres after TRF2ΔB expression (Fig. 3-12A). Additionally, mouse cells that express a hypomorphic allele of Rad50 (Rad50^{S/S}) also efficiently undergo TRF2ΔB mediated deletions (Table 3-2). Unlike primary human NBS fibroblasts, both Nbs1^{ΔB/ΔB} cells and Rad50^{S/S} cells are competent for the localization of the Mre11 complex to the nucleus [359, 360]. While Nbs1 is required to prevent TRF2ΔB mediated telomere deletion, the ability of hypomorphic alleles of Nbs1 and Rad50 to support TRF2ΔB telomere deletions suggests that the loss of the Mre11 complex from the nucleus is necessary for a rescue of TRF2ΔB-mediated deletions. This possibility should be further tested using mouse and human cells deficient for Mre11 or Rad50.

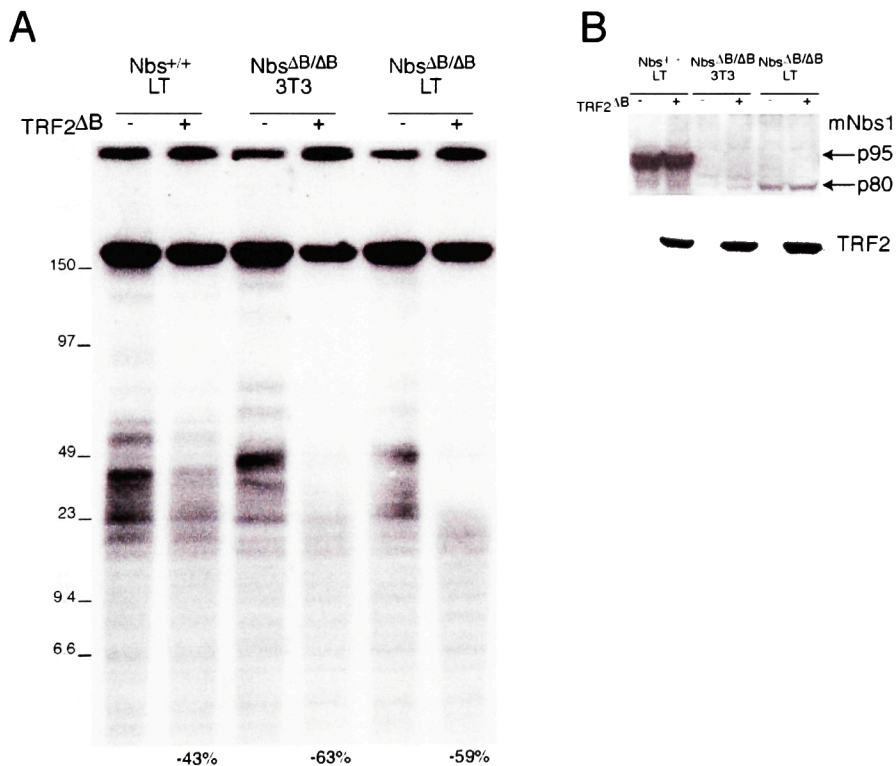


Figure 3-12. Telomeres from Nbs1^{ΔB/ΔB} MEFs still undergo TRF2ΔB-mediated shortening.

(A) CHEF gel telomere blot of Nbs1^{ΔB/ΔB} cells. The indicated MEF type was selected for TRF2ΔB expression for 5 days and harvested from DNA and protein. Blots were quantitated for telomeric repeats as described in Fig. 3-5. The loss of telomeric repeats compared to vector control samples prepared in parallel is indicated below each sample. (B) Western blot of lysates prepared from Nbs1^{ΔB/ΔB} and control MEFs. Nbs1^{ΔB/ΔB} MEFs express a C-terminal truncation of Nbs1 (p80).

Factors that do not abrogate TRF2 Δ B induced deletions

Because of its interaction with TRF2 and known function in modifying TRF2, I tested whether the ATM kinase was required for TRF2 Δ B mediated-deletions. I expressed vector and TRF2 Δ B retroviruses into two ATM deficient primary human cell lines. After 8 days of selection, both lines of ATM-deficient fibroblasts still lost telomeric repeats.

Although telomeric sequence loss appeared to be slightly more efficient (~two-fold) in IMR90 fibroblasts that were processed in parallel, the quantity of telomere loss in the ATM deficient cells was comparable to the levels of telomeric sequence loss that occurred in other cell types including HeLa1.2.11, HCT116, and HTC75 (Fig. 3-4, 3-10, 3-11). Thus, I conclude that ATM is not required for TRF2 Δ B mediated deletions.

Table 3-2. Human mutations that do not abrogate TRF2 Δ B-induced telomere signal loss

Cell line	Gene defect	Telomere signal loss	Days in selection	Source
IMR90	--	34%	8	ATCC
AG02496	ATM	16%	8	ATCC
AG04405	ATM	17%	8	ATCC
AG03141	WRN	19%	7	Coriell
AG06300C	WRN	+	7	Coriell
AG05013	RecQL4	+	7	Coriell
HCT15	Msh6	17%	6	ATCC
HCT116	Mlh1	18%	6	[361]
HCT116+chr 3	Mlh1 rescue	13%	6	[361]
RS-SCID	Artemis	+	7	[362]
SCID	Rag2	+	7	[362]
BJ/hTERT	--	34%, 43%*	5	Clontech
BJ/hTERT	+vanillin	29%, 24%*	5	Clontech
HeLa1.2.11	--	19%*	5	--
HeLa1.2.11	+vanillin	27%*	5	--

Cell lines were infected with TRF2 Δ B and a vector control in parallel and the percentage telomeric signal loss in TRF2 Δ B infected cells compared to the vector control cells was determined as described in the Experimental Procedures. All samples were normalized by Hoechst fluorometry prior to loading. Cells were treated with the DNA-PK inhibitor vanillin at 30 μ M. '+' indicates samples that were not quantitated but showed clear telomere shortening and signal loss. '*' indicates samples that were not normalized for a chromosome internal control band prior to quantitation.

Because the Werner (WRN) helicase associates with TRF2 and regulates HR, I expressed TRF2 Δ B in fibroblasts deficient for the WRN helicase (AG03141). Quantitative telomere blots indicated that these cells still responded to TRF2 Δ B expression by deleting telomeric sequences. One additional WRN deficient line (AG06300C) and one cell lines deficient for the RecQ-like helicase 4 (RecQL4; AG05013), also showed clear telomere shortening and loss after TRF2 Δ B expression (Table 3-2). I conclude that WRN and RecQL4 are not required for efficient TRF2 Δ B mediated deletion. Additional experiments with other RecQ deficient cell lines including BLM helicase deficient and WRN/BLM doubly deficient mouse cell lines will be required to assess more completely possible contributions of the RecQ helicases to HR mediated telomere deletions.

ERCC1/XPF modulates the efficiency of HR in *S. cerevisiae* and mammals. Because I suspected that HR was involved in the TRF2 Δ B-mediated telomere deletions, I tested the effect of the endonuclease on the process. In ERCC1 deficient MEFs, expression of TRF2 Δ B was still capable of catalyzing telomere deletions as assessed by quantitative telomere blots. Thus, ERCC1 does not appear to be essential for TRF2 Δ B-mediated deletion in mammalian cells. Human cell lines with hypomorphic mutations in XPF may be useful in determining whether this TRF2-associated endonuclease has more subtle contributions in modulating HR mediated deletions at mammalian telomeres. In addition, it may be worthwhile examining whether ERCC1 deficient cells possess a defect in HR of telomeres even without the expression of the TRF2 Δ B allele.

Table 3-2. Mouse mutations that do not abrogate TRF2^{ΔB} induced telomere signal loss

Cell line	Gene defect	Telomere signal loss	Days in selection	Source
88-17:3T3	--	43%	5	[360]
25-2:3T3	Nbs ^{ΔB/ΔB}	63%	5	[360]
25-2:SV40LT	Nbs ^{ΔB/ΔB}	59%	5	[360]
824-5	Rad50 ^{S/S}	19%*, 29%*	4, 7	[359]
Immort MEFs	--	30%	4, 7	[363]
Immort MEFs	ERCC1	18%	5	[363]
Immort MEFs	--	14%	4	[364]
Immort MEFs	DNA-PKcs	10%	4	[364]
Immort MEFs	--	19%	4	[365]
Immort MEFs	Ku86	23%	4	[365]
RH3:E1A	--	44%	5	[366]
RH4:E1A	MSH2	50%	5	[366]
MC5:3T3	--	19%	5	[367]
MC2:3T3	MLH1	18%	5	[367]
B4:SV40LT	--	43%	5	[368]
B4:SV40LT	MSH2	49%	5	(Edelmann, unpublished)
B4:SV40LT	MLH1	13%	5	[368]

Cell lines were infected with TRF2^{ΔB} and a vector control in parallel and the percentage telomeric signal loss in TRF2^{ΔB} infected cells compared to the vector control cells was determined as described in the Experimental Procedures. '+' indicates samples that were not quantitated but showed patent telomere shortening and signal loss. '*' indicates samples that were not normalized for a chromosome internal control band prior to quantitation. MEFs were immortalized by introduction of SV40LT, spontaneous immortalization, or due to their p53^{-/-} genotype.

Mismatch repair inhibits the recombination of mismatched sequences. To test for a possible effect of MMR on TRF2^{ΔB}-mediated HR, I introduced TRF2^{ΔB} into both mouse and human cell lines deficient for components of MMR. In two independently targeted lines of mouse cells deficient for Msh2, TRF2^{ΔB} deleted telomeres at similar efficiencies in the mutant and matched control fibroblasts [366, 369] (Table 3-3). Furthermore, the absence of Mlh1 in either mouse or human cells (HCT116) did not abrogate TRF2^{ΔB} mediated deletions compared control cells. The deletion of MMR

does not significantly alter rates of TRD in budding yeast. Similarly, the impairment of MMR in human cells did not strongly affect TRF2 Δ B mediated telomere deletions.

The dual functions of NHEJ factors in telomere maintenance and DSB break repair suggested that it might also affect possible HR events at telomeres. To assess the possible contributions of NHEJ, I expressed TRF2 Δ B in mouse and human cells lacking various components on the NHEJ joining machinery. I found that Ku86^{-/-}-p53^{-/-} and DNA-PKcs^{-/-} MEFs deleted telomeres at rates comparable to wild-type mouse fibroblasts (Table 3-3). Vanillin specifically inhibits the activity of DNA-PKcs but not other PIKK kinases [370]. After the chemical inhibition of DNA-PKcs through vanillin, cells underwent TRF2 Δ B-mediated telomere deletions at levels comparable to untreated control cells. DNA-PKcs deficient MEFs or the cells treated with wortmannin, a less-specific inhibitor of DNA-PKcs, show substantially decreased efficiencies of retroviral integration and undergo apoptosis presumably due to unrepaired abortive retroviral integration events [371, 372]. Consistent with these findings, both BJ/hTERT and HeLa1.2.11 cells treated with vanillin were much less efficiently infected and many HeLa1.2.11 cells died by apoptosis during the infection process. These observations suggest that DNA-PK was at least partially inhibited by vanillin in these experiments. Furthermore, human cells deficient for the NHEJ nuclease Artemis also responded to TRF2 Δ B similar to control Rag2 deficient fibroblasts that were infected in parallel. Neither the mutant mouse fibroblast nor human cell lines inhibited for NHEJ demonstrated significant differences in the efficiency of TRF2 Δ B-mediated telomere deletions.

TRF2 Δ B induces t-loop sized circular DNAs

Mammalian telomeres occur in a t-loop conformation. The inappropriate resolution of t-loops through homologous recombination could explain the deletions caused by TRF2 Δ B. If the expression of TRF2 Δ B resulted in the inappropriate deletion

of t-loops, then the expected products of such a process should be a shortened telomere and a circular telomeric DNA whose size corresponded the original size of the t-loop.

It is possible to detect circular DNA through neutral-neutral 2D gel electrophoresis. 2D gels were developed Brewer and Fangman to analyze the replication intermediates of plasmids that contained autonomously replicating sequences (ARS) [373]. In the first dimension, using low voltages and agarose concentrations, DNA fragments are separated according to their MW. In the second dimension, DNA molecules are fractionated in the presence of ethidium bromide (0.3 $\mu\text{g/ml}$) at high voltage in high percentages of agarose to emphasize the shape of DNA molecules. The second dimension serves to separate molecules according to their shape; the more highly structured a molecule is, the more it is retarded in its mobility in the second dimension. More recently, the technique has been modified to allow for the detection of different types of DNA structures (i.e. linear, circular, supercoiled, ss DNA) [374].

I used this modified version of neutral-neutral 2D gel electrophoresis to analyze the telomeres of cells expressing TRF2 Δ B or a vector control. The 2D telomere blots of HeLa1.2.11 cells expressing TRF2 Δ B had two prominent features when compared with control cells. As expected based on 1D genomic blots, the telomere of TRF2 Δ B expressing cells were shortened compared to control cells (Fig. 3-13). In addition, TRF2 Δ B expression generated a new arc of telomeric DNA whose migration was consistent with that of relaxed, double-stranded circles (Fig. 3-13). Expression of TRF2 Δ B also induced the formation of this novel arc in IMR90 (Fig. 3-18) and mouse cells (Fig. 3-16). These telomeric circles were not strongly induced by overexpression of TRF1 (Fig. 3-14A) or TRF2 Δ B Δ M (Fig. 3-14D), confirming their specificity for the TRF2 Δ B allele. The structure of the telomeric molecules comprising the new arc was confirmed by their co-migration with ligase circularized λ /HindIII DNA fragments when the samples were loaded just adjacent to one another on the same gel (Fig. 3-14).

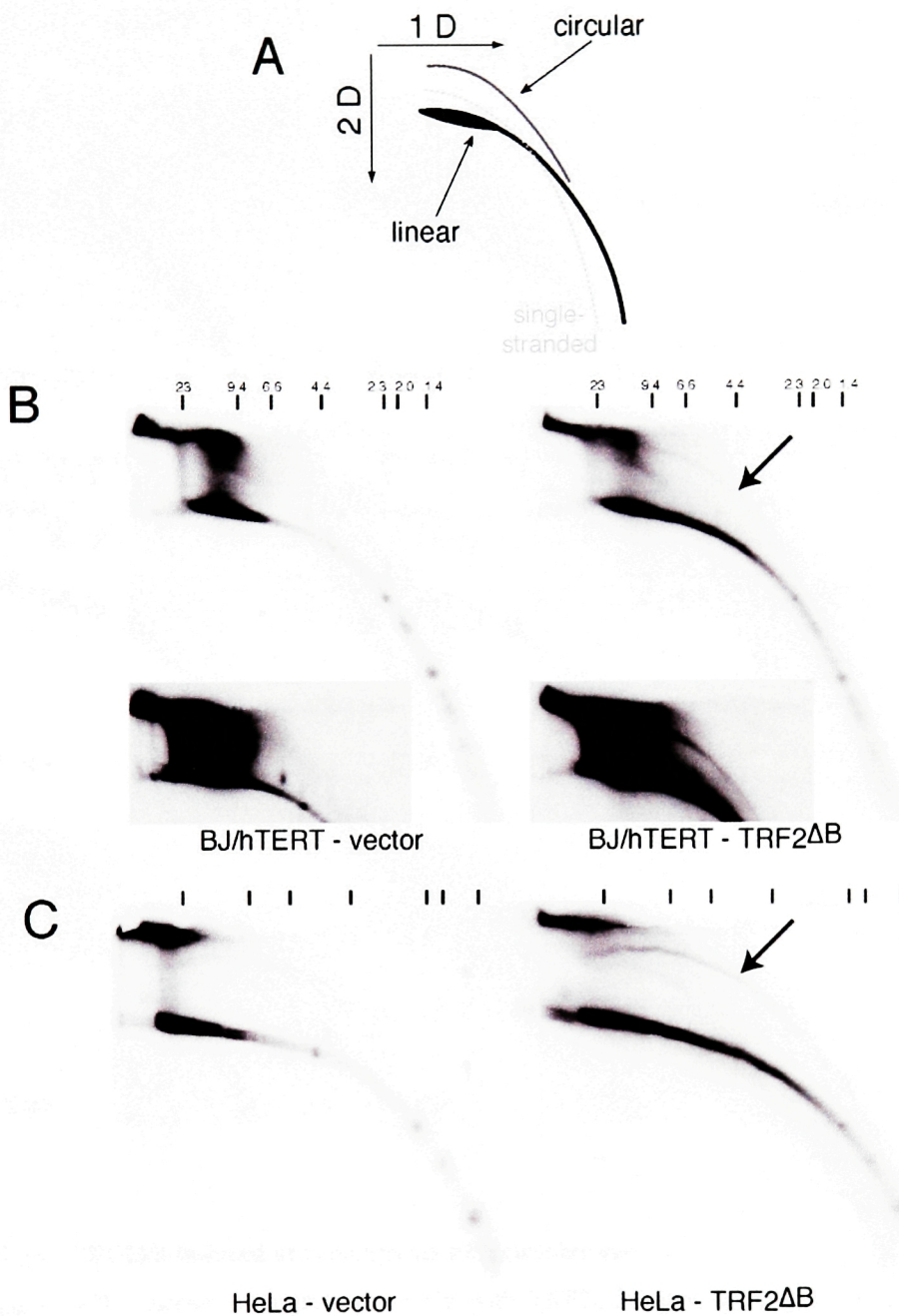


Figure 3-13. TRF2ΔB induces an arc consistent with relaxed telomeric circles detectable by 2D gels.

(A) Schematic of the expected migration patterns of circular ds DNA, linear ds DNA, and linear ss DNA. Molecules are separated by size (1D) and then shape (2D) in the indicated directions [375]. (B) 2D gel analysis of TRF2ΔB expressing cells. BJ/hTERT (right) cells were infected with the indicated viruses and harvested at day 5 of selection. Genomic DNA was isolated and digested with *Mbo*I and *Alu*I. After Hoechst quantitation, equal amounts of the digested DNA (10-15 μg) was separated by 2D gel analysis. Blots were transferred to Nylon and probed for telomeric repeats (Sty11 probe). The MW marker is labeled along the 1D axis. Arrows indicate the telomeric circles induced by TRF2ΔB. Also note the shortened TRFs in the linear ds DNA arc. (Inset) Long exposure of BJ1/hTERT cells demonstrating the presence of low levels of circles in vector control cells. (C) HeLa1.2.11 cells were analyzed by 2D gel as described in (B).

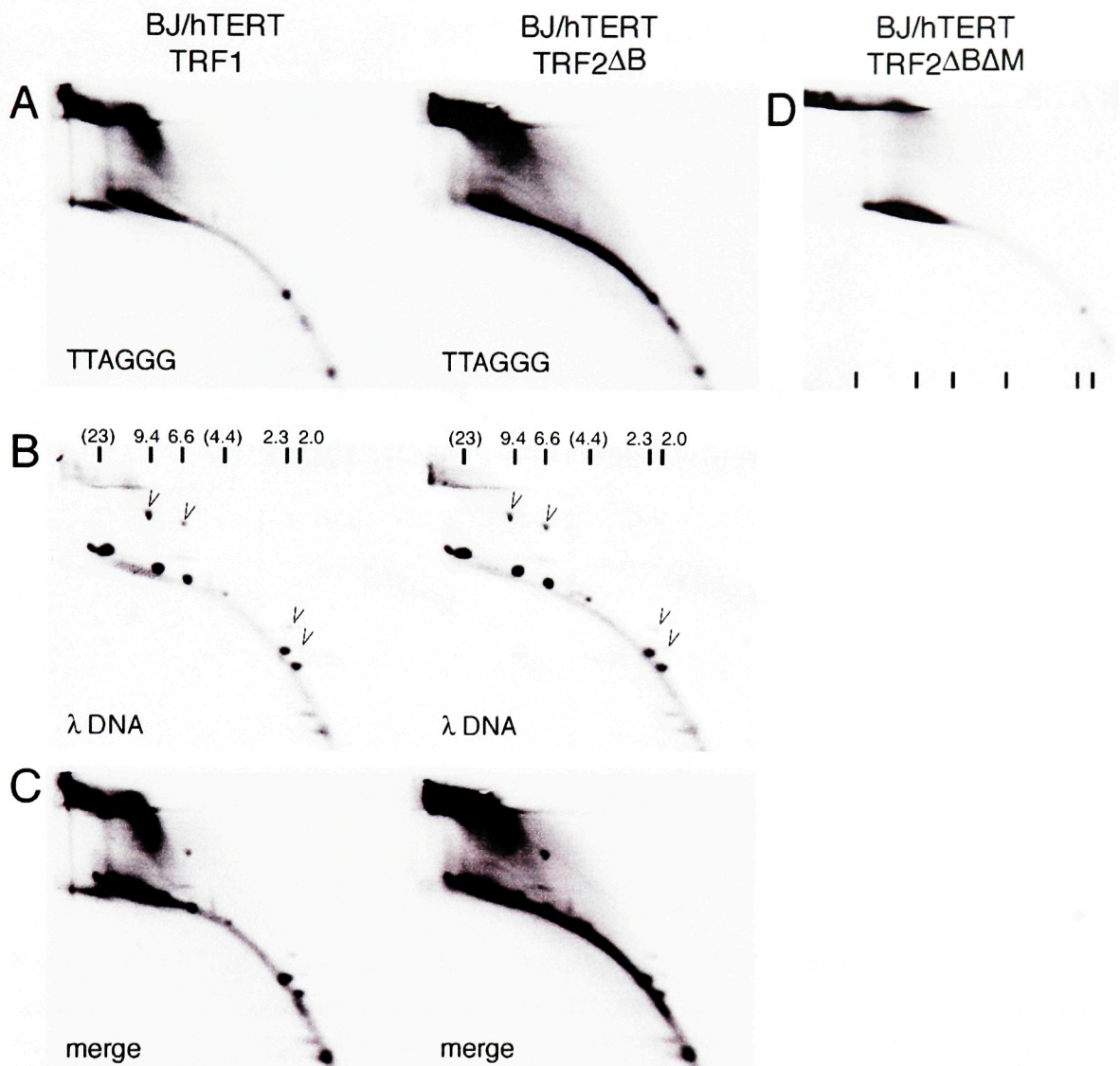


Figure 3-14. TRF2 Δ B-induced arc comigrates with circular marker.

Circularized MW markers comigrate precisely with TRF2 Δ B-induced telomeric circles on 2D gels. BJ/hTERT cells were infected with TRF1 or TRF2 Δ B viruses and prepared as described in Fig. 3-13. The digested genomic DNA was loaded just adjacent to T4 DNA ligase circularized λ /*Hind*III marker (500 ng). The blots were probed for the λ /*Hind*III fragments (B), stripped, and reprobed for telomere repeats (A). Images were merged in Photoshop (C) to confirm the co-migration of the predicted circular molecules. Arrowheads indicate the position of the ligase circularized MW marker. The 23 and 4.4 kb λ /*Hind*III fragments do not circularize because their ends are not complementary (Cos and *Hind*III). (D) BJ/hTERT cells expressing TRF2 Δ B Δ M do not induce telomeric circles. BJ/hTERT cells were infected with TRF2 Δ B Δ M and harvested after 5 days of selection.

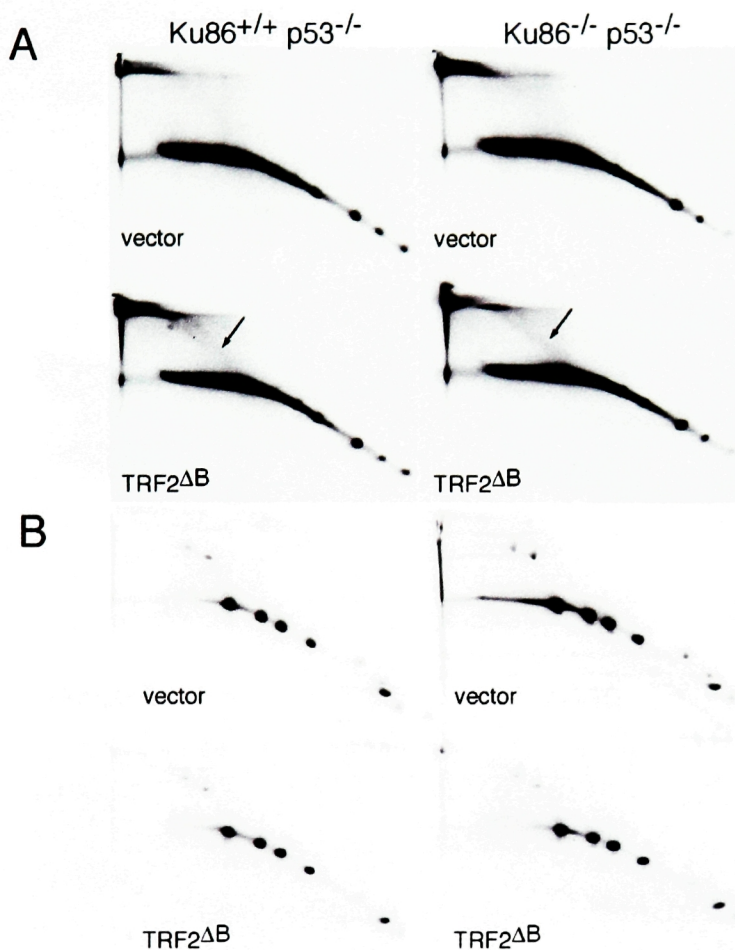


Figure 3-15. TRF2 Δ B-induced relaxed telomeric circles are detected in mouse cells.

MEFs of the indicated genotypes were infected with TRF2 Δ B or vector control retroviruses and harvested 4 days after selection. Genomic DNA from 1.5×10^6 cells was digested in plugs with *Mbo*I and *Alu*I, and separated by CHEF gel in the 1st dimension and by standard 2D gel conditions in the 2nd dimension. DNAs were loaded adjacent to partially circularized λ -*Hind*III fragments cast in agarose gels resulting in co-migration of the fragments in the 2nd dimension. The blots were probed for the λ -*Hind*III fragments (B), stripped, and reprobed for telomere repeats (A). Arrows in the top panels point to circular telomeric DNA, which migrates with the circularized λ -*Hind*III fragments.

Many different structures can possess greatly retarded mobilities in the presence of ethidium bromide in high concentrations of agarose. Although unlikely, it was possible that the TRF2 Δ B-induced telomeric arc could be due to DNA replication or recombination intermediates that had migration profiles similar to circular molecules. mobility in the second dimension. For example, it could be conceived that TRF2 Δ B could somehow stabilize the t-loop structure.

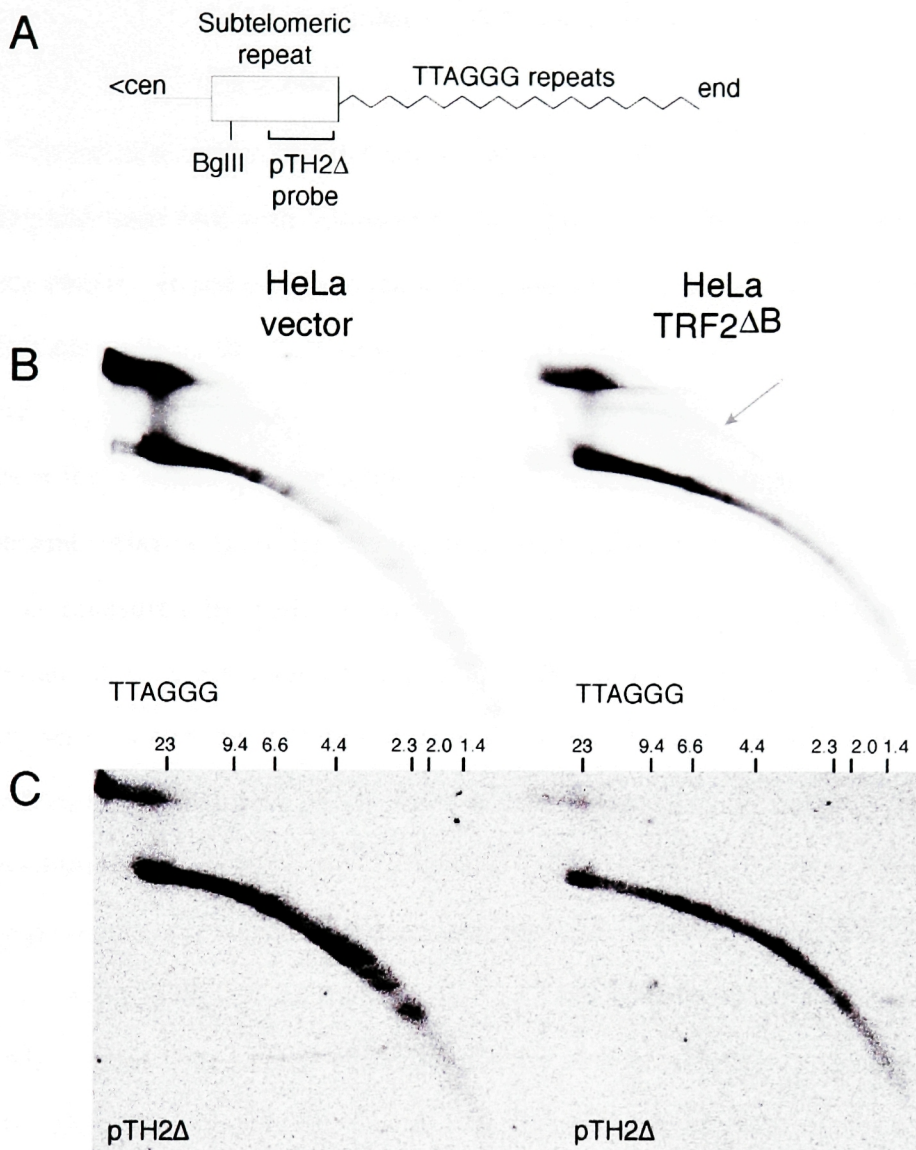


Figure 3-16. TRF2 Δ B-induced circular telomeric DNAs do not contain subtelomeric DNA.

(A) The schematic diagrams the position of the pTH2 Δ probe that is present at ~10% of human telomeres. The indicated DNA was digested with *Eco*RI and *Bgl*III and probed with pTH2 Δ (C), stripped, and reprobred with a Sty11 (B). Relaxed circles are only visible when telomeric circles are used as the probe.

To test this, I probed *Bgl*III and *Eco*RI digested DNA with a subtelomeric repeat element present which was previously found to be present at approximately 10% of human chromosome ends (pTH2 Δ) [349]. If the TRF2 Δ B were telomeric circles, then they should be comprised solely of telomeric DNA. In contrast, if the TRF2 Δ B structures

represented replication intermediates of stabilized t-loops, then the arc would still be recognized by the pTH2Δ probe.

The subtelomeric probe did not reveal any non-linear arcs (Fig. 3-16C); however, reprobing the same blot with telomere repeats (Fig. 3-16C) revealed the presence of the telomeric circles. Based on the absence of subtelomeric repeats in the circles, I conclude that TRF2ΔB induces the formation of structures that are composed solely of terminal telomeric repeats. Because it is likely that other DNA structures like t-loops or replication forks would possess subtelomeric DNA, it is likely that the TRF2ΔB-induced arc represents relaxed ds circles relaxed ds telomeric circles.

As measured by EM, the size of t-loops correlates with telomere length for mammalian cells. Specifically, HeLa1.2.11 cells that have telomeres between 15-40 kb in length possess a range of t-loop sizes, the longest of which are 25 kb in length [134]. As an additional correlation between the telomeric circles and t-loops, I found that the size distribution of telomeric circles induced by TRF2ΔB correlated with this expected size range of t-loops for each particular cell type. For example, TRF2ΔB induced telomeric circles in HeLa1.2.11 (mean TRF ~23 kb) cells that ranged from about 3kb to over 20kb. In contrast, IMR90 cells that possess shorter telomeres (~6-10 kb telomeres) generated circles from ~3-9 kb (Fig. 3-17). Thus, the generation of circular telomeric repeats requires the telomere either already be present in a t-loop configuration or that it proceed through a t-loop intermediate prior to HJ resolution. Therefore, the rapid deletion events associated with the formation of telomeric circles, including those induced by the expression of TRF2ΔB, will hereafter described as t-loop HR. More general events involving homologous recombination at telomeres will be described as telomere HR.

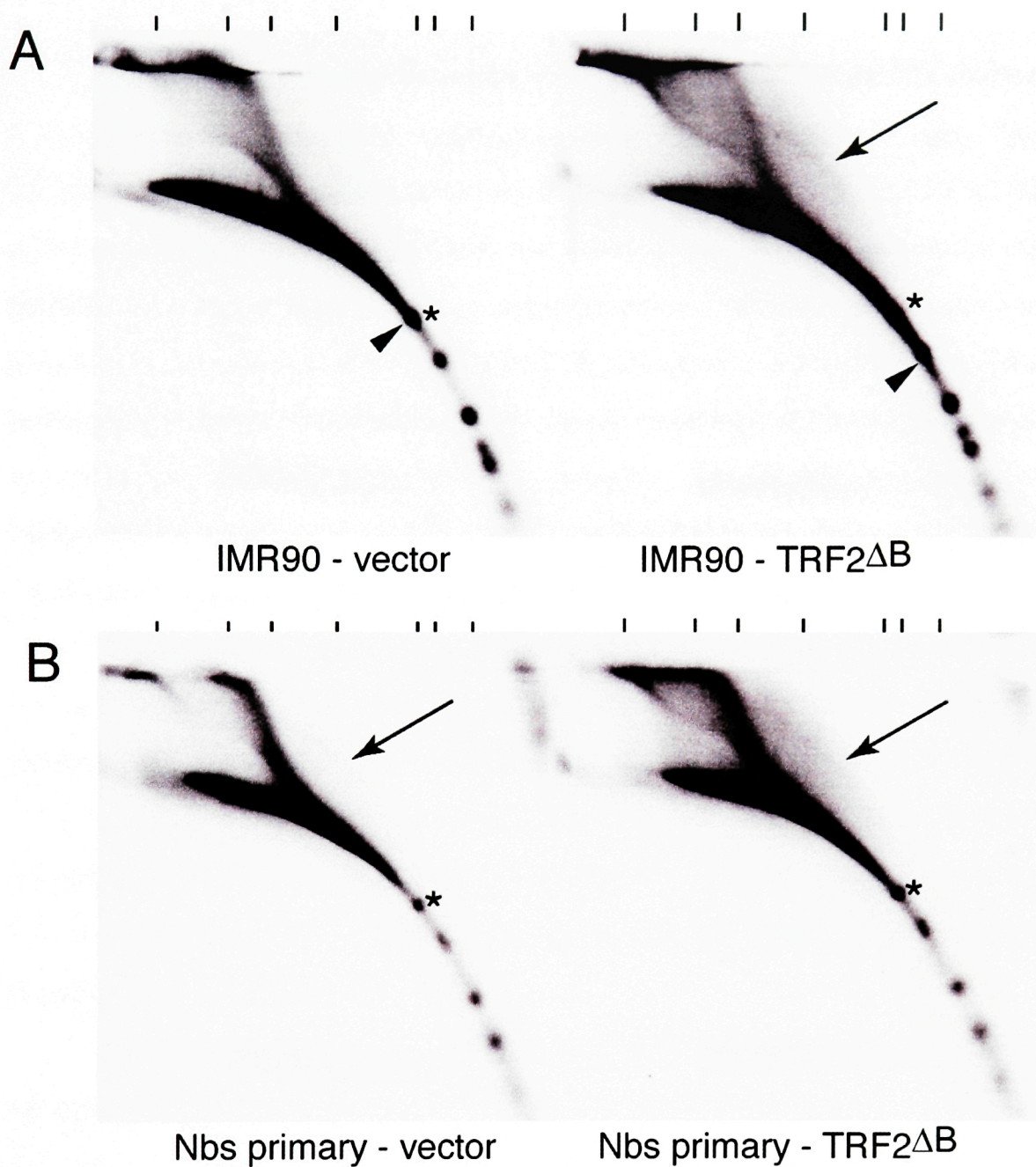


Figure 3-17. Comparison of telomeric circles in primary IMR90 and Nbs1 fibroblasts.

IMR90 or Nbs1 fibroblasts (Coriell, GM07166B) were infected with the indicated virus. Eight μg of *Mbo*I and *Alu*I digested genomic DNA was separated on 2D gels. **(A)** 2D analysis of IMR90 cells. TRF2 Δ B induces shortening of the TRF range. The arrowhead highlights the shift in the TRF length range when compared to an immobile interstitial repeat labeled with the asterisk. Arrow points to telomeric circles induced by TRF2 Δ B. **(B)** 2D analysis of primary Nbs1 cells. TRF2 Δ B does not induce shortening of the TRF range. The TRF length range does not shift appreciably when compared to an immobile interstitial repeat labeled with the asterisk. TRF2 Δ B does not strongly induce the formation of telomeric circles. Primary Nbs1 cells possess higher levels of background telomeric circles than IMR90 cells.

Due to the limitations of the resolution in the 2D gels, circular products derived from very short telomeres (<2 kb) could not be detected as a separated circle arcs. This limitation prohibited the analysis of circular products in cell lines with short TTAGGG repeat regions (e.g., HTC75, HCT116, and NBS1-LB1). Larger t-loops have the potential for a higher degree of branch migration prior to cleavage. More extensive branch migration would allow for more hybridizing sequences to interrupt potential nicks in the relaxed circular structure (Fig. 3-20); thus, it might enhance the preservation of nicked circular structures during DNA preparations. Alternatively, large tracts of telomeric DNA could be maintained episomally or even replicated while smaller circles might lack the ability to recruit binding factors essential to their preservation.

Extended exposures of 2D gels of IMR90, BJ/hTERT, HeLa1.2.11 genomic DNA revealed the presence of low amounts of telomeric circles even in vector control or uninfected cells (Fig. 3-13, 3-17). The presence of the arc in unperturbed BJ/hTERT fibroblasts indicates that circular telomeric DNA are not strictly a result of TRF2 Δ B expression but may also be generated in small amounts by normal telomere metabolism. This finding is consistent with the occurrence of occasional signal free ends in metaphase spreads of control cells (Fig. 3-7).

Although unperturbed primary IMR90 and BJ fibroblasts had very low amounts of telomeric circles in 2D gel analysis, in most analyses these arcs were not detectable without extended exposures of the 2D blots. However, I found that primary Nbs1 fibroblasts expressing vector control possessed a more readily detectable arc of circular telomeric DNA (Fig. 3-17B). Importantly, consistent with the rescue we observed by quantitative Southern analyses, the expression of TRF2 Δ B did not result in an induction of the telomeric circles or a shortening of TRFs when compared to the vector control. Thus, although the effects of TRF2 Δ B-mediated t-loop HR require Nbs1, in the absence

of Nbs1, cells still seem capable of mediating some level of TRF2 Δ B- independent t-loop HR. However, the role of Nbs1 in modulating t-loop HR appears to be more complex.

Preliminary analysis of telomeres with non-denaturing 2D in-gel hybridization

The expression of TRF2 Δ B resulted in the accumulation of excess single stranded DNA at the telomere (Fig. 3-6). Much of the excess ss DNA induced by TRF2 Δ B was retarded in its mobility in 1D gels run in the presence of ethidium bromide suggesting that the ss DNA might possess non-linear structures. To test this possibility, I performed non-denaturing 2D in-gel hybridization on DNA prepared in parallel from vector control and TRF2 Δ B expressing BJ/hTERT cells.

Consistent with my previous 1D in-gel analyses, DNA from TRF2 Δ B-expressing cells was notable for its excess ss telomeric DNA in both strands, but especially marked in the G strand. The additional ss signal did not co-migrate with the arc of circular telomeric DNA, which was visible only after the gels had been denatured. From the 2D in-gel analysis, I conclude that the TRF2 Δ B-induced ss DNA is not present as long stretches of ss DNA within the telomeric circles. However, this does not exclude the possibility that there are short stretches of single stranded DNA on the telomeric circles.

Surprisingly, in both vector control and TRF2 Δ B expressing cells, there were two discernable populations of molecules possessing ss G-rich DNA. The weaker of these two populations migrated just off of the arc of double stranded linear DNA. Curiously, the expression of TRF2 Δ B resulted in an induction of this second population of ss G-rich telomeric DNAs. It is unclear what the second, non-linear population of molecules represents and whether the molecules have significance in telomere maintenance. The analysis of telomeres by 2D in-gel hybridization is still very preliminary and requires further analysis before any conclusions can be drawn.

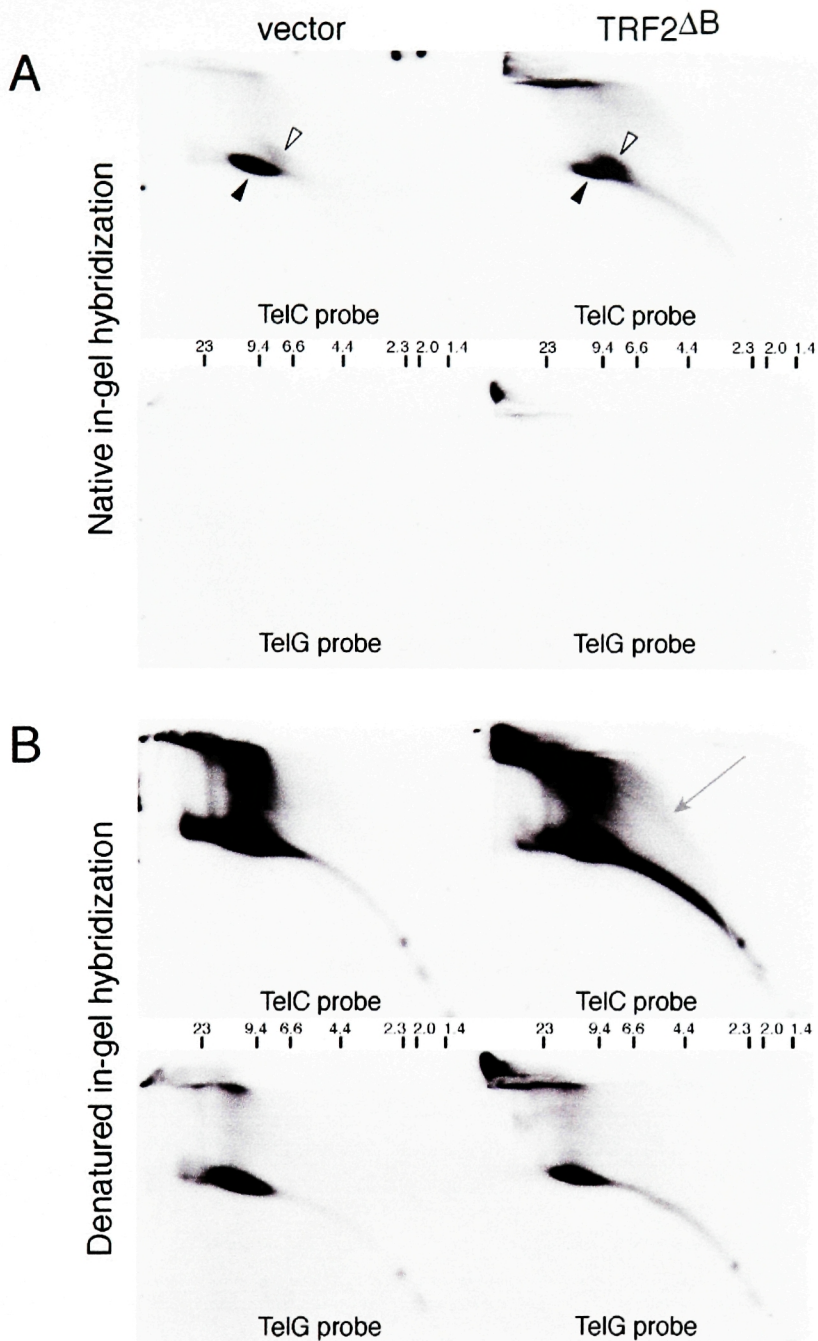


Figure 3-18. TRF2 Δ B induces ss DNA that does not comigrate with telomeric circles in native 2D in-gel hybridizations.

(A) DNA from BJ/hTERT cells was prepared as described in Fig. 3-13. Equal loading was confirmed by EtBr staining. Gels were dried at 45°C for 2 hrs. The same gel were first probed under native (A) and denaturing (B) conditions with an end-labeled (CCCTAA)₄ or (TTAGGG)₄ probe as indicated. Closed arrowhead indicates the expected position of TRFs that possess short overhangs. Open arrowhead indicates an unknown nucleic acid structure that possesses ss G-rich DNA and does not migrate as linear ds DNA; this structure is induced by the expression of TRF2 Δ B. Arrow indicates the 2D telomeric circles detectable in denaturing but not non-denaturing conditions.

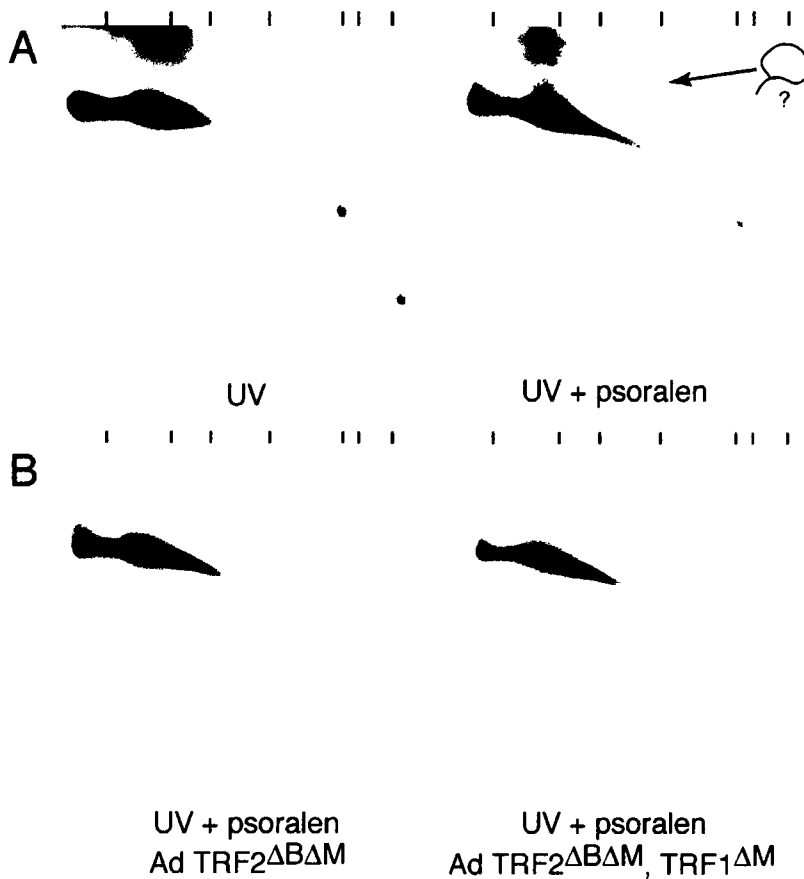


Figure 3-19. Telomeric circles can be visualized after UV cross-linking in the presence of psoralen.

Nuclei were prepared from uninfected BJ/hTERT (A) cells or subsequent to a 48 hr infection with the indicated adenovirus (@400 MOI total) (B). Nuclei were treated with UV (365 nm) with or without psoralen according to condition previously described for t-loop preparation [134]. DNA was prepared and separated by 2D gel as previously described. 2D gels were depurinated for 30 min in 0.5 N HCl prior to a standard Southern protocol. Hybridizations and washes were performed at 55°C.

Preliminary attempts at analysis of t-loop structure by 2D gels

Because circular telomeric DNAs were readily detected on 2D gels, it might also be possible to detect t-loops using this analysis. To address this, I performed 2D gel analyses on genomic DNA, which had been UV-crosslinked in the presence of psoralen, prior to preparation. These conditions have previously been shown to enhance the detection of t-loops by EM, as the structures would normally be lost due to branch migration during standard genomic preparations. The psoralen crosslinking caused the telomeric DNA to be much more difficult to detect by telomere Southern blot. In order to improve the sensitivity, psoralen crosslinked DNA was depurinated in 0.5 N HCl for 30

minutes (rather than 0.25 N for 30 min). In addition, blots were hybridized and washed at 55°C (rather than 65°C).

Using these modified conditions for 2D gel analysis, I was able to detect an arc of products that migrated like relaxed circles. Importantly, this arc was detected only in the presence of psoralen (Fig. 3-19). It is important to note that the overall signal strength of telomere blots after UV irradiation (with or without psoralen) are much lower (at least 10 fold) than normal telomere blots. Thus, the psoralen-induced circular arc only constituted a very small proportion (<1%) of the overall telomeric signal. Furthermore, the strength of this arc did not change with the expression of TRF2 Δ B Δ M as might be expected based on the predicted requirements for t-loop formation (Fig. 3-19B). It has been shown that TRF1 promotes the recruitment of TRF2 to telomeres via an interaction with Tin2 [142, 162]. Thus, because it was possible that TRF1 promoted the recruitment of some TRF2 even in the absence of its Myb domain, I infected cells with both TRF2 Δ B Δ M and TRF1 Δ M and found that the psoralen-induced circular structures also persisted under these conditions. Additional experiments will be required determine whether 2D gels are a valid methodology for analysis of t-loops. It will be especially important to examine the psoralen-dependent arc by EM to order to confirm the migration of t-loop structures in the arc.

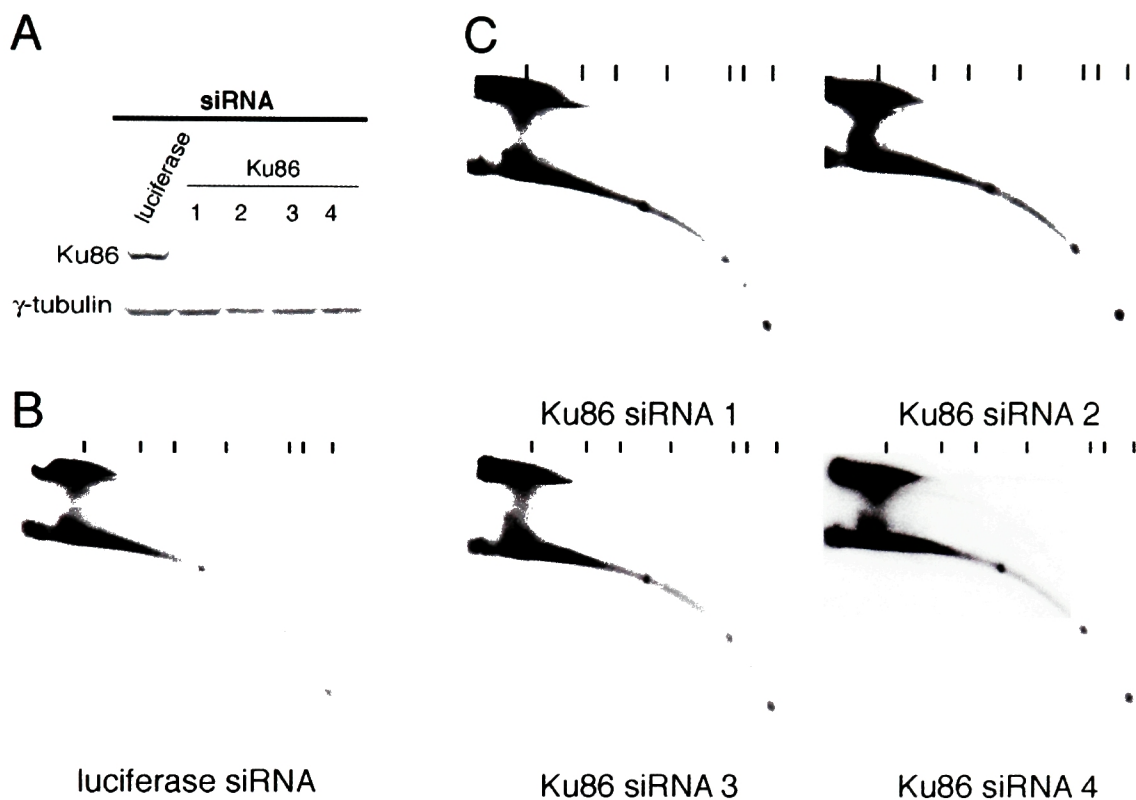


Figure 3-20. Depletion of Ku86 does not induce telomeric circles.

(A) Western blot of lysates from HeLa1.2.11 after Ku86 siRNA. Cells were twice with 24 hr intervals with the indicated siRNA and lysates were harvested 48 hrs after the 2nd transfection. (B) HeLa1.2.11 cells treated with control luciferase siRNA (B) and Ku86 siRNAs (C) have similar levels of telomeric circles.

Inhibition of Ku86 does not induce telomeric circles

Ku deficient mouse cells have been reported to have shorter telomeres. In addition, it was found that human somatic cells heterozygous for Ku had higher frequencies of signal free ends on metaphase spreads [210]. Although TRF2 Δ B mediated deletions were not affected by the absence of Ku86, it is possible that Ku has a TRF2-independent role in modulating HR at telomeres. I tested whether the loss of NHEJ alone would be sufficient to induce HR mediated telomere deletions in HeLa1.2.11 cells. The depletion of Ku86 by siRNA did not result in an obvious loss of telomeric repeats or the strong induction of circular telomeric DNAs (Fig. 3-20). By necessity, these experiments were transient. It is possible that the longer periods of Ku86 depletion are necessary to

effect changes in t-loop HR. In addition, it is possible that the Ku86 does exert an effect on t-loop HR or telomeric recombination that is missed due to a relative insensitivity of 1D and 2D genomic blotting assays. The latter concern could be addressed by analyzing Ku inhibited cells with other markers for t-loop HR, like the occurrence of signal free ends. More careful studies will be required to delineate subtle changes in the rate or efficiency of t-loop HR in the absence of NHEJ.

DNA damage may induce telomere deletions through t-loop HR

The loss of telomeric repeats has been reported to be an early step in DNA damage induced apoptosis though these results are disputed [376-378]. Furthermore, it is thought that the accumulation of oxidative damage at telomeres contributes significantly to telomere shortening [379]. To begin to assess a possible role for telomere HR in DNA damage induced telomere shortening, HeLa1.2.11 were harvested for genomic DNA 8 hr after treatments with either UV (120 J/m²) or camptothecin (10 μM).

Both of these treatments resulted in the accumulation of apoptotic cells. When TRFs in these cells were analyzed by 2D gel, there was an obvious induction of telomeric circles. Currently, it is not clear whether the telomeric circles are the result of DNA damage to telomeres or whether telomere cleavage through t-loop HR is a general outcome during the induction of apoptosis. The induction of apoptosis without inducing DNA damage and vice versa should be able to distinguish between these possibilities. It will be interesting to dissect the possible relationships between t-loop HR and both DNA damage at telomeres and apoptosis.

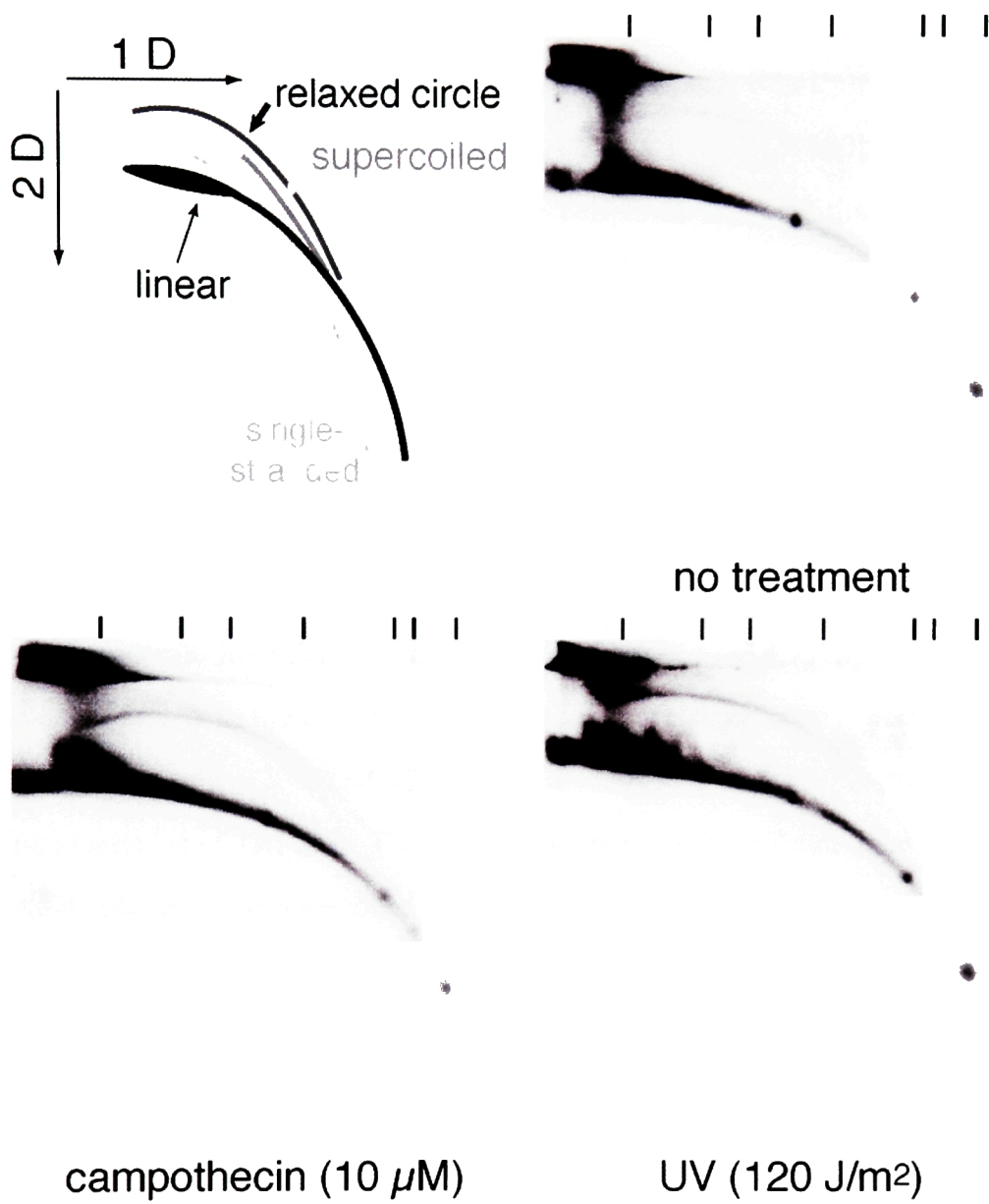


Figure 3-21. DNA damaging agents induce t-loop HR.

HeLa.1.2.11 cells were harvested for genomic DNA 8 hr after the indicated treatments. Both DNA damaging agents resulted in an induction of telomeric circles.

Telomeric circles in ALT cells

As described in the introduction, HR has been implicated in human telomere maintenance in the absence of telomerase, or ALT [342, 343, 380]. The low amounts of telomeric circles in telomerase positive cell lines suggests that HR at telomeres is normally tightly regulated. I predicted that if telomere maintenance by ALT involved an activation of telomeric HR, then telomeric circles should be more abundant in ALT cells. Genomic DNA was prepared from six different ALT cell lines (VA13/2RA, Saos-2, SUSM-1, U2-OS, and MeT-4A). These ALT lines had diverse tissue origins and pathways of transformation [326]. Using 2D gels, I found that five out of six lines possessed a strong arc of telomeric circles (Fig. 3-22). GM847 cells had a circle arc of more moderate intensity, one that was comparable to HeLa1.2.11 cells. The circular telomeric DNA in the five ALT cell lines appeared significantly more abundant than in telomerase positive cells and were comparable to the levels of telomeric circles caused by the expression of TRF2 Δ B. Furthermore, in four of the ALT cell types, an additional arc, which migrated like supercoiled circular DNA, was also detected.

Because of the possible link between ALT and t-loop HR, I examined the levels of telomeric proteins in different ALT cells. All cells appeared to have comparable levels of TRF2, hRap1, Ku70, and Ku86 in comparison to non-ALT cells. However, the Met-4A cell lines appears to have (~4 fold) elevated levels of TRF2, notable with two distinct antibodies against TRF2. This finding was independently confirmed in a separate experiment (Wu and de Lange, unpublished). The significance of the increased level of TRF2 in these cells is not known.

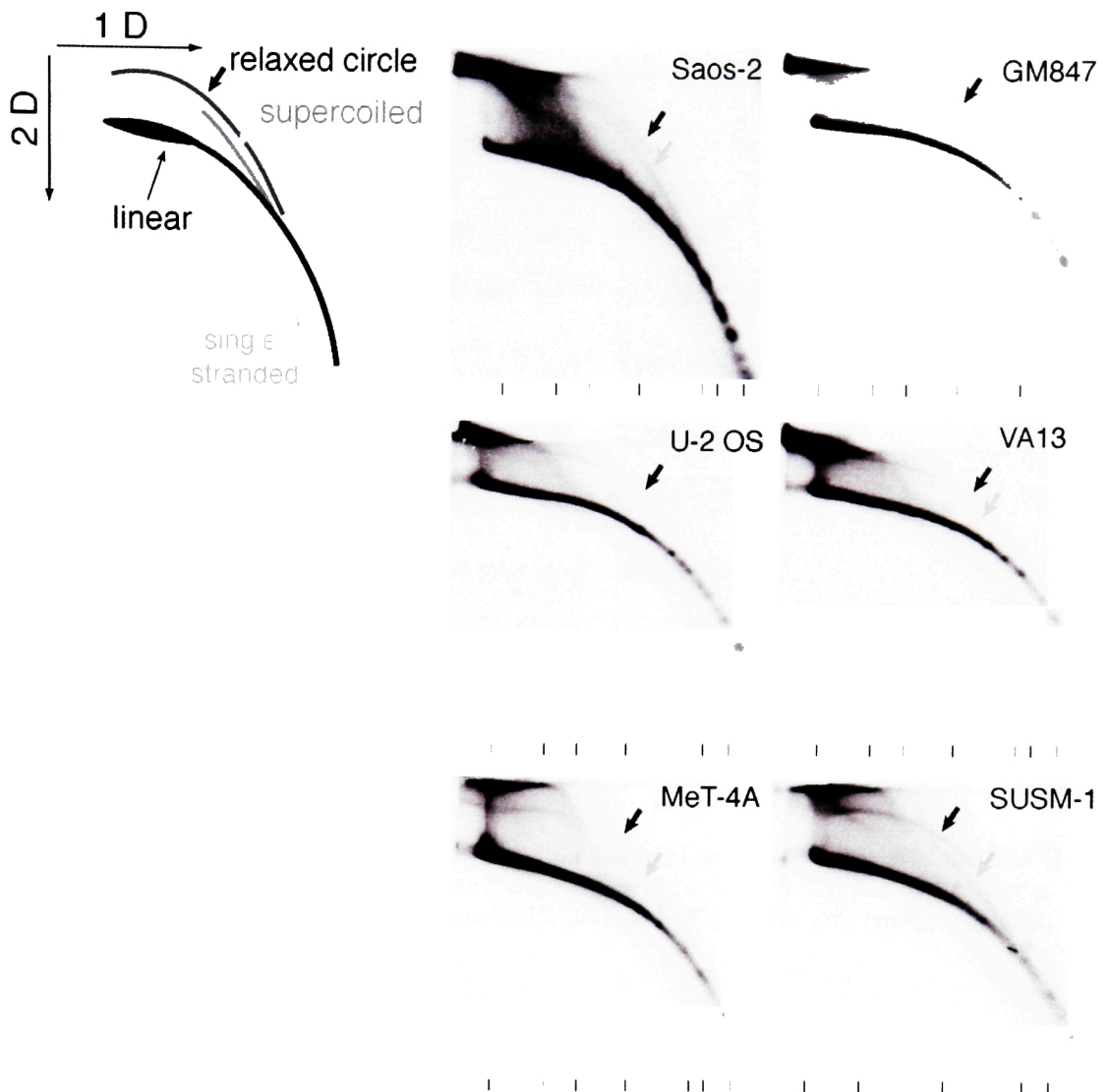


Figure 3-22. ALT cell lines have increased amounts of circular telomeric DNA.

Genomic DNA was prepared from 6 ALT lines, digested with *MboI* and *AluI*, and 10 μ g was separated for 2D analysis. Five out of six lines (not GM847) had patently elevated levels of circular telomeric DNA (black arrow) when compared to non-ALT cell lines. Four out of six lines (Saos-2, U-2 OS, MeT-4A, and SUSM-1) possessed an additional arc of supercoiled circular telomeric DNA (gray arrow).

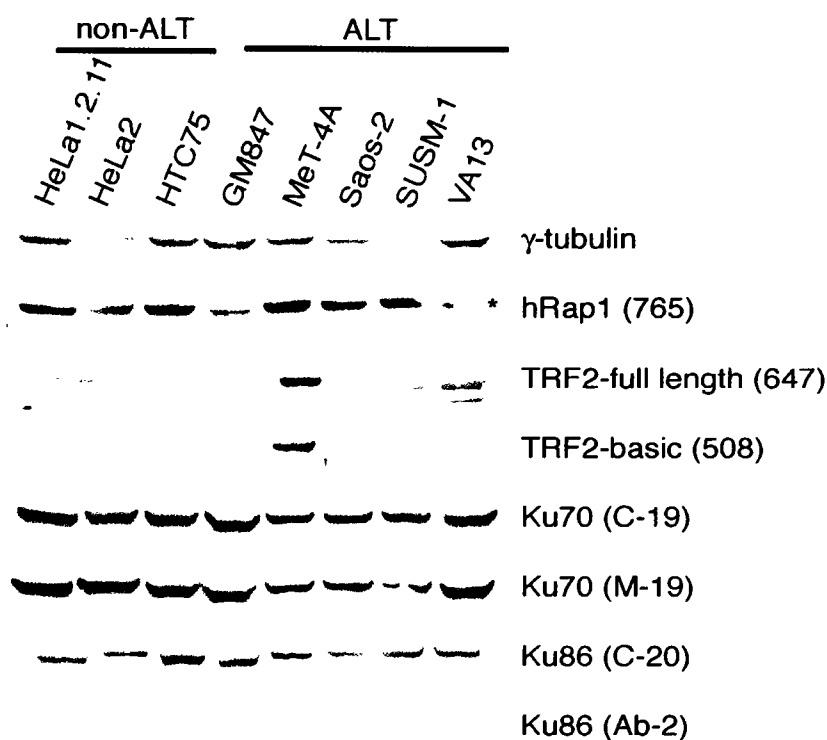


Figure 3-23. Telomere protein expression in ALT cells.

Lysates from the indicated cell types were probed with the indicated antibody. Asterisk represents a transfer artifact. The only notable difference was the increased (~3-4 fold) level of TRF2 in MeT-4A cells. This was noted for two separate antibodies against TRF2 (508 and 647). ALT cell lysates (Laemmli buffer) were a gift from Josh Silverman.

DISCUSSION

The telomeres of mouse and human structures are coated by TRF2 and maintained in t-loops, both of which are thought to sequester chromosome ends and protect them from non-homologous end joining and DNA damage signaling. The expression of a mutant allele of TRF2 that lacks its basic N-terminus results in the induction of telomere dysfunction that is distinct from the telomere capping caused by TRF2 inhibition and characterized by the catastrophic deletion of telomeric sequences, which was accompanied by DNA damage foci and cellular senescence. Genetically, the process is dependent on XRCC3, a component of the proposed CX3 HJ resolvase, and Nbs1, a member of the Mre11 complex; both factors have been implicated in HR. CO-FISH analysis revealed that TRF2 Δ B-induced deletion events can occur after DNA replication

and preferentially affected leading strand telomeres. Finally, using 2D gels, the products of TRF2 Δ B mediated t-loop HR are detected as relaxed telomeric circles. Based on these molecular and genetic clues, we have demonstrated that homologous recombination (HR) mediated deletion of telomeres, called t-loop HR, happens at mammalian telomeres. The detection of small amounts of telomeric circles in unperturbed cells suggests that t-loop HR occurs in normal cells and may explain the strong stochastic element of telomere shortening and cellular senescence. In addition, I find that many ALT cell lines, which are thought to maintain their telomeres through recombination, have elevated levels of telomeric circles.

A role for Rad51 paralogs at the telomere

The data in this chapter show that XRCC3 is required for efficient TRF2 Δ B mediated telomere deletions. We propose that TRF2 prevents the RAD51C-XRCC3 associated HJ resolvase activity from resolving t-loops (Fig. 3-24). This model would be consistent with the recent finding that XRCC3 plays a role in the completion of HR repair events initiated by factors including Rad54 and Rad51B [381]. However, studies have also implicated XRCC3 in early events in HR, like Rad51 loading. Thus, we cannot exclude the possibility that XRCC3 acts early to promote the formation of Holliday junctions at telomeres. CHIP analyses indicate that Rad51C is not present in significant amounts at human telomeres [298]. We suspect that telomeres must have a mechanism to prevent the association of the putative CX3 resolvase to protect t-loop from resolution.

Previous studies have demonstrated that two other Rad52 epistasis group proteins, Rad54 and Rad51D, have protective roles at telomeres. Specifically, mouse cells deficient for Rad51D or Rad54 have modestly shorter telomeres and a slightly increased frequency of telomere end-to-end fusions. These data suggest that factors involved in HR may have a positive role in normal telomere maintenance. For example, HR factors may be required to repair DNA interstrand crosslinks, which would otherwise result in replication fork collapse in S-phase. Thus, it is possible that actions of the CX3 complex

can be specifically coordinated to promote the repair of damaged telomere but not the resolution of t-loop junctions. In future studies, it will be useful to determine how other factors that have been implicated in general HR (Rad51, Rad51B, Rad51C, Rad51D, XRCC2, BRCA1, and BRCA2) affect t-loop HR.

Complex roles for the Mre11-complexity in telomere HR

Mre11 and Rad50 are required for efficient TRD in *S. cerevisiae*. Although budding yeast possess a functional ortholog of Nbs1 in Xrs2, it does not appear to be required for TRD. In contrast, in mammalian cells, Nbs1 is required for efficient t-loop HR. The defect in efficient TRF2 Δ B mediated telomere deletion could be secondary to the loss of nuclear localization of Mre11 and Rad50 in Nbs1 cells. Indeed, I have found that hypomorphic alleles of Rad50 and Nbs1 (Rad50^{S/S} and Nbs1 ^{Δ B/ Δ B}) and an S-phase checkpoint deficient Nbs1 (S343A) are all competent for TRF2 Δ B mediated telomere deletion. For all of the hypomorphic alleles, the Mre11 complex is still capable of localizing to the nucleus [356, 359, 360]. Thus, it is likely that the Mre11 complex rather than Nbs1 per se is required for t-loop HR. Mouse A-TLD cells and human Mre11 deficient cells, like Nbs fibroblasts, have severely compromised levels of the Mre11 complex, which localizes to the cytoplasm [382, 383]. Using these cells, it should be possible to tested confirm the requirement of the Mre11 complex in t-loop HR.

The diverse functions of the Mre11 complex make it difficult to propose its precise role in promoting t-loop HR. One possibility is that the complex promotes the formation of a true HJ from a t-loop after TRF2 Δ B (Fig. 3-24). Curiously, I observe that Nbs1 deficient primary fibroblasts have increased amounts of telomeric circles. It is possible that one of the functions of TRF2-bound, telomeric Mre11 complex is to inhibit t-loop recombination events. It might do so by promoting the repair of damaged telomeric DNA while excluding factors involved in HR. However, upon expression of TRF2 Δ B and the loss of HR inhibition, the Mre11 complex would take on the pathological role of promoting t-loop HR.

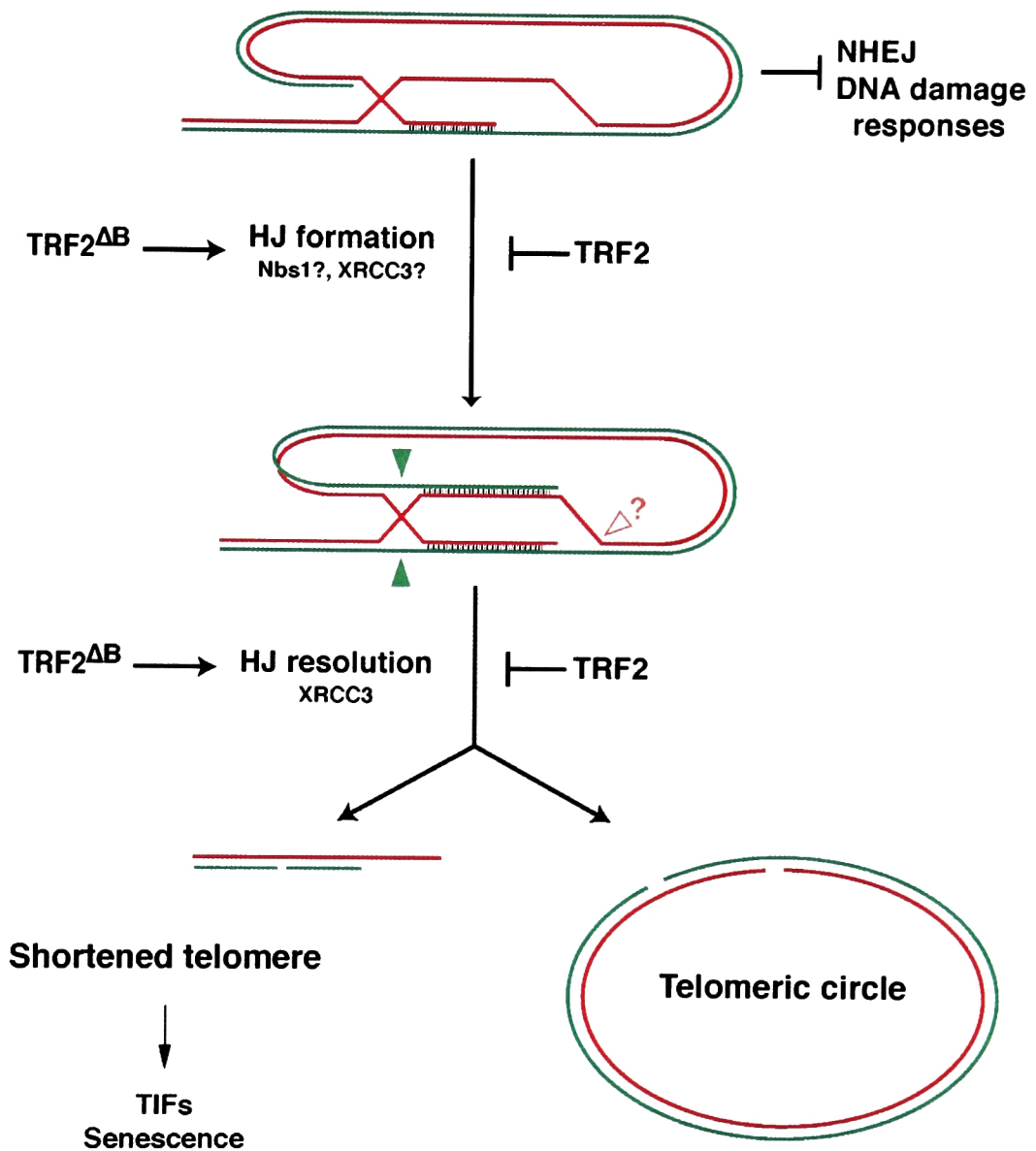


Figure 3-24. Model for t-loop HR.

Model for t-loop HR. Mammalian telomeres are thought to be protected from NHEJ by the TRF2 mediated formation of t-loops. Branch migration at the strand invasion site of the telomere terminus results in the formation of a Holliday junction. Two steps lead to t-loop deletion. Cleavage of the C-strand at two positions by a HJ resolvase (green arrow heads). This process is proposed to require XRCC3. The second step involves nicking of the D loop by an unknown nuclease (open arrow head). The products are a shortened telomere and a relaxed telomeric circle. The shortened telomere might activate a DNA damage response and induce senescence. The basic domain of TRF2 is proposed to suppress t-loop HR either by inhibiting branch migration and/or strand cleavage.

Preferential deletion of parent C strand telomeres

My data showed that TRF2 Δ B mediated deletions occur preferentially on the telomeres containing the parental C. As replication origins are not thought to fire within the telomere, the parental C strand gives rise to the leading strand replication product. Already, there have been strand specific differences observed in post-replicative telomere fusions caused by TRF2 inhibition or by NHEJ pathway deficiency [132]. For post-replicative telomere fusions, it is also leading strand telomeres that appear to be more susceptible to fusion. Telomere uncapping as assayed by TIF formation also appears to preferentially affect one of two sister telomeres [125].

The asymmetry between sister telomeres must ultimately derive from either the different parental DNA (C vs. G strand) sequence or the manner in which a sister telomere is synthesized (leading vs. lagging). A transient, preferential loading of single stranded repeat binding factors like Pot1 and associated proteins on the nascent parental G strand could protect it during and after DNA replication. Alternatively, lagging strand DNA synthesis is known to recruit proteins like PCNA and mismatch repair complexes [384]. Any of these proteins could also contribute to the preferential protection of the lagging strand from deletions.

Furthermore, leading strand replication is predicted to generate a blunt ended product. It is possible that leading strand telomeres could form true HJs rather than t-loops after the expression of TRF2 Δ B. These true HJ would be preferentially resolved by the CX3 resolvase. Finally, it is possible that TRF2 Δ B is asymmetrically distributed on leading and lagging strand replication products resulting in the preferential impairment of one sister. Expressing TRF2 Δ B in the presence of mutant or null alleles of the asymmetrically distributed proteins (e.g. Pot1 Δ OB, MMR null lines) may help to distinguish between the different mechanisms of sister asymmetry. Determining which

factors contribute to sister telomere asymmetry is an interesting problem to explore in future studies.

Changes in telomere end structure by TRF2 Δ B

The expression of TRF2 Δ B resulted in an increased amount of ss G- and C-rich DNA at telomeres. Although the precise structure of this excess ss DNA is not known, it is clear that it does not exhibit the standard sensitivity to ExoI as canonical G-rich overhangs. Furthermore, the high apparent molecular weight of much of the ss DNA suggests that it forms secondary structures that retard its mobility. This secondary structure is not caused by fusions or an increase in telomere length, as these higher MW TRFs are not visible under denaturing gel conditions. It is possible that these extra ss DNA represent hybridizations between ss G- and C- rich telomeres of different telomeres. This might also explain the marked increase in the number of telomere associations that are noted by FISH analyses. The role of TRF2 Δ B in causing the excess ss DNA at telomeres is not clear. The resection of DSBs to generate 3' overhangs is a common step in the repair of DSBs and some of TRF2 Δ B-mediated ssDNA could be a result of this process. Furthermore, TRF2 Δ B could cause telomeres to be more susceptible to nucleases and/or transcription. These possibilities are explored more thoroughly in the discussion.

Possible roles of the basic domain of TRF2

The inhibition of TRF2 by dominant negative TRF2 Δ B Δ M or by its conditional deletion in mouse cells does not result in t-loop HR ((Smogorzewska et al., 2002); G. Celli and TdL, in preparation). Similarly, telomere end-to-end fusions are not observed upon the expression of TRF2 Δ B making it a unique dissociation of function mutant. It is likely that the expression of the TRF2 Δ B Δ M allele of TRF2 disrupts the formation of t-loops, a necessary first step in t-loop HR. This is consistent with the fact that both TRF2 and TRF2 Δ B are competent for t-loop formation in vitro while TRF2 Δ B Δ M is not (Stansel and Griffiths, unpublished). Furthermore, we have found that the Mre11

complex is required for efficient t-loop recombination. While TRF2 Δ B still efficiently targets the Mre11 complex to telomeric DNA, the inhibition of TRF2 may result in relatively less accumulation of the Mre11 complex to telomeres.

The TRF2 Δ B is a separation of function mutant of the TRF2 gene. While it is competent for the inhibition of NHEJ, it appears to have lost its ability to inhibit HR. The occurrence of baseline levels of t-loop HR in the absence of TRF2 Δ B expression indicate that the TRF2 Δ B allele has lost regulation over a process that normally occurs in mammalian cells. Based on ChIP analysis of HTC75 lines, TRF2 Δ B effectively displaces endogenous TRF2 from telomeres (Fig. 3-2B).

Precisely how the basic domain of TRF2 inhibits t-loop HR is unclear. The simplest explanation is that basic domain recruits factor(s) that inhibit HR. Intriguingly, Rad51D, BLM, and WRN localize to telomeres and are all known to regulate HR. It would be interesting to determine whether any of these proteins interact specifically with the basic domain of TRF2. However, based on phenotypes of Rad51D deficient MEFs and BLM or WRN deficient human cells, it appears that the null phenotypes of neither Rad51D nor BLM are similar to the expression of TRF2 Δ B. Therefore, even if these factors were involved in t-loop HR, they would need to act in concert with each other or with additional factors. It is also possible that the basic domain interacts with a novel factor that negatively regulates HR at telomeres. Previous yeast-2-hybrid assays and large scale IPs of TRF2 did not yield candidate molecules that were known to regulate HR. However, this does not rule out lower abundance or transient interactions between TRF2 and novel factors involved in inhibiting t-loop HR. To address the possible role of the basic domain, it may be helpful to overexpress the basic domain and target it to the nucleus. It is possible that the nucleoplasmic localization of the basic domain could titrate necessary factors from the telomere and recapitulate the phenotypes of TRF2 Δ B.

A possible contribution of t-loop HR for general studies of HR

The biochemical assays of HR have been very informative but still yield limited insight to the complexity of HR *in vivo*. Genetic analyses of HR in mammalian has been possible by following the long term outcomes of *I-SceI* induced double stranded breaks in known marker genes [385]. The *I-SceI* induced double strand break system has also been very informative but can only assess the long-term products of the process. As HR at telomeres may have some of the same properties and requirements as HR at other genomic loci, t-loop HR may provide a third, complementary approach for the study of HR. The use of t-loop HR in more general settings would require a precisely controlled induction of t-loop HR in concert with an improved ability to quantitate the circular products of t-loop recombination. Insight in the control of HR at mammalian telomeres will be important for the understanding of telomere dynamics and may also reveal mechanisms by which t-loop or general HR can be manipulated.

An explanation for the stochastic nature of cellular senescence

TRF2 Δ B expression in primary cells causes the rapid induction of cellular senescence. TRF2 Δ B induced cellular senescence in the absence of telomere end-to-end fusions is likely to be caused by the stochastic deletion of one or more telomeres to a length that is ultimately too short to be functionally capped. The TIFs visible in TRF2 Δ B expressing cells would be the consequence of these critically shortened telomeres. *In vivo*, cells appear to senesce with a few large DNA damage foci some of which may represent uncapped telomeres. TRF2 Δ B models the stochastic shortening of genuine senescence better than TRF2 Δ B Δ M, which uncaps all telomeres, regardless of length. Thus, the stochastic telomere shortening and associated senescence triggered by TRF2 Δ B may be a better model for telomere-induced senescence.

The earliest models of telomere attrition predicted that the end replication problem would lead to progressive attrition of all telomere ends. However, experiments with primary fibroblasts clearly indicate that entry into senescence is not a synchronized event. When individual cells are taken from a clonal colony of fibroblasts, those

individual cells go on to form new colonies of dramatically different size. While some subcloned cells divide a similar number of times when compared to their siblings in the original clone, many subclonal population entered senescence within a few divisions; in many cases, subcloned cells were unable to divide at all (Smith and Whitney, 1980).

To explain these stochastic features of senescence, models speculated that both slow, progressive telomere shortening combined with rapid, stochastic shortening events must work in concert to limit cellular lifespan in primary human cells [17]. These predictions have been validated by the assessment of length in an individual telomere (XpYp) using a recently developed protocol called STELA (Baird et al., 2003). Using STELA, Baird and colleagues have documented the abrupt appearance of very short telomeres whose length differs dramatically from the bulk telomeres that undergo progressive shortening.

We have found that unperturbed human cell lines (e.g., BJ/hTERT and IMR90) possess a low, but detectable amount of telomeric circles by 2D gel analysis. The size range of these telomeric circles is consistent with the abrupt shortening events monitored by STELA (Fig. 1-1). Depending on its frequency, t-loop HR could be the major cause of cellular senescence.

Additional sources of telomeric circles

There are almost certainly other factors that could contribute to stochastic telomere shortening. Oxidative damage at the telomere, especially at guanine residues, could be processed to ss DNA gaps. The gap, if unrepaired, might result in a truncated telomere after replication. Also, the possible formation of G-quartet like structures in the G rich DNA could result in a rapid truncation of a telomere during S-phase if it is not properly unwound by helicases prior to replication for progression. My preliminary results indicate that the levels of telomeric circles may also be elevated after cells are treated with DNA damaging. It will be very interesting to understand how specific types

of DNA damage at the telomere and t-loop HR interact with each other and how these processes coalesce to affect telomere length and protection.

I have detected telomeric circles at low levels in unperturbed cells. These circles may represent aberrant attempts at repairing telomeric damage. Previous studies have demonstrated that the treatment of cells with DNA damaging agents resulted in an increase in the amount of small polydispersed circular DNAs; these so-called spcDNAs included telomeric DNA [338, 339]. Unlike any other sequences in the genome, a DSB within a direct repeat sequence can use homology from its own sequence downstream rather than a homologous template on a separate chromosome. The result of this aberrant repair reaction is the persistence of the DSB and the generation of circular DNAs of the repeated sequence.

Manipulating t-loop HR: Implications for cellular senescence

In this study, I have been able to delineate two of the factors involved in catalyzing t-loop HR, Nbs1 and XRCC3. If it were possible to abrogate t-loop HR, then the progressive shortening of telomeres should be the only factor contributing to telomere attrition. Cells without t-loop HR would be predicted to have a greatly extended proliferative capacity and would also be expected to senesce more or less synchronously. Using a combination of 2D gel analyses and STELA to monitor stochastic shortening events, it should be possible to explore the contribution of t-loop HR to cellular senescence. XRCC3 does not appear to be essential for some somatic cells; thus, it may be possible to stably deplete XRCC3 through short hairpin RNA interference in primary cells. Cells depleted for XRCC3 and vector control cells could be monitored in parallel to study the possible contributions of t-loop HR to telomere shortening. Studies designed to monitor the rates of t-loop HR would require the analysis of cells using both 2D gels and STELA. As described earlier, in concert with other HR factors (Rad54, Rad51D), XRCC3 may be required the repair of damaged telomeres. If this is the case, then it may not be possible to extend cellular lifespan by inhibiting HR at telomeres. Doing so might

eliminate shortening by t-loop HR, but it would ultimately result in the rapid shortening of telomeres due to unrepaired DNA damage.

Telomeric circles in ALT cells

HR has been proposed to mediate telomere elongation in telomerase negative ALT cells. Consistent with this possibility, we find that most ALT cell lines have elevated levels of telomeric circles. These telomeric circles may partly explain the detection of extrachromosomal telomeric DNA in ALT cells (Ford et al., 2001; Tokutake et al., 1998). In *K. lactis*, a minority of cells that survive the loss of telomerase may maintain their telomeres using telomeric circles as templates for rolling circle replication [324]. It is possible that the telomeric circles may contribute to a similar process in ALT cells. For telomeric circles to contribute to multiple rounds of rolling circle replication, the telomeric circles would need to be covalently ligated. The participation of such circles in replication could result in the supercoiling of the covalently closed circles. Consistent with this possibility, we find that most of the ALT cell lines possess another strong arc of supercoiled telomeric DNA. This supercoiled arc is just detectable in HeLa1.2.11 but not other cell lines, even after the expression of TRF2 Δ B, suggesting that there may be differences between the way that t-loop HR is deregulated after TRF2 Δ B expression in comparison with ALT cells.

The increased amounts of telomeric circles may not directly contribute to telomere maintenance but, instead, may be an unavoidable consequence of relaxed restrictions on HR at telomeres in the ALT cells. Previous studies have suggested that deletion events may be common at the telomeres in ALT cells. For example, an ALT cell line with tagged telomeres showed stochastic telomere deletions [386]. In addition, compared with spreads from telomerase positive cells, metaphase spreads from ALT cell lines have a higher frequency of signal free chromosome ends [334]. Even if telomeric circles do not contribute directly to ALT telomere maintenance, 2D gel analysis could still serve as an additional marker for the presence of ALT telomere maintenance.

The similarities between ALT and TRF2 Δ B mediated t-loop HR suggest that defects in the same pathway may be involved in both processes. It would be interesting to explore whether ALT cell lines possessed mutations in the TRF2 pathways. My preliminary studies suggest that there are no gross defects in the expression of TRF2, hRap1, or Ku70/86 in many ALT cell lines (GM847, SaOS-2, SUSM-1, VA13, and MeT-4A). However, I did find that MeT-4A cells possessed elevated levels (~4-fold) TRF2 protein compared to all of the telomerase positive cells (Fig. 2-23). This elevation represents a genuine elevation of protein level as it was detected with two separate antibodies against TRF2 and has subsequently been reproduced in independent cell lysates. However, the significance of this elevation is not known. The sequence of the basic domain of TRF2 is wild-type in all ALT cell lines tested (Wu and de Lange, unpublished). In future studies, we will clone and sequence the full length TRF2 from each of the mutant cell lines to test for possible mutations in other regions of the protein. This effort may be especially interesting in MeT-4a cells because of a notable abnormality in TRF2 expression levels.

In addition, we have sequenced through full-length hRap1 in the ALT cell lines. All sequences were normal except for the VA-13/2RA cell line. This cell line possesses a single nucleotide polymorphism in its third exon which results in a K324E missense mutation. However, this AA polymorphism is also present in the WI-38 cell line from which VA-13 cells were derived. As WI-38 cells are not ALT cells, it is not clear whether it is relevant for the ALT phenotype. This possibility that this polymorphism predisposes cells to ALT type telomere mechanisms is currently being tested. We will continue in our analysis of the TRF2 pathway in ALT cells as any mutations in these cell types would be helpful in understanding the regulation of t-loop HR in vivo.

Telomerase may counteract catastrophic telomere deletions

The ability of telomerase to add TTAGGG repeats to chromosome ends counteracts the progressive erosion of telomeres caused by the end replication problem.

Thus, it made sense that telomerase need only be expressed at high levels in proliferative tissues like stem cells. However, the simple idea that telomerase counteracts only slow telomere attrition has recently been met with some confounding factors. Importantly, telomerase expression markedly improves the growth of ALT cells and primary fibroblasts even when its expression did not result in telomere elongation [387, 388]. It has also been noted that primary fibroblasts express low amounts of telomerase. The inhibition of telomerase with a dominant negative telomerase or RNA interference results in a restricted lifespan [37]. Because this inhibition of telomerase did not appear to change the rate of telomere shortening, it had seemed that telomerase has an important role in maintaining a 'capped' telomere structure.

Because we observe that t-loop recombination occurs in unperturbed primary cells, we suggest that telomerase functions to counteract not only the end replication problem but also t-loop deletion events. While t-loop HR stochastically renders individual telomeres virtually undetectable by standard telomere blotting, the majority of the other telomeres would maintain their normal size. Consequently, it would appear as if the mean telomere length and shortening rate had not been affected. We propose that in at least some of these experiments, telomerase is required for cell proliferation through its reconstitution of telomeres deleted by t-loop HR.

CHAPTER 4: DISCUSSION

Preamble

Arguably the most important function of telomeres in any organism is to prevent the chromosome end from being processed as a standard double strand break. In the late 1930's, H.J. Müller became aware of this critical function of telomeres when he observed that terminal deletions and inversions are never recovered in the offspring of irradiated *Drosophila* embryos [389]. Around the same time, Barbara McClintock described how broken chromosomes, in contrast to natural chromosome ends, form dicentric chromosomes that go through cycles of breakage and fusion during repeated rounds of cell division [69, 70]. Since the original deduction that telomeres were important, specialized structures of chromosomes, many molecular details of their protection have been described. Most eukaryotes possess a special enzyme, telomerase, that adds defined repeat sequences to the ends of the chromosome. Although one highly touted function of telomerase is to circumvent the end-replication problem, this function is actually not essential as many cell types that effectively lack telomerase (e.g. primary somatic cells, ALT cells) still have functional telomeres. Thus, perhaps even more important than its function in maintaining telomere length, telomerase adds specific telomeric repeats that function as the binding sites for sequence-specific DNA binding proteins that in turn interact with additional proteins to form the functional telomeric complex. The functional telomeric complex not only ensures that the ends of chromosomes are protected from standard DNA damage processes but also functions to regulate its own length. Some of the protective functions of the telomere are intrinsic to the telomere binding proteins themselves while other protective functions depend on interaction with and modulation of existing DNA damage response factors.

In a general sense, this thesis explores how DNA damage response pathways interact with mammalian telomeres. In Chapter 2, I characterize the human homolog of *Tel2*, a gene that affects telomere length and telomeric silencing in *S. cerevisiae* and the

response to DNA damage in *C. elegans*. In Chapter 3, I use a dissociation-of-function mutant of TRF2, TRF2 Δ B, to understand how HR affects telomere metabolism. In this discussion, I will briefly review the findings of each chapter and speculate more generally about the possible contributions of Tel2 and HR to telomere metabolism.

Possible roles of Tel2 in mammalian cells

Summary of Tel2 phenotypes

I have found that endogenous human Tel2 (hTel2) localized predominantly to the nuclei of human cells where it possessed a granular staining pattern. Surprisingly, hTel2 also localized to the centrosome. This centrosomal localization of hTel2 was confirmed using several different antibodies and was also found to be true for mouse homolog of Tel2. The granular nuclear staining pattern of hTel2 showed some foci of enrichment. These foci colocalized with PML nuclear bodies including some Cajal bodies, but not telomeres in primary cells and telomerase positive cell lines. In ALT cells, Tel2 localized with some telomeres in the ALT associated PML-NBs. Tel2 did not interact with any known telomeric proteins by IP. In addition, a ChIP with antibodies against Tel2 did not demonstrate a strong enrichment of telomeric DNA. However, the overexpression of hTel2 resulted in a modest (~10-20 bp/PD) telomere elongation in both HTC75 and SK-HEP-1 cells. Curiously, the expression of an N-terminal epitope tagged hTel2 may impair Tel2's telomere elongating effects. In addition to a moderate effect on telomere length, hTel2 overexpression resulted in the suppression of the accumulation of cells in G2 following IR. The depletion of Tel2 by two distinct siRNAs resulted in cell death by apoptosis. Furthermore, Tel2 depletion resulted in a modest accumulation of aberrant mitotic cells that arrested with multipolar spindles and disorganized chromatin. Finally, metaphase chromosomes from cells hTel2 depleted cells appeared to be defective in condensation and were curly in their appearance.

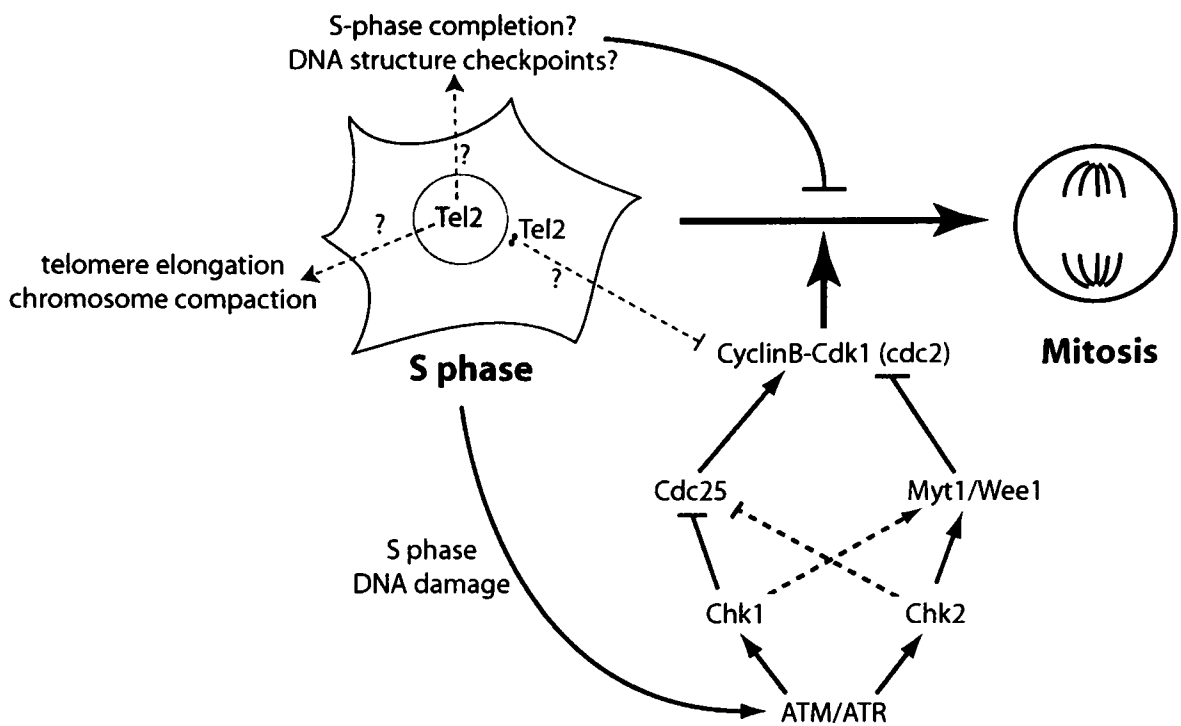


Figure 4-1. Possible functions in S-phase for hTel2.

DNA damage that occurs during S-phase activates defined signaling pathways that halt S-phase progression. In addition to these known pathways, mammalian cells are thought to monitor additional unknown cues that halt cell cycle progression in the absence of complete replication. Many functions of hTel2 may be related to functions in S phase. hTel2 elongates telomeres, a process that happens late in S-phase for yeast and throughout S-phase in human cells. In addition, the depletion of hTel2 results in a modest enrichment of mitotic cells with aberrantly compacted chromosomes. A defect in chromosome compaction at the end of S-phase or a premature onset of mitosis in the absence of hTel2 could explain these defects.

A speculative model for a conserved function of Tel2 in monitoring chromatin

The possible involvement of Tel2 in the diverse processes including telomere length maintenance, chromosome compaction, mitotic progression, and IR dependent G2 accumulation make it difficult to ascribe a single function to Tel2. It is tempting to speculate that Tel2 is involved in the poorly defined replication checkpoint that governs progression from G2 to M. Unknown upstream sensors of DNA structure are thought to inhibit progression into mitosis until the completion of S-phase. This inhibition could occur through known signaling pathways (Myt1/Wee1 kinase and Cdc25 phosphatase) or it may act directly at the level of inhibiting Cyclin B-Cdk1 kinase activity until cells are ready to progress into mitosis. Plk1 has been shown to promote the Cdc25 phosphatase and inhibit the Myt/Wee1 kinase ultimately resulting in a positive feedback loop

reinforcing CyclinB-Cdk1 activity. However, the upstream regulation of Plk1 is not well understood. DNA damage can inhibit Cdk1 activation through the activation of the DNA damage kinases ATM, ATR, and Chk1, which in turn inhibit Cdc25 and Plk1. However, ATR and ATM null mouse cells still do not progress into mitosis when S phase is slowed by HU or aphidicolin [390]. Thus, unlike *S. cerevisiae*, other sensors are likely to be involved in monitoring DNA structure and replication through S-phase.

Drawing from our observations and the phenotypes of *tel2/rad-5/clk-2* mutants in other systems, I speculate that Tel2 is involved in monitoring chromatin during S-phase for replication forks or incompletely condensed chromatin in order to promote their repair and to inhibit progression to G2/M until S phase is complete. Consistent with other hypomorphic alleles of Tel2, one might expect to observe the spontaneous accumulation of DNA damage (*rad-5*), chromosome loss (*tel2*), and defects in cell cycle arrest (*rad-5/clk-2*). A role for *Tel2* in monitoring S-phase might also explain the hypersensitivity of Tel2 depleted fibroblasts to hydroxyurea [237]. In a more severe absence of Tel2, cells would attempt to enter mitosis prematurely despite incomplete DNA replication or DNA condensation. The mitotic arrest that results after hTel2 depletion would result from a spindle-checkpoint dependent arrest of aberrant mitoses. The apoptosis caused by Tel2 depletion would be a result of the failed mitoses or gross defects in chromosome segregation. In this model, the possible localization of Tel2 to centrosomes might be related to its regulation of mitotic kinases, especially CyclinB-Cdk1 and Plk1, both of which appear to be activated on centrosomes first [391].

In *S. cerevisiae*, the replication of yeast telomeres has been shown to happen late in S-phase. *Tel2* mutants may be especially compromised in the protection of these late firing origins thus impairing the complete replication of telomeres. A role for Tel2 in telomere replication would be consistent with the observation that Tel2 associates with telomeric chromatin during S-phase (Runge K., personal communication). The extension of telomeres by telomerase is also thought to happen late in S-phase and, thus, may also

be affected by premature entry into mitosis [200]. Finally, chromatin condensation through the recruitment of the Sir proteins at telomeres, a process which is necessary for TPE, might also be inhibited by the premature entry into mitosis.

Mammalian telomeres fire asynchronously in S-phase, so any effects of Tel2 mutation on telomere maintenance in mammals would be less apparent but could still be exerted at the level of telomere replication [392, 393]. My preliminary suggests that Tel2 mediated telomere elongation is dependent on telomerase. Additional studies in primary and ALT cells will be necessary to confirm the telomerase dependence of Tel2 telomere elongation. Determining the effects of hTel2 depletion on telomere length are absolutely necessary to confirm its proposed role as a positive regulator of telomere length. If the depletion results in the expected telomere shortening, it will be interesting to determine whether Tel2 affects the stability of telomerase or the access of telomerase to telomeric chromatin.

If Tel2 is important for regulating S-phase progression, it is possible that its overexpression could improve the cell's ability to progress through S-phase even after DNA damage. Perhaps consistent with this model, I found that the overexpression could promote progression to G2 after DNA damage. Importantly, according to this model, the depletion of Tel2 should compromise S-phase DNA damage checkpoints. This prediction will be tested in mouse cells with a conditional allele of Tel2.

Recently, mouse Tel2 has been found to be an essential gene (Takai and de Lange, unpublished). Although Tel2 is essential at the cellular level, cells that have a conditional allele of Tel2 have been generated. In a p53 deficient setting, the loss of mTel2 resulted in cell cycle arrest. The cells senesce, but did not undergo apoptosis. The difference between the response of MEFs and HeLa cells could be due to the absence of p53 in the MEFs; alternatively, the depletion of hTel2 in HeLa could work synergistically with unknown defects in HeLa2 cells to induce apoptosis. Importantly, the expression of exogenous mTel2 rescued the defects of the presumed Tel2 MEFs,

indicating that the defect in cell proliferation were specifically due to the loss of Tel2p. Finally, consistent with a decreased BrdU incorporation after Tel2 depletion (Fig. 2-13E), Tel2 null MEFs had reduced levels of cells in S-phase as assessed by FACS for both DNA content and BrdU incorporation. These conditionally targeted fibroblasts should be a powerful tool for understanding the essential functions of the gene. Because the gene is essential, it may also be informative to study the phenotypes of mice heterozygous for Tel2. For example, Tel2 may be haploinsufficient for the maintenance of telomere length, so telomere length blots of cells from heterozygous mice may be informative. Furthermore, as *C. elegans* that possess the *clk-2* mutation have an extended lifespan, it may be interesting to monitor the development and lifespan of Tel2 heterozygous mice.

Although it is more satisfying to attribute a conserved function for the many known homologs of Tel2/Rad-5/Clk-2, it is also possible that the proteins have been implicated in diverse processes because they have evolved to have different roles. The lack of obviously conserved domains with known function may support this more conservative interpretation of the results. As more information comes from other model systems and Tel2 null mouse cells, we should be better equipped to understand the essential role of Tel2 in mammalian cells and its possible role in DNA damage checkpoints and telomere function.

TRF2 protects chromosome ends from HR

Summary of telomere deprotection by TRF2 Δ B

TRF2 protects telomeres from being recognized as DNA damage and being processed by NHEJ. Although these functions of TRF2 were first described using a dominant negative allele, TRF2 Δ B Δ M, they have subsequently been confirmed with knockout MEFs (Celli and de Lange, unpublished). In the course of my studies with an allele of TRF2 that lacks its basic amino terminus, I have found that TRF2 also protects telomeres from HR. The expression of TRF2 Δ B caused rapid telomere shortening that

was visible by FISH and Southern blots. Cell lines deficient for proteins previously implicated in HR, XRCC3 and Nbs1, were resistant to TRF2 Δ B mediated telomere deletion. Furthermore, I used 2D gels to detect relaxed telomeric circles as the deletion products of TRF2 Δ B mediated telomere HR. I found that low levels of telomeric circles were detectable in normal cells suggesting that telomere HR could contribute to stochastic telomere shortening even in the absence of TRF2 Δ B expression. Finally, most ALT cells, which have proposed to maintain their telomeres by HR, have higher levels of telomeric circles than non-ALT cells. Collectively, these studies demonstrate that TRF2 protects telomere from deletion by HR and suggests that telomere HR has an important role in telomere maintenance.

Inhibition of telomere HR – an explanation for Ku’s diverse roles at telomeres?

NHEJ factors including Ku, XRCC4, and DNA-PK inhibit HR in mammalian cells [315]. Furthermore, yKu inhibits TRD in *S. cerevisiae*. However, my studies did not implicate NHEJ in TRF2 Δ B mediated t-loop HR. Based on quantitative telomere blots, the extent of TRF2 Δ B mediated telomere HR events were similar in Ku86 in mouse cells, DNA-PK null mouse cells, or Artemis deficient human cells. The inhibition of DNA-PK catalytic activity with vanillin also did not affect TRF2 Δ B mediated deletions. It is possible that NHEJ and TRF2 function in separate pathways to protect telomeres from HR. Thus, some of the cells that I analyzed for TRF2 Δ B epistasis, like Ku deficient MEFs, may have already experienced telomere HR events and reached a shorter telomere length equilibrium. To address this possibility, it would be necessary to inhibit NHEJ and induce TRF2 Δ B telomere HR simultaneously. Such experiments may be possible by depleting the Ku heterodimer through RNA interference concomitant with the induction of TRF2 Δ B. It is possible that more careful analyses like these will reveal any subtle effects that NHEJ factors have on t-loop HR.

As described in the introduction, the inactivation of Ku in a variety of organisms results in disparate effects on telomere length and function. In *S. pombe*, *S. cerevisiae*,

mouse, and human cells, the inactivation of the Ku heterodimer is associated with telomere shortening. In contrast, in *Arabidopsis*, the loss of Ku70 results in a telomerase dependent telomere elongation and loss of length regulation. In *S. cerevisiae*, *Arabidopsis*, and human cells, the loss of Ku is also associated with an increase in the length of single-stranded G overhang at telomeres. A loss of control over telomere HR mediated deletions could provide a unifying explanation for at least some of the diverse telomere phenotypes resulting from the loss of Ku. If the Ku heterodimer were normally required to inhibit intra-telomeric HR events, then the telomere shortening in yeast and mammalian cells lacking Ku could be explained by increased rates of telomere HR mediated deletions. In *Arabidopsis*, the loss of Ku might also result in increased rates of inter-telomeric recombination as evidenced by a loss of telomere length homogeneity. However, in contrast to yeast and mammalian cells, in *Arabidopsis*, telomerase appears to compensate for the increased rates of telomere loss by overelongating the telomeres. Consistent with this interpretation, the dual loss of telomerase in conjunction with Ku in *Arabidopsis* or *S. pombe* results in exaggerated telomere shortening and the rapid onset of senescence. Thus, it is possible that one of the primary functions of Ku at the telomere of many organisms is to prevent telomere HR events.

A role for other telomere binding proteins in telomere HR?

In this thesis, I have studied the process of telomere HR using a mutant allele of TRF2, TRF2 Δ B. In future studies, exploring the role of other known telomere binding proteins in telomere HR may give us a better understanding of both telomere HR and TRF2's role in regulating the process. In particular, hRap1 and hPot1 may be worthwhile candidates to investigate. Studies with hRap1 may be informative because it is a direct binding partner of TRF2. Furthermore, length studies using various mutant alleles of hRap1 indicate that it can affect the length heterogeneity of telomeres. Specifically, expression of a mutant allele of hRap1 lacking the BRCT domain hRap1 Δ Br results in telomere elongation and a homogenization of the size range of telomeres. It is possible

that the BRCT domain of hRap1 positively regulates t-loop recombination events at the telomere. The expression of hRap1 Δ Br would decrease normal levels of t-loop HR resulting in telomere elongation and more length homogeneity. Although the hRap1 interaction domain is intact in TRF2 Δ B, the absence of the basic domain may have more subtle effects on their interaction.

Currently, hPot1 is the only ss DNA binding protein of mammalian telomeres. As discussed in the introduction of Chapter 3, ss DNA plays an essential role in promoting HR. Thus, hPot1 may be important for regulating the formation of heteroduplex DNA within telomeric tracts. The loss of Pot1 in *S. pombe* results in the complete loss of telomeric and telomere associated sequences. It is important to note that currently there is no evidence that the deletion of *S. pombe* telomeres is related to HR. Furthermore, in human cells, interfering with the activity of hPot1 with a mutant lacking the ss DNA binding domain or depletion of hPot1 through RNA interference results in telomere elongation rather than telomere shortening. Thus, it seems unlikely that a straightforward loss of hPot1 function would result in telomere HR. However, the role of hPot1 in telomere HR may be analogous to that of TRF2. Interfering with TRF2 function results in NHEJ and telomere fusions; likewise, a more subtle perturbation of hPot1 may reveal possible roles in telomere HR. I have also observed that the expression of TRF2 results in an increased amount of ss DNA at telomeres. It may be interesting to know whether the increased ss DNA at telomeres affects the manner in which hPot1 is regulated at telomeres. A more careful analysis of other telomeric proteins, especially hRap1 and hPot1, may help to uncover TRF2's specific role in modulating telomere HR and yield a more general understanding of how the process is regulated at mammalian telomeres.

A role for TRF2 in chromatin at telomeres?

The telomeres of *S. cerevisiae* are maintained in a transcriptionally silenced, “closed” chromatin configuration state. Rap1 is involved in recruiting Sir3 and Sir4 to telomeres and other silent loci to establish transcriptional silencing [91, 394]. In addition,

Ku recruits and/or activates Sir4 to promote silencing of the telomere [395]. The deletion of either Sir3 or Ku alters TRD in *S. cerevisiae* both increasing its frequency and decreasing the precision of the deletion events. The inhibition of transcription by the chromatin at yeast telomeres may also be related to the suppression of telomere HR. In particular, the *hpr1* Δ mutant that shows a 10-fold increase in the rate of TRD is also known to promote intrachromatid recombination between repeats in a transcription dependent manner [318]. Thus, at the very least, the state of chromatin at the telomere can modulate the rate of TRD. Other studies have suggested that chromatin state can be a critical factor in preventing HR. In particular, studies in *S. cerevisiae* show that the Ty repeat element exhibits low levels of recombination due to its maintenance in a closed, nuclease-insensitive chromatin, a configuration that can be propagated to flanking DNA sequences [396].

In mammalian cells, there is increasing evidence that telomeres are heterochromatic or compacted in a “closed” chromatin state. In one study, it was found that expression of a luciferase gene incorporated next to a newly formed telomere was repressed 10 fold compared to randomly integrated chromosomal loci [397]. In mouse cells, telomeric DNA appears to be associated with di- and tri-methylated H3-Lys9 [398]. Furthermore, mice deficient for factors known to be involved in the establishment of heterochromatin including SUV39 DN and triple Rb knockout mice have defects in telomere length maintenance [398, 399].

The simplest explanation for the actions of the TRF2 Δ B would be that the protein fails to recruit factor(s) that directly inhibit HR. However, a strict increase in telomere HR may not explain the increased frequency of telomere associations and the increased amount of single stranded DNA at telomeres. I suggest that increased telomere HR could be a consequence of a more general alteration of telomeric chromatin. For example, the basic domain of TRF2 could be involved in recruiting factors that maintain telomeres in a “closed” chromatin configuration. If TRF2 were required for maintaining compact,

nuclease-insensitive telomeric chromatin, then the expression of TRF2 Δ B would result in an opening of telomeric chromatin making it both more susceptible to inappropriate transcription, nuclease activity, and HR. Aberrant transcription or nuclease activity at telomeres could explain the excess single-stranded DNA at TRF2 Δ B expressing telomeres. Non-covalent interaction between the ss DNA of different telomeres would explain the telomere association visualized by FISH. If the telomeric chromatin is “opened” by the expression of TRF2 Δ B, it should be possible to detect differences in the sensitivity of the telomeres to DNase I and micrococcal nuclease. It has previously been observed that RNA transcripts corresponding to telomeric repeats are detectable in human cells (de Lange, unpublished data). It may be worthwhile to determine whether these RNA transcripts become more abundant after the expression of TRF2 Δ B.

A role for telomeric circles in telomere maintenance?

Telomeric circles are not limited to mammalian cells. Previously, it was found that *Xenopus* embryos possessed telomeric circles early in their development [375]. In addition, the mitochondria of some *Candida* species use 750 bp direct repeat sequences as telomeric sequences. Circular telomeric DNA that corresponded to multimers of 750 bp were visualized by EM [400]. As the linear mitochondria of *Candida* are not thought to be extended by a telomerase enzyme, it is possible that telomere circles provide a means of telomere elongation in those mitochondria. The recombination of telomeric circles into linear chromosome ends would result in the elongation of shorter chromosome ends.

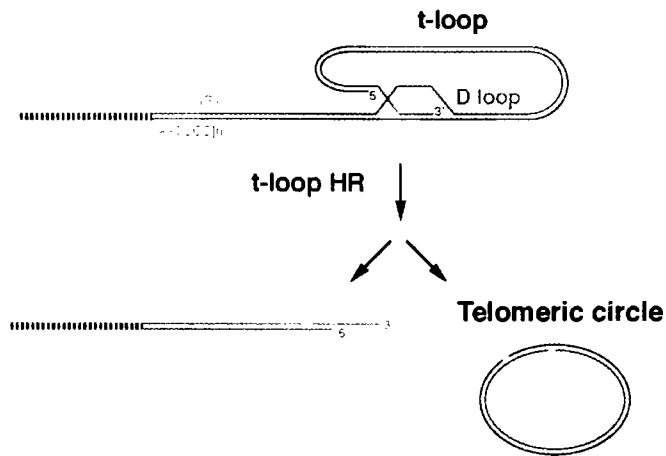
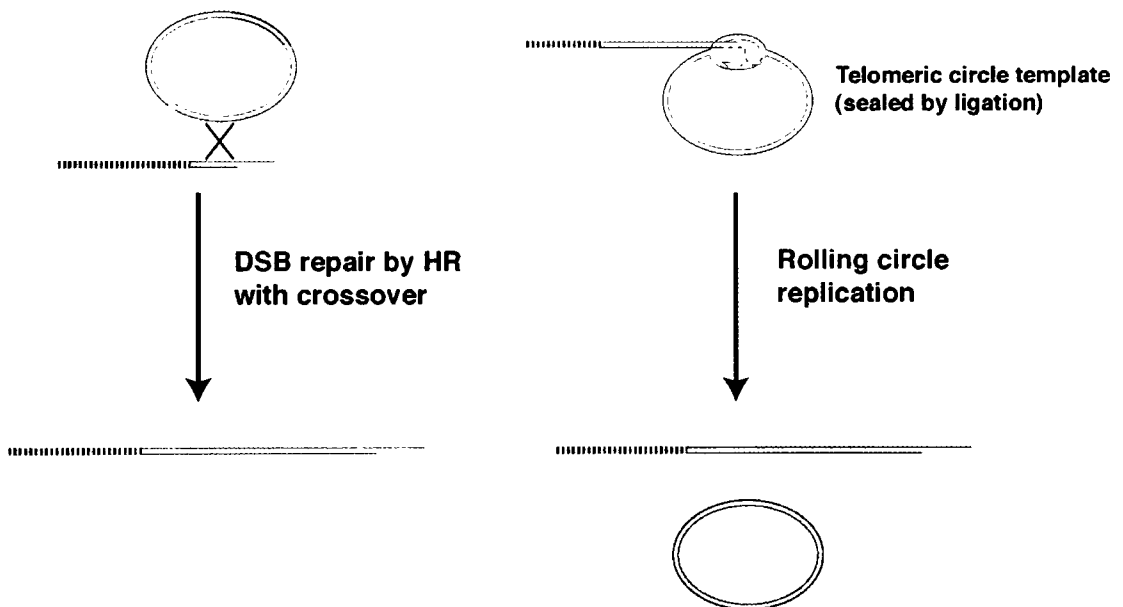
A**B**

Figure 4-2. Possible contributions of telomeric circles in ALT telomere lengthening.

(A) T-loop HR events are predicted to generate relaxed circles of telomeric DNA. (B) The telomeric circles may be used in ALT cell telomere maintenance. (*left*) Circles could be incorporated into some telomeres through HR directed DSB repair of a shortened telomere. This model does not result in an increase in the total amount of telomeric DNA. (*right*) Alternatively, after ligation of nicked telomeric circles, they could become substrates for rolling circle replication.

However, the recombination of circular telomeric DNAs onto short ALT telomeres would not result in a net increase in the amount of telomeric DNA in the cell. It is possible that telomeres could actually be replicated during S-phase. Even the

occasional replication of telomeric circles would allow for a potentially limitless source of telomeric DNA for incorporation into DNA ends.

As an alternative model, telomeric circles could be used as templates for rolling circle replication. Rolling circle replication of telomeres with telomeric circles would result in the formation of telomeric DNA that is not semi-conservative (i.e. both strands are newly synthesized in one S-phase). It may be possible to distinguish DNA that results from non-conservative replication through a modification of CO-FISH techniques. It will be an interesting challenge to determine whether telomeric circles are important to the telomere maintenance of ALT cells. It may also be interesting to determine whether the injection of telomeric circles into normal cells undergoing telomere crisis may promote the cell's ability to activate non-telomerase (ALT) mechanisms of telomere maintenance.

Possible applications of telomere HR

If telomere HR is a primary factor in driving cellular senescence, then the modulation of t-loop HR may have clinical applications. Because t-loop HR appears to be regulated by a very short domain in TRF2, it may be possible to screen for small molecules that modulate these functions of TRF2. The modulation of t-loop HR may be more practical than attempting to alter the *in vivo* activity of telomerase whose regulation appears to be largely controlled at the level of protein expression. By inhibiting t-loop HR, it may be possible to delay the onset of cellular senescence. Such a strategy would be expected to be beneficial for patients who suffer from diseases that result from excess telomere shortening or an inability to counteract telomere shortening. The depletion of stem cells in conditions like Werner's syndrome and dyskeratosis congenita are thought to be secondary to accelerated telomere shortening. Cells that possessed an extended proliferative capacity due to the inhibition of t-loop HR would still possess an intrinsic limit to their replicative potential. Therefore, the hypothetical inhibition of t-loop HR

would have therapeutic advantages over the ectopic expression of telomerase because it would not be expected to promote tumorigenesis.

Furthermore, the short-term enhancement of telomere HR through small molecules may have roles in advancing telomerase-based cancer therapy. Telomerase inhibition results in the rapid induction of senescence *in vitro* [401]. The rapid onset of telomerase inhibition may be explained by t-loop HR mediated stochastic deletion events. The existence of this pathway *in vivo* makes the inhibition of telomerase a more attractive therapeutic option in treating cancer. Furthermore, it may be possible to promote t-loop HR with small molecules that mimic the action of the TRF2 Δ B allele. The coordinated inhibition of telomerase with a promotion of t-loop HR might make the inhibition of telomerase an especially effective treatment regimen. A promotion of t-loop HR might be expected to result in a transient promotion of ALT survivor cells, but these survivors would be expected to lose their ability to maintain their telomeres through telomere HR upon withdrawal of the t-loop HR promoting agent. Although any clinical applications of t-loop HR are highly speculative and would require significant develop, the potential promise of treating human disease demands continued investigations of this pathway in mammalian cells.

CHAPTER 5:
MATERIALS AND METHODS

Cell culture

WI-38 (ATCC), IMR90 (ATCC), AG06300 (WRN-) (Coriell), AG03141 (WRN-) (Coriell), AG05013 (RTS-) (Coriell), AG04405A (ATM-) (ATCC), and AG02496 (ATM-) (ATCC) were grown in DMEM with 100U of penicillin and 0.1 mg of streptomycin, 2 mM L-glutamine, 0.1 mM non-essential amino acids (Gibco), 1 mM sodium pyruvate (Sigma) and 15%FBS. RS-SCID/P80 (Artemis-) [362] and RS-SCID/P83 (Rag2-) [362] were grown in RPMI with supplements and 15%FBS. U-2 OS (ATCC) and Saos-2 (ATCC) were grown in McCoy's 5a medium with supplements and 10% or 15% FBS, respectively. GM847, VA13, HTC75, HeLa1.2.11, NBS1-LB1 [357], Phoenix amphotropic, Phoenix ecotropic packaging cells were grown in DMEM with supplements and 10%FBS. BJ/hTERT (Clontech) were grown according to the manufacturer's specifications. NIH/3T3, Rad50^{S/S} (824-5) [359], Nbs^{ΔB/ΔB} and littermates (54-4, 88-17, 25-1, 25-2) [360], ERCC1^{-/-} and littermate [363], DNA-PKcs^{-/-} [364], and Ku86^{-/-}p53^{-/-} and Ku86^{+/+}p53^{-/-} [365] were grown in DMEM with supplements and 10% FBS (or 15% heat inactivated FBS and 50 μM 2-mercaptoethanol for primary MEFs).

Cells were passaged by pre-rinsing and 5-10 min incubation with Trypsin-EDTA (Gibco, 0.25%) and seeding at fixed densities indicated in the text. Cells were counted with a Coulter Counter Z1 Particle counter. Population doublings were determined by the following formula: PD = original PD + [ln (# cells at passage/# cells seeded) / ln(2)] implemented in Excel and graphed in Graph Prism.

Plasmids and retroviral gene delivery

Tagged and untagged alleles of Tel2 were cloned by PCR from a full-length cDNA clone as (RZPD ID: DKFZp434A073) into the pLPC vector. Either pLPC_puro or pWZL_hygro were used to deliver untagged alleles of TRF2. Primary MEFs were transformed with pBabe_neoSV40largeTAg (gift from Greg Hannon) at early passage. Retroviral gene delivery was performed as described [11] except that cells were infected

3 times at 12 hr intervals. Briefly, Phoenix packaging cells (293T derived cell lines) were transfected with 15 μg of the relevant plasmid DNA (see below for 293T transfection details). The media was refreshed 12 hrs later. 36 hours after the transfection, the media, now containing viral particles, was filtered through a 0.5 μm filter and combined with 5-10% FBS, 5-10% fresh media, and polybrene to 4 $\mu\text{g}/\text{ml}$. This mixture was placed on target cells and repeated twice at 12 hr intervals. The ATM and Nbs primary fibroblasts were infected 3 times at 24 hr intervals. Most retrovirally infected cells were selected in the appropriate drugs (puromycin 2 $\mu\text{g}/\text{ml}$, hygromycin 90 $\mu\text{g}/\text{ml}$, or G418 600 $\mu\text{g}/\text{ml}$) for 4-5 days until uninfected control cells were completely selected. HCT116 and HCT116 derivative cell lines were selected in 120 $\mu\text{g}/\text{ml}$ hygromycin; ERCC1+/+ and ERCC1-/- cells were selected in 3 $\mu\text{g}/\text{ml}$ puromycin. Infection of NIH/3T3 cells proved to be very efficient (>90% expression after 3 rounds). Thus, for better preservation of telomere signals, FISH and CO-FISH was performed on NIH/3T3 cells immediately after a 24 hr recovery from 2, 12-hour infections without selection.

In vitro transcription / translation

In vitro transcription and translation were performed using the Promega TNT coupled reticulocyte system TnT system according to the manufacturer's recommendations. Briefly, the following reagents are mixed and incubated for 1hr: 12.5 μl reticulocyte lysate, 1 μl TNT buffer, 0.5 μl polymerase (T7 or T3), 0.5 μl amino acids – methionine, 2 μl S³⁵-labeled methionine, 0.5 μl RNasin, 5.5 μl H₂O, 2.5 μl of 0.2 $\mu\text{g}/\mu\text{l}$ DNA. 3 μl of sample was loading with with 2 \times Laemmli buffer on SDS-PAGE. The gel was incubated with Amplify (Amersham) for 15 min, transferred to Whatmann paper, dried on a gel dryer at 80°C for 30 min, and exposed to film.

Table 5-1. Antibodies used in Chapter 2.

Name	Antigen	Type	Reactivity	Dilution	Source
TRF1 – 371	TRF1 - FL protein	Rb, poly	Hu	IF 1:3000 WB 1:2000 ChIP: 25 μ l crude	
TRF2 – 647	TRF2 - FL protein	Rb, poly	Hu, M	IF, WB 1:2000 ChIP: 25 μ l crude	
Upstate α TRF2	TRF2 peptide	M, mono	Hu	IF 1:500 WB 1:1000	Upstate
hRap1 765	hRap1	Rb, poly	Hu, M	IF, WB 1:3000 ChIP: 25 μ l crude	
Tin2 - 864	Tin2	Rb, poly	Hu	IF, WB 1:2000	
Mre11 - 874	Mre11	Rb, poly	Hu	IF, WB 1:1000 ChIP: 25 μ l crude	
Hp95 #16/9	Human Nbs/p95	Rb, poly	Hu	WB 1:20,000	John Petrini
9E10	Myc	M, mono	--	IF, WB 1:1000	Oncogene
M2	FLAG	M, mono	--	IF, WB 1:10,000 ChIP: 5 μ g	Sigma
GTU88	γ tubulin	M, mono	Hu, M	IF, WB 1:20,000	Sigma
GNS1	cyclin B	M, mono	Hu	IF 1:200	Santa Cruz
BRCA-1, Ab-1	BRCA1	M, mono	Hu	IF 1:400	Oncogene (OP-92)
α phospho – Histone H3	phospho peptide	M, mono	Hu	IF 1:400	Cell Signaling 6G3
PML (PG-M3)	AA 37-51	M, mono	Hu	IF 1:200	Cell Signaling 6G3
Coilin - C28020	Coilin, p80	M, mono	Hu	IF 1:1000	Becton Dickinson
Centrin	Centrin	Rb, poly	Hu	IF 1:1000	J. Salisburg
CREST	autoimmune	Hu, poly	Hu	IF 1:2	Tarun Kapoor
CENP-F	autoimmune	Hu, poly	Hu	IF 1:5000	E. Tan
Tel2A	C term pep	Rb, poly	Hu	IF 1:100	
Tel2B	C term pep	Rb, poly	Hu	IF, WB 1:100	
Tel2C	FL protein	Rb, poly	Hu	IF, WB 1:1000	

Rb, rabbit; Hu, human; IF - immunofluorescence; WB - Western blot

Table 5-2. Antibodies used in Chapter 3.

Name	Antigen	Type	Reactivity	Dilution	Source
TRF1 - 371	TRF1 - FL protein	Rb, poly	Hu	IF, WB 1:3000 ChIP: 25 μ l crude	
TRF2 - 647	TRF2 - FL protein	Rb, poly	Hu, M	IF, WB 1:2000 ChIP: 25 μ l crude	
TRF2 - 508 (basic domain)	N term peptide	Rb, poly	Hu, M	WB 1:500 ChIP: 25 μ l crude	
hRap1 - 765	hRap1	Rb, poly	Hu, M	IF, WB 1:3000 ChIP: 25 μ l crude	
Mre11 - 874	Mre11	Rb, poly	Hu	IF, WB 1:1000 ChIP: 25 μ l crude	
Hp95 #16/9	Nbs/p95	Rb, poly	Hu	WB 1:20,000	John Petrini
93/5 Nbs (p95)	Mouse p95	Rb, poly	M	WB 1:10,000	John Petrini
Ku70 (C-19)	C term peptide	Goat, poly	Hu, M	WB 1:1000	Santa Cruz
Ku70 (M-19)	C term peptide	Goat, poly	Hu, M	WB 1:1000	Santa Cruz
Ku86 (C-20)	C term peptide	Goat, poly	Hu, M	WB 1:1000	Santa Cruz
Ku86 (Ab-2)	B cell nuclei	M, mono	Hu, M	WB 1:250	NeoMarkers
9E10	Myc	M, mono	--	IF, WB 1:1000	Oncogene
M2	FLAG	M, mono	--	IF, WB 1:10,000 ChIP: 5 μ g	Sigma
53BP1	53BP1	M, mono	Hu	IF 1:10	Thanos Hazalonetis
α phospho - Histone H3	phospho peptide	M, mono	Hu	IF 1:400	Cell Signaling 6G3
XRCC3	peptide	Rb, poly	Hu	WB 5 μ g/ml	Chemicon

Rb, rabbit; Hu, human; IF - immunofluorescence; WB - Western blot

Transfection of 293T cells

Twenty-four hours prior to transfection, 293T cells were plate at $4-5 \times 10^6$ cells per 10 cm plate so that cells are 40-50% confluent at the time of transfection. Up to 2 ml of a DNA-calcium chloride mix (856 μ l H₂O, 124 μ l 2 M CaCl₂, 5-10 μ g/ml DNA) was mixed dropwise into an equal amount of 2 x HBS (50 mM HEPES pH 7.05, 10 mM KCl, 12 mM dextrose, 280 mM NaCl, 1.5 mM Na₂PO₄) while being vortexed. Immediately

after mixing, 1 ml of the now precipitated DNA solution is added dropwise onto a 10 cm plate. After 12-16 hrs, the media is refreshed. Cells were harvested ~24 hr later.

Immunoprecipitations

Relevant cells--one 10 cm plate of transfected 293T cells, one 10 cm plate of HCT116 cells, or one 15 cm plates of infected IMR90 cells--were harvested by flushing cells off the plate with cold PBS. 293T cells were pelleted by in cold PBS and lysed in 0.5 ml IP lysis buffer (50 mM Tris-HCl pH 7.4, 1% Triton X-100, 0.1% SDS, 150 mM NaCl, 1 mM EDTA, 1 mM DTT, 1 mM PMSF, 1XProtease inhibitor mix [Roche]) and gently resuspended with a pipette. The lysate was transferred to an Eppendorf tube, vortexed for 3-5 sec and kept on ice for 5 min. Next, 25 μ l pf 5 M NaCl was added to each tube, raising the sodium concentration to 400 mM. HCT116 cells and IMR90 cells were lysed in Buffer C 20 mM HEPES-KOH pH 7.9, 420 mM KCl, 25% [v/v] glycerol, 0.1 mM EDTA, 5 mM MgCl₂, 1 mM DTT, 5 mM fresh PMSF, 0.2% [v/v] NP-40, and 1XProtease inhibitor cocktail [Roche]). After 10 min on ice, the samples were vortexed, incubated on ice for an additional 5 min prior to the dropwise addition of 0.5 μ l ice-old H₂O with mixing. Lysates were centrifuged at 14,000 rpm for 10 min at 4°C. The resulting supernatant represent the input lysate. The Bradford assay was used to determine protein concentration of the input lysate. Protein concentrations of input lysates were normalized by the addition of the appropriate amount of lysis buffer or Buffer C. A fraction of input was set aside for subsequent Western blots.

Indicated amounts of antibody were added to 0.5-1 ml of lysate. Samples were nutated at 4°C for at least 5 hr (up to O/N). 60 μ l of a Protein G sepharose slurry (50% [v/v] Protein-G sepharose [Amersham] in PBS in 1 mg/ml BSA) was added to each tube and samples were nutated at 4°C for 1 hr. (For generating Protein G sepharose slurry, 3-4 ml of beads are placed into a Falcon tube, spun down down 1 K for 1 min at 4°C, and washed with PBS twice. The beads were resuspended in 10 ml of 5% BSA in PBS and keep on ice for 30 minutes, washed three times with PBS, and stored with an equal

volume of PBS containing 0.02% sodium azide at 4°C.) Then, the Protein-G beads were pelleted at 4,000 rpm for 5 sec at 4°C and washed with 1 ml cold lysis buffer. The was repeated 3 times and beads were pelleted. After removal of buffer, beads were suspended in 45-60 μ l 2X Laemmli buffer is added to each pellet. Pellets and Laemmli buffer were boiled for 10 min and stored at -20°C.

Whole cell lysates and Western blots

For whole cell lysates, cell were trypsinized, washed with PBS, counted and resuspended at 2×10^4 cells/ml, an equal volume of 4XLaemmli buffer (0.24 mM Tris-HCl, 4% SDS, 20% glycerol, 10% beta-mercaptoethanol, 0.004% bromophenol blue) was added. The viscous lysates were boiled for 10 min and DNA was sheared through a 28 gauge insulin syringe. For buffer C extracts, cells were trypsinized, washed once with media, twice with ice-cold PBS, and incubated in Buffer C on ice for 30 min. After centrifugation at 4°C for 10 min at 14,000 rpm, the supernatant was collected and the Bradford assay was used to determine protein concentration. The extract was then combined with Laemmli buffer and boiled for 10 min.

Protein samples were separated by SDS-PAGE and blotted onto nitrocellulose membranes. Membranes were blocked in 10% non-fat powdered milk in PBST (0.5% Tween-20 in PBS) for 30 min at RT and incubated with primary antibodies in 1% milk in PBST at 4°C O/N. Membranes were washed three times in PBST, incubated with secondary antibody in 1% milk in PBST for 30 min at RT, washed three times with PBST, and once with H₂O. ECL (Amersham) was applied to membranes, which were exposed to film.

siRNA transfections

The following sequences were used as siRNAs:

Tel2.2 - 5' G.G.A.G.G.A.G.U.U.U.G.C.C.U.C.G.G.C.C.dT.dT 3'

Tel2.3 - 5' C.U.C.C.G.U.G.G.C.C.G.G.C.C.A.C.U.U.C.dT.dT 3'

Ku86.1 - 5' U.C.C.U.C.A.A.G.U.C.G.G.C.G.U.G.G.C.U.dT.dT 3'

Ku86.2 - 5' A.G.U.C.A.G.C.U.G.G.A.U.A.U.U.A.U.A.A.dT.dT 3'

Ku86.3 - 5' G.A.C.U.U.G.C.G.G.C.A.A.U.A.C.A.U.G.U.dT.dT 3'

Ku86.4 - 5' U.C.C.U.C.G.A.U.U.U.C.A.G.A.G.A.U.U.A.dT.dT 3'

GFP and luciferase siRNA sequences were previously published [Novina, 2002 #2692] [Elbashir, 2001 #2290]. All siRNAs were obtained from Dharmacon. HeLa2 were transfected using OligofectamineTM (Invitrogen). Briefly, 2.0×10^5 of HeLa2 or 1.0×10^5 of U2OS cells per well of a 6-well plate were plated 18-24 hr prior to transfection. Transfections were done twice with a 24 hr interval. Cells were processed 12-60 hr after the second transfection as indicated. As a control, cells were mock treated or treated with GFP or luciferase siRNAs.

Fluorescence activated cell sorting (FACS) analysis

Cells were collected from a 10 cm plate by trypsinization, spun down at 1000 rpm, washed in 5 ml PBS, spun down again, and resuspended in 100 μ l of PBS. Two ml of ice cold 70% ethanol was added dropwise while vortexing. Cells were stored at 4°C. Prior to FACS, cells were spun down and resuspended in propidium iodide mix (500 μ l PBS, 100 μ g Rnase, 25 μ g propidium iodide). After a 30 min incubation, cells were analyzed on a Becton Dickinson FACS-Scan II.

Immunofluorescence

Cells were plated on dishes with coverslips. Cells were rinsed with PBS, fixed with 2% paraformaldehyde in PBS for 10 min at room temperature, washed twice (5 min) with PBS, and permeabilized with 0.5% NP-40 or 0.5% Triton X-100 in PBS for 10 min at room temperature and washed three times with PBS. Cells were blocked with PBG (0.2% (w/v) cold water fish gelatin (Sigma), 0.5% (w/v) BSA (Sigma) in PBS) for at least 30 minutes at RT. Cells were stored in 0.5xPBG with 0.02% sodium azide at 4°C. Coverslips were placed on parafilm in a foil-covered tray next to wet paper towels to keep the cells moist. Cells were incubated with primary antibody diluted in PBG O/N at

4°C (see Table 5-1), washed three times with PBG at RT, incubated with secondary antibody diluted 1:250 in PBG for 30-40 min at RT, and washed three times with PBG at RT. 4,6-diamidino-2-phenylindole (DAPI) was added to the last wash at 0.1 µg/ml. Coverslips were rinsed twice with PBS and sealed onto glass slides with embedding media (1 mg/ml p-phenylene diamine (Sigma) in 50% glycerol in 1xPBS).

For methanol fixation, cells were rinsed in PBS and then plunged into methanol (-20°C) and fixed for 5 min at -20°C. Cells were washed three times with PBS and blocked with PBG for 30 min. Cells were immediately processed for IF, no additional permeabilization was necessary.

For Triton X-100 extraction, cells can be extracted prior to fixation with Triton X-100 buffer or cytoskeleton extraction (CSK) buffer. For Triton X-100 extraction, cells were rinsed with PBS and extracted with Triton X-100 extraction buffer (0.5% Triton X-100, 20 mM HEPES-KOH pH 7.9, 50 mM NaCl, 3 mM MgCl₂, and 300 mM sucrose) at 4°C for 5 min. Cells were then rinsed twice with PBS and fixed with 3% paraformaldehyde/ 2% sucrose for 10 min at RT, washed twice with PBS, and again permeabilized in Triton X-100 buffer for 10 min at RT, washed twice with PBS.

For CSK extraction, cells were rinsed with PBS and first incubated in cytoskeleton buffer [10 mM piperazine-*N,N'*-bis(2-ethanesulfonic acid) (PIPES; pH 6.8), 100 mM NaCl, 300 mM sucrose, 3 mM MgCl₂, 1 mM EGTA, 0.5% Triton X-100] for 5 min on ice followed by an incubation in cytoskeleton stripping buffer (10 mM Tris-HCl [pH 7.4], 10 mM NaCl, 3 mM MgCl₂, 1% [v/v] Tween 40, 0.5% [v/v] sodium deoxycholate) for 5 min on ice. Cells were washed 3 times in cold PBS, fixed in % paraformaldehyde/ 2% sucrose for 10 min at RT, and permeabilized with 0.5% Triton X-100 solution for 10 min at RT. Subsequent incubation were complete with the standard IF protocol. Images were captured using an Axioplan2 Zeiss microscope with a Hamamatsu CCD digital camera using OpenLab software. Images were merged in OpenLab and processed with Adobe Photoshop.

Senescence associated (SA) β -galactosidase assay

This procedure was adapted from [402]. Cells were plated on coverslips or in 2 well chamber glass slide (LabTek) at a density of 3×10^4 cells per chamber or coverslip. On the second day after plating, the cells were washed with PBS, fixed for 5 min in 2% formaldehyde/0.2% glutaraldehyde (v/v) in PBS, washed in PBS, and stained with X-gal at 1 mg/ml in SA buffer (150 mM NaCl, 2 mM $MgCl_2$, 5 mM $K_3Fe(CN)_6$, and 40 mM NaP_i at pH 6.0) for 12 hr at 37°C.

Chromatin Immunoprecipitation (ChIP)

ChIP was performed as previously described [85]. Cells from 2 15 cm plates were harvested, washed with PBS, fixed in 1% formaldehyde in PBS for 60 min at RT, washed in PBS, and lysed in 1% SDS, 50 mM Tris-HCl, pH 8.0, 10 mM EDTA at a density of 1×10^7 cells/ml. Lysates were sonicated to obtain chromatin fragments <1 kb, and centrifuged for 10 min at 4 °C. Two-hundred μ l of lysate was diluted with 1.2 ml 0.01% SDS, 1.1% Triton X-100, 1.2 mM EDTA, 16.7 mM Tris-HCl, pH 8.0, and 150 mM NaCl was supplemented with antibody (typically 25 μ l crude serum or 5 μ l 9E10), mutated overnight at 4 °C, supplemented with 30 μ l protein G Sepharose beads (Amersham; blocked with 30 μ g bovine serum albumin (BSA) and 5 μ g sheared *Escherichia coli* DNA), and incubated for 30 min at 4 °C. IP pellets were washed with 0.1% SDS, 1% Triton X-100, 2 mM EDTA, pH 8.0, 20 mM Tris-HCl, pH 8.0, containing 150 mM NaCl in the first wash and 500 mM NaCl in the second wash. Further washes were with 0.25 M LiCl, 1% NP-40, 1% Na-deoxycholate, 1 mM EDTA, pH 8.0, 10 mM Tris-HCl, pH 8.0, and with 10 mM Tris-HCl, pH 8.0, 1 mM EDTA. Chromatin was eluted from the beads with 500 μ l 1% SDS, 0.1 M Na_2CO_3 . After addition of 20 μ l of 5 M NaCl, crosslinks were reversed for 4 h at 65 °C. Samples were supplemented with 20 μ l of 1 M Tris-HCl, pH 6.5, 10 μ l of 0.5 M EDTA, and 20 μ g DNase free RNase A, and incubated at 37 °C for 30 min. Samples were then digested with 40 μ g proteinase K for 60 min at 37 °C, phenol extracted, and the DNA was precipitated overnight at -20 °C

with 1 ml ethanol. The precipitate was dissolved in 100 μ l water, denatured at 95 °C for 5 min, and dot blotted onto Hybond membranes in 2 \times SSC (80% was loaded for the detection of telomeric sequences, and 10% for Alu sequences). Membranes were treated with 1.5 M NaCl, 0.5 N NaOH for 10 min, and with 1 M NaCl, 0.5 M Tris-HCl, pH 7.0, for 10 min. Hybridization with a 800-bp Klenow-labelled TTAGGG probe or an Alu probe was performed as described below. Membranes were washed four times in 2 \times SSC and exposed overnight to PhosphorImager screen. The quantification of the percent precipitated DNA was done with the ImageQuant software. All lysates were normalized for cell number. For the total telomeric DNA samples, two 50- μ l aliquots (corresponding to one-quarter and one-eighth of the amount of lysate used in the IPs) were processed along with the rest of the samples at the step of reversing the crosslinks. The average of the telomeric signal in two total fractions was taken for the reference value (total DNA), and the percentage of each immunoprecipitation sample was calculated based on the signal relative to the corresponding total DNA signal. Therefore, the calculated CHIP yield takes into account changes in telomere length.

Genomic DNA extraction

Genomic DNA was prepared as described previously [11]. Approximately 10^7 cells were harvested by trypsinization, washed with cold PBS, and collected by centrifugation at 1000 \times g for 5 min. Cells were suspended in 1 ml of Tris/NaCl/EDTA (TNE, 10 mM Tris-HCl pH 7.4, 100 mM NaCl, 10 mM EDTA), lysed by squirting into 1 ml of TNES (TNE + 1% SDS) containing 0.1 mg/ml proteinase K (added fresh), and incubated at 37°C O/N. Phenol extraction with 2 ml of phenol/chloroform/isoamyl-alcohol (50:49:1) was performed in a 15 ml phase-lock tube (Eppendorf) by gently mixing for 5 min followed by centrifugation at 3,500 \times g for 5 min. DNA was collected from the water phase by precipitation with 2 ml iso-propanol after addition of 200 μ l 3 M sodium acetate pH 5.2 at room temperature. The DNA was collected and dissolved in 300 μ l TE (10 mM

Tris-HCl pH 7.4, 1 mM EDTA) containing DNase-free, heat-inactivated RNase A (1 mg/ml) for 2 hours at 37°C, followed by incubation for 1 hour after addition of 200 μ l of TNE containing 0.1 mg/ml proteinase K. The DNA was phenol extracted and precipitated with iso-propanol as above using adjusted volumes and 2 ml phase-lock tubes and dissolved in 100 μ l TE and digested with the indicated enzymes. Approximately \sim 20 μ g of genomic DNA was digested in a final volume of 100 μ l, using the appropriate restriction enzymes. 2 μ l of each digested genomic DNA was quantitated in 2 ml of Hoechst 33258 dye at 1 μ g/ml in TNE. DNA samples were measured at least twice to ensure accuracy of the measurements.

Pulsed-field gel electrophoresis sample preparation

MEFs were trypsinized washed once in PBS and resuspended in PBS at 3.0×10^7 cells / ml and warmed to 50°C. The PBS-cell suspension was then mixed with an equal volume of 2% agarose in PBS to a final concentration of 1.5×10^7 cells / ml. The agarose mixture was allowed to equilibrate at 50°C for 5 min, and 100 μ L of the mixture was pipetted into a disposable plug-caster (Bio-Rad). The plugs were allowed to set at 4°C for 15 min. Plugs were incubated in 1 ml per plug of Proteinase K digestion buffer (10 mM Tris pH 7.9, 250 mM EDTA pH 8.0, 0.2% sodium deoxycholate, 1% sodium lauryl sarcosine, and 500 mg/ml fresh Proteinase K) at 50°C overnight. The plugs were washed three times for 1 hr in 1 ml per plug of TE. PMSF (1 mM final from 100 mM freshly made stock in methanol) was included in the final wash in TE. The plugs are now stable at 4°C for several months. Prior to digestion, the plugs were washed again for 1 hr in TE and 20 min in water. Next, the plug was equilibrated for 1 hr in 1ml per plug of the appropriate restriction digest buffer for 1 hr. The plug was then was then changed into 1 mL pre plug of fresh restriction digest buffer with 120 units of the indicated enzyme and 10 μ g RNase A for at least 12hrs. After digestion, plugs were washed in 1 ml pre plug of TE for 30 min and equilibrated in 0.5 \times TBE for 20 min. The plugs were fractionated on a

CHEF-DRII PFGE (Biorad) in a 1% agarose gel in 0.5×TBE at 6 V/cm for 20 hrs at 14°C. The gels were blotted to nylon membranes and probed first with a 550-bp mTRF2 probe prepared by PCR using the primers 2MF2 (5'-ACCGCTGGGTGCTCAAG-3') and 2MB8 (5'-TTCTGGATAACAGGGTGGG-3'). To strip the blots, boiling 0.1%SDS in water was poured over the blots and was allowed to cool to room temperature. Blots were then probed for telomeric repeats as described below.

Telomere Southern blots

Between 2 to 4 µg of digested DNA and MW markers were loaded with 6× DNA loading buffer (0.25% Orange G, 15% Ficoll [w/v] 400 (Pharmacia) in ddH₂O) on a 20×20 cm 0.7% agarose gel in 0.5×TBE with ethidium bromide (gel-volume ~300 ml; 3 µl of 10 mg/ml ethidium bromide stock). Load 4 µl Mw markers in lanes 1 and 24. The gel was run for 1 hr at 30 V. The gel was then run until the Orange G front reached the bottom of the gel (e.g., O/N at 45V). A picture of the gel was taken to ensure even loading. The run was continued until the 1.3 kb marker was near the bottom of the gel. This takes ~800-900 V•hrs total. Another picture was taken with a ruler to mark the location of the ladder. The gel was gently agitated in depurination solution (0.25 M HCl) for 30 min, then in denaturation solution (1.5M NaCl; 0.5M NaOH) twice for 30 min, and finally in neutralization solution (1M Tris 7.4; 1.5M NaCl) twice for 30 min. The gel was blotted onto pre-wet Hybond Nylon filters in 20×SSC O/N. Filters were handled with forceps and gloves at all times. The filter with DNA was wrapped with SaranWrap and auto-crosslinked (DNA side up) in a Stratalinker (Promega). The filter was rinsed with 2×SSCm, water, and prehybridized for at least 45 min 1 hr at 65°C in a hybridization oven (Hybaid) in Churh hybridization buffer (500 mM NaPO₄ pH 7.2, 2 mM EDTA pH 8.0, 70 mg/ml SDS, 10 mg/ml BSA).

Measurement of reduction in telomeric repeat signal after TRF2 Δ B expression

Cells were infected with vector or TRF2 Δ B retroviruses and processed in parallel. Cells were harvested, genomic DNA isolated, digested with the indicated restriction enzymes, and quantified in duplicate by Hoechst fluorescence after digestion. Equal amounts of DNA (2-4 μ g) were fractionated and equal loading was confirmed by EtBr staining. Blots were first probed for a loading control. For human DNA one of two control probes were used--a 475 bp Histone H1.3 or a 23 kb genomic DNA fragment gel isolated from *Mbo*I + *Alu*I digested genomic DNA that contains unknown repetitive sequences lacking *Mbo*I/*Alu*I sites. The blots were exposed on PhosphorImager screens, and the loading control signal was quantified using Imagequant. For mouse DNA, the mTRF2 probe was used as described above and bands representing the mTRF2 gene were used as loading control. The blots were then stripped by boiling in 0.1% SDS, rinsed in 2xSSC, hybridized with a TTAGGG repeat probe (pSP73.Sty11; [403]), and the telomere signal was quantified in Imagequant. The telomeric signal was normalized to the loading control for all lanes and the normalized values for vector and TRF2 Δ B infected samples were compared and expressed as % signal change in the TRF2 Δ B samples.

Detection of ssDNA telomeric DNA (in-gel hybridization)

This assay was adapted from [350]. Briefly, DNA samples prepared and gel-fractionated as described above were dried on Whatman 3MM filter paper (at 50°C until completely dry). Whatman paper was removed by soaking the gel in water. The gel was prehybridized in Church mix (0.5 M Na₂HPO₄ pH 7.2, 1 mM EDTA, 7% SDS, 1% BSA) for 30 min at 50°C and hybridized in Church mix o/n at 50°C with 4 ng [CCCTAA]₄ or [TTAGGG]₄ of a γ -³²P-ATP an end-labeled probe. The gel was washed three times in 4xSSC for 30 min at room temperature, and once with 4xSSC, 0.1% SDS at 55°C and exposed to a PhosphorImager screen. Subsequently the gel was denatured in 0.5 M NaOH, 1.5 M NaCl for 30 min, neutralized in 0.5 M Tris-HCl pH 7.5, 3 M NaCl for 20 min, and hybridized to the same probe in Church mix O/N at 55°C. The gel was

washed and exposed as above. Where indicated, the DNA was incubated with 50 units of Exonuclease I (Amersham) in 10 mM Tris-HCl pH 8, 1 mM EDTA, 10 mM MgCl₂, 20 mM KCl, 10 mM -mercaptoethanol for 6 hours at 37°C prior to restriction digestion. After Exo I digestion, DNA were phenol:chloroform extracted, precipitated, resuspended and digested with the indicated enzymes.

Alkaline gel electrophoresis

This protocol was done as previously described [130]. Genomic DNA was digested with *MboI/AluI* and was fractionated on a native 0.7% agarose gel or adjusted to 10 mM EDTA, mixed with 0.2 volumes of 6× alkaline loading buffer (0.3 M NaOH, 6 mM EDTA, 18% Ficoll, 0.15% bromocresol green, 0.25% xylene cyanol FF), and run in duplicate on a 0.5% alkaline agarose gel in 50 mM NaOH/1 mM EDTA (pH 8.0) for 27 hr at 50V at 4°C with two changes of running buffer. Half of the alkaline gel, as well as the native gel, was subsequently treated with 0.25 N HCl, denatured, neutralized, blotted in 20SSC onto a nylon membrane, and hybridized with the TTAGGG probe as described above. To verify complete denaturation of the DNA, the other half of the gel was neutralized for 45 min, soaked in 2_ SSC for 30 min at room temperature, dried for 30 min at room temperature on a gel drier, and hybridized with the same probe. A telomeric DNA marker ladder was prepared by digesting a TTAGGG repeat bearing pTH5 plasmid with *HindIII* and religation.

2D gel electrophoresis and genomic blotting

Neutral-neutral 2D gel electrophoresis was performed according to the protocols established by Brewer and Fangman (<http://fangman-brewer.genetics.washington.edu/2Dgel.html>) with the modifications described by Cohen and Lavi (1996). Genomic DNA samples were digested O/N in 100µl. For non-transformed fibroblasts (IMR90, hTERT-BJ1, BJ), about 1/3 of a genomic prep from 1-2×10⁷ cells are necessary for a gel. The first dimension is a 0.4% agarose gel in 1×TBE (~140ml without ethidium bromide

[EtBr]) poured in a Bio-Rad Wide Mini Sub Cell GT (15 x 11 cm tray) using a comb with narrow, thin teeth (4mm x 1.2mm thick). Between 8-15 μ g of digested was loaded into each well. Sample and in the adjacent lane 3 μ l ladder (~750 μ g). Gel was run for 24 hrs at RT at 10-14V (<1V/cm). The buffer was refreshed after ~12hrs. The Orange G dye should just be at the bottom of the gel after the run. The gel was stained with 0.3 μ g/ml EtBr in 1 \times TBE for 20 min. The gel was examined on a **long** wave UV light box and using a clean razor, sample lanes were quickly excised making certain the left edge was straight, vertical, and close to the sample. About half of the DNA ladder lane was included when the excision was made on the right side. The gel excised lanes were manipulated with a plastic ruler to manipulate the slices helps greatly. The second dimension was 1.1% agarose gel in 1 \times TBE with 0.3 μ g/ml EtBr (~340ml). The excised lanes were placed in a 20 \times 20cm gel support orthogonal to the first direction of electrophoresis. The 20 \times 20 gel box will hold up to 4 samples. The agarose was cooled to 55 $^{\circ}$ C and EtBr was added to 0.3 μ g/ml. The gel was poured around the 1D lanes until they were just covered. The gel was run at RT ~150V (4-5V/cm) for 4hrs. To facilitate subsequent manipulations, cut the gel in half horizontally. The gels were processed for Southern blots as described previously.

Circularized λ DNA ladder was generated by ligating *Hind*III digested λ DNA (NEB) at 5 ng/ μ l overnight at 16 $^{\circ}$ C. The ligated DNA was ethanol precipitated in the presence of glycogen and resuspended at 500 ng/ μ l. To generate the ladder probe, *Hind*III cut λ DNA was digested with *Bst*EII and gel purified. Approximately 2 μ g of the digested λ DNA was labeled with T4 PNK and γ -³²P-ATP. For 2D in-gel hybridizations, gels were handled as described previously for G-overhang assays with the exception that the gels required 3hrs at 44C under vacuum for complete drying.

Methanol:Acetic Acid (3:1) metaphase spreads

Cells were grown to ~40% confluence in a 10-15 cm culture dish. Cells were incubated for 30min – 2 hrs in the regular medium +0.1mg/ml demecolcin (colcemide; Sigma). By harvesting time, the effects of the colcemide were obvious, there were many more refractile cells and many cells with a spiky margin. Cells were harvested by trypsinization and spun down in 15 ml conical tube (at 1000rpm). The supernatant was removed, and cells were **gently** resuspended in 5 ml of 75 mM KCl (prewarmed to 37°C). Cells were incubated at 37°C for 7 min. The tube was periodically inverted to keep the cells suspended. If the cells started clumping during the incubation, a few drops of fixative (3:1 methanol:glacial acetic acid, prepared fresh and kept on ice) were added and clumps were gently resuspended. Cells were spun down at 1000rpm for 5 min. The KCl was decanted gently and cells were resuspended fully in the remaining KCl (~250 μ l) by tapping. 500 μ l of fixative was added dropwise while the cells were gently being shaken on a vortexer (<1000 rpm). Another 500 μ l of fixative was added slowly. Finally, tubes were filled to 15 ml with the fixative and stored at 4°C O/N or longer. Cells can be stored at -20°C at this stage for months. Cells were spun down (1000rpm) and refixed prior to spreading. Fixative was decanted and cells were resuspended cells in the remaining fixative (~0.5 ml left) (may vary depending on cell number). A few slides were soaked in in cold water. Wet paper towels were set on top of a heating block set to 70°C. Cells were dropped on the water-wetted slide and gently washed once with fresh fixative dropped across the top of the slide. Slides were placed for a minute on the humidified 70°C block. The slides were checked under a phase contrast microscope for

spreading efficiency. The process was repeated at different dilutions if necessary. The slides were stacked upright on a slide holder and dried O/N in a fume hood.

Formaldehyde metaphase chromosome spreads

Metaphase cells were enriched as described above. Cells were trypsinized and counted. Cells were spun down at 1000 rpm for 5 min. RSB (10 mM Tris pH 7.4, 10 mM NaCl, 5 mM MgCl₂) was added to a final concentration of $3-4 \times 10^6$ cells/ml. Cells were resuspended in RSB buffer by gentle tapping. Cells were incubated in RSB buffer at 37°C for 10 min. Cells were immediately placed on ice. Cells were spun down in a CytoSpin at 1000 rpm for 1 min. Cell area was demarked with a hydrophobic marking pen and cells were fixed and processed for IF as described as above.

FISH and CO-FISH

FISH was performed using a FITC conjugated PNA probe specific for the G-strand (FITC-5'-(CCCTAA)₃-3') (Applied Biosystems) as previously described [352]. CO-FISH was done as described previously [132]. Cells were grown in the presence of BrdU:C (3:1, 10 μM final) for 18 hrs with the inclusion of demecolcine (0.1 μg/ml) for the final 2 hrs. Metaphases were harvested and prepared as previously described. Slides were treated with 0.5 mg/ml RNase A (in PBS, DNase free) for 10 min at 37°C. Next, slides were stained with 0.5 μg/ml Hoechst 33258 (Sigma) in 2×SSC for 15 min at RT. Slides were then expose slides to 365-nm UV light (Stratalinker 1800 UV irradiator) for 30 min (equivalent to 5.4×10^3 J/m²). Digest the BrdU/BrdC-substituted DNA strands with at least 500 μl of 3 U/μl of Exonuclease III (Promega) in buffer supplied by the manufacturer (50 mM Tris-HCl, 5 mM MgCl₂, and 5 mM DTT, pH 8.0) at RT for 10 min. Slides were denatured in 70% formamide, 2×SSC at 70-80°C on a heat block. Slides were dehydrated in an ice cold ethanol series--70%, 85%, 100%. Dried slides were stored at RT. The regular protocol for FISH was then followed. For dual CO-FISH

both Tam-TelG (1:2000) and FITC-TelC (1:1000) probes were added together to the hybridization mix during the FISH protocol. CO-FISH was performed using either the FITC-TelC probe or a TAMRA conjugated PNA probe specific for the C-strand (TAMRA-5-(TTAGGG)₃-3') (Applied Biosystems) except. For simultaneous visualization of both strands, following the standard CO-FISH degradation, both the FITC-TelC and TAMRA-TelG probes were added to the hybridization buffer to 0.5 $\mu\text{g/ml}$. The slides were then denatured at 80°C, hybridized at room temperature, and processed as usual.

Sister chromatid exchange (SCE) detection by αBrdU

BrdU (Sigma) was added to 10 μM to rapidly cycling cells for 16 hrs (<1 cell cycle). The pulse time may vary based on the cell cycle time of the cell being using. The cells were chased with 50 μM thymidine for 20 hrs. Metaphases were enriched and prepared through methanol:acetic acid fixation as described above. Spreads were rehydrated in PBS and fixed with formaldehyde as described in the FISH protocol. Following formaldehyde fixation, chromosome were denatured for 10 min at 80°C in 90% deionized formamide/10% 2 \times SSC (pH 7.2). The spreads were dehydrated through an ice-cold Ethanol series. Slides were incubated for 1hr with FITC conjugated αBrdU (Sigma). Slides were washed 3 \times 5 min in PBG. DAPI was added to the second wash.

REFERENCES

1. Berube, N.G., J.R. Smith, and O.M. Pereira-Smith, *The genetics of cellular senescence*. Am J Hum Genet, 1998. **62**(5): p. 1015-9.
2. Hayflick, L., *The Limited in Vitro Lifetime of Human Diploid Cell Strains*. Exp Cell Res, 1965. **37**: p. 614-36.
3. Hayflick, L., *How and why we age*. Exp Gerontol, 1998. **33**(7-8): p. 639-53.
4. Shelton, D.N., et al., *Microarray analysis of replicative senescence*. Curr Biol, 1999. **9**(17): p. 939-45.
5. Smith, J.R. and O.M. Pereira-Smith, *Replicative senescence: implications for in vivo aging and tumor suppression*. Science, 1996. **273**(5271): p. 63-7.
6. Alcorta, D.A., et al., *Involvement of the cyclin-dependent kinase inhibitor p16 (INK4a) in replicative senescence of normal human fibroblasts*. Proc Natl Acad Sci U S A, 1996. **93**(24): p. 13742-7.
7. Olovnikov, A.M., *A theory of marginotomy. The incomplete copying of template margin in enzymic synthesis of polynucleotides and biological significance of the phenomenon*. J Theor Biol, 1973. **41**(1): p. 181-90.
8. Watson, J.D., *Origin of concatemeric T7 DNA*. Nat New Biol, 1972. **239**(94): p. 197-201.
9. Harley, C.B., A.B. Futcher, and C.W. Greider, *Telomeres shorten during ageing of human fibroblasts*. Nature, 1990. **345**(6274): p. 458-60.
10. Blasco, M.A., et al., *Telomere shortening and tumor formation by mouse cells lacking telomerase RNA*. Cell, 1997. **91**(1): p. 25-34.
11. Karlseder, J., A. Smogorzewska, and T. de Lange, *Senescence induced by altered telomere state, not telomere loss*. Science, 2002. **295**(5564): p. 2446-9.
12. Smith, J.R. and R.G. Whitney, *Intraclonal variation in proliferative potential of human diploid fibroblasts: stochastic mechanism for cellular aging*. Science, 1980. **207**(4426): p. 82-4.
13. Baird, D.M., et al., *Extensive allelic variation and ultrashort telomeres in senescent human cells*. Nat Genet, 2003. **33**(2): p. 203-7.

14. Martin-Ruiz, C., et al., *Stochastic variation in telomere shortening rate causes heterogeneity of human fibroblast replicative life span*. J Biol Chem, 2004. **279**(17): p. 17826-33.
15. von Zglinicki, T., *Role of oxidative stress in telomere length regulation and replicative senescence*. Ann N Y Acad Sci, 2000. **908**: p. 99-110.
16. Varley, H., et al., *Molecular characterization of inter-telomere and intra-telomere mutations in human ALT cells*. Nat Genet, 2002. **30**(3): p. 301-5.
17. Rubelj, I. and Z. Vondracek, *Stochastic mechanism of cellular aging--abrupt telomere shortening as a model for stochastic nature of cellular aging*. J Theor Biol, 1999. **197**(4): p. 425-38.
18. Lindsey, J., et al., *In vivo loss of telomeric repeats with age in humans*. Mutat Res, 1991. **256**(1): p. 45-8.
19. Bodnar, A.G., et al., *Extension of life-span by introduction of telomerase into normal human cells* Science, 1998. **279**(5349): p. 349-52.
20. Hastie, N.D., et al., *Telomere reduction in human colorectal carcinoma and with ageing* Nature, 1990. **346**(6287): p. 866-8.
21. Wright, W.E., et al., *Telomerase activity in human germline and embryonic tissues and cells*. Dev Genet, 1996. **18**(2): p. 173-9.
22. Greider, C.W. and E.H. Blackburn, *The telomere terminal transferase of Tetrahymena is a ribonucleoprotein enzyme with two kinds of primer specificity*. Cell, 1987. **51**(6): p. 887-98.
23. Nakamura, T.M., et al., *Telomerase catalytic subunit homologs from fission yeast and human* Science, 1997. **277**(5328): p. 955-9.
24. Meyerson, M., et al., *hEST2, the putative human telomerase catalytic subunit gene, is up-regulated in tumor cells and during immortalization*. Cell, 1997. **90**(4): p. 785-95.
25. Singer, M.S. and D.E. Gottschling, *TLC1: template RNA component of Saccharomyces cerevisiae telomerase* Science, 1994. **266**(5184): p. 404-9.
26. Shippen-Lentz, D. and E.H. Blackburn, *Functional evidence for an RNA template in telomerase*. Science, 1990. **247**(4942): p. 546-52.

27. Greider, C.W. and E.H. Blackburn, *A telomeric sequence in the RNA of Tetrahymena telomerase required for telomere repeat synthesis*. Nature, 1989. **337**(6205): p. 331-7.
28. Chen, J.L., M.A. Blasco, and C.W. Greider, *Secondary structure of vertebrate telomerase RNA*. Cell, 2000. **100**(5): p. 503-14.
29. Dandjinou, A.T., et al., *A phylogenetically based secondary structure for the yeast telomerase RNA*. Curr Biol, 2004. **14**(13): p. 1148-58.
30. Lingner, J., et al., *Reverse transcriptase motifs in the catalytic subunit of telomerase* Science, 1997. **276**(5312): p. 561-7.
31. Greider, C.W., *Telomerase is processive*. Mol Cell Biol, 1991. **11**(9): p. 4572-80.
32. Shippen-Lentz, D. and E.H. Blackburn, *Telomere terminal transferase activity from Euplotes crassus adds large numbers of TTTTGGGG repeats onto telomeric primers*. Mol Cell Biol, 1989. **9**(6): p. 2761-4.
33. Wenz, C., et al., *Human telomerase contains two cooperating telomerase RNA molecules*. Embo J, 2001. **20**(13): p. 3526-34.
34. Beattie, T.L., et al., *Functional multimerization of the human telomerase reverse transcriptase*. Mol Cell Biol, 2001. **21**(18): p. 6151-60.
35. Smogorzewska, A. and T. de Lange, *Regulation of telomerase by telomeric proteins*. Ann Rev Biochem, 2004. **73**: p. 177-208.
36. Teixeira, M.T., et al., *Telomere Length Homeostasis Is Achieved via a Switch between Telomerase- Extendible and -Nonextendible States*. Cell, 2004. **117**(3): p. 323-35.
37. Masutomi, K., et al., *Telomerase maintains telomere structure in normal human cells*. Cell, 2003. **114**(2): p. 241-53.
38. Lin, S.Y. and S.J. Elledge, *Multiple tumor suppressor pathways negatively regulate telomerase*. Cell, 2003. **113**(7): p. 881-9.
39. Liu, Y., et al., *The telomerase reverse transcriptase is limiting and necessary for telomerase function in vivo*. Curr Biol, 2000. **10**(22): p. 1459-62.
40. Feng, J., et al., *The RNA component of human telomerase*. Science, 1995. **269**(5228): p. 1236-41.

41. Kim, N.W., et al., *Specific association of human telomerase activity with immortal cells and cancer*. Science, 1994. **266**(5193): p. 2011-5.
42. Shay, J.W. and S. Bacchetti, *A survey of telomerase activity in human cancer*. Eur J Cancer, 1997. **33**(5): p. 787-91.
43. Hiyama, E., et al., *Telomerase activity in gastric cancer*. Cancer Res, 1995. **55**(15): p. 3258-62.
44. Greenberg, R.A., et al., *Short dysfunctional telomeres impair tumorigenesis in the INK4a(delta2/3) cancer-prone mouse*. Cell, 1999. **97**(4): p. 515-25.
45. Seger, Y.R., et al., *Transformation of normal human cells in the absence of telomerase activation*. Cancer Cell, 2002. **2**(5): p. 401-13.
46. Bryan, T.M., et al., *Telomere elongation in immortal human cells without detectable telomerase activity*. Embo J, 1995. **14**(17): p. 4240-8.
47. Counter, C.M., et al., *Telomere shortening associated with chromosome instability is arrested in immortal cells which express telomerase activity*. Embo J, 1992. **11**(5): p. 1921-9.
48. Seto, A.G., et al., *A bulged stem tethers Est1p to telomerase RNA in budding yeast*. Genes Dev, 2002. **16**(21): p. 2800-12.
49. Evans, S.K. and V. Lundblad, *Est1 and Cdc13 as comediators of telomerase access*. Science, 1999. **286**(5437): p. 117-20.
50. Hughes, T.R., et al., *The Est3 protein is a subunit of yeast telomerase*. Curr Biol, 2000. **10**(13): p. 809-12.
51. Reichenbach, P., et al., *A human homolog of yeast est1 associates with telomerase and uncaps chromosome ends when overexpressed*. Curr Biol, 2003. **13**(7): p. 568-74.
52. Beernink, H.T., et al., *Telomere maintenance in fission yeast requires an est1 ortholog*. Curr Biol, 2003. **13**(7): p. 575-80.
53. Snow, B.E., et al., *Functional conservation of the telomerase protein est1p in humans*. Curr Biol, 2003. **13**(8): p. 698-704.
54. Seto, A.G., et al., *Saccharomyces cerevisiae telomerase is an Sm small nuclear ribonucleoprotein particle*. Nature, 1999. **401**(6749): p. 177-80.

55. Lukowiak, A.A., et al., *The snoRNA domain of vertebrate telomerase RNA functions to localize the RNA within the nucleus*. Rna, 2001. **7**(12): p. 1833-44.
56. Jady, B.E., E. Bertrand, and T. Kiss, *Human telomerase RNA and box H/ACA scaRNAs share a common Cajal body-specific localization signal*. J Cell Biol, 2004. **164**(5): p. 647-52.
57. Zhu, Y., et al., *Telomerase RNA accumulates in Cajal bodies in human cancer cells*. Mol Biol Cell, 2004. **15**(1): p. 81-90.
58. Dokal, I., *Dyskeratosis congenita in all its forms*. Br J Haematol, 2000. **110**(4): p. 768-79.
59. Vulliamy, T., et al., *Association between aplastic anaemia and mutations in telomerase RNA*. Lancet, 2002. **359**(9324): p. 2168-70.
60. Ruggero, D., et al., *Dyskeratosis congenita and cancer in mice deficient in ribosomal RNA modification*. Science, 2003. **299**(5604): p. 259-62.
61. Vulliamy, T., et al., *Disease anticipation is associated with progressive telomere shortening in families with dyskeratosis congenita due to mutations in TERC*. Nat Genet, 2004. **36**(5): p. 447-9.
62. Wong, J.M., L. Kusdra, and K. Collins, *Subnuclear shuttling of human telomerase induced by transformation and DNA damage*. Nat Cell Biol, 2002. **4**(9): p. 731-736.
63. Teixeira, M.T., et al., *Intracellular trafficking of yeast telomerase components*. EMBO Rep, 2002. **3**(7): p. 652-9.
64. Allsopp, R.C., et al., *Telomere length predicts replicative capacity of human fibroblasts*. Proc Natl Acad Sci U S A, 1992. **89**(21): p. 10114-8.
65. Shampay, J., J.W. Szostak, and E.H. Blackburn, *DNA sequences of telomeres maintained in yeast*. Nature, 1984. **310**(5973): p. 154-7.
66. Yu, G.L., et al., *In vivo alteration of telomere sequences and senescence caused by mutated Tetrahymena telomerase RNAs*. Nature, 1990. **344**(6262): p. 126-32.
67. Prescott, J. and E.H. Blackburn, *Telomerase RNA mutations in Saccharomyces cerevisiae alter telomerase action and reveal nonprocessivity in vivo and in vitro*. Genes Dev, 1997. **11**(4): p. 528-40.

68. Marusic, L., et al., *Reprogramming of telomerase by expression of mutant telomerase RNA template in human cells leads to altered telomeres that correlate with reduced cell viability*. Mol Cell Biol, 1997. **17**(11): p. 6394-401.
69. McClintock, B., *The fusion of broken ends of sister half-chromatids following chromatid breakage at meiotic anaphase*, in *The discovery and characterization of transposable elements. The collected papers of Barbara McClintock*. 1938, Garland Publishing, Inc.: New York and London. p. 1-48.
70. McClintock, B., *The stability of broken ends of chromosomes in Zea mays*. Genetics, 1941. **26**: p. 234-282.
71. Klobutcher, L.A., et al., *All gene-sized DNA molecules in four species of hypotrichs have the same terminal sequence and an unusual 3' terminus*. Proc Natl Acad Sci U S A, 1981. **78**(5): p. 3015-9.
72. Gottschling, D.E. and V.A. Zakian, *Telomere proteins: specific recognition and protection of the natural termini of Oxytricha macronuclear DNA*. Cell, 1986. **47**(2): p. 195-205.
73. Horvath, M.P., et al., *Crystal structure of the Oxytricha nova telomere end binding protein complexed with single strand DNA*. Cell, 1998. **95**(7): p. 963-74.
74. Froelich-Ammon, S.J., et al., *Modulation of telomerase activity by telomere DNA-binding proteins in Oxytricha*. Genes Dev, 1998. **12**(10): p. 1504-14.
75. Mitton-Fry, R.M., et al., *Conserved structure for single-stranded telomeric DNA recognition*. Science, 2002. **296**(5565): p. 145-7.
76. Garvik, B., M. Carson, and L. Hartwell, *Single-stranded DNA arising at telomeres in cdc13 mutants may constitute a specific signal for the RAD9 checkpoint*. Mol Cell Biol, 1995. **15**(11): p. 6128-38.
77. Grandin, N., S.I. Reed, and M. Charbonneau, *Stn1, a new Saccharomyces cerevisiae protein, is implicated in telomere size regulation in association with Cdc13*. Genes Dev, 1997. **11**(4): p. 512-27.
78. Chandra, A., et al., *Cdc13 both positively and negatively regulates telomere replication*. Genes Dev, 2001. **15**(4): p. 404-14.
79. Baumann, P. and T.R. Cech, *Pot1, the putative telomere end-binding protein in fission yeast and humans*. Science, 2001. **292**(5519): p. 1171-5.

80. Lei, M., P. Baumann, and T.R. Cech, *Cooperative Binding of Single-Stranded Telomeric DNA by the Pot1 Protein of Schizosaccharomyces pombe*. *Biochemistry*, 2002. **41**(49): p. 14560-8.
81. Loayza, D., et al., *DNA binding features of human POT1: A nonamer 5'-TAGGGTTAG-3' minimal binding site, sequence specificity, and internal binding to multimeric sites*. *J Biol Chem*, 2004. **279**(13): p. 13241-8.
82. Baumann, P., E. Podell, and T.R. Cech, *Human pot1 (protection of telomeres) protein: cytolocalization, gene structure, and alternative splicing*. *Mol Cell Biol*, 2002. **22**(22): p. 8079-87.
83. Liu, D., et al., *PTOP interacts with POT1 and regulates its localization to telomeres*. *Nat Cell Biol*, 2004.
84. Ye, J.Z., et al., *POT1-interacting protein PIP1: a telomere length regulator that recruits POT1 to the TIN2/TRF1 complex*. *Genes Dev*, 2004. **18**(14): p. 1649-54.
85. Loayza, D. and T. De Lange, *POT1 as a terminal transducer of TRF1 telomere length control*. *Nature*, 2003. **424**(6943): p. 1013-8.
86. Colgin, L.M., et al., *Human POT1 Facilitates Telomere Elongation by Telomerase*. *Curr Biol*, 2003. **13**(11): p. 942-6.
87. Armbruster, B.N., et al., *Rescue of an hTERT mutant defective in telomere elongation by fusion with hPot1*. *Mol Cell Biol*, 2004. **24**(8): p. 3552-61.
88. Dionne, I. and R.J. Wellinger, *Cell cycle-regulated generation of single-stranded G-rich DNA in the absence of telomerase*. *Proc Natl Acad Sci U S A*, 1996. **93**(24): p. 13902-7.
89. Larrivee, M., C. LeBel, and R.J. Wellinger, *The generation of proper constitutive G-tails on yeast telomeres is dependent on the MRX complex*. *Genes Dev*, 2004. **18**(12): p. 1391-6.
90. Shore, D. and K. Nasmyth, *Purification and cloning of a DNA binding protein from yeast that binds to both silencer and activator elements*. *Cell*, 1987. **51**(5): p. 721-32.
91. Moretti, P., et al., *Evidence that a complex of SIR proteins interacts with the silencer and telomere-binding protein RAP1*. *Genes Dev*, 1994. **8**(19): p. 2257-69.

92. Cockell, M., et al., *The carboxy termini of Sir4 and Rap1 affect Sir3 localization: evidence for a multicomponent complex required for yeast telomeric silencing.* J Cell Biol, 1995. **129**(4): p. 909-24.
93. Liu, C., X. Mao, and A.J. Lustig, *Mutational analysis defines a C-terminal tail domain of RAP1 essential for Telomeric silencing in Saccharomyces cerevisiae.* Genetics, 1994. **138**(4): p. 1025-40.
94. Liu, C. and A.J. Lustig, *Genetic analysis of Rap1p/Sir3p interactions in telomeric and HML silencing in Saccharomyces cerevisiae.* Genetics, 1996. **143**(1): p. 81-93.
95. Chien, C.T., et al., *Targeting of SIR1 protein establishes transcriptional silencing at HM loci and telomeres in yeast.* Cell, 1993. **75**(3): p. 531-41.
96. Conrad, M.N., et al., *RAP1 protein interacts with yeast telomeres in vivo: overproduction alters telomere structure and decreases chromosome stability.* Cell, 1990. **63**(4): p. 739-50.
97. Wotton, D. and D. Shore, *A novel Rap1p-interacting factor, Rif2p, cooperates with Rif1p to regulate telomere length in Saccharomyces cerevisiae.* Genes Dev, 1997. **11**(6): p. 748-60.
98. Hardy, C.F., L. Sussel, and D. Shore, *A RAP1-interacting protein involved in transcriptional silencing and telomere length regulation.* Genes Dev, 1992. **6**(5): p. 801-14.
99. Marcand, S., E. Gilson, and D. Shore, *A protein-counting mechanism for telomere length regulation in yeast* Science, 1997. **275**(5302): p. 986-90.
100. Broccoli, D., et al., *Human telomeres contain two distinct Myb-related proteins, TRF1 and TRF2.* Nat Genet, 1997. **17**(2): p. 231-5.
101. Bianchi, A., et al., *TRF1 binds a bipartite telomeric site with extreme spatial flexibility.* Embo J, 1999. **18**(20): p. 5735-44.
102. Griffith, J., A. Bianchi, and T. de Lange, *TRF1 promotes parallel pairing of telomeric tracts in vitro.* J Mol Biol, 1998. **278**(1): p. 79-88.
103. van Steensel, B. and T. de Lange, *Control of telomere length by the human telomeric protein TRF1* Nature, 1997. **385**(6618): p. 740-3.

104. Ancelin, K., C. Brun, and E. Gilson, *Role of the telomeric DNA-binding protein TRF2 in the stability of human chromosome ends*. *Bioessays*, 1998. **20**(11): p. 879-83.
105. Sbodio, J.I. and N.W. Chi, *Identification of a tankyrase-binding motif shared by IRAP, TAB182, and human TRF1 but not mouse TRF1. NuMA contains this RXXPDG motif and is a novel tankyrase partner*. *J Biol Chem*, 2002. **277**(35): p. 31887-92.
106. Smith, S., et al., *Tankyrase, a poly(ADP-ribose) polymerase at human telomeres*. *Science*, 1998. **282**(5393): p. 1484-7.
107. Cook, B.D., et al., *Role for the related poly(ADP-Ribose) polymerases tankyrase 1 and 2 at human telomeres*. *Mol Cell Biol*, 2002. **22**(1): p. 332-42.
108. Kaminker, P.G., et al., *TANK2, a new TRF1-associated PARP, causes rapid induction of cell death upon overexpression*. *J Biol Chem*, 2001. **276**: p. 35891-99.
109. Chang, W., J.N. Dynek, and S. Smith, *TRF1 is degraded by ubiquitin-mediated proteolysis after release from telomeres*. *Genes Dev*, 2003. **17**(11): p. 1328-33.
110. Smith, S. and T. de Lange, *Tankyrase promotes telomere elongation in human cells*. *Curr Biol*, 2000. **10**(20): p. 1299-302.
111. Kim, S.H., P. Kaminker, and J. Campisi, *TIN2, a new regulator of telomere length in human cells*. *Nat Genet*, 1999. **23**(4): p. 405-12.
112. Ye, J.Z. and T. De Lange, *TIN2 is a tankyrase 1 PARP modulator in the TRF1 telomere length control complex*. *Nat Genet*, 2004. **36**(6): p. 618-23.
113. Guglielmi, B. and M. Werner, *The yeast homolog of human PinX1 is involved in rRNA and small nucleolar RNA maturation, not in telomere elongation inhibition*. *J Biol Chem*, 2002. **277**(38): p. 35712-9.
114. Lin, J. and E.H. Blackburn, *Nucleolar protein PinX1p regulates telomerase by sequestering its protein catalytic subunit in an inactive complex lacking telomerase RNA*. *Genes Dev*, 2004. **18**(4): p. 387-96.
115. Dynek, J.N. and S. Smith, *Resolution of sister telomere association is required for progression through mitosis*. *Science*, 2004. **304**(5667): p. 97-100.

116. Smogorzewska, A., et al., *Control of human telomere length by TRF1 and TRF2*. Mol Cell Biol, 2000. **20**(5): p. 1659-68.
117. Ancelin, K., et al., *Targeting assay to study the cis functions of human telomeric proteins: evidence for inhibition of telomerase by TRF1 and for activation of telomere degradation by TRF2*. Mol Cell Biol, 2002. **22**(10): p. 3474-87.
118. Zhu, X.D., et al., *Cell-cycle-regulated association of RAD50/MRE11/NBS1 with TRF2 and human telomeres*. Nat Genet, 2000. **25**(3): p. 347-52.
119. D'Amours, D. and S.P. Jackson, *The Mre11 complex: at the crossroads of dna repair and checkpoint signalling*. Nat Rev Mol Cell Biol, 2002. **3**(5): p. 317-27.
120. Ranganathan, V., et al., *Rescue of a telomere length defect of Nijmegen breakage syndrome cells requires NBS and telomerase catalytic subunit*. Curr Biol, 2001. **11**(12): p. 962-6.
121. Li, B., S. Oestreich, and T. de Lange, *Identification of human Rap1: implications for telomere evolution*. Cell, 2000. **101**(5): p. 471-83.
122. Li, B. and T. De Lange, *Rap1 affects the length and heterogeneity of human telomeres*. Mol Biol Cell, 2003.
123. O'Connor, M.S., et al., *The human Rap1 protein complex and modulation of telomere length*. J Biol Chem, 2004. **279**(27): p. 28585-91.
124. van Steensel, B., A. Smogorzewska, and T. de Lange, *TRF2 protects human telomeres from end-to-end fusions*. Cell, 1998. **92**(3): p. 401-13.
125. Takai, H., A. Smogorzewska, and T. de Lange, *DNA damage foci at dysfunctional telomeres*. Curr Biol, 2003. **13**(17): p. 1549-56.
126. d'Adda di Fagagna, F., S.H. Teo, and S.P. Jackson, *Functional links between telomeres and proteins of the DNA-damage response*. Genes Dev, 2004. **18**(15): p. 1781-99.
127. Bakkenist, C.J., et al., *Disappearance of the telomere dysfunction-induced stress response in fully senescent cells*. Cancer Res, 2004. **64**(11): p. 3748-52.
128. Karlseder, J., et al., *p53- and ATM-dependent apoptosis induced by telomeres lacking TRF2*. Science, 1999. **283**(5406): p. 1321-5.
129. Smogorzewska, A. and T. de Lange, *Different telomere damage signaling pathways in human and mouse cells*. Embo J, 2002. **21**(16): p. 4338-48.

130. Smogorzewska, A., et al., *DNA Ligase IV-Dependent NHEJ of Deprotected Mammalian Telomeres in G1 and G2*. *Curr Biol*, 2002. **12**(19): p. 1635.
131. Zhu, X.D., et al., *ERCC1/XPF Removes the 3' Overhang from Uncapped Telomeres and Represses Formation of Telomeric DNA-Containing Double Minute Chromosomes*. *Mol Cell*, 2003. **12**(6): p. 1489-98.
132. Bailey, S.M., et al., *Strand-specific Postreplicative Processing of Mammalian Telomeres*. *Science*, 2001(293): p. 2462-2465.
133. Herbig, U., et al., *Telomere shortening triggers senescence of human cells through a pathway involving ATM, p53, and p21(CIP1), but not p16(INK4a)*. *Mol Cell*, 2004. **14**(4): p. 501-13.
134. Griffith, J.D., et al., *Mammalian telomeres end in a large duplex loop*. *Cell*, 1999. **97**(4): p. 503-14.
135. Cesare, A.J., et al., *Telomere looping in P. sativum (common garden pea)*. *Plant J*, 2003. **36**(2): p. 271-9.
136. Munoz-Jordan, J.L., et al., *t-loops at trypanosome telomeres*. *Embo J*, 2001. **20**(3): p. 579-88.
137. Murti, K.G. and D.M. Prescott, *Telomeres of polytene chromosomes in a ciliated protozoan terminate in duplex DNA loops*. *Proc Natl Acad Sci U S A*, 1999. **96**(25): p. 14436-9.
138. Nikitina, T. and C.L. Woodcock, *Closed Chromatin Loops at the Ends of Chromosomes*. *Journal Cell Biology*, 2004. **in press**.
139. Stansel, R.M., T. de Lange, and J.D. Griffith, *T-loop assembly in vitro involves binding of TRF2 near the 3' telomeric overhang*. *EMBO J*, 2001. **20**: p. E5532-5540.
140. de Lange, T. and J. Petrini, *A new connection at human telomeres: association of the Mre11 complex with TRF2*. *Cold Spring Harb Symp Quant Biol*, 2000. **LXV**: p. 265-273.
141. Opresko, P.L., et al., *The Werner Syndrome Helicase and Exonuclease Cooperate to Resolve Telomeric D Loops in a Manner Regulated by TRF1 and TRF2*. *Mol Cell*, 2004. **14**(6): p. 763-774.

142. Ye, J.Z., et al., *TIN2 binds TRF1 and TRF2 simultaneously and stabilizes the TRF2 complex on telomeres*. J Biol Chem, 2004.
143. de Lange, T., *Protection of mammalian telomeres*. Oncogene, 2002. **21**(4): p. 532-40.
144. Karlseder, J., et al., *The Telomeric Protein TRF2 Binds the ATM Kinase and Can Inhibit the ATM-Dependent DNA Damage Response*. PLoS, 2004. **in press**.
145. Park, C.H. and A. Sancar, *Formation of a ternary complex by human XPA, ERCC1, and ERCC4(XPF) excision repair proteins*. Proc Natl Acad Sci U S A, 1994. **91**(11): p. 5017-21.
146. de Laat, W.L., et al., *DNA structural elements required for ERCC1-XPF endonuclease activity*. J Biol Chem, 1998. **273**(14): p. 7835-42.
147. Dantzer, F., et al., *Functional interaction between poly(ADP-Ribose) polymerase 2 (PARP-2) and TRF2: PARP activity negatively regulates TRF2*. Mol Cell Biol, 2004. **24**(4): p. 1595-607.
148. Deng, Z., et al., *Telomeric proteins regulate episomal maintenance of Epstein-Barr virus origin of plasmid replication*. Mol Cell, 2002. **9**(3): p. 493-503.
149. Dantzer, F., et al., *Base excision repair is impaired in mammalian cells lacking Poly(ADP-ribose) polymerase-1*. Biochemistry, 2000. **39**(25): p. 7559-69.
150. Schreiber, V., et al., *Poly(ADP-ribose) polymerase-2 (PARP-2) is required for efficient base excision DNA repair in association with PARP-1 and XRCC1*. J Biol Chem, 2002. **277**(25): p. 23028-36.
151. Tong, W.M., et al., *DNA strand break-sensing molecule poly(ADP-Ribose) polymerase cooperates with p53 in telomere function, chromosome stability, and tumor suppression*. Mol Cell Biol, 2001. **21**(12): p. 4046-54.
152. Samper, E., et al., *Normal telomere length and chromosomal end capping in poly(ADP-ribose) polymerase-deficient mice and primary cells despite increased chromosomal instability*. J Cell Biol, 2001. **154**(1): p. 49-60.
153. d'Adda di Fagagna, F., et al., *Functions of poly(ADP-ribose) polymerase in controlling telomere length and chromosomal stability*. Nat Genet, 1999. **23**(1): p. 76-80.

154. Alexander, M.K. and V.A. Zakian, *Rap1p telomere association is not required for mitotic stability of a C(3)TA(2) telomere in yeast*. *Embo J*, 2003. **22**(7): p. 1688-96.
155. Cooper, J.P., et al., *Regulation of telomere length and function by a Myb-domain protein in fission yeast* *Nature*, 1997. **385**(6618): p. 744-7.
156. Spink, K.G., R.J. Evans, and A. Chambers, *Sequence-specific binding of Taz1p dimers to fission yeast telomeric DNA*. *Nucleic Acids Res*, 2000. **28**(2): p. 527-33.
157. Godhino Ferreira, M. and J. Promisel Cooper, *The fission yeast Taz1 protein protects chromosomes from Ku-dependent end-to-end fusions*. *Mol Cell*, 2001. **7**(1): p. 55-63.
158. Kanoh, J. and F. Ishikawa, *spRap1 and spRif1, recruited to telomeres by Taz1, are essential for telomere function in fission yeast*. *Curr Biol*, 2001. **11**(20): p. 1624-30.
159. Chikashige, Y. and Y. Hiraoka, *Telomere binding of the Rap1 protein is required for meiosis in fission yeast*. *Curr Biol*, 2001. **11**(20): p. 1618-23.
160. Nimmo, E.R., et al., *Defective meiosis in telomere-silencing mutants of Schizosaccharomyces pombe* *Nature*, 1998. **392**(6678): p. 825-8.
161. Cooper, J.P., Y. Watanabe, and P. Nurse, *Fission yeast Taz1 protein is required for meiotic telomere clustering and recombination*. *Nature*, 1998. **392**(6678): p. 828-31.
162. Kim, S.H., et al., *TIN2 mediates functions of TRF2 at human telomeres*. *J Biol Chem*, 2004.
163. Iwano, T., et al., *Importance of TRF1 for functional telomere structure*. *J Biol Chem*, 2004. **279**(2): p. 1442-8.
164. Lustig, A.J. and T.D. Petes, *Identification of yeast mutants with altered telomere structure*. *Proc Natl Acad Sci U S A*, 1986. **83**(5): p. 1398-402.
165. Dahlen, M., et al., *Regulation of telomere length by checkpoint genes in Schizosaccharomyces pombe*. *Mol Biol Cell*, 1998. **9**(3): p. 611-21.
166. Ritchie, K.B., J.C. Mallory, and T.D. Petes, *Interactions of TLC1 (which encodes the RNA subunit of telomerase), TEL1, and MEC1 in regulating telomere length in the yeast Saccharomyces cerevisiae*. *Mol Cell Biol*, 1999. **19**(9): p. 6065-75.

167. Naito, T., A. Matsuura, and F. Ishikawa, *Circular chromosome formation in a fission yeast mutant defective in two ATM homologues*. Nat Genet, 1998. **20**(2): p. 203-6.
168. Takata, H., et al., *Reciprocal association of the budding yeast ATM-related proteins Tell and Mec1 with telomeres in vivo*. Mol Cell, 2004. **14**(4): p. 515-22.
169. Hande, M.P., et al., *Extra-chromosomal telomeric DNA in cells from Atm(-/-) mice and patients with ataxia-telangiectasia*. Hum Mol Genet, 2001. **10**(5): p. 519-28.
170. Metcalfe, J.A., et al., *Accelerated telomere shortening in ataxia telangiectasia*. Nat Genet, 1996. **13**(3): p. 350-3.
171. Craven, R.J. and T.D. Petes, *Involvement of the checkpoint protein Mec1p in silencing of gene expression at telomeres in Saccharomyces cerevisiae*. Mol Cell Biol, 2000. **20**(7): p. 2378-84.
172. Bi, X., S.C. Wei, and Y.S. Rong, *Telomere Protection without a Telomerase; The Role of ATM and Mre11 in Drosophila Telomere Maintenance*. Curr Biol, 2004. **14**(15): p. 1348-53.
173. Silva, E., et al., *ATM Is Required for Telomere Maintenance and Chromosome Stability during Drosophila Development*. Curr Biol, 2004. **14**(15): p. 1341-7.
174. Oikemus, S.R., et al., *Drosophila atm/telomere fusion is required for telomeric localization of HP1 and telomere position effect*. Genes Dev, 2004. **18**(15): p. 1850-61.
175. Craven, R.J. and T.D. Petes, *Dependence of the regulation of telomere length on the type of subtelomeric repeat in the yeast Saccharomyces cerevisiae*. Genetics, 1999. **152**(4): p. 1531-41.
176. Smith, J., H. Zou, and R. Rothstein, *Characterization of genetic interactions with RFA1: the role of RPA in DNA replication and telomere maintenance*. Biochimie, 2000. **82**(1): p. 71-8.
177. Mallory, J.C., et al., *Amino acid changes in Xrs2p, Dun1p, and Rfa2p that remove the preferred targets of the ATM family of protein kinases do not affect DNA repair or telomere length in Saccharomyces cerevisiae*. DNA Repair (Amst), 2003. **2**(9): p. 1041-64.

178. Nakamura, T.M., B.A. Moser, and P. Russell, *Telomere binding of checkpoint sensor and DNA repair proteins contributes to maintenance of functional fission yeast telomeres*. Genetics, 2002. **161**(4): p. 1437-52.
179. Ahmed, S. and J. Hodgkin, *MRT-2 checkpoint protein is required for germline immortality and telomere replication in C. elegans*. Nature, 2000. **403**(6766): p. 159-64.
180. Hofmann, E.R., et al., *Caenorhabditis elegans HUS-1 Is a DNA Damage Checkpoint Protein Required for Genome Stability and EGL-1-Mediated Apoptosis*. Curr Biol, 2002. **12**(22): p. 1908-18.
181. Corda, Y., et al., *Interaction between Set1p and checkpoint protein Mec3p in DNA repair and telomere functions* Nat Genet, 1999. **21**(2): p. 204-8.
182. Longhese, M.P., et al., *Checkpoint proteins influence telomeric silencing and length maintenance in budding yeast*. Genetics, 2000. **155**(4): p. 1577-91.
183. Grandin, N., C. Damon, and M. Charbonneau, *Cdc13 prevents telomere uncapping and Rad50-dependent homologous recombination*. Embo J, 2001. **20**(21): p. 6127-39.
184. Askree, S.H., et al., *A genome-wide screen for Saccharomyces cerevisiae deletion mutants that affect telomere length*. Proc Natl Acad Sci U S A, 2004. **101**(23): p. 8658-63.
185. Hande, P., et al., *Elongated telomeres in scid mice*. Genomics, 1999. **56**(2): p. 221-3.
186. Espejel, S., et al., *Shorter telomeres, accelerated ageing and increased lymphoma in DNA-PKcs-deficient mice*. EMBO Rep, 2004. **5**(5): p. 503-9.
187. Jaco, I., et al., *Role of mammalian Rad54 in telomere length maintenance*. Mol Cell Biol, 2003. **23**(16): p. 5572-80.
188. Goytisolo, F.A., et al., *The absence of the DNA-dependent protein kinase catalytic subunit in mice results in anaphase bridges and in increased telomeric fusions with normal telomere length and G-strand overhang*. Mol Cell Biol, 2001. **21**(11): p. 3642-51.
189. Espejel, S., et al., *Functional interaction between DNA-PKcs and telomerase in telomere length maintenance*. Embo J, 2002. **21**(22): p. 6275-87.

190. Bailey, S.M., et al., *DNA double-strand break repair proteins are required to cap the ends of mammalian chromosomes*. Proc Natl Acad Sci U S A, 1999. **96**(26): p. 14899-904.
191. Gilley, D., et al., *DNA-PKcs is critical for telomere capping*. Proc Natl Acad Sci U S A, 2001. **98**(26): p. 15084-8.
192. Bailey, S.M., et al., *Dysfunctional mammalian telomeres join with DNA double-strand breaks*. DNA Repair (Amst), 2004. **3**(4): p. 349-57.
193. d'Adda di Fagagna, F., et al., *Effects of DNA nonhomologous end-joining factors on telomere length and chromosomal stability in mammalian cells*. Curr Biol, 2001. **11**(15): p. 1192-6.
194. Boulton, S.J. and S.P. Jackson, *Identification of a Saccharomyces cerevisiae Ku80 homologue: roles in DNA double strand break rejoining and in telomeric maintenance*. Nucleic Acids Res, 1996. **24**(23): p. 4639-48.
195. Porter, S.E., et al., *The DNA-binding protein Hdf1p (a putative Ku homologue) is required for maintaining normal telomere length in Saccharomyces cerevisiae*. Nucleic Acids Res, 1996. **24**(4): p. 582-5.
196. Nugent, C.I., et al., *Telomere maintenance is dependent on activities required for end repair of double-strand breaks*. Curr Biol, 1998. **8**(11): p. 657-60.
197. Polotnianka, R.M., J. Li, and A.J. Lustig, *The yeast Ku heterodimer is essential for protection of the telomere against nucleolytic and recombinational activities*. Curr Biol, 1998. **8**(14): p. 831-4.
198. Peterson, S.E., et al., *The function of a stem-loop in telomerase RNA is linked to the DNA repair protein Ku*. Nat Genet, 2001. **27**(1): p. 64-7.
199. Stellwagen, A.E., et al., *Ku interacts with telomerase RNA to promote telomere addition at native and broken chromosome ends*. Genes Dev, 2003.
200. Taggart, A.K., S.C. Teng, and V.A. Zakian, *Est1p as a cell cycle-regulated activator of telomere-bound telomerase*. Science, 2002. **297**(5583): p. 1023-6.
201. Gravel, S., et al., *Yeast Ku as a regulator of chromosomal DNA end structure*. Science, 1998. **280**(5364): p. 741-4.

202. Maringele, L. and D. Lydall, *EXO1-dependent single-stranded DNA at telomeres activates subsets of DNA damage and spindle checkpoint pathways in budding yeast yku70Delta mutants*. Genes Dev, 2002. **16**(15): p. 1919-33.
203. Tsukamoto, Y., J. Kato, and H. Ikeda, *Budding yeast Rad50, Mre11, Xrs2, and Hdf1, but not Rad52, are involved in the formation of deletions on a dicentric plasmid*. Mol Gen Genet, 1997. **255**(5): p. 543-7.
204. Baumann, P. and T.R. Cech, *Protection of telomeres by the Ku protein in fission yeast*. Mol Biol Cell, 2000. **11**(10): p. 3265-75.
205. Hsu, H.L., et al., *Ku is associated with the telomere in mammals*. Proc Natl Acad Sci U S A, 1999. **96**(22): p. 12454-8.
206. Bianchi, A. and T. de Lange, *Ku binds telomeric DNA in vitro*. J Biol Chem, 1999. **274**(30): p. 21223-7.
207. Hsu, H.L., et al., *Ku acts in a unique way at the mammalian telomere to prevent end joining*. Genes Dev, 2000. **14**(22): p. 2807-12.
208. Song, K., et al., *Interaction of human Ku70 with TRF2*. FEBS Lett, 2000. **481**(1): p. 81-5.
209. Li, G., C. Nelsen, and E.A. Hendrickson, *Ku86 is essential in human somatic cells*. Proc Natl Acad Sci U S A, 2002. **99**(2): p. 832-7.
210. Myung, K., et al., *Regulation of telomere length and suppression of genomic instability in human somatic cells by Ku86*. Mol Cell Biol, 2004. **24**(11): p. 5050-9.
211. Samper, E., et al., *Mammalian Ku86 protein prevents telomeric fusions independently of the length of TTAGGG repeats and the G-strand overhang*. EMBO Rep, 2000. **1**(3): p. 244-52.
212. Riha, K., et al., *Telomere length deregulation and enhanced sensitivity to genotoxic stress in Arabidopsis mutants deficient in Ku70*. Embo J, 2002. **21**(11): p. 2819-26.
213. Wei, C., et al., *Effects of double-strand break repair proteins on vertebrate telomere structure*. Nucleic Acids Res, 2002. **30**(13): p. 2862-70.

214. Boulton, S.J. and S.P. Jackson, *Components of the Ku-dependent non-homologous end-joining pathway are involved in telomeric length maintenance and telomeric silencing*. *Embo J*, 1998. **17**(6): p. 1819-28.
215. Ritchie, K.B. and T.D. Petes, *The Mre11p/Rad50p/Xrs2p complex and the Tel1p function in a single pathway for telomere maintenance in yeast*. *Genetics*, 2000. **155**(1): p. 475-9.
216. Wilson, S., et al., *The role of Schizosaccharomyces pombe Rad32, the Mre11 homologue, and other DNA damage response proteins in non-homologous end joining and telomere length maintenance*. *Nucleic Acids Res*, 1999. **27**(13): p. 2655-61.
217. Hartsuiker, E., et al., *Fission yeast Rad50 stimulates sister chromatid recombination and links cohesion with repair*. *Embo J*, 2001. **20**(23): p. 6660-71.
218. Ueno, M., et al., *Molecular characterization of the Schizosaccharomyces pombe nbs1+ gene involved in DNA repair and telomere maintenance*. *Mol Cell Biol*, 2003. **23**(18): p. 6553-63.
219. Chahwan, C., et al., *The fission yeast Rad32 (Mre11)-Rad50-Nbs1 complex is required for the S-phase DNA damage checkpoint*. *Mol Cell Biol*, 2003. **23**(18): p. 6564-73.
220. Diede, S.J. and D.E. Gottschling, *Exonuclease activity is required for sequence addition and Cdc13p loading at a de novo telomere*. *Curr Biol*, 2001. **11**(17): p. 1336-40.
221. Tsukamoto, Y., A.K. Taggart, and V.A. Zakian, *The role of the Mre11-Rad50-Xrs2 complex in telomerase-mediated lengthening of Saccharomyces cerevisiae telomeres*. *Curr Biol*, 2001. **11**(17): p. 1328-35.
222. Ciapponi, L., et al., *The Drosophila mre11/rad50 complex is required to prevent both telomeric fusion and chromosome breakage*. *Curr Biol*, 2004. **14**(15): p. 1360-6.
223. Lundblad, V. and J.W. Szostak, *A mutant with a defect in telomere elongation leads to senescence in yeast*. *Cell*, 1989. **57**(4): p. 633-43.

224. Lendvay, T.S., et al., *Senescence mutants of Saccharomyces cerevisiae with a defect in telomere replication identify three additional EST genes*. Genetics, 1996. **144**(4): p. 1399-412.
225. Kota, R.S. and K.W. Runge, *The yeast telomere length regulator TEL2 encodes a protein that binds to telomeric DNA*. Nucleic Acids Res, 1998. **26**(6): p. 1528-35.
226. Kota, R.S. and K.W. Runge, *Tel2p, a regulator of yeast telomeric length in vivo, binds to single- stranded telomeric DNA in vitro*. Chromosoma, 1999. **108**(5): p. 278-90.
227. Hartman, P.S. and R.K. Herman, *Radiation-sensitive mutants of Caenorhabditis elegans*. Genetics, 1982. **102**(2): p. 159-78.
228. Ahmed, S., et al., *C. elegans RAD-5/CLK-2 defines a new DNA damage checkpoint protein*. Curr Biol, 2001. **11**(24): p. 1934-44.
229. Gartner, A., et al., *A conserved checkpoint pathway mediates DNA damage-- induced apoptosis and cell cycle arrest in C. elegans*. Mol Cell, 2000. **5**(3): p. 435-43.
230. Lakowski, B. and S. Hekimi, *Determination of life-span in Caenorhabditis elegans by four clock genes*. Science, 1996. **272**(5264): p. 1010-3.
231. Benard, C., et al., *The C. elegans maternal-effect gene clk-2 is essential for embryonic development, encodes a protein homologous to yeast Tel2p and affects telomere length*. Development, 2001. **128**(20): p. 4045-55.
232. Lim, C.S., et al., *C. elegans clk-2, a gene that limits life span, encodes a telomere length regulator similar to yeast telomere binding protein Tel2p*. Curr Biol, 2001. **11**(21): p. 1706-10.
233. Cheung, I., et al., *Strain-specific telomere length revealed by single telomere length analysis in Caenorhabditis elegans*. Nucleic Acids Res, 2004. **32**(11): p. 3383-91.
234. Runge, K.W. and V.A. Zakian, *TEL2, an essential gene required for telomere length regulation and telomere position effect in Saccharomyces cerevisiae*. Mol Cell Biol, 1996. **16**(6): p. 3094-105.
235. Levis, R.W., et al., *Transposons in place of telomeric repeats at a Drosophila telomere*. Cell, 1993. **75**(6): p. 1083-93.

236. Lamers, M.H., et al., *The crystal structure of DNA mismatch repair protein MutS binding to a G x T mismatch*. Nature, 2000. **407**(6805): p. 711-7.
237. Jiang, N., et al., *Human CLK2 links cell cycle progression, apoptosis, and telomere length regulation*. J Biol Chem, 2003. **278**(24): p. 21678-84.
238. Stavropoulos, D.J., et al., *The Bloom syndrome helicase BLM interacts with TRF2 in ALT cells and promotes telomeric DNA synthesis*. Hum Mol Genet, 2002. **11**(25): p. 3135-3144.
239. Takahashi, Y., et al., *PML nuclear bodies and apoptosis*. Oncogene, 2004. **23**(16): p. 2819-24.
240. Bernardi, R. and P.P. Pandolfi, *Role of PML and the PML-nuclear body in the control of programmed cell death*. Oncogene, 2003. **22**(56): p. 9048-57.
241. Schul, W., et al., *The RNA 3' cleavage factors CstF 64 kDa and CPSF 100 kDa are concentrated in nuclear domains closely associated with coiled bodies and newly synthesized RNA*. Embo J, 1996. **15**(11): p. 2883-92.
242. Grande, M.A., et al., *PML-containing nuclear bodies: their spatial distribution in relation to other nuclear components*. J Cell Biochem, 1996. **63**(3): p. 280-91.
243. Gorisch, S.M., et al., *Nuclear body movement is determined by chromatin accessibility and dynamics*. Proc Natl Acad Sci U S A, 2004.
244. Elbashir, S.M., et al., *Duplexes of 21-nucleotide RNAs mediate RNA interference in cultured mammalian cells*. Nature, 2001. **411**(6836): p. 494-8.
245. Gruss, O.J., et al., *Chromosome-induced microtubule assembly mediated by TPX2 is required for spindle formation in HeLa cells*. Nat Cell Biol, 2002. **4**(11): p. 871-9.
246. Du, J. and G.J. Hannon, *Suppression of p160ROCK bypasses cell cycle arrest after Aurora-A/STK15 depletion*. Proc Natl Acad Sci U S A, 2004. **101**(24): p. 8975-80.
247. Van Vugt, M.A., et al., *Polo-like Kinase-1 Is Required for Bipolar Spindle Formation but Is Dispensable for Anaphase Promoting Complex/Cdc20 Activation and Initiation of Cytokinesis*. J Biol Chem, 2004. **279**(35): p. 36841-54.
248. Fukagawa, T., et al., *Dicer is essential for formation of the heterochromatin structure in vertebrate cells*. Nat Cell Biol, 2004. **6**(8): p. 784-91.

249. Boy de la Tour, E. and U.K. Laemmli, *The metaphase scaffold is helically folded: sister chromatids have predominantly opposite helical handedness*. Cell, 1988. **55**(6): p. 937-44.
250. Ohnuki, Y., *Demonstration of the spiral structure of human chromosomes*. Nature, 1965. **208**(13): p. 916-7.
251. Xu, B., et al., *Two molecularly distinct G(2)/M checkpoints are induced by ionizing irradiation*. Mol Cell Biol, 2002. **22**(4): p. 1049-59.
252. Chang, S., et al., *Essential role of limiting telomeres in the pathogenesis of Werner syndrome*. Nat Genet, 2004. **36**(8): p. 877-82.
253. Barr, F.A., H.H. Sillje, and E.A. Nigg, *Polo-like kinases and the orchestration of cell division*. Nat Rev Mol Cell Biol, 2004. **5**(6): p. 429-40.
254. Hirano, T., R. Kobayashi, and M. Hirano, *Condensins, chromosome condensation protein complexes containing XCAP-C, XCAP-E and a Xenopus homolog of the Drosophila Barren protein*. Cell, 1997. **89**(4): p. 511-21.
255. Hudson, D.F., et al., *Condensin is required for nonhistone protein assembly and structural integrity of vertebrate mitotic chromosomes*. Dev Cell, 2003. **5**(2): p. 323-36.
256. Ono, T., et al., *Differential contributions of condensin I and condensin II to mitotic chromosome architecture in vertebrate cells*. Cell, 2003. **115**(1): p. 109-21.
257. Ono, T., et al., *Spatial and temporal regulation of Condensins I and II in mitotic chromosome assembly in human cells*. Mol Biol Cell, 2004. **15**(7): p. 3296-308.
258. Holliday, R., *The Induction of Mitotic Recombination by Mitomycin C in Ustilago and Saccharomyces*. Genetics, 1964. **50**: p. 323-35.
259. Haber, J.E., et al., *Repairing a double-strand chromosome break by homologous recombination: revisiting Robin Holliday's model*. Philos Trans R Soc Lond B Biol Sci, 2004. **359**(1441): p. 79-86.
260. Ogawa, T., et al., *Similarity of the yeast RAD51 filament to the bacterial RecA filament*. Science, 1993. **259**(5103): p. 1896-9.

261. Benson, F.E., A. Stasiak, and S.C. West, *Purification and characterization of the human Rad51 protein, an analogue of E. coli RecA*. *Embo J*, 1994. **13**(23): p. 5764-71.
262. Baumann, P., F.E. Benson, and S.C. West, *Human Rad51 protein promotes ATP-dependent homologous pairing and strand transfer reactions in vitro*. *Cell*, 1996. **87**(4): p. 757-66.
263. Sung, P., *Catalysis of ATP-dependent homologous DNA pairing and strand exchange by yeast RAD51 protein*. *Science*, 1994. **265**(5176): p. 1241-3.
264. Symington, L.S., *Role of RAD52 epistasis group genes in homologous recombination and double-strand break repair*. *Microbiol Mol Biol Rev*, 2002. **66**(4): p. 630-70, table of contents.
265. Milne, G.T. and D.T. Weaver, *Dominant negative alleles of RAD52 reveal a DNA repair/recombination complex including Rad51 and Rad52*. *Genes Dev*, 1993. **7**(9): p. 1755-65.
266. Shen, Z., et al., *Specific interactions between the human RAD51 and RAD52 proteins*. *J Biol Chem*, 1996. **271**(1): p. 148-52.
267. Rijkers, T., et al., *Targeted inactivation of mouse RAD52 reduces homologous recombination but not resistance to ionizing radiation*. *Mol Cell Biol*, 1998. **18**(11): p. 6423-9.
268. Yamaguchi-Iwai, Y., et al., *Homologous recombination, but not DNA repair, is reduced in vertebrate cells deficient in RAD52*. *Mol Cell Biol*, 1998. **18**(11): p. 6430-5.
269. Petukhova, G., S. Stratton, and P. Sung, *Catalysis of homologous DNA pairing by yeast Rad51 and Rad54 proteins*. *Nature*, 1998. **393**(6680): p. 91-4.
270. Van Komen, S., et al., *Functional cross-talk among Rad51, Rad54, and replication protein A in heteroduplex DNA joint formation*. *J Biol Chem*, 2002. **277**(46): p. 43578-87.
271. Essers, J., et al., *Disruption of mouse RAD54 reduces ionizing radiation resistance and homologous recombination*. *Cell*, 1997. **89**(2): p. 195-204.
272. Dronkert, M.L., et al., *Mouse RAD54 affects DNA double-strand break repair and sister chromatid exchange*. *Mol Cell Biol*, 2000. **20**(9): p. 3147-56.

273. Welch, P.L. and M.C. King, *BRCA1 and BRCA2 and the genetics of breast and ovarian cancer*. Hum Mol Genet, 2001. **10**(7): p. 705-13.
274. Moynahan, M.E., A.J. Pierce, and M. Jasin, *BRCA2 is required for homology-directed repair of chromosomal breaks*. Mol Cell, 2001. **7**(2): p. 263-72.
275. Xia, F., et al., *Deficiency of human BRCA2 leads to impaired homologous recombination but maintains normal nonhomologous end joining*. Proc Natl Acad Sci U S A, 2001. **98**(15): p. 8644-9.
276. Sharan, S.K., et al., *Embryonic lethality and radiation hypersensitivity mediated by Rad51 in mice lacking Brca2*. Nature, 1997. **386**(6627): p. 804-10.
277. Wong, A.K., et al., *RAD51 interacts with the evolutionarily conserved BRC motifs in the human breast cancer susceptibility gene brca2*. J Biol Chem, 1997. **272**(51): p. 31941-4.
278. Moynahan, M.E., et al., *Brca1 controls homology-directed DNA repair*. Mol Cell, 1999. **4**(4): p. 511-8.
279. Moynahan, M.E., T.Y. Cui, and M. Jasin, *Homology-directed dna repair, mitomycin-c resistance, and chromosome stability is restored with correction of a Brca1 mutation*. Cancer Res, 2001. **61**(12): p. 4842-50.
280. Liu, N., et al., *XRCC2 and XRCC3, new human Rad51-family members, promote chromosome stability and protect against DNA cross-links and other damages*. Mol Cell, 1998. **1**(6): p. 783-93.
281. Cartwright, R., et al., *The XRCC2 DNA repair gene from human and mouse encodes a novel member of the recA/RAD51 family*. Nucleic Acids Res, 1998. **26**(13): p. 3084-9.
282. Cartwright, R., et al., *Isolation of novel human and mouse genes of the recA/RAD51 recombination-repair gene family*. Nucleic Acids Res, 1998. **26**(7): p. 1653-9.
283. Albala, J.S., et al., *Identification of a novel human RAD51 homolog, RAD51B*. Genomics, 1997. **46**(3): p. 476-9.
284. Pittman, D.L., L.R. Weinberg, and J.C. Schimenti, *Identification, characterization, and genetic mapping of Rad51d, a new mouse and human RAD51/RecA-related gene*. Genomics, 1998. **49**(1): p. 103-11.

285. Thacker, J., *A surfeit of RAD51-like genes?* Trends Genet, 1999. **15**(5): p. 166-8.
286. Masson, J.Y., et al., *Identification and purification of two distinct complexes containing the five RAD51 paralogs.* Genes Dev, 2001. **15**(24): p. 3296-307.
287. Masson, J.Y., et al., *Complex formation by the human RAD51C and XRCC3 recombination repair proteins.* Proc Natl Acad Sci U S A, 2001. **98**(15): p. 8440-6.
288. Kurumizaka, H., et al., *Homologous-pairing activity of the human DNA-repair proteins Xrcc3.Rad51C.* Proc Natl Acad Sci U S A, 2001. **98**(10): p. 5538-43.
289. Sigurdsson, S., et al., *Mediator function of the human Rad51B-Rad51C complex in Rad51/RPA-catalyzed DNA strand exchange.* Genes Dev, 2001. **15**(24): p. 3308-18.
290. Pierce, A.J., et al., *XRCC3 promotes homology-directed repair of DNA damage in mammalian cells.* Genes Dev, 1999. **13**(20): p. 2633-8.
291. Izsvak, Z., et al., *Healing the wounds inflicted by sleeping beauty transposition by double-strand break repair in mammalian somatic cells.* Mol Cell, 2004. **13**(2): p. 279-90.
292. French, C.A., et al., *Role of mammalian RAD51L2 (RAD51C) in recombination and genetic stability.* J Biol Chem, 2002. **277**(22): p. 19322-30.
293. Brenneman, M.A., et al., *XRCC3 controls the fidelity of homologous recombination: roles for XRCC3 in late stages of recombination.* Mol Cell, 2002. **10**(2): p. 387-95.
294. Yoshihara, T., et al., *XRCC3 deficiency results in a defect in recombination and increased endoreduplication in human cells.* Embo J, 2004. **23**(3): p. 670-80.
295. Deans, B., et al., *Homologous recombination deficiency leads to profound genetic instability in cells derived from Xrcc2-knockout mice.* Cancer Res, 2003. **63**(23): p. 8181-7.
296. Takata, M., et al., *Chromosome instability and defective recombinational repair in knockout mutants of the five Rad51 paralogs.* Mol Cell Biol, 2001. **21**(8): p. 2858-66.
297. Liu, Y., et al., *RAD51C is required for Holliday junction processing in mammalian cells.* Science, 2004. **303**(5655): p. 243-6.

298. Tarsounas, M., et al., *Telomere maintenance requires the RAD51D recombination/repair protein*. Cell, 2004. **117**(3): p. 337-47.
299. Gangloff, S., C. Soustelle, and F. Fabre, *Homologous recombination is responsible for cell death in the absence of the Sgs1 and Srs2 helicases*. Nat Genet, 2000. **25**(2): p. 192-4.
300. Saintigny, Y., et al., *Homologous recombination resolution defect in werner syndrome*. Mol Cell Biol, 2002. **22**(20): p. 6971-8.
301. Karow, J.K., et al., *The Bloom's syndrome gene product promotes branch migration of holliday junctions*. Proc Natl Acad Sci U S A, 2000. **97**(12): p. 6504-8.
302. Constantinou, A., et al., *Werner's syndrome protein (WRN) migrates Holliday junctions and co-localizes with RPA upon replication arrest*. EMBO Rep, 2000. **1**(1): p. 80-4.
303. Wu, L. and I.D. Hickson, *The Bloom's syndrome helicase suppresses crossing over during homologous recombination*. Nature, 2003. **426**(6968): p. 870-4.
304. Ira, G., et al., *Srs2 and Sgs1-Top3 suppress crossovers during double-strand break repair in yeast*. Cell, 2003. **115**(4): p. 401-11.
305. Sun, H., R.J. Bennett, and N. Maizels, *The Saccharomyces cerevisiae Sgs1 helicase efficiently unwinds G-G paired DNAs*. Nucleic Acids Res, 1999. **27**(9): p. 1978-84.
306. Opresko, P.L., et al., *Telomere binding protein TRF2 binds to and stimulates the Werner and Bloom syndrome helicases*. J Biol Chem, 2002. **277**(43): p. 41110-9.
307. Ivanov, E.L. and J.E. Haber, *RAD1 and RAD10, but not other excision repair genes, are required for double-strand break-induced recombination in Saccharomyces cerevisiae*. Mol Cell Biol, 1995. **15**(4): p. 2245-51.
308. Fishman-Lobell, J. and J.E. Haber, *Removal of nonhomologous DNA ends in double-strand break recombination: the role of the yeast ultraviolet repair gene RAD1*. Science, 1992. **258**(5081): p. 480-4.
309. Niedernhofer, L.J., et al., *The structure-specific endonuclease Ercc1-Xpf is required to resolve DNA interstrand cross-link-induced double-strand breaks*. Mol Cell Biol, 2004. **24**(13): p. 5776-87.

310. Nicholson, A., et al., *Regulation of mitotic homeologous recombination in yeast. Functions of mismatch repair and nucleotide excision repair genes.* Genetics, 2000. **154**(1): p. 133-46.
311. Niedernhofer, L.J., et al., *The structure-specific endonuclease Ercc1-Xpf is required for targeted gene replacement in embryonic stem cells.* Embo J, 2001. **20**(22): p. 6540-9.
312. Buermeier, A.B., et al., *Mammalian DNA mismatch repair.* Annu Rev Genet, 1999. **33**: p. 533-64.
313. Sugawara, N., et al., *Heteroduplex rejection during single-strand annealing requires Sgs1 helicase and mismatch repair proteins Msh2 and Msh6 but not Pms1.* Proc Natl Acad Sci U S A, 2004. **101**(25): p. 9315-20.
314. Allen, C., et al., *DNA-dependent protein kinase suppresses double-strand break-induced and spontaneous homologous recombination.* Proc Natl Acad Sci U S A, 2002. **99**(6): p. 3758-63.
315. Pierce, A.J., et al., *Ku DNA end-binding protein modulates homologous repair of double-strand breaks in mammalian cells.* Genes Dev, 2001. **15**(24): p. 3237-42.
316. Kyrion, G., K.A. Boakye, and A.J. Lustig, *C-terminal truncation of RAP1 results in the deregulation of telomere size, stability, and function in Saccharomyces cerevisiae.* Mol Cell Biol, 1992. **12**(11): p. 5159-73.
317. Li, B. and A.J. Lustig, *A novel mechanism for telomere size control in Saccharomyces cerevisiae.* Genes Dev, 1996. **10**(11): p. 1310-26.
318. Prado, F., J.I. Piruat, and A. Aguilera, *Recombination between DNA repeats in yeast hpr1delta cells is linked to transcription elongation.* Embo J, 1997. **16**(10): p. 2826-35.
319. Chavez, S., et al., *A protein complex containing Tho2, Hpr1, Mft1 and a novel protein, Thp2, connects transcription elongation with mitotic recombination in Saccharomyces cerevisiae.* Embo J, 2000. **19**(21): p. 5824-34.
320. Bucholc, M., Y. Park, and A.J. Lustig, *Intrachromatid excision of telomeric DNA as a mechanism for telomere size control in Saccharomyces cerevisiae.* Mol Cell Biol, 2001. **21**(19): p. 6559-73.

321. Lundblad, V. and E.H. Blackburn, *An alternative pathway for yeast telomere maintenance rescues est1- senescence*. Cell, 1993. **73**(2): p. 347-60.
322. Le, S., et al., *RAD50 and RAD51 define two pathways that collaborate to maintain telomeres in the absence of telomerase*. Genetics, 1999. **152**(1): p. 143-52.
323. McEachern, M.J. and E.H. Blackburn, *Cap-prevented recombination between terminal telomeric repeat arrays (telomere CPR) maintains telomeres in Kluyveromyces lactis lacking telomerase*. Genes Dev, 1996. **10**(14): p. 1822-34.
324. Natarajan, S. and M.J. McEachern, *Recombinational telomere elongation promoted by DNA circles*. Mol Cell Biol, 2002. **22**(13): p. 4512-21.
325. Rizki, A. and V. Lundblad, *Defects in mismatch repair promote telomerase-independent proliferation*. Nature, 2001. **411**(6838): p. 713-6.
326. Henson, J.D., et al., *Alternative lengthening of telomeres in mammalian cells*. Oncogene, 2002. **21**(4): p. 598-610.
327. Lansdorp, P.M., et al., *Telomeres in the haemopoietic system*. Ciba Found Symp, 1997. **211**: p. 209-18.
328. Yeager, T.R., et al., *Telomerase-negative immortalized human cells contain a novel type of promyelocytic leukemia (PML) body*. Cancer Res, 1999. **59**(17): p. 4175-9.
329. Grobelny, J.V., A.K. Godwin, and D. Broccoli, *ALT-associated PML bodies are present in viable cells and are enriched in cells in the G(2)/M phase of the cell cycle*. J Cell Sci, 2000. **113 Pt 24**: p. 4577-85.
330. Wu, G., W.H. Lee, and P.L. Chen, *NBS1 and TRF1 colocalize at PML bodies during late S/G2 phases in immortalized telomerase-negative cells: Implication of NBS1 in alternative lengthening of telomeres*. J Biol Chem, 2000.
331. Yankiwski, V., et al., *Nuclear structure in normal and Bloom syndrome cells*. Proc Natl Acad Sci U S A, 2000. **97**(10): p. 5214-9.
332. Nabetani, A., O. Yokoyama, and F. Ishikawa, *Localization of hRad9, hHus1, hRad1 and hRad17, and caffeine-sensitive DNA replication at ALT (alternative lengthening of telomeres)-associated promyelocytic leukemia body*. J Biol Chem, 2004.

333. Johnson, F.B., et al., *The Saccharomyces cerevisiae WRN homolog Sgs1p participates in telomere maintenance in cells lacking telomerase*. *Embo J*, 2001. **20**(4): p. 905-13.
334. Perrem, K., et al., *Coexistence of alternative lengthening of telomeres and telomerase in hTERT-transfected GM847 cells*. *Mol Cell Biol*, 2001. **21**(12): p. 3862-75.
335. Ogino, H., et al., *Release of telomeric DNA from chromosomes in immortal human cells lacking telomerase activity*. *Biochem Biophys Res Commun*, 1998. **248**(2): p. 223-7.
336. Tokutake, Y., et al., *Extra-chromosomal telomere repeat DNA in telomerase-negative immortalized cell lines*. *Biochem Biophys Res Commun*, 1998. **247**(3): p. 765-72.
337. Sugimoto, M., et al., *Reconsideration of senescence, immortalization and telomere maintenance of Epstein-Barr virus-transformed human B-lymphoblastoid cell lines*. *Mech Ageing Dev*, 1999. **107**(1): p. 51-60.
338. Regev, A., et al., *Telomeric repeats on small polydisperse circular DNA (spcDNA) and genomic instability*. *Oncogene*, 1998. **17**(26): p. 3455-61.
339. Cohen, S., A. Regev, and S. Lavi, *Small polydispersed circular DNA (spcDNA) in human cells: association with genomic instability*. *Oncogene*, 1997. **14**(8): p. 977-85.
340. Katoh, M., et al., *A repressor function for telomerase activity in telomerase-negative immortal cells*. *Mol Carcinog*, 1998. **21**(1): p. 17-25.
341. Razak, Z.R., et al., *p53 differentially inhibits cell growth depending on the mechanism of telomere maintenance*. *Mol Cell Biol*, 2004. **24**(13): p. 5967-77.
342. Dunham, M.A., et al., *Telomere maintenance by recombination in human cells*. *Nat Genet*, 2000. **26**: p. 447-450.
343. Londono-Vallejo, J.A., et al., *Alternative lengthening of telomeres is characterized by high rates of telomeric exchange*. *Cancer Res*, 2004. **64**(7): p. 2324-7.
344. Konrad, J.P., et al., *Cloning and characterisation of the chicken gene encoding the telomeric protein TRF2*. *Gene*, 1999. **239**(1): p. 81-90.

345. Amsterdam, A., et al., *Identification of 315 genes essential for early zebrafish development*. Proc Natl Acad Sci U S A, 2004.
346. Smogorzewska, A., *Functional analysis of the human telomeric protein TRF2*, in *Molecular Genetics and Cell Biology*. 2001, The Rockefeller University: New York. p. 246.
347. Sedelnikova, O.A., et al., *Senescing human cells and ageing mice accumulate DNA lesions with unrepairable double-strand breaks*. Nat Cell Biol, 2004. **6**(2): p. 168-70.
348. d'Adda di Fagagna, F., et al., *A DNA damage checkpoint response in telomere-initiated senescence*. Nature, 2003. **426**(6963): p. 194-198.
349. de Lange, T., et al., *Structure and variability of human chromosome ends*. Mol Cell Biol, 1990. **10**(2): p. 518-27.
350. McElligott, R. and R.J. Wellinger, *The terminal DNA structure of mammalian chromosomes*. EMBO J, 1997. **16**(12): p. 3705-14.
351. Zijlmans, J.M., et al., *Telomeres in the mouse have large inter-chromosomal variations in the number of T2AG3 repeats*. Proc Natl Acad Sci U S A, 1997. **94**(14): p. 7423-8.
352. Lansdorp, P.M., et al., *Heterogeneity in telomere length of human chromosomes*. Hum Mol Genet, 1996. **5**(5): p. 685-91.
353. Bailey, S.M., et al., *CO-FISH reveals inversions associated with isochromosome formation*. Mutagenesis, 1996. **11**(2): p. 139-44.
354. Meyne, J. and E.H. Goodwin, *Direction of DNA sequences within chromatids determined using strand-specific FISH*. Chromosome Res, 1995. **3**(6): p. 375-8.
355. Haber, J.E., *The many interfaces of Mre11*. Cell, 1998. **95**(5): p. 583-6.
356. Lee, J.H., et al., *Distinct functions of Nijmegen breakage syndrome in ataxia telangiectasia mutated-dependent responses to DNA damage*. Mol Cancer Res, 2003. **1**(9): p. 674-81.
357. Kraakman-van der Zwet, M., et al., *Immortalization and characterization of Nijmegen Breakage syndrome fibroblasts*. Mutat Res, 1999. **434**(1): p. 17-27.
358. Lim, D.S., et al., *ATM phosphorylates p95/nbs1 in an S-phase checkpoint pathway*. Nature, 2000. **404**(6778): p. 613-7.

359. Bender, C.F., et al., *Cancer predisposition and hematopoietic failure in Rad50(S/S) mice*. Genes Dev, 2002. **16**(17): p. 2237-51.
360. Williams, B.R., et al., *A murine model of Nijmegen breakage syndrome*. Curr Biol, 2002. **12**(8): p. 648-53.
361. Umar, A., et al., *Correction of hypermutability, N-methyl-N'-nitro-N-nitrosoguanidine resistance, and defective DNA mismatch repair by introducing chromosome 2 into human tumor cells with mutations in MSH2 and MSH6*. Cancer Res, 1997. **57**(18): p. 3949-55.
362. Moshous, D., et al., *Artemis, a novel DNA double-strand break repair/V(D)J recombination protein, is mutated in human severe combined immune deficiency*. Cell, 2001. **105**(2): p. 177-86.
363. Weeda, G., et al., *Disruption of mouse ERCC1 results in a novel repair syndrome with growth failure, nuclear abnormalities and senescence*. Curr Biol, 1997. **7**(6): p. 427-39.
364. Gao, Y., et al., *A targeted DNA-PKcs-null mutation reveals DNA-PK-independent functions for KU in V(D)J recombination*. Immunity, 1998. **9**(3): p. 367-76.
365. Zhu, C., et al., *Ku86-deficient mice exhibit severe combined immunodeficiency and defective processing of V(D)J recombination intermediates*. Cell, 1996. **86**(3): p. 379-89.
366. de Wind, N., et al., *Inactivation of the mouse Msh2 gene results in mismatch repair deficiency, methylation tolerance, hyperrecombination, and predisposition to cancer*. Cell, 1995. **82**(2): p. 321-30.
367. Prolla, T.A., et al., *Tumour susceptibility and spontaneous mutation in mice deficient in Mlh1, Pms1 and Pms2 DNA mismatch repair*. Nat Genet, 1998. **18**(3): p. 276-9.
368. Edelmann, W., et al., *Meiotic pachytene arrest in MLH1-deficient mice*. Cell, 1996. **85**(7): p. 1125-34.
369. Schrader, C.E., et al., *Reduced isotype switching in splenic B cells from mice deficient in mismatch repair enzymes*. J Exp Med, 1999. **190**(3): p. 323-30.
370. Durant, S. and P. Karran, *Vanillins--a novel family of DNA-PK inhibitors*. Nucleic Acids Res, 2003. **31**(19): p. 5501-12.

371. Daniel, R., et al., *Wortmannin potentiates integrase-mediated killing of lymphocytes and reduces the efficiency of stable transduction by retroviruses*. Mol Cell Biol, 2001. **21**(4): p. 1164-72.
372. Daniel, R., R.A. Katz, and A.M. Skalka, *A role for DNA-PK in retroviral DNA integration*. Science, 1999. **284**(5414): p. 644-7.
373. Brewer, B.J., V.A. Zakian, and W.L. Fangman, *Replication and meiotic transmission of yeast ribosomal RNA genes*. Proc Natl Acad Sci U S A, 1980. **77**(11): p. 6739-43.
374. Cohen, S. and S. Lavi, *Induction of circles of heterogeneous sizes in carcinogen-treated cells: two-dimensional gel analysis of circular DNA molecules*. Mol Cell Biol, 1996. **16**(5): p. 2002-14.
375. Cohen, S. and M. Mechali, *Formation of extrachromosomal circles from telomeric DNA in Xenopus laevis*. EMBO Rep, 2002. **3**(12): p. 1168-74.
376. Multani, A.S., et al., *Caspase-dependent apoptosis induced by telomere cleavage and TRF2 loss*. Neoplasia, 2000. **2**(4): p. 339-45.
377. Ramirez, R., et al., *Massive telomere loss is an early event of DNA damage-induced apoptosis*. J Biol Chem, 2003. **278**(2): p. 836-42.
378. Jeyapalan, J., et al., *The Role of Telomeres in Etoposide Induced Tumour Cell Death*. Cell Cycle, 2004. **3**(9).
379. von Zglinicki, T., R. Pilger, and N. Sitté, *Accumulation of single-strand breaks is the major cause of telomere shortening in human fibroblasts*. Free Radic Biol Med, 2000. **28**(1): p. 64-74.
380. Bechter, O.E., J.W. Shay, and W.E. Wright, *The Frequency of Homologous Recombination in Human ALT Cells*. Cell Cycle, 2004. **3**(5).
381. Sasaki, M.S., et al., *Recombination repair pathway in the maintenance of chromosomal integrity against DNA interstrand crosslinks*. Cytogenet Genome Res, 2004. **104**(1-4): p. 28-34.
382. Carson, C.T., et al., *The Mre11 complex is required for ATM activation and the G2/M checkpoint*. Embo J, 2003. **22**(24): p. 6610-20.

383. Theunissen, J.W., et al., *Checkpoint failure and chromosomal instability without lymphomagenesis in Mre11(ATLD1/ATLD1) mice*. Mol Cell, 2003. **12**(6): p. 1511-23.
384. Pavlov, Y.I., I.M. Mian, and T.A. Kunkel, *Evidence for preferential mismatch repair of lagging strand DNA replication errors in yeast*. Curr Biol, 2003. **13**(9): p. 744-8.
385. Richardson, C. and M. Jasin, *Recombination between two chromosomes: implications for genomic integrity in mammalian cells*. Cold Spring Harb Symp Quant Biol, 2000. **65**: p. 553-60.
386. Murnane, J.P., et al., *Telomere dynamics in an immortal human cell line*. Embo J, 1994. **13**(20): p. 4953-62.
387. Zhu, J., et al., *Telomerase extends the lifespan of virus-transformed human cells without net telomere lengthening* Proc Natl Acad Sci U S A, 1999. **96**(7): p. 3723-8.
388. Stewart, S.A., et al., *Telomerase contributes to tumorigenesis by a telomere length-independent mechanism*. Proc Natl Acad Sci U S A, 2002.
389. Muller, H.J., *The remaking of chromosomes*. The Collecting Net, Woods Hole, 1938. **8**: p. 182-195.
390. Brown, E.J. and D. Baltimore, *Essential and dispensable roles of ATR in cell cycle arrest and genome maintenance*. Genes Dev, 2003. **17**(5): p. 615-28.
391. Jackman, M., et al., *Active cyclin B1-Cdk1 first appears on centrosomes in prophase*. Nat Cell Biol, 2003. **5**(2): p. 143-8.
392. Zou, Y., et al., *Asynchronous replication timing of telomeres at opposite arms of mammalian chromosomes*. Proc Natl Acad Sci U S A, 2004. **101**(35): p. 12928-33.
393. Hultdin, M., et al., *Replication timing of human telomeric DNA and other repetitive sequences analyzed by fluorescence in situ hybridization and flow cytometry*. Exp Cell Res, 2001. **271**(2): p. 223-9.
394. Marcand, S., et al., *Silencing of genes at nontelomeric sites in yeast is controlled by sequestration of silencing factors at telomeres by Rap 1 protein*. Genes Dev, 1996. **10**(11): p. 1297-309.

395. Mishra, K. and D. Shore, *Yeast Ku protein plays a direct role in telomeric silencing and counteracts inhibition by rif proteins*. *Curr Biol*, 1999. **9**(19): p. 1123-6.
396. Ben-Aroya, S., et al., *The compact chromatin structure of a Ty repeated sequence suppresses recombination hotspot activity in Saccharomyces cerevisiae*. *Mol Cell*, 2004. **15**(2): p. 221-31.
397. Baur, J.A., et al., *Telomere position effect in human cells*. *Science*, 2001. **292**(5524): p. 2075-7.
398. Garcia-Cao, M., et al., *Epigenetic regulation of telomere length in mammalian cells by the Suv39h1 and Suv39h2 histone methyltransferases*. *Nat Genet*, 2004. **36**(1): p. 94-9.
399. Garcia-Cao, M., et al., *A role for the Rb family of proteins in controlling telomere length*. *Nat Genet*, 2002.
400. Tomaska, L., et al., *Extragenomic double-stranded DNA circles in yeast with linear mitochondrial genomes: potential involvement in telomere maintenance*. *Nucleic Acids Res*, 2000. **28**(22): p. 4479-87.
401. Hahn, W.C., et al., *Inhibition of telomerase limits the growth of human cancer cells*. *Nat Med*, 1999. **5**(10): p. 1164-70.
402. Dimri, G.P., et al., *A biomarker that identifies senescent human cells in culture and in aging skin in vivo*. *Proc Natl Acad Sci U S A*, 1995. **92**(20): p. 9363-7.
403. de Lange, T., *Human telomeres are attached to the nuclear matrix*. *Embo J*, 1992. **11**(2): p. 717-24.